ANALYSIS OF BOLT AND RIVET STRUCTURAL FASTENERS SUBJECTED TO DYNAMIC AND QUASI-STATIC SHEAR LOADINGS

A Thesis

by

CHRISTOPHER PAUL RABALAIS

Submitted to the Office of Graduate and Professional Studies of
Texas A&M University
in partial fulfillment of the requirements for the degree of

MASTER OF SCIENCE

Chair of Committee,	W. Lynn Beason
Committee Members,	Peter B. Keating
	Dara Childs
Head of Department,	Robin Autenrieth

May 2015

Major Subject: Civil Engineering

ABSTRACT

Non-pretensioned bolted, pretensioned bolted, and riveted lap-spliced specimens were tested to observe how the fasteners' shear strengths were affected by (1) loading type, (2) fastener type, (3) number of shear planes, and (4) joint configuration. A 200,000-lbf capacity dynamic loader was used to fail the specimens under a monotonic dynamic or quasi-static load. The applied force and acceleration were measured by load cells and accelerometers above and below the specimen.

The test data were normalized by the number of shear planes loaded in each test, actual cross-sectional area per shear plane, and ultimate static tensile strength of the respective fastener type. A statistical analysis (ANOVA and t-test) was conducted on data sets from the 224 tests to determine the significant factors affecting the fastener shear strength.

Conclusions from the analysis indicated that the loading type factor has the most significant effect on shear capacity. A fastener's dynamic shear strength is increased by a ratio of 1.72 to 1.78 over its quasi-static shear capacity regardless of fastener type, when both are normalized to the fastener's ultimate static tensile strength. The joint configuration and shear type generally did not have a practical effect from an engineering standpoint on the shear capacity of bolted fasteners. Shear type did have an effect on riveted specimens under quasi-static loadings. Joint configuration only affected the response of riveted specimens under dynamic loadings.

DEDICATION

I would like to dedicate this thesis to the special people in my life who have formed me into the person I have become. First, to my Mom and Dad, you taught me how to be the best person I can be and never do anything halfway. You have pushed me, whether I thought I needed it or not, to never give up and pursue the things that would help me in the long run. Thank you for your never-ending support in all things, whether it was on the playing field, in the classroom, or in life. You have made me the man I am today.

Second, to my fiancée, Katie, thank you for being my better half and putting up with all my antics. I love you, and I can't wait to spend the rest of my life with you.

Third, to my sister, Lauren, thank you for being there all these years and know that you can accomplish anything you want if you put your mind to it.

Fourth, to my grandparents: Meemaw Freda, thank you for your never-ending support and encouraging words, and Meemaw Alice, although you are no longer with us, thank you for your support while you were here, and I know you would be so proud of me.

Lastly, to all the faculty members who pushed me to where I am today especially Mrs. Philips and Mrs. Reid for your challenges to me in high school and for your encouragement to me to pursue engineering, and Dr. Griffin, for being a royal pain in those CVEN courses at Louisiana Tech but challenging me to think critically in my academics and life.

ACKNOWLEDGEMENTS

I would like to acknowledge the efforts of all those who helped make the completion of this thesis possible.

First, and foremost, I must recognize the efforts put in by engineers and technicians from the USACE-ERDC, especially those in the GSL-StEB. They helped formulate the research problem, design and fabricate the specimens, assist in completing the tests, and guide me through the analysis of the data. The most special thanks goes to Dr. C. Kennan Crane, a research structural engineer with GSL-StEB, who mentored me throughout the research process and provided funding sources for the research. Also, the technicians who helped physically with completing the tests need special recognition. Joseph Bonelli, a contractor with GSL-StEB, was the main technician in charge of assisting with completing the research tests. The tests could not have been completed without his assistance. He and I were supported during testing by Ched Gorrondona, T.J. Beard, and Tyler Temple, also technicians with GSL-StEB. I would also like to acknowledge Lennie Gonzelez-Roman and Edgardo Ruiz, research structural engineers with GSL-StEB, for designing the test specimens and gripping mechanisms. Bob Walker, research civil engineer with GSL-StEB, and Patrick Kieffer, research mechanical engineer with GSL-SvEB, assisted Dr. Crane and me in determining the correct analysis methods of the data. Other acknowledgements are for the efforts of Cliff Grey, of ERDC's Instrumentation Branch, and Oscar Reihsman, of USACE's Information Technology group, who helped to provide the instrumentation setup, as well

as Mickey Blackmon and technicians of the USACE-Public Works System Machine Shop who helped to design and fabricate the test specimens and gripping mechanism. Also, a big thanks goes to Dr. Paul Allison who tested the ASTM E8 specimens.

Secondly, I would like to acknowledge and thank the Department of Homeland Security (Interagency Agreement HSHQDS-09-X-00320) and Federal Highway Administration (Interagency Agreement DTFH61-10-X-30028) for funding this research project and many others. Our goal as engineers is to make the lives of people safer, better, and easier to live in. We could not do this without your financial support.

Thirdly, I would like to acknowledge Vincent Chiarito, research structural engineer with StEB, who first helped me, as a high school junior, obtain a job working in StEB. If it weren't for him, I would not have the opportunities I have been given to pursue a career in civil engineering research.

Lastly, I would like to acknowledge members of my thesis advisory committee at Texas A&M University. Dr. W. Lynn Beason, my committee chair and academic advisor during the pursuit of my master's degree, helped to guide me through the trials of graduate school and thesis writing. Dr. Peter Keating, from who I had the pleasure of taking several structural engineering courses at TAMU, and Dr. Dara Childs, a mechanical engineering professor at TAMU, helped to guide me through the completion of the thesis requirements.

NOMENCLATURE

AISC	American Institute for Steel Construction
ANSI	American National Standards Institute
ASTM	American Society for Testing and Materials
ASCE	American Society of Civil Engineers
ERDC	Engineer Research and Development Center
fps	Frames per second
g's	Gravitational Acceleration: 1 g = 32.2 ft/s^2 = 9.81 m/s^2
GSL	Geotechnical and Structures Laboratory
Hz	Hertz, unit of frequency
kip	Kilo-Pound, one-thousand (1000) pounds, unit of force
ksi	Kips per square inch, unit of pressure
lbf	Pound, unit of force
psi	Pounds per square inch, unit of pressure
RCRBSJ	Research Council for Riveted and Bolted Structural Joints
RCSC	Research Council for Structural Connectors
StEB	Structural Engineering Branch
SvEB	Survivability Engineering Branch
TAMU	Texas A&M University
USACE	United States Army Corps of Engineers

TABLE OF CONTENTS

Page

LIST OF FIGURES

Page

LIST OF TABLES

Page

1. INTRODUCTION

Many national landmark bridges, such as the iconic Golden Gate Bridge and the Brooklyn Bridge, are relatively old, opened in 1937 and 1883, respectively. These bridges were designed and constructed using older standards. Therefore, these bridges and others might have significant structural vulnerabilities, such as weaker than expected joints, members, or fasteners. Also, most pre-1950s bridges were built using hot-driven rivets as the fasteners in structural connections rather than high-strength bolts and nuts, which is today's standard fastener for structural connections. Additionally, no in-depth design standard or provisions for dynamic loadings, such as American Institute for Steel Construction's (AISC) Seismic Provisions for Steel Structures which was first published in 1990, existed when pre-1950s bridges were designed and built.

In the past 100 years, millions of dollars have been spent researching types of structural connections as well as the fasteners themselves. The Research Council for Structural Connections (RCSC) was formed in 1947 as the Research Council on Riveted and Bolted Structural Joints (RCRBSJ) for this specific purpose. This council was instrumental in determining bolts could be a 1-to-1 replacement for rivets, as bolts had the same static bearing strength as rivets, could be tightened to introduce clamping forces like rivets did when cooled, and were a more reliable fastener for fatigue strength in place of rivets. Bolts and rivets were tested to determine their shear load capacity and tensile load capacity, as well as the combined loading of shear and tension. A few other types of loadings were researched as well, such as static and fatigue loadings. However,

one scenario has yet to be tested on either bolts or rivets: a short duration monotonic dynamic load that causes a shear/bearing failure in the fasteners in 1 to 6 milliseconds.

Due to recent events, civil engineers are very aware of the threat of monotonic dynamic impacts critically damaging or destroying important areas, such as an iconic landmark and/or main transportation arteries that allow people, goods, and support to steadily move across normally impassable areas. Knowing this, it is surprising to realize that there is vital research on bolts and rivets, literally the pieces that hold the transportation system together, that has yet to be completed. There are a number of instances where dynamically loaded axial members were connected in such a way that the fasteners experienced a short duration shear loading when the connected members experienced short duration axial loadings. This is why it is important to Department of Homeland Security (DHS), Federal Highway Administration (FHWA), United States Army Corps of Engineers—Engineer Research and Development Center (USACE-ERDC), the sponsors of this research, that the dynamic shear strength of bolts and rivets be researched.

The research performed in this thesis determined dynamic shear capacities of common fasteners used in structural connections and compared the responses of different types of fasteners to each other. Specifically, two bolt types (non-pretensioned and pretensioned) and hot-driven rivets were tested. Each of these fasteners was tested with three main variables: single or double shear, five different fastener configurations, and quasi-static or short duration dynamic loading. Therefore, the four main factors

affecting the ultimate shear strength of a fastener were analyzed in this thesis: fastener type, shear type, joint configuration, and loading type.

This thesis is divided into seven major sections. Section 2 lists the research objectives of this thesis. Section 3 presents a literature review that covers the topics of history of structural connection research, current design guides, comparison of bolt and rivet strengths, tests of shear strength of fasteners, and fastener capacities under various types of loadings.

Section 4 presents details about the testing setup. Included are discussions of the test specimen types and configurations, the methods used for collecting test data, the description of the test machine, the method for processing load cell and acceleration data, and the overall test matrix.

Section 5 discusses the results of the experiments outlined in Section 4. Included is the table of results for all test specimens by joint configuration and fastener type. In addition, this section presents photographs of typical bolted and riveted test specimens in place ready for testing for each joint configuration.

Section 6 discusses the statistical analysis completed on the data presented in Section 5. Using traditional analysis of variance (ANOVA) techniques, a four-factor factorial experimental design was conducted on the data presented in Section 5. The four factors considered included fastener type, joint configuration, shear type (double or single shear), and loading type (quasi-static or dynamic). Based on the results of this ANOVA, individual comparisons of mean values were conducted using the Students' t-

test statistic to compare the mean values so that the full significance of the results can be better understood.

Section 7 condenses the analysis into a list of conclusions that can be taken from the test results, and Section 8 presents the recommendations for future testing.

References and the appendices follow the recommendations. Appendix A presents shop drawings for each of the five specimen configurations tested. Appendix B presents the technical information on and existing operating procedures for the 200-Kip Dynamic Loader used to test the specimens. Appendix C presents data plots from each individual dynamic test and all plots from similar quasi-static test sets.

2. RESEARCH PLAN AND OBJECTIVES

The purpose of the research presented in this thesis was to develop an experimental plan that examined the behavior of various structural fasteners that are subjected to both quasi-static and dynamic shear loads.

Research conducted by the RCSC and others was reviewed and analyzed to determine the most appropriate type of specimens and variables to be tested in this research prior to any testing for this thesis. It was determined to fabricate specimens that incorporate axial bars and fasteners, as shown in Figure 1, based on the literature review. These specimens were designed so that failure would occur in the fastener when exposed to an axial loading. An axial tension load, shown as the value "P" in Figure 1, was applied to the test specimen. The fastener, which is perpendicular to the axial load and denoted by the dashed lines in Figure 1, failed in direct shear. The shear plane(s) of failure are denoted by the circles in Figure 1.

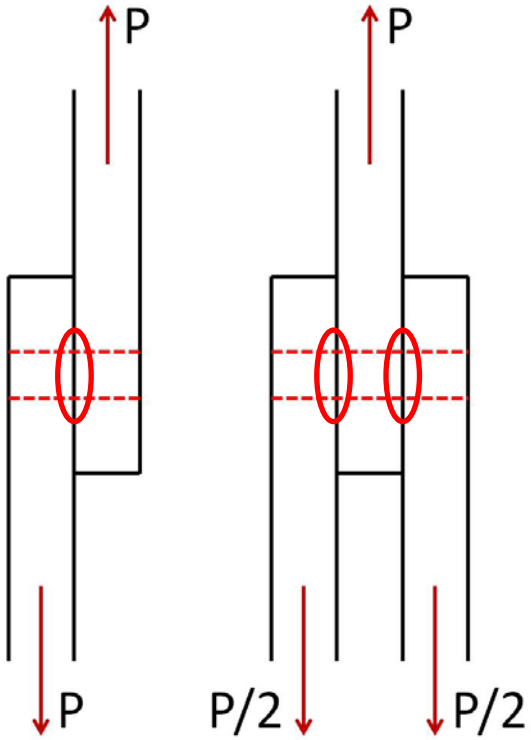

Figure 1: Free Body Diagram Example of Single Shear (Left) and Double Shear (Right).

The loading of the specimens was performed by using a rapid-loading testing apparatus housed at USACE-ERDC-Vicksburg. The 200-Kip Dynamic Loader is capable of applying multiple loading rates to the specimen, with an approximate range of loading rates of 10 to 100,000 lbf/msec. The loader was operated at the maximum loading rate possible and slowest loading rate possible for the dynamic loading type and quasi-static loading type tests, respectively. Failure of the fasteners occurred in approximately 1 to 6 milliseconds for the dynamic loading type and in approximately 500 to 4000 milliseconds for the quasi-static loading type. The actual loading rate for each specimen type was dependent on the fastener type.

The results of these tests were normalized to the number of fasteners and shear planes in the specimen and the average measured ultimate static tensile strength of the respective fastener type. A statistical analysis was conducted on these results to determine the effects of the chosen variable on the specimen response. The conclusions of this analysis satisfied the research objectives for this thesis as outlined below.

This thesis has the following three primary objectives.

1. Determine the dynamic and quasi-static shear strength of the three most commonly used types of structural fasteners: pretensioned bolts, non-pretensioned bolts, and hot-driven rivets,
2. Compare dynamic shear strength to quasi-static shear strength for each fastener type in order to determine an applicable dynamic increase ratio for each.
3. Determine if dynamic shear strength of the structural fasteners is affected by fastener type, joint patterns, and/or number of shear planes, and verify that the quasi-static shear strength is not affected by fastener type, joint patterns, and number of shear planes as shown in previous research,

These objectives will enable DHS, FHWA, and USACE-ERDC, the research sponsors, to have a more accurate understanding of the behaviors of structural fasteners under dynamic loadings so that results of previous research experiments can be better interpreted.

3. LITERATURE REVIEW

The following critical literature review summarized articles pertaining to experiments performed using similar types of structural fastener and connection specimens to those that will be tested in this thesis. The main topics covered in the review are history of structural connection research, current design guides, comparison of bolt and rivet strengths, tests of shear strength of fasteners, and capacities under various types of loads. These topics helped demonstrate why certain methodologies were used in the thesis research testing. The methods used for this thesis was discussed in Section 4.

It is important to note that the majority of the papers were written in the late 1940s through the 1960s. This was mainly due to the formation of the RCRBSJ (now RCSC) in 1947. Since the research push by the RCSC in the mid-1900s, very little research has been performed on structural fasteners.

3.1 History of Structural Connections Research

Rivets were the fastener of choice for the earliest iron and steel construction projects. Engineers understood that the hot-driven rivets could induce clamping forces, but it was almost impossible to determine the amount of clamping force created once the rivet had cooled (Kulak et al. 1987). The first publication on riveting was released in the mid-1800s by British engineers detailing the erection of two new bridges in Wales and the properties of the materials used during construction, according to A. E. R. deJonge's

bibliography on riveted joints and Higgins and Ruble 1955. Since then, very little has been written about riveted connections (Stewart 1954). The early research showed that the slip resistance caused by clamping forces could not be designed, since the amount of clamping force could not be reliably predicted even though it was known to exist in the structural connections (Kulak et al. 1987).

Published research on high strength bolts for use in structural connections did not begin until the 1930s. In 1934, Batho and Bateman presented to the Steel Structures Committee of Scientific and Industrial Research of Great Britain the idea that high strength bolts could be used as fasteners for steel structures and that the bolts could be tightened sufficiently to prevent slip provided the bolt has a minimum yield strength of 54 ksi (Kulak et al. 1987). Wilbur Wilson and F. P. Thomas, from the University of Illinois at Urbana, released “Fatigue Tests of Riveted Joints” in 1938, which introduced the idea that a high strength bolt, when “screwed up to give a high tension in bolts”, could perform better than a rivet under fatigue conditions (Stewart 1954).

This idea was furthered by G. A. Maney, 1946 when he developed a balanced joint design for reverse loadings using bolts. These tests also proved the need for washers under the bolt head and nut. By 1947, the hardened washer was determined to be the best tool for keeping bolt tension under the reverse loading (Stewart 1954). This was the same year the RCRBSJ was formed. The research conducted by the RCRBSJ expedited the use of high strength bolts over rivets in structural applications (Stewart 1954).

The RCRBSJ, in conjunction with ASTM, created tentative specifications for materials to be used in high strength bolts which were approved in 1949. These specifications, along with continued research by the RCRBSJ, led to the release of the first specification for bolted structural joints in 1951. Revised editions of RCRBSJ, now known as the RCSC, specifications and other research projects have allowed for refinement of specifications for bolt installation and joint design, such as the development of ASTM A307 standard strength bolt and ASTM A325 and ASTM A490 high strength bolts (Kulak et al. 1987). These advances in bolted specifications led to riveted structural connections becoming obsolete.

3.2 Current Design Guides

Two professional groups set the main standards for steel construction, AISC and RCSC. The earliest design guide and specifications were released in 1923 for AISC and 1951 for RCSC.

AISC specifications and design guides detail the general design guidelines and construction practices for all components of steel construction. A new edition of AISC Steel Design Manual is released every 5-10 years. RCSC only releases specifications and design guides on specific structural joints and the fasteners that are included in those joints. A new specification for structural bolts has been released nearly every 5 years since 1951, with the most recent specification released in 2009. The specifications allow for bolted joints to be designed for friction resistance, a slip-critical joint, or for bearing of the bolt, a non-slip-critical joint.

The most recent design guide for rivets, however, was published in 1987 by Kulak, et al. in the “Guide to Design Criteria for Bolted and Riveted Joints, Second Edition”. The most recent AISC design manual did not include specifications for rivets. Past specifications allowed for riveted joints to be designed only for bearing strength of the rivet, as the friction developed during the hot-driven process was difficult and unreliable to determine.

3.3 Comparison of Bolted and Riveted Strengths

Researchers from universities across the nation and the RCRBSJ compared the performance of these bolts to the existing riveted connections as soon as high strength bolts were hypothesized as replacement fasteners for rivets in structural joints. The economic impacts, such as fastener, labor, and equipment costs of bolt installation versus rivet installation, were also researched. Many of these tests were detailed in Munse (1970).

Most of the summarized research in Munse (1970) focused on static and fatigue loading conditions, as well as the effects that fastener type has on the transfer of load from member to member. Munse (1970) detailed five projects conducted at the University of Illinois covering a wide breadth of topics; bearing pressure on joints, joint patterns, and strength of fasteners under combined tension and shear are discussed. Most of the research was completed during the time when high strength bolts were becoming the fastener of choice for new construction and for replacement of loosened riveted connections. Section 2.4.3 of Munse (1970) noted that the high strength bolt went from

being frowned on as a permanent fastener to being tested in laboratories across the country and to being used heavily in the field in a matter of a decade or so.

The research summarized in Munse (1970), as well as Baron and Larson (1955) and several other papers that focused on fatigue loadings of structural joints, noted the importance of clamping forces in the performance of the joint regardless of the fastener type; Baron and Larson tested cold- and hot-driven ASTM A141 standard rivets and ASTM A325 high strength bolts. Wright and Munse (1952) noted the importance of the clamping force, as well as the type of faying surface, or the surface where structural members are joined together to make physical contact with one another, in determining the load-slip relationship of a joint. Wright and Munse (1952) also noted, however, that the type of faying surface was less important to the load-slip relationship in riveted joints than those in bolted joints. Conclusions of these tests determined that ultimately the faying surface and initial tension in either fastener had no effect on the ultimate strength of the connection under static loadings. In the first bolt specification concerning bolting of structures, the RCRBSJ indicated that a high strength bolt could replace a rivet on a "one-to-one" basis even though high strength bolts had a much higher ultimate strength than A141 rivets (Chesson 1964). The specifications also stated that the replacement could only be used on joints where the load was transferred solely through shear in the fasteners (Higgins 1955).

Early structural engineers were reluctant to use bolts to replace the rivet based on their fear of the tightened nut coming loose and ending up with the same situation with loosening rivets. Multiple researchers at University of Illinois, Lehigh University, and

others in conjunction with the RCRBSJ conducted several series of fatigue tests in order to determine if this situation would indeed happen. These tests were designed to indicate if the bolts may work loose and compared their performance to the widely used riveted joints. Carter et al. (1955) reasoned that the bearing of the rivet directly on the fastener hole after driving was the reason for fatigue failure of riveted joints, and the bolt would alleviate this failure if the bolt was fully tightened and did not initially bear on the fastener hole. The resulting compression would also help reduce crack propagations at the fastener hole.

Field tests and laboratory tests where rivets were replaced by bolts in connections with cyclic dynamic loadings were detailed by Higgins (1951) and followed up in Higgins and Ruble (1955). These tests concluded that bolted connections performed much better than rivets in fatigue testing. Baron and Larson (1955) and Carter et al. (1955) arrived at the same conclusion. Field tests indicated that the bolts did not loosen after six years of observations when they were properly tightened, whereas a similar riveted joint had several fasteners work loose (Higgins and Ruble 1955). Every fully tightened bolt in laboratory tests did not come loose even after 8,000,000 loading cycles (Higgins 1951). The results also showed that the number of shear planes was not a factor in performance of the joint (Carter et al. 1955).

These and other tests at the University of Illinois proved the bolt could be used in a wider range of connections than previously thought. These conclusions, as well as several economic factors, led to the bolt rapidly replacing the rivet as the fastener of choice during the 1950s. Bolts were more expensive in initial costs in the 1950s but were

cheaper and easier to install. The need for temporary construction bolts was eliminated since bolts could replace rivets. The need for rivet installation equipment and moving of this equipment was eliminated as well. More bolts could be placed in a day, and there was much less noise with an impact wrench used to install bolts compared with an air hammer used to install rivets. It was also cheaper to perform maintenance on joints after construction (Higgins and Ruble 1955). The use of high strength bolts also increased due to the shortage of riveters and the small amount of training a person needed to learn how to properly install a bolt.

3.4 Tests Conducted on Riveted Joints

Few tests were conducted on the performance of riveted connections in the first years after the creation of the RCRBSJ. Some tests were conducted in the 1930s, like Wilson and Oliver's "Tension Tests of Rivets" (Wilson and Oliver 1930). In Munse (1970), bolted tests outnumber the riveted tests by a ratio of almost 2:1. The research that was performed, however, tested specimens in combined tension and shear and observed the effects of initial tension in the rivet due to cooling.

Wilson and Oliver (1930) originally tested over 80 riveted specimens to observe the effect of head type on performance of a riveted connection subjected to tension. However, the testing revealed that as the grip length, the distance between the heads of the rivet, increases, the tensile strength of the joint decreases, but the internal initial tensile stress of the rivet increases. The conclusions stated that even though initial tension of the rivet could vary from 70 to 90% of the yield stress of the rivet, this tension

did not affect the ability of the rivet to resist an external tensile load. However, tests did not show how the initial tension affects the rivet in shear.

Munse and Cox (1956) sought to determine the effects of combined loading on the performance of rivets. They tested a variety of rivets under multiple loading conditions and were able to develop an elliptical curve that relates the combined stress the rivet can take from pure tension to pure shear, and they were able relate the ultimate shear values to ultimate stress of the material. This equation, which is still used in the AISC design criteria (Kulak et al. 1987) and codified in the AISC Steel Design Manual, is shown in Equation (1),

$$\boldsymbol{S = r * S_e} \quad \textbf{(1)}$$

where S is the ultimate strength of the fastener, S_e is the ultimate shear strength of the fastener, and r is calculated as shown in Equation (2),

$$\boldsymbol{r = 1.333 * \sqrt{\frac{1+m^2}{(1.333)^2+m^2}}} \quad \textbf{(2)}$$

where m is the ratio of tensile component force divided by the shear component force. The test results also indicated that for ultimate strength of the rivet for any combination of tension and shear loadings was not affected by the rivet being hot or cold formed. Figure 2 shows the interaction curve describing the relationship between the shear and tension capacity of the rivets at various states of combined shear and tension forces on the fastener from tests in Kulak et al. (1987).

Higgins and Munse (1952) extended Munse and Cox's research to include over 230 rivets. The resulting equation, shown in Equation (3), was mathematically the same as Equation (1) but is easier to use,

$$\frac{a^2}{1.00^2} + \frac{b^2}{1.33^2} = 1.0 \qquad (3)$$

where *a* and *b* are the ratios of shear and tensile component forces, respectively. These papers developed the value for ratio of shear strength to ultimate tensile strength for design. The AISC design guide (Kulak et al. 1987) suggested using a factor of 0.75 to determine the shear stress capacity of a rivet versus the tensile stress capacity based on the research by Munse, Cox, and Higgins. It is important to note that the tensile strength was based on the un-driven rivet's ultimate tensile strength. This strength is much easier to determine than the driven rivet ultimate tensile strength. Kulak et al. (1987) and Schenker et al. (1954) stated that the ultimate tensile strength of the driven rivet was approximately 20% greater than the un-driven strength when machine driving is used. Therefore, if the ratio of shear stress to tensile strength was based upon the driven rivet's ultimate tensile strength, the value would be approximately 0.625. This value was similar to the Kulak et al. (1987) value for available shear stress in bolts of 0.6.

Further testing also examined the relationship of shear stress of the rivet to tensile stress of the connected material in order to create a balanced design that the connection would either fail in shear of the rivet or tension rupture of the connected material. Jones (1956) determined that the bearing ratio had no effect on the performance of the joint, and could actually be used at a higher value than recommended

in codes at the time. This meant that a riveted joint with three connected members bearing on the fastener (double shear) would perform the same as one with two connected members bearing on the fastener (single shear).

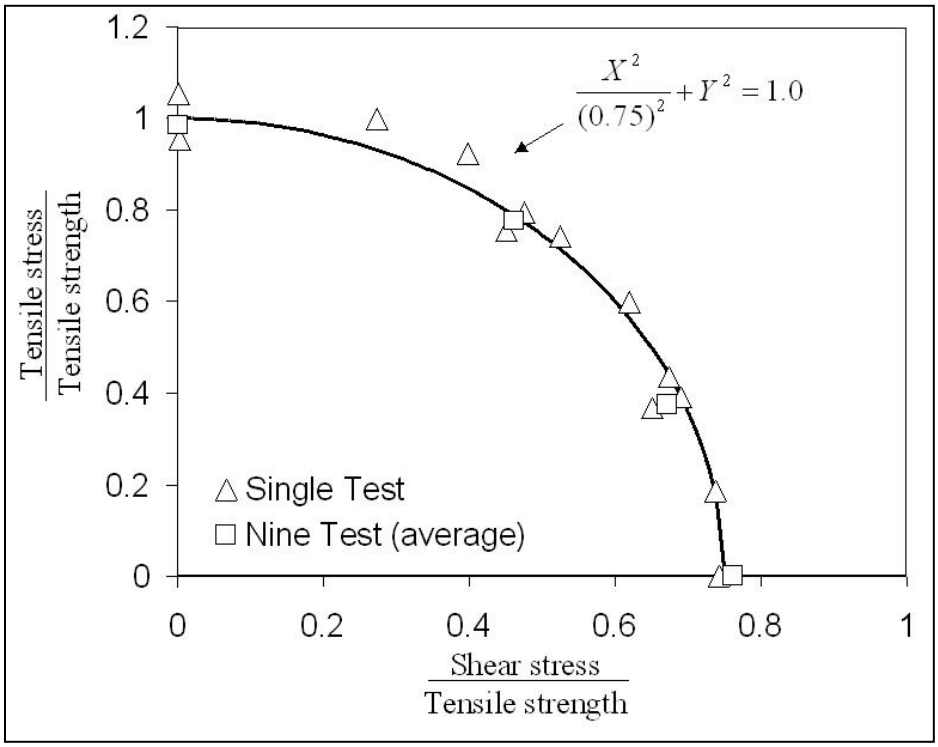

Figure 2: Interaction Curve for Combined Shear and Tension Stress as a Ratio of Ultimate Tensile Strength of Rivets (Kulak et al. 1987).

3.5 Tests Conducted on Bolted Joints

It was shown in a previous sub-section that much testing was completed on bolted joints and the bolts themselves under the direction of the RCRBSJ. This sub-section focuses only on the tests that influenced the reasoning for testing specimens in the specifications detailed in Section 4.

Bolts demonstrated their superiority to rivets based on the fatigue testing of bolts, as noted in the section comparing bolted and riveted joints. Munse et al. (1955) replicated previous tests and concluded that bolted joints, when tightened correctly, would provide a 25% gain in strength over that of riveted joints. Other research was completed on observing the effects of bolt tension on joint performance. Wallaert and Fisher (1962), Higgins and Ruble (1955), Munse et al. (1955), Kaplan (1959), and Bendigo et al. (1963) concluded that the amount of bolt pre-tension had no effect on the ultimate shear strength of the bolts. The overarching conclusion of these researchers was that no matter the bolted joint configuration, number of shear planes, number of bolts in the joint, the strength of bolt, or fatigue or static loadings, the amount of tension developed on the bolt during installation would not appreciably affect the overall shear strength of the bolt.

Several more tests observed the effects of clamping and contact surface type on the load-slip relationship of the joint. Munse et al. (1955), Foreman and Rumpf (1961), and Hectman et al. (1955) concluded that applying a clamping force and the type of faying surface greatly affected the amount of force the joint could handle before slipping. Foreman and Rumpf (1961) went further to state that the joint pattern in large joints also affected the load-slip relationship. However, Hectman et al. (1955) determined that the properties of the joints such as the lap plate thickness, faying area, and bolt pattern had no major effect on the shear developed in the bolts prior to major slip.

The ultimate shear strength of a fastener in design specifications researched for this thesis was given as a ratio to the fastener's ultimate tensile strength. The AISC design guide (Kulak et al. 1987) and AISC manual state that the ratio of shear stress to tensile stress in bolts is 0.62 whereas the ratio of shear stress to tensile stress in rivets is 0.75. The interaction curve for combined shear and tension loading on a bolt is given in Figure 3. The bolt interaction curve has a similar shape to the curve for rivets shown in Figure 2. The reduction of the strength ratio from rivets to bolts was seen in the single bolt, double shear tests completed by Kaplan in 1959. He and Wallaert and Fisher (1962) investigated multiple bolt diameters and determined that bolt diameter did not affect the overall shear strength of the fastener, but will change the amount of deformation "because the bolt shearing area increases faster than that of the bolt bearing area" (Wallaert and Fisher 1962). Chesson (1964) noted that the shear strength was also reduced to 0.80 of the ultimate shear strength when the shear plane is located in the threads versus the shank of the bolt. This reduction in strength accounted for the reduction in cross-sectional surface area caused by the threads. Also, if a load was placed through the shank of a bolt, the number of shear planes would not matter; a double shear joint would have twice the capacity of a single shear joint, and vice versa (Bendigo et al. 1963).

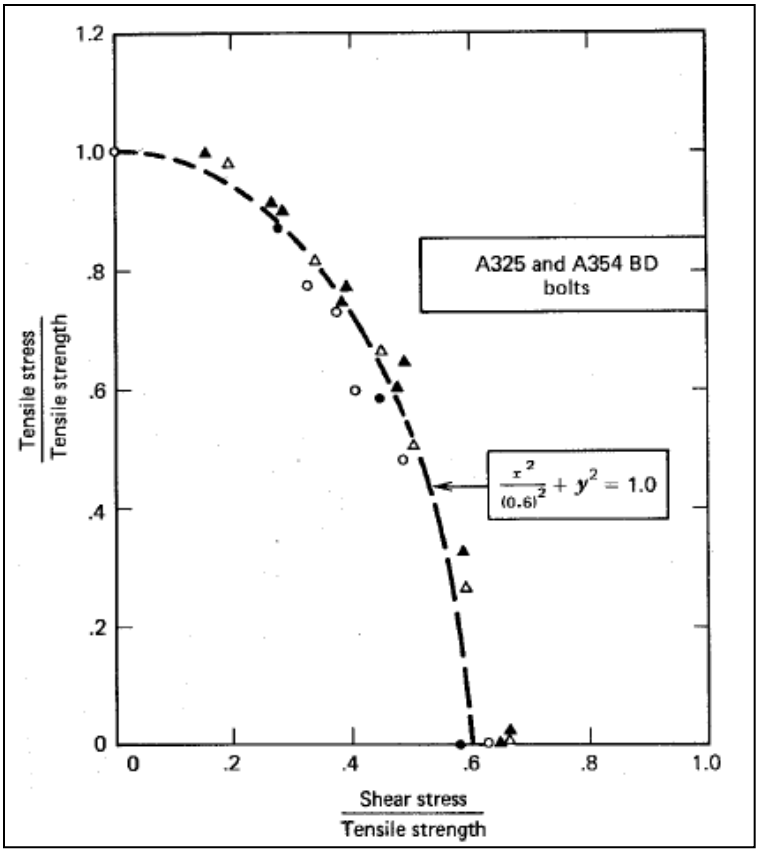

Figure 3: Interaction Curve for Combined Shear and Tension Stress as a Ratio of Ultimate Tensile Strength of Bolts (Kulak et al. 1987).

Bendigo et al. (1963) also observed an effect called “unbuttoning” in long bolted joints, which were joints that had more than 7 fasteners in a line along the loading axis. Their tests showed that the end fastener of the long joint being tested would fail prematurely before all the fasteners in the line could develop their full shear stress.

All the work on bolted joint capacity and behavior allowed the RCRBSJ (RCSC) to place new specifications for bolts replacing rivets. A141 standard rivets could be replaced on a three-to-two basis with A325 high strength bolts and a two-to-one basis

with the higher strength A490 high strength bolt, but only for smaller joints (Chesson 1964).

3.6 Summary

From reviewing the past literature on testing of riveted and bolted structural joints, it was obvious that significant testing had been completed on these fasteners, especially high strength bolts. The two types of fasteners performed similarly under static loadings, but the high strength bolt outperformed the rivet in fatigue strength and economic benefits. Rivets have essentially been removed as a fastener to use in standard design practices for steel construction because of this realization.

However, many old structures constructed with rivets, as well as those constructed with bolts, still stand and are threatened by one loading situation that has not been researched: a short duration monotonic dynamic loading causing failure of a fastener or joint in 1 to 6 milliseconds. One test series conducted by the Naval Research Laboratory in the 1950s tested bolts under shock loadings. However, these bolts were tested for tension failures and failed using repeated blows with a constant weight and not with a single load with a varying intensity (Clements 1956).

The following sections of this thesis detail the use of information gleaned from past researchers to develop a testing procedure for determining the dynamic shear capacity of similar bolts and rivets.

4. TEST DESIGN

In this section, details are presented about the testing setup. Included are discussions of the test specimen types and configurations, the methods used for collecting test data, the description of the loading machine, the description of the gripping mechanism, and the overall test matrix.

4.1 Test Specimens

A test specimen for this thesis was defined as the combination of plates and fastener(s) to create a structural joint. The connected plates were a combination of ½-inch and 1-inch-thick A36 mild structural steel plates. Each specimen consisted of either two ½-inch plates or two ½-inch plates and one 1-inch plate, for single and double shear tests, respectively, and one of five joint configurations milled into each plate. The specimen plates were designed by Lennie Gonzalez-Roman, a research structural engineer with Geotechnical and Structures Laboratory—Structural Engineering Branch (GSL-StEB), such that the only possible failure in the test specimen would occur from failure of the fastener in shear. A plate design was developed using connection design specifications listed in AISC Steel Design Manual, 14th Edition. The design used the "worst-case-scenario" design strengths of the test specimen components, such as highest specified fastener strength and cross-sectional area, largest number of fasteners, double shear of the fastener, and lowest specified plate strength. This design process would prevent failure caused by plate tension yielding, tension rupture, bearing/tear-out failure,

and block shear rupture. Figure 4 shows the typical plate designs for the 1-inch and ½-inch-thick plate specimens. The six top holes were 1-1/16 inches in diameter, and the one to four bottom holes, depending on joint configuration, were 9/16 inches in diameter. All dimensions in Figure 4 were to the center of the appropriate hole.

The fasteners used in the experiments were ASTM A307 Grade B standard strength bolts (ASTM 2010) and ASTM A502 Grade 2 standard strength rivets (ASTM 2003). Each fastener type had a nominal diameter of ½ inch. ASTM A307 standard strength bolts were used instead of an ASTM A325 or ASTM A490 high strength bolts even though ASTM A325 or A490 high strength bolts are typically used in actual bolted structural joints. ASTM A307 bolts were chosen because A307 bolts and A502 rivets have similar mechanical properties. This was done to ensure the response of the bolted and riveted specimens were as close as possible to each other. All bolted fasteners had threads in the shear plane. It is notable that threads are typically not included in the shear plane in actual structural applications. However, ATSM A307 bolts are not used in structural joints. Also, A307 bolts are not manufactured with the threads excluded from the shear plane in the lengths required for this thesis's research.

The plate specimens were reused in bolted specimen tests to speed up the testing of the specimens. Measurements were obtained with a micrometer after several tests. The measurements showed no hole elongation or deformation had occurred during testing. The plate specimens were not reused for riveted specimens due to the construction of the specimen. See section 4.1.2.4 for details about riveted specimens.

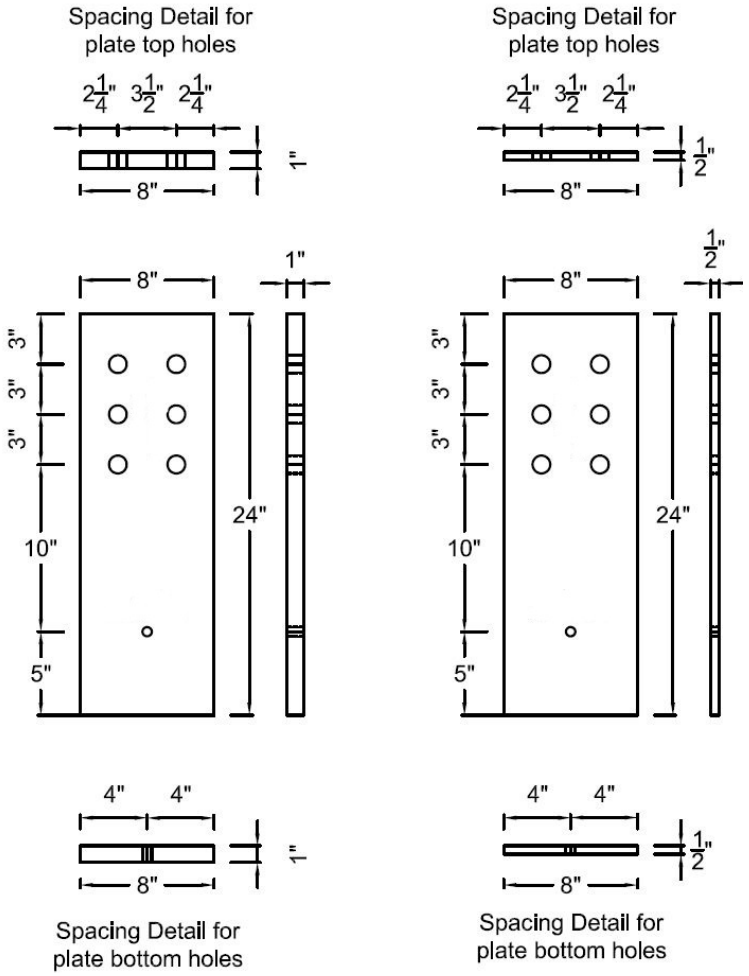

Figure 4: Typical Plate Test Specimens.

4.1.1 Joint Configurations

This thesis research tested five different joint configurations. These joint configurations were selected to model typical joint patterns found in bridge and other structural connections and to keep the specimen response under the load capacity of the rapid loading machine described in a later sub-section. Figure 5 below shows the selected joint configurations.

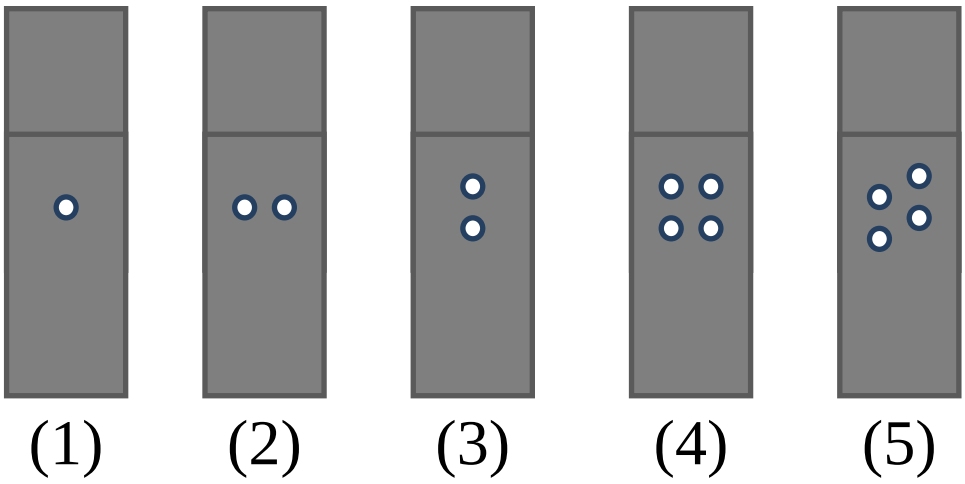

Figure 5: Five Joint Configurations for Testing.

The first configuration was a single fastener in the center of the plate specimen, like that shown in Figure 4 and Figure 5, (1). This joint configuration was selected as the control joint configuration for the test series. It allowed for the determination of the capacity of a single fastener in both single and double shear. That capacity was then compared to other joint configurations to determine effects of multiple fasteners at a joint.

The second and third joint configurations utilized different two-fastener configurations. Joint Configuration 2 has two fasteners in a horizontal line, Figure 5, (2). Joint Configuration 3 has two fasteners in a vertical line, Figure 5, (3). These two-fastener configurations were selected to determine if a “zippering” effect could be seen. Fasteners in Joint Configuration 2 would resist a load at the same time, whereas fasteners in Joint Configuration 3 would not resist the total load simultaneously if there was a zippering effect. One fastener would develop its full shear capacity and fail prior

to the next fastener in the line developing its full capacity. This “zippering” effect was seen in Bendigo (1963), which observed long joints that have more than 5 or 6 fasteners in a single line along the tensile axis. The end fasteners in Bendigo (1963) developed a shear failure before the middle fasteners developed their full strength. The test results from Joint Configurations 2 and 3 would help to determine if a joint under a monotonic impact/dynamic load showed the same results as Bendigo (1963), but for the smallest multiple fastener joint possible.

The fourth and fifth joint configurations utilized different four-fastener configurations. Joint Configuration 4 has four fasteners in a square pattern, Figure 5, (4). Joint Configuration 5 has four fasteners in a staggered configuration, Figure 5, (5). These four-fastener joint configurations were chosen because they more closely mimicked the interaction between fasteners seen in actual structural joints. The staggered joint was chosen because it is the most typical joint configuration in use in the field as staggering of fasteners increases the efficiency of large joints under static loads (Munse 1970).

4.1.2 Fastener Types

The types of structural fasteners can be reduced to three main categories that were detailed in AISC structural connection specifications: non-pretensioned bolts, pretensioned bolts, and rivets. Non-pretensioned bolts and pretensioned bolts were detailed in the connection specifications of the most recent AISC code as non-slip critical connections and slip critical connections, respectively. Rivets were once widely

used but were relegated to the appendices of AISC code and were completely removed in the latest (14^{th}) edition of AISC code.

The nominal diameter of each type of fastener used in this thesis is ½ inches. Bolts tested in single shear had a nominal 2-inch bolt length, and those tested in double shear had a nominal 3-inch bolt length. The effective cross-sectional area (accounting for threads included in the shear plane) is 0.1419 in^2. The ultimate tensile strengths of these bolts were determined and detailed in Subsection 4.1.2.1. The rivets have an effective diameter of 9/16 (0.5625) inches (effective cross-sectional area of 0.2463 in^2) due to the filling of the oversized hole in the connected plates during the hot-driving process. Figure 6 shows the typical fastener types prior to testing. Subsections 4.1.2.2 through 4.1.2.4 detailed the specifications for each type of fastener.

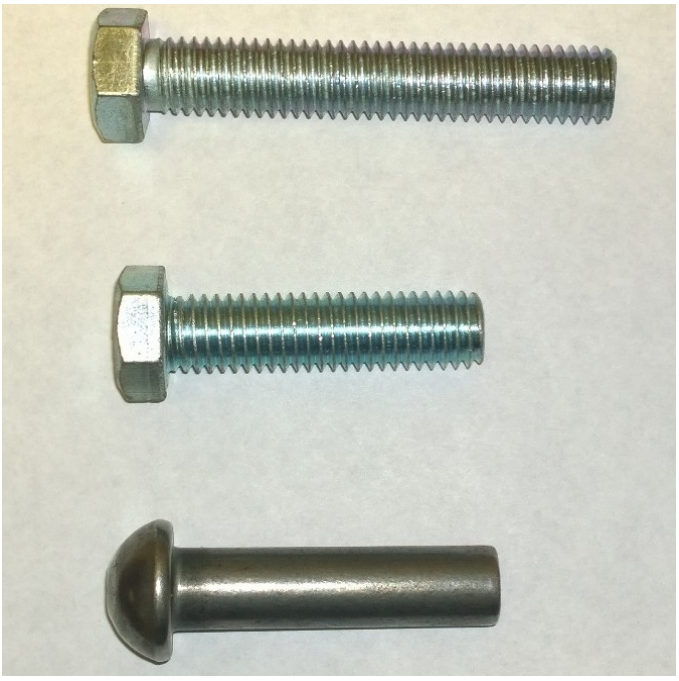

Figure 6: Typical Fastener Specimen; Top to Bottom: ASTM A307 Bolt for Double Shear specimens, ASTM A307 Bolt for Single Shear Specimens, and Un-Driven, Un-Heated ASTM A502 Rivet.

4.1.2.1 Ultimate Tensile Strength of Fasteners

AISC 14th Edition indicated that the available nominal shear strength of a bolt is 56.3% of the ultimate tensile strength of the fastener. The ultimate force on each shear plane for the specimens tested in this thesis was normalized to the ultimate tensile strength of the respective bolt. This allowed for correct comparisons of the ultimate shear capacities of the double- and single-shear bolted specimens.

A series of tests was completed to determine the ultimate tensile capacity of the two sizes of bolts using ASTM F606 standard testing procedures (ASTM 2011). The double and single shear bolts were each tested six times using the setup shown in Figure

7 and Figure 8. The tests were conducted with a MTS 810 Material Test System. The data were collected at a 30-Hz sample rate using the loader's controlling software. The speed of the free-running cross head was at most 0.07 inches/minute (maximum speed per ASTM F606 is 1 inch/minute). The results of the ASTM F606 ultimate tensile strength testing is listed in Table 1. The average ultimate tensile strength of the double- and single-shear bolts was as 72 ksi and 86 ksi, respectively.

It is important to note that ASTM F606 testing procedures did not provide for tensile testing of hot driven rivets. The actual ultimate tensile strength of the rivets tested was unknown. The ultimate driven rivet tensile strength was difficult to determine in other manners due to the small size of the driven specimens and the change in the material during the heating and driving processes. However, samples of undriven rivets were milled and tested to ASTM E8 specifications (ASTM 2013). The average ultimate undriven rivet tensile strength was 77 ksi. An estimated value for driven rivet strength was calculated using the increase factor of 1.2 as it is stated in Kulak et al. (1987) and Schenker (1954). This factor was the ratio of the un-driven to driven rivet ultimate tensile strengths when the rivet is driven using hydraulics, as performed for this thesis. Therefore, the estimated driven rivet ultimate tensile strength is 92 ksi.

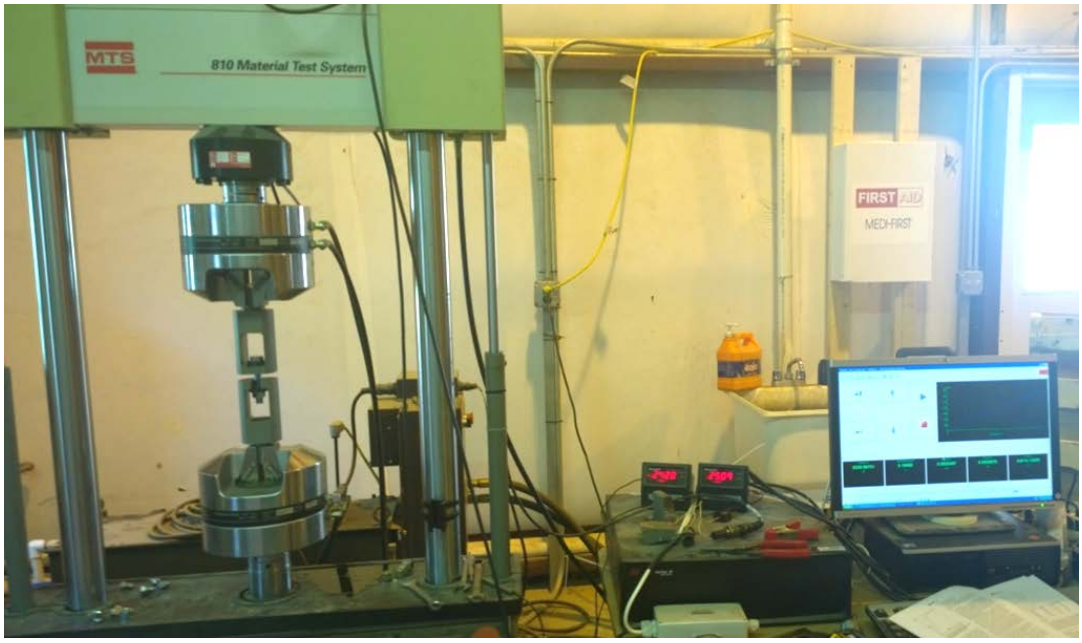

Figure 7: Test Setup for ASTM F606 Tensile Tests.

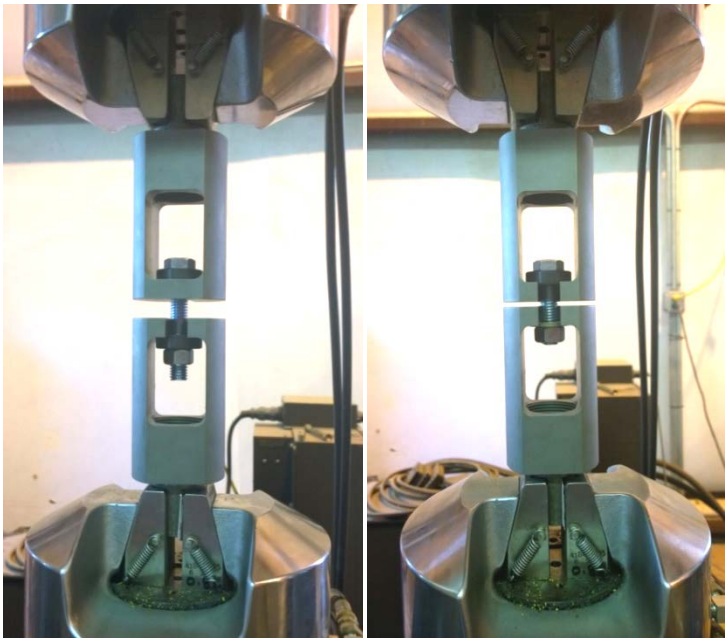

Figure 8: Typical ASTM F606 Test Setup for, from Left to Right, Double and Single Shear Bolts.

Table 1: ASTM F606 Testing Results of Double and Single Shear Bolts

F606 Testing of Bolt Ultimate Tensile Strength			
Single Shear Bolts		Double Shear Bolts	
Test Number	Ultimate Tensile Load, lbf	Test Number	Ultimate Tensile Load, lbf
1	11751	1	10096
2	12204	2	10073
3	12167	3	10350
4	12285	4	10171
5	12147	5	10181
6	12333	6	10392
Average Ultimate Load, lbf	12148	Average Ultimate Load, lbf	10210
Average Ultimate Stress, ksi	86	Average Ultimate Stress, ksi	72
Standard Deviation, ksi	1.4	Standard Deviation, ksi	0.93

4.1.2.2 Pretensioned Bolts

A pretensioned bolt is a bolt that is tensioned sufficiently during installation to where the resulting frictional force is enough to transfer the design load through the faying surfaces without placing a bearing load onto the bolt, according to the AISC 14th Edition. AISC commonly called this connection a slip critical connection. The pretensioned bolts were tensioned using slip critical connection design standards, but the joint still failed when the bolt(s) failed in shear, not when the joint slipped (failure criteria for slip critical connections). The tension force in the bolt is developed by

placing torque onto the bolt and nut. The torque induces tension in the bolt and clamping forces onto the connected members.

It is customary to use bolt tension calibrators to determine the calibrated torque to achieve the desired pretension in field construction where it is necessary to develop sufficient clamping force to assure a properly performing slip critical connection. This torque level is then applied to all bolts used in construction. The bolts tested in this thesis were tested to full shear plane failure of the fastener rather than slip failure of the joint. Therefore, the joint slipped before shear plane failure of the bolt was ultimately reached regardless of the level of pretension.

However, a bolt tension calibrator was not accessible for this project. Empirical relationships between the applied torque and bolt tension are often used to assure that the bolt has a significant tensile force when a bolt tension calibrator was not available. One such empirical relationship was developed by G. A. Maney (1946). He performed experiments to develop a relationship between the applied torque and tension on the bolt. The resulting relationship is described in Equation (4),

$$\boldsymbol{T = K * D * P} \qquad \textbf{(4)}$$

where *T* is the torque, *K* is the torque coefficient, *D* is the nominal bolt diameter, and *P* is the tension required in the bolt. Munse et al. (1955) determined a K value of 0.2 could be used to obtain an approximate value of the torque/tension on the bolt. This formula is still used in current applications where a bolt tension calibrator is not available. Many

prominent bolt retailers and manufacturers, such as Fastenal and Portland Bolt and Manufacturing Company, have accepted the use of this formula to develop torque to tension relationship tables (McKinnon 2007, Torque 2009). Therefore, it was decided to rely on Equation (4) to establish the relationship between torque and tensile force.

It was determined to induce a bolt tension force of at least 70% of the minimum specified ultimate tensile strength for the experiments presented herein. This criterion satisfied the minimum bolt pretension requirements specified in AISC 14th Edition. The minimum specified ultimate tensile strength is 60 ksi for A307 bolts. The minimum required torque for the pretensioned bolts was 69 ft-lbf. However, the actual ultimate tensile strength of the specific bolts used in these experiments as shown in Table 1 was 72 ksi and 86 ksi for double and single shear bolts, respectively. The actual ultimate tensile strength was considerably larger than the minimum specified ultimate tensile strength as is often the case. Therefore, the amount of torque applied for the pretensioned bolt tests was increased to 75 ft-lbf to ensure that each joint had an adequate amount of clamping force based on AISC criteria. This level of torque corresponded to a tensile stress of 46 ksi or an internal force of approximately 6500 lbf according to Equation (4) and using a torque coefficient of 0.2.

4.1.2.3 Non-Pretensioned Bolts

Non-pretensioned bolts (or snug-tightened bolts) are defined as bolts that do not depend on clamping forces to transfer loads from member to member. The forces are transferred through the shear strength of the structural fasteners. All of the strength in

these joints is based on the bolt shear strength. Failure of the structure/joint occurs when the bolts are sheared (Bendigo et al. 1963).

The non-pretensioned bolts tested were hand-tightened. This was to ensure that there was no significant frictional component acting on the specimen, and that all the force was transferred through the shear plane(s) of the fastener.

4.1.2.4 Hot-Driven Rivets

A hot-driven rivet is a permanent mechanical fastener that resists shear and tension forces through a solid steel shaft. The design of riveted joints is based on the shear resistance of the un-driven rivet diameter and strength. The latest ASTM standard regarding rivets was A502 and was last issued in 2003 (ASTM 2003).

The hot-driving process does two things to the rivet that are not considered when determining the design strength of a riveted joint: the rivet develops tension caused by the axial shrinkage of the rivet as it cooled and the rivet almost fills the hole, as shown for the cast iron rivet in Figure 9. Both of these effects of hot-driving rivets help the riveted joint to resist slip (Higgins 1955).

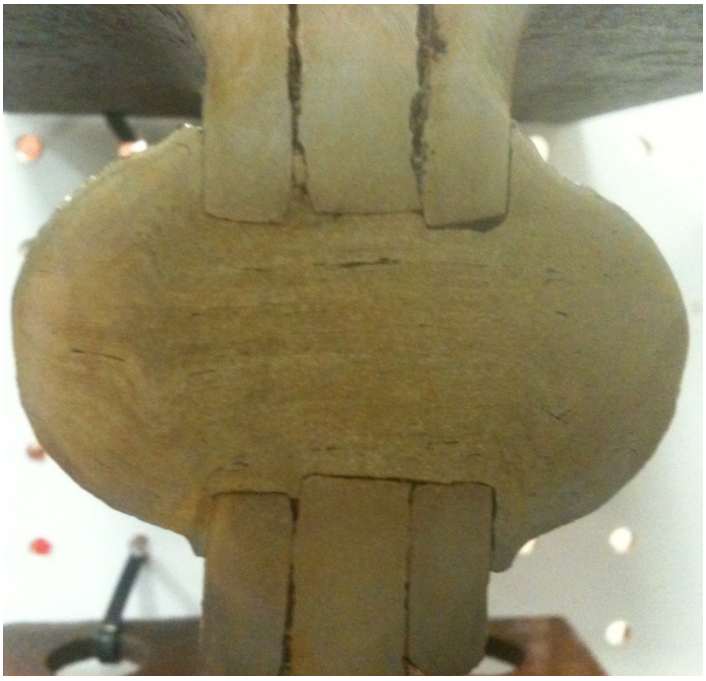

Figure 9: Typical Hot-Driven Cast Iron Riveted Connection Cross-Section.

The rivets tested in this thesis were A502 Grade 2 and were hot driven like the typical rivets used in structural joints. The rivets were placed in the plate test specimens by Ballard Forge in Seattle, WA. Rivets were heated and driven by a hydraulic riveter at a range of 1500 to 1950 degrees Fahrenheit. Dimensions of the rivet conform to ANSI Standard B18.1.2. Figure 10 is an example of how the rivets were placed and prepared to be driven. Note that the rivets placed for this thesis were not driven using pneumatic hammers like rivets driven in the field. The hydraulic riveter was used in most shop fabrications and was considered to be equivalent to the field driving process. Also, the rivets for double shear specimens have a smaller cross-section than the single shear rivets, confirming Wilson and Oliver's (1930) conclusion that the longer the grip of a rivet, the less the rivet will fill the hole. The riveted specimens that were tested exhibit

this characteristic as the average diameter of double shear rivets was 0.545 inches for a stress area of 0.233 inches^2. Comparatively, the average diameter of single shear rivets was 0.560 inches for a stress area of 0.246 inches^2.

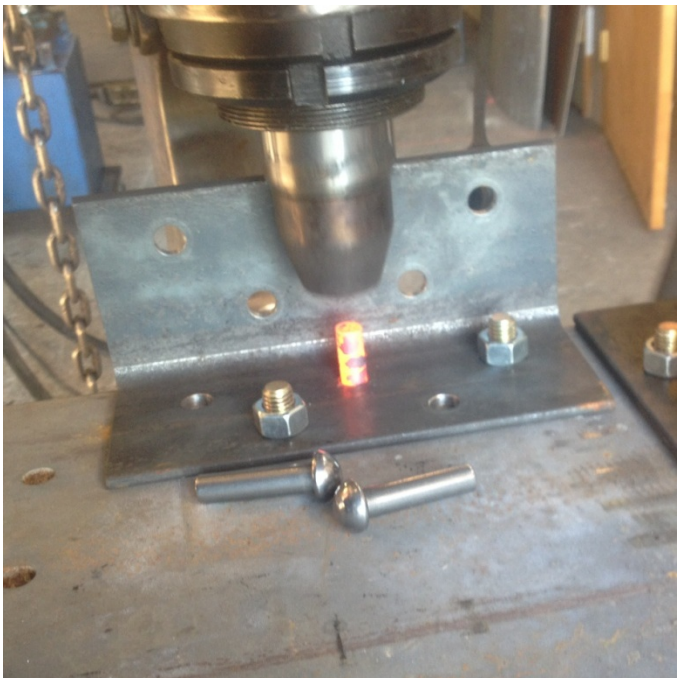

Figure 10: Typical Hot-Driven Rivet Being Driven.

4.2 Testing Machine and Instrumentation

The test specimens described in section 4.1 were tested using the 200-Kip Dynamic Loader, shown in Figure 11. This unique loader is located at USACE-ERDC in Vicksburg, MS and has been used for many test series since the 1970s. A uniaxial tension load was applied to the test specimen by using a compressible fluid to apply pressure above and below a piston. The test specimen was attached to the piston and reaction structure above the piston. The bottom portion of the specimen and piston

moved downwards when pressure below the piston was released. The upper portion of the specimen remained stationary and resisted movement resulting in an axial tension load applied to the specimen. Typical operating pressures of the compressible fluid for tests completed in this thesis ranged from 1500 psi to 3000 psi depending on the number of fasteners in the specimen.

Figure 11: 200-Kip Dynamic Loader.

The pressure was released by a rapid opening solenoid valve through a variable sized orifice. The size of the orifice controlled the flow rate of the compressed fluid exiting the loader, thereby controlling the loading rate on the specimen. However, the actual load rate was dictated by the specimen's response to the load. The orifice sizes used for this research were 4.5 inches, when the valve's main orifice was fully open, and 1/16 inch, the smallest bypass orifice available for use on loader, and the valve's main orifice was fully closed, for dynamic and quasi-static loading types, respectively.

The typical time for the applied load to fail the test specimens was 1 to 6 msec for dynamic loading and 500 to 4000+ msec for quasi-static loading. The load duration for quasi-static loadings was long enough, or the loading rate was slow enough, to negate any dynamic effects on the test specimen's response even though the quasi-static loading type load duration was not long enough to be deemed a static load per ASTM standards. Figure 12 and Figure 13 show a typical load versus time curve for dynamic and quasi-static loadings, respectively. The chosen figures were from tests with the same fastener type, shear type, and joint configuration but have a different loading type applied. The load duration for this dynamic loading type was approximately 300 times shorter than the load duration for the quasi-static loading type. This difference was large enough for dynamic effects on the specimen response to be determined.

Appendix B contains specific details on the 200-Kip Dynamic Loader, its mechanics, and existing operating procedure.

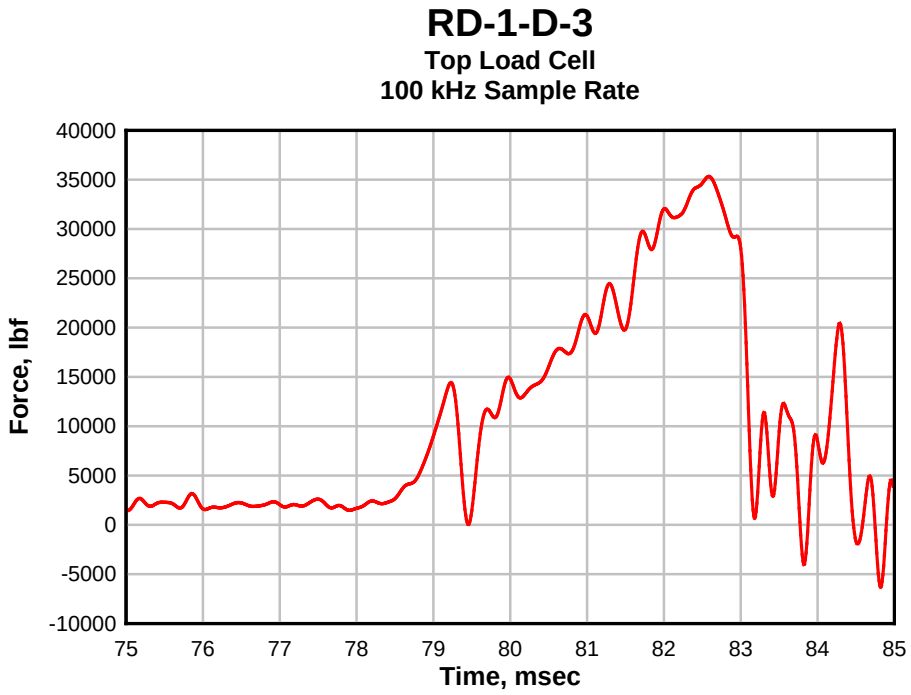

Figure 12: Typical Total Load vs. Time Curve for Dynamic Loading Type.

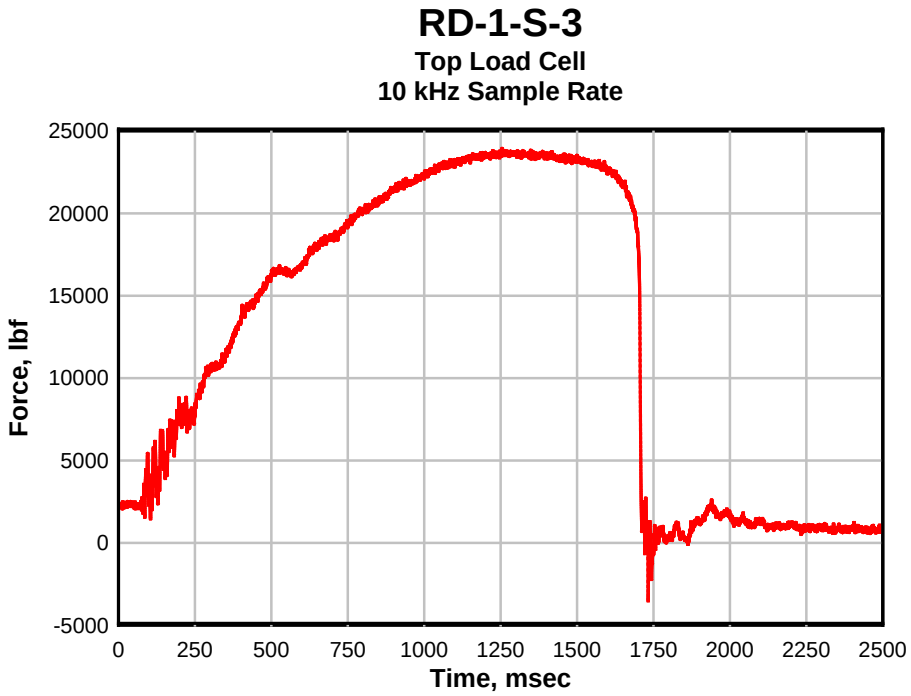

Figure 13: Typical Total Load vs. Time Curve for Quasi-Static Loading Type.

Two load cells and two accelerometers were used to measure the forces and accelerations, respectively, during testing. One of each was placed both above and below the specimen. The two load cells were specifically designed for the 200-Kip Loader and were integrated into the loader structure. The load cells were comprised of a series of strain gauges arranged around a specific diameter steel rod. The load cells' maximum working capacity was 200 kips. The load cells were calibrated in such a way that a positive load measurement corresponded to tension and negative load measurement corresponded to compression in the load cell.

The accelerometers were mounted in tandem with the load cells. Two Sigma 7270A 20K piezoresistive accelerometers were used initially, but they were damaged during testing of one specimen. Two PCB Electronics Model 3991A1120KG piezoresistive accelerometers were used in their place for the remainder of the tests. All four accelerometers had a peak sensitivity of 20,000 g's. The accelerometers were mounted to the specimen in a vertical orientation to measure the acceleration of the specimen in the direction of loading. The accelerometers were calibrated such that a positive acceleration measurement corresponded to the specimen accelerating up, and a negative acceleration measurement corresponded to the specimen accelerating down.

All the data were recorded using a Hi-Techniques Synergy P data acquisition system. The data from the instrumentation used for this test series was collected at a 100 kHz to 1000 kHz sampling rate for the dynamic loading type tests and at a 10 kHz sampling rate for the quasi-static loading type tests. Acquisition of the data was triggered remotely when the rapid-opening valve was fired.

Phantom v4.3 and v5.1 high-speed cameras were used to record footage at 8113 fps for dynamic tests and 1000 fps for quasi-static tests. The resolution of the footage is limited to 256 pixels by 256 pixels because of the frame rate needed to accurately capture footage for dynamic tests. The camera was triggered simultaneously with the data acquisition system. The high-speed camera footage was used to aid in determining the time of maximum load and failure of the specimen.

Appendix B contains specific details about the instrumentation used for this research.

4.3 Gripping Mechanism

A new gripping mechanism was designed and fabricated in order for the test specimens to be attached to the 200-Kip Dynamic Loader and load cells. The grips were fabricated in the USACE-ERDC Machine Shop in Vicksburg, MS.

The grip assembly was designed in a similar manner as the plate specimens to ensure that the only failure in the assembly would occur in the test specimens. This required that the grips be extremely large and be able to withstand loads larger than the 200-kip capacity of the loader. The grips also had to be designed so that the specimen could attach to the loader and load cells while also limiting/eliminating the slip of the test specimen in the grip.

Figure 14 shows the final gripping mechanism assembly for single- and double-shear test specimens in this test series. ‘A’ and ‘B’ were the ½-inch thick and 1-inch thick shims, respectively. The shims allowed the test specimen to be centered along the

applied uniaxial tension force. The height and width dimensions of the shims are shown in Figure 15. ‘C’ was the fastener(s) being tested as described in section 4.1.2. ‘D’ was the main “T’ grip, detailed in Figure 16. The “T” grip connected the test specimen to the loader. It was milled out of SAE 4140 high yield strength alloy steel. Threads were milled into grip to allow it to attach to the load cells on the loader. ‘E’ was the set of SAE 4140 steel plates, detailed in Figure 17. These plates connected the test specimen to the main “T” grip. The plates on the bottom grip were replaced with 1-inch-thick A36 steel plates after the first two tests. The inertial forces caused by the extra steel caused concerns about the longevity of the loader. The top plates remained at 2-inches thick as the inertial force developed by the top grip (acceleration of the grip multiplied by mass of the grip) was negligible compared to inertial force developed by the bottom grip. ‘F’ was twelve 1-inch-diameter A490 high strength bolts. The bolts transferred load to the grip from the specimen. Six bolts attached the plate to the main “T” grip, and the other six attached the plate to the test specimen. These bolts were tightened sufficiently to prevent slip in the grip using the methods detailed in section 4.1.2.2. The A490 bolts in pretensioned and non-pretensioned bolt tests were torqued to 125-150 ft-lbf., and the A490 bolts were torqued to 350-375 ft-lbf in the riveted specimen tests to ensure no slips occurred for the higher capacity riveted specimens. The torque was also increased to check if any specimen slipped inside the grips, which occurred as the initial test data had intriguing accelerometer data. However, the data from both sets of tests were similar, indicating the accelerometer response was independent of grip bolt torque increase.

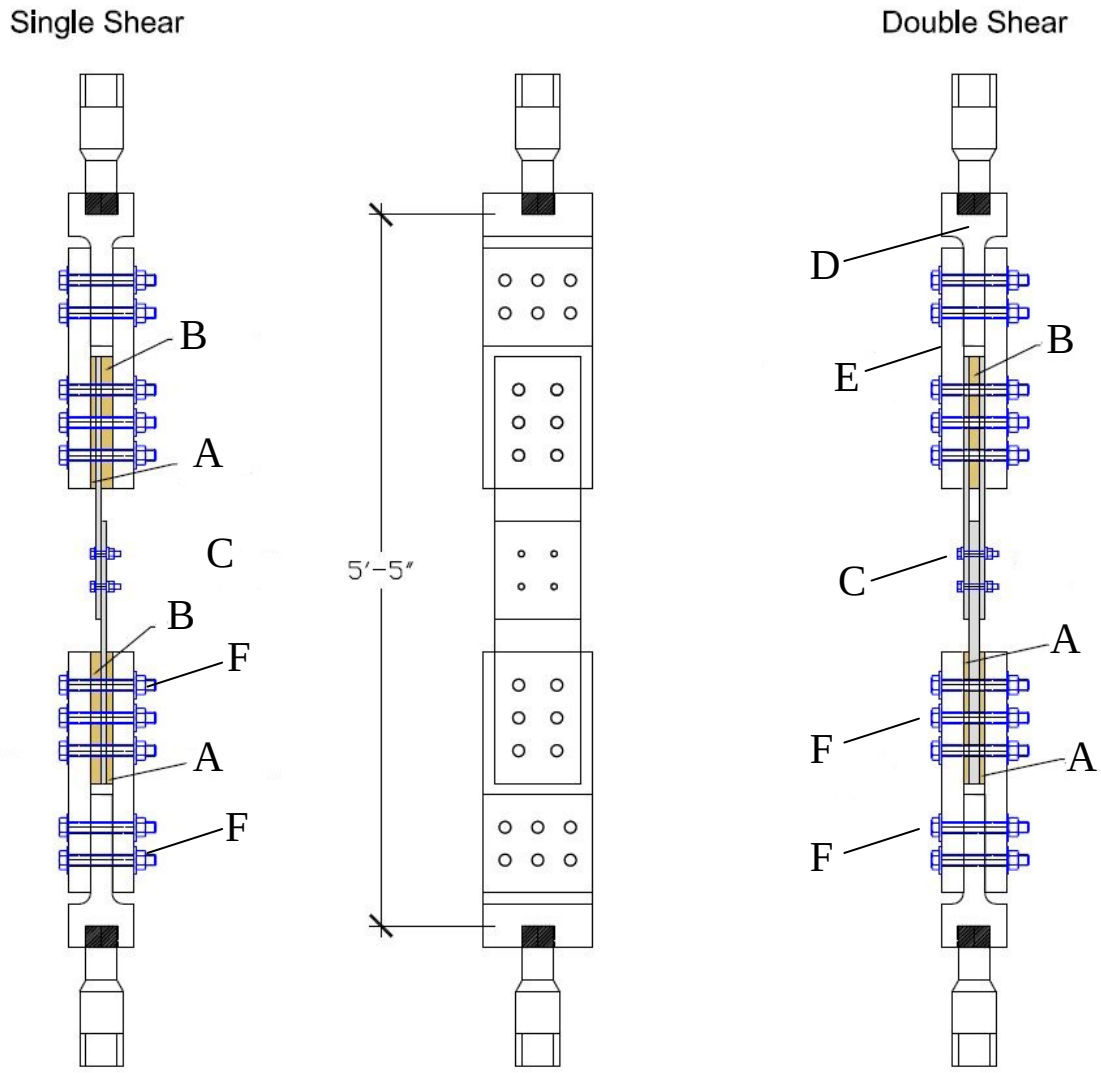

Figure 14: Gripping Mechanism Assembly.

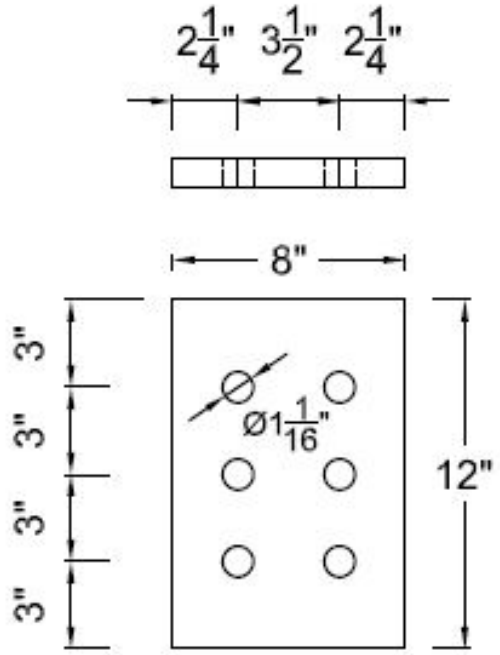

Figure 15: ½-inch and 1-inch Shims Height and Width Dimensions.

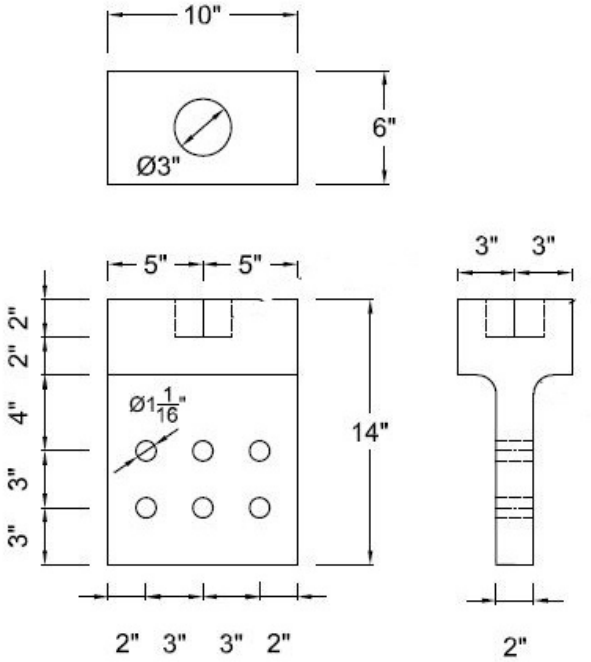

Figure 16: Main "T" Grip Dimensions.

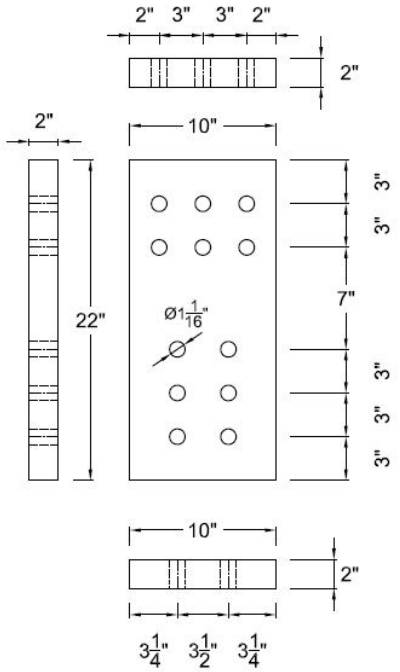

Figure 17: Gripping Plate Dimensions.

4.4 Test Matrix

The test matrix details the completed testing schedule. Each joint configuration was tested at least three times, or four for riveted specimens, for each type of structural fastener, for each loading type, and for each shear type. Therefore, at least twelve tests were completed for each joint configuration, shear type, and loading type combination. Some test combinations had more tests added than others due to malfunctions during testing of previous tests of that combination.

The labeling system for test names in the test series was in the following order: *Structural Fastener Type/Shear Type-Joint Configuration-Loading Type-Test Number.*

The list of initials used in the test name is shown in Table 2. For example, the non-pretensioned, double shear, two fasteners-horizontal, dynamic loading, test number 2 had the test name ND-2-D-2. The riveted, single shear, single fastener, dynamic loading, test number 4 had the test name: RS-1-D-4. Table 3 is the complete test matrix that details the number and type of tests conducted and the dates they were completed. A total of 224 tests were conducted.

Table 2: List of Initials Used in Test Name.

Test Characteristic	Label	Description
Structural Fastener Type	N	Non-Pretensioned Bolts
	R	Rivets
	S	Pretensioned Bolts
Shear Type	D	Double Shear
	S	Single Shear
Joint Configuration	1	Single Fastener
	2	Two Fasteners—Horizontal
	3	Two Fasteners—Vertical
	4	Four Fasteners—Square
	5	Four Fasteners—Staggered
Loading Type	D	Dynamic
	S	Quasi-Static

Table 3: Experimental Test Matrix

Test Name	Fastener Type	Shear Type	Joint Configuration	Loading Type	Test Number	Test Date
SD-1-D-1T	Pretensioned	Double	1	Dynamic	1	6/26/2013
SD-1-D-2T	Pretensioned	Double	1	Dynamic	2	6/26/2013
SD-1-D-3T	Pretensioned	Double	1	Dynamic	3	6/26/2013
SD-1-D-4T	Pretensioned	Double	1	Dynamic	4	7/8/2013
SD-1-D-5T	Pretensioned	Double	1	Dynamic	5	7/9/2013
SD-1-D-6T	Pretensioned	Double	1	Dynamic	6	7/9/2013
ND-1-D-1	Non-Pretensioned	Double	1	Dynamic	1	7/9/2013
ND-1-D-2	Non-Pretensioned	Double	1	Dynamic	2	7/9/2013
ND-1-D-3	Non-Pretensioned	Double	1	Dynamic	3	7/9/2013
RD-1-D-1	Riveted	Double	1	Dynamic	1	12/30/2013
RD-1-D-2	Riveted	Double	1	Dynamic	2	12/30/2013
RD-1-D-3	Riveted	Double	1	Dynamic	3	12/30/2013
RD-1-D-4	Riveted	Double	1	Dynamic	4	12/30/2013
SD-1-S-1	Pretensioned	Double	1	Quasi-Static	1	7/16/2013
SD-1-S-2	Pretensioned	Double	1	Quasi-Static	2	7/16/2013
SD-1-S-3	Pretensioned	Double	1	Quasi-Static	3	12/16/2013
SD-1-S-4	Pretensioned	Double	1	Quasi-Static	4	12/19/2013
SD-1-S-5	Pretensioned	Double	1	Quasi-Static	5	12/19/2013
ND-1-S-1	Non-Pretensioned	Double	1	Quasi-Static	1	11/25/2013
ND-1-S-2	Non-Pretensioned	Double	1	Quasi-Static	2	11/25/2013
ND-1-S-3	Non-Pretensioned	Double	1	Quasi-Static	3	11/26/2013
ND-1-S-4	Non-Pretensioned	Double	1	Quasi-Static	4	12/16/2013
RD-1-S-1	Riveted	Double	1	Quasi-Static	1	1/2/2014
RD-1-S-2	Riveted	Double	1	Quasi-Static	2	1/2/2014
RD-1-S-3	Riveted	Double	1	Quasi-Static	3	1/2/2014
RD-1-S-4	Riveted	Double	1	Quasi-Static	4	1/2/2014
SS-1-D-1	Pretensioned	Single	1	Dynamic	1	7/16/2013
SS-1-D-2	Pretensioned	Single	1	Dynamic	2	7/17/2013
SS-1-D-3	Pretensioned	Single	1	Dynamic	3	7/18/2013
SS-1-D-4	Pretensioned	Single	1	Dynamic	4	7/18/2013
SS-1-D-5	Pretensioned	Single	1	Dynamic	5	12/23/2013
NS-1-D-1	Non-Pretensioned	Single	1	Dynamic	1	7/18/2013
NS-1-D-2	Non-Pretensioned	Single	1	Dynamic	2	7/18/2013
NS-1-D-3	Non-Pretensioned	Single	1	Dynamic	3	7/19/2013
NS-1-D-4	Non-Pretensioned	Single	1	Dynamic	4	7/19/2013
NS-1-D-5	Non-Pretensioned	Single	1	Dynamic	5	7/19/2013
NS-1-D-6	Non-Pretensioned	Single	1	Dynamic	6	7/19/2013
NS-1-D-7	Non-Pretensioned	Single	1	Dynamic	7	12/23/2013
RS-1-D-1	Riveted	Single	1	Dynamic	1	12/23/2013
RS-1-D-2	Riveted	Single	1	Dynamic	2	12/24/2013
RS-1-D-3	Riveted	Single	1	Dynamic	3	12/24/2013
RS-1-D-4	Riveted	Single	1	Dynamic	4	12/24/2013

Table 3, continued.

Test Name	Fastener Type	Shear Type	Joint Configuration	Loading Type	Test Number	Test Date
SS-1-S-1	Pretensioned	Single	1	Quasi-Static	1	12/19/2013
SS-1-S-2	Pretensioned	Single	1	Quasi-Static	2	12/20/2013
SS-1-S-3	Pretensioned	Single	1	Quasi-Static	3	12/20/2013
NS-1-S-1	Non-Pretensioned	Single	1	Quasi-Static	1	12/20/2013
NS-1-S-2	Non-Pretensioned	Single	1	Quasi-Static	2	12/20/2013
NS-1-S-3	Non-Pretensioned	Single	1	Quasi-Static	3	12/23/2013
RS-1-S-1	Riveted	Single	1	Quasi-Static	1	12/30/2013
RS-1-S-2	Riveted	Single	1	Quasi-Static	2	12/31/2013
RS-1-S-3	Riveted	Single	1	Quasi-Static	3	12/31/2013
RS-1-S-4	Riveted	Single	1	Quasi-Static	4	12/31/2013
SD-2-D-1	Pretensioned	Double	2	Dynamic	1	8/1/2013
SD-2-D-2	Pretensioned	Double	2	Dynamic	2	8/1/2013
SD-2-D-3	Pretensioned	Double	2	Dynamic	3	8/1/2013
SD-2-D-4	Pretensioned	Double	2	Dynamic	4	8/6/2013
ND-2-D-1	Non-Pretensioned	Double	2	Dynamic	1	8/6/2013
ND-2-D-2	Non-Pretensioned	Double	2	Dynamic	2	8/6/2013
ND-2-D-3	Non-Pretensioned	Double	2	Dynamic	3	8/6/2013
RD-2-D-1	Riveted	Double	2	Dynamic	1	1/9/2014
RD-2-D-2	Riveted	Double	2	Dynamic	2	1/9/2014
RD-2-D-3	Riveted	Double	2	Dynamic	3	1/9/2014
RD-2-D-4	Riveted	Double	2	Dynamic	4	1/9/2014
SD-2-S-1	Pretensioned	Double	2	Quasi-Static	1	8/6/2013
SD-2-S-2	Pretensioned	Double	2	Quasi-Static	2	8/7/2013
SD-2-S-3	Pretensioned	Double	2	Quasi-Static	3	8/7/2013
ND-2-S-1	Non-Pretensioned	Double	2	Quasi-Static	1	8/7/2013
ND-2-S-2	Non-Pretensioned	Double	2	Quasi-Static	2	8/7/2013
ND-2-S-3	Non-Pretensioned	Double	2	Quasi-Static	3	8/7/2013
RD-2-S-1	Riveted	Double	2	Quasi-Static	1	1/6/2014
RD-2-S-2	Riveted	Double	2	Quasi-Static	2	1/6/2014
RD-2-S-3	Riveted	Double	2	Quasi-Static	3	1/7/2014
RD-2-S-4	Riveted	Double	2	Quasi-Static	4	1/7/2014
SS-2-D-1	Pretensioned	Single	2	Dynamic	1	8/8/2013
SS-2-D-2	Pretensioned	Single	2	Dynamic	2	8/8/2013
SS-2-D-3	Pretensioned	Single	2	Dynamic	3	8/8/2013
NS-2-D-1	Non-Pretensioned	Single	2	Dynamic	1	8/8/2013
NS-2-D-2	Non-Pretensioned	Single	2	Dynamic	2	8/8/2013
NS-2-D-3	Non-Pretensioned	Single	2	Dynamic	3	8/8/2013
RS-2-D-1	Riveted	Single	2	Dynamic	1	1/8/2014
RS-2-D-2	Riveted	Single	2	Dynamic	2	1/8/2014
RS-2-D-3	Riveted	Single	2	Dynamic	3	1/8/2014
RS-2-D-4	Riveted	Single	2	Dynamic	4	1/9/2014
RS-2-D-5	Riveted	Single	2	Dynamic	5	1/9/2014
RS-2-D-6	Riveted	Single	2	Dynamic	6	1/9/2014

Table 3, continued.

Test Name	Fastener Type	Shear Type	Joint Configuration	Loading Type	Test Number	Test Date
SS-2-S-1	Pretensioned	Single	2	Quasi-Static	1	8/7/2013
SS-2-S-2	Pretensioned	Single	2	Quasi-Static	2	8/7/2013
SS-2-S-3	Pretensioned	Single	2	Quasi-Static	3	8/7/2013
NS-2-S-1	Non-Pretensioned	Single	2	Quasi-Static	1	8/7/2013
NS-2-S-2	Non-Pretensioned	Single	2	Quasi-Static	2	8/7/2013
NS-2-S-3	Non-Pretensioned	Single	2	Quasi-Static	3	8/8/2013
RS-2-S-1	Riveted	Single	2	Quasi-Static	1	1/7/2014
RS-2-S-2	Riveted	Single	2	Quasi-Static	2	1/8/2014
RS-2-S-3	Riveted	Single	2	Quasi-Static	3	1/8/2014
RS-2-S-4	Riveted	Single	2	Quasi-Static	4	1/8/2014
SD-3-D-1	Pretensioned	Double	3	Dynamic	1	7/24/2013
SD-3-D-2	Pretensioned	Double	3	Dynamic	2	7/24/2013
SD-3-D-3	Pretensioned	Double	3	Dynamic	3	7/24/2013
ND-3-D-1	Non-Pretensioned	Double	3	Dynamic	1	7/24/2013
ND-3-D-2	Non-Pretensioned	Double	3	Dynamic	2	7/24/2013
ND-3-D-3	Non-Pretensioned	Double	3	Dynamic	3	7/24/2013
RD-3-D-1	Riveted	Double	3	Dynamic	1	1/17/2014
RD-3-D-2	Riveted	Double	3	Dynamic	2	1/17/2014
RD-3-D-3	Riveted	Double	3	Dynamic	3	1/17/2014
RD-3-D-4	Riveted	Double	3	Dynamic	4	1/28/2014
SD-3-S-1	Pretensioned	Double	3	Quasi-Static	1	7/25/2013
SD-3-S-2	Pretensioned	Double	3	Quasi-Static	2	7/25/2013
SD-3-S-3	Pretensioned	Double	3	Quasi-Static	3	7/25/2013
ND-3-S-1	Non-Pretensioned	Double	3	Quasi-Static	1	7/25/2013
ND-3-S-2	Non-Pretensioned	Double	3	Quasi-Static	2	7/25/2013
ND-3-S-3	Non-Pretensioned	Double	3	Quasi-Static	3	7/25/2013
RD-3-S-1	Riveted	Double	3	Quasi-Static	1	3/28/2014
RD-3-S-2	Riveted	Double	3	Quasi-Static	2	3/28/2014
RD-3-S-3	Riveted	Double	3	Quasi-Static	3	3/28/2014
RD-3-S-4	Riveted	Double	3	Quasi-Static	4	3/30/2014
SS-3-D-1	Pretensioned	Single	3	Dynamic	1	7/26/2013
SS-3-D-2	Pretensioned	Single	3	Dynamic	2	7/30/2013
SS-3-D-3	Pretensioned	Single	3	Dynamic	3	7/31/2013
NS-3-D-1	Non-Pretensioned	Single	3	Dynamic	1	7/31/2013
NS-3-D-2	Non-Pretensioned	Single	3	Dynamic	2	8/1/2013
NS-3-D-3	Non-Pretensioned	Single	3	Dynamic	3	8/1/2013
RS-3-D-1	Riveted	Single	3	Dynamic	1	1/16/2014
RS-3-D-2	Riveted	Single	3	Dynamic	2	1/16/2014
RS-3-D-3	Riveted	Single	3	Dynamic	3	1/17/2014
RS-3-D-4	Riveted	Single	3	Dynamic	4	1/17/2014
SS-3-S-1	Pretensioned	Single	3	Quasi-Static	1	7/25/2013
SS-3-S-2	Pretensioned	Single	3	Quasi-Static	2	7/26/2013
SS-3-S-3	Pretensioned	Single	3	Quasi-Static	3	7/26/2013

Table 3, continued.

Test Name	Fastener Type	Shear Type	Joint Configuration	Loading Type	Test Number	Test Date
NS-3-S-1	Non-Pretensioned	Single	3	Quasi-Static	1	7/26/2013
NS-3-S-2	Non-Pretensioned	Single	3	Quasi-Static	2	7/26/2013
NS-3-S-3	Non-Pretensioned	Single	3	Quasi-Static	3	7/26/2013
RS-3-S-1	Riveted	Single	3	Quasi-Static	1	3/30/2014
RS-3-S-2	Riveted	Single	3	Quasi-Static	2	4/16/2014
RS-3-S-3	Riveted	Single	3	Quasi-Static	3	4/16/2014
RS-3-S-4	Riveted	Single	3	Quasi-Static	4	4/16/2014
SD-4-D-1	Pretensioned	Double	4	Dynamic	1	8/8/2013
SD-4-D-2	Pretensioned	Double	4	Dynamic	2	8/9/2013
SD-4-D-3	Pretensioned	Double	4	Dynamic	3	8/9/2013
SD-4-D-4	Pretensioned	Double	4	Dynamic	4	8/12/2013
ND-4-D-1	Non-Pretensioned	Double	4	Dynamic	1	8/9/2013
ND-4-D-2	Non-Pretensioned	Double	4	Dynamic	2	8/9/2013
ND-4-D-3	Non-Pretensioned	Double	4	Dynamic	3	8/9/2013
RD-4-D-1	Riveted	Double	4	Dynamic	1	4/18/2014
RD-4-D-2	Riveted	Double	4	Dynamic	2	4/18/2014
RD-4-D-3	Riveted	Double	4	Dynamic	3	4/18/2014
RD-4-D-4	Riveted	Double	4	Dynamic	4	4/18/2014
RD-4-D-5	Riveted	Double	4	Dynamic	5	4/18/2014
RD-4-D-6	Riveted	Double	4	Dynamic	6	4/18/2014
SD-4-S-1	Pretensioned	Double	4	Quasi-Static	1	8/9/2013
SD-4-S-2	Pretensioned	Double	4	Quasi-Static	2	8/9/2013
SD-4-S-3	Pretensioned	Double	4	Quasi-Static	3	8/9/2013
ND-4-S-1	Non-Pretensioned	Double	4	Quasi-Static	1	8/12/2013
ND-4-S-2	Non-Pretensioned	Double	4	Quasi-Static	2	8/12/2013
ND-4-S-3	Non-Pretensioned	Double	4	Quasi-Static	3	8/12/2013
RD-4-S-1	Riveted	Double	4	Quasi-Static	1	3/25/2014
RD-4-S-2	Riveted	Double	4	Quasi-Static	2	3/26/2014
RD-4-S-3	Riveted	Double	4	Quasi-Static	3	3/26/2014
RD-4-S-4	Riveted	Double	4	Quasi-Static	4	3/26/2014
SS-4-D-1	Pretensioned	Single	4	Dynamic	1	8/12/2013
SS-4-D-2	Pretensioned	Single	4	Dynamic	2	8/12/2013
SS-4-D-3	Pretensioned	Single	4	Dynamic	3	8/12/2013
NS-4-D-1	Non-Pretensioned	Single	4	Dynamic	1	8/13/2013
NS-4-D-2	Non-Pretensioned	Single	4	Dynamic	2	8/13/2013
NS-4-D-3	Non-Pretensioned	Single	4	Dynamic	3	8/13/2013
RS-4-D-1	Riveted	Single	4	Dynamic	1	4/16/2014
RS-4-D-2	Riveted	Single	4	Dynamic	2	4/16/2014
RS-4-D-3	Riveted	Single	4	Dynamic	3	4/16/2014
RS-4-D-4	Riveted	Single	4	Dynamic	4	4/16/2014
RS-4-D-5	Riveted	Single	4	Dynamic	5	4/16/2014
RS-4-D-6	Riveted	Single	4	Dynamic	6	4/18/2014
SS-4-S-1	Pretensioned	Single	4	Quasi-Static	1	8/13/2013

Table 3, continued.

Test Name	Fastener Type	Shear Type	Joint Configuration	Loading Type	Test Number	Test Date
SS-4-S-2	Pretensioned	Single	4	Quasi-Static	2	8/13/2013
SS-4-S-3	Pretensioned	Single	4	Quasi-Static	3	8/13/2013
NS-4-S-1	Non-Pretensioned	Single	4	Quasi-Static	1	8/13/2013
NS-4-S-2	Non-Pretensioned	Single	4	Quasi-Static	2	8/13/2013
NS-4-S-3	Non-Pretensioned	Single	4	Quasi-Static	3	8/13/2013
RS-4-S-1	Riveted	Single	4	Quasi-Static	1	3/27/2014
RS-4-S-2	Riveted	Single	4	Quasi-Static	2	3/28/2014
RS-4-S-3	Riveted	Single	4	Quasi-Static	3	3/28/2014
RS-4-S-4	Riveted	Single	4	Quasi-Static	4	3/28/2014
SD-5-D-1T	Pretensioned	Double	5	Dynamic	1	10/4/2013
SD-5-D-2T	Pretensioned	Double	5	Dynamic	2	10/7/2013
SD-5-D-1	Pretensioned	Double	5	Dynamic	3	10/23/2013
SD-5-D-2	Pretensioned	Double	5	Dynamic	4	10/23/2013
SD-5-D-3	Pretensioned	Double	5	Dynamic	5	10/23/2013
ND-5-D-1	Non-Pretensioned	Double	5	Dynamic	1	10/24/2013
ND-5-D-2	Non-Pretensioned	Double	5	Dynamic	2	10/24/2013
ND-5-D-3	Non-Pretensioned	Double	5	Dynamic	3	10/25/2013
RD-5-D-1	Riveted	Double	5	Dynamic	1	3/19/2014
RD-5-D-2	Riveted	Double	5	Dynamic	2	3/19/2014
RD-5-D-3	Riveted	Double	5	Dynamic	3	3/19/2014
RD-5-D-4	Riveted	Double	5	Dynamic	4	3/19/2014
SD-5-S-1T	Pretensioned	Double	3	Quasi-Static	1	10/3/2013
SD-5-S-2T	Pretensioned	Double	4	Quasi-Static	2	10/4/2013
SD-5-S-1	Pretensioned	Double	5	Quasi-Static	3	10/25/2013
SD-5-S-2	Pretensioned	Double	5	Quasi-Static	4	10/29/2013
SD-5-S-3	Pretensioned	Double	5	Quasi-Static	5	10/29/2013
ND-5-S-1	Non-Pretensioned	Double	5	Quasi-Static	1	10/29/2013
ND-5-S-2	Non-Pretensioned	Double	5	Quasi-Static	2	11/5/2013
ND-5-S-3	Non-Pretensioned	Double	5	Quasi-Static	3	11/5/2013
RD-5-S-1	Riveted	Double	5	Quasi-Static	1	3/21/2014
RD-5-S-2	Riveted	Double	5	Quasi-Static	2	3/21/2014
RD-5-S-3	Riveted	Double	5	Quasi-Static	3	3/25/2014
RD-5-S-4	Riveted	Double	5	Quasi-Static	4	3/25/2014
SS-5-D-1	Pretensioned	Single	5	Dynamic	1	11/15/2013
SS-5-D-2	Pretensioned	Single	5	Dynamic	2	11/15/2013
SS-5-D-3	Pretensioned	Single	5	Dynamic	3	11/15/2013
NS-5-D-1	Non-Pretensioned	Single	5	Dynamic	1	11/21/2013
NS-5-D-2	Non-Pretensioned	Single	5	Dynamic	2	11/21/2013
NS-5-D-3	Non-Pretensioned	Single	5	Dynamic	3	11/21/2013
RS-5-D-1	Riveted	Single	5	Dynamic	1	3/18/2014
RS-5-D-2	Riveted	Single	5	Dynamic	2	3/18/2014
RS-5-D-3	Riveted	Single	5	Dynamic	3	3/18/2014
RS-5-D-4	Riveted	Single	5	Dynamic	4	3/18/2014

Table 3, continued.

Test Name	Fastener Type	Shear Type	Joint Configuration	Loading Type	Test Number	Test Date
SS-5-S-1	Pretensioned	Single	5	Quasi-Static	1	11/8/2013
SS-5-S-2	Pretensioned	Single	5	Quasi-Static	2	11/8/2013
SS-5-S-3	Pretensioned	Single	5	Quasi-Static	3	11/13/2013
NS-5-S-1	Non-Pretensioned	Single	5	Quasi-Static	1	11/14/2013
NS-5-S-2	Non-Pretensioned	Single	5	Quasi-Static	2	11/14/2013
NS-5-S-3	Non-Pretensioned	Single	5	Quasi-Static	3	11/14/2013
RS-5-S-1	Riveted	Single	5	Quasi-Static	1	3/20/2014
RS-5-S-2	Riveted	Single	5	Quasi-Static	2	3/20/2014
RS-5-S-3	Riveted	Single	5	Quasi-Static	3	3/20/2014
RS-5-S-4	Riveted	Single	5	Quasi-Static	4	3/20/2014

5. RESULTS

In this section, the results of the experiments using the approach described in Section 4 are given. Included is the table of results for each joint configuration and photographs of typical bolted and riveted test specimens for each joint configuration in place ready for testing.

The upper load cell and accelerometer data for the dynamic tests was processed in the method outlined in Appendix B to determine the total load applied to the specimen during testing. This method was developed and published in Flathau (1971) specifically for the 200-Kip Dynamic Loader. Other data processing outlined in Appendix B, such as filtering, was typical of the techniques used by USACE-ERDC-GSL-StEB.

All data values shown in "Quasi-Static Load" or "Dynamic Load" columns of Tables 4 through 13 were values from the upper load cell and accelerometer. Data values in the "Ratio of Shear…" column were the average ratio of ultimate shear stress to ultimate static tensile strength seen by a single shear plane on the fastener (values were normalized by the number of shear planes in the test). Values in the "Ratio…" column that are footnoted were excluded from analysis.

Data plots consisting of the load cell data, inertial load, total load, and velocity of the specimen are shown in Appendix C.

5.1 Joint Configuration 1 Results

Results from fasteners tested in Joint Configuration 1 are presented in this subsection. The results from bolted specimens are presented in Table 4, and results from riveted specimens are presented in Table 5. Figure 18 and Figure 19 show a typical bolted test specimen in place for testing in double and single shear, respectively. Figure 20 and Figure 21 show a typical riveted test specimen in place for testing double and single shear, respectively.

Table 4: Test Results of Joint Configuration 1, Bolted Specimens.

Test Name	Ultimate Tensile Strength, ksi	Stress Area, $in.^2$	Quasi-Static Load, lbf	Dynamic Load, lbf	Shear Load Per Plane, lbf	Shear Stress per plane, psi	Ratio of Ult. Shear Stress to U.T.S., ksi/ksi
SD-1-D-1T	72	0.1419	-	-	-	-	-[1]
SD-1-D-2T	72	0.1419	N/A	20361	10180	71744	0.996
SD-1-D-3T	72	0.1419	-	-	-	-	-[2]
SD-1-D-4T	72	0.1419	N/A	20160	10080	71038	0.987
SD-1-D-5T	72	0.1419	N/A	26641	13321	93874	1.304
SD-1-D-6T	72	0.1419	N/A	27767	13883	97841	1.359
ND-1-D-1	72	0.1419	N/A	25176	12588	88711	1.232
ND-1-D-2	72	0.1419	N/A	15429	7714	54366	0.755
ND-1-D-3	72	0.1419	N/A	20103	10051	70835	0.984
SD-1-S-1	72	0.1419	-	-	-	-	-[1]
SD-1-S-2	72	0.1419	-	-	-	-	-[1]
SD-1-S-3	72	0.1419	10731	N/A	5365	37812	0.525
SD-1-S-4	72	0.1419	10357	N/A	5179	36496	0.507
SD-1-S-5	72	0.1419	10426	N/A	5213	36739	0.510
ND-1-S-1	72	0.1419	9336	N/A	4668	32895	0.457
ND-1-S-2	72	0.1419	11403	N/A	5701	40180	0.558
ND-1-S-3	72	0.1419	11225	N/A	5613	39554	0.549
ND-1-S-4	72	0.1419	11144	N/A	5572	39269	0.545
SS-1-D-1	86	0.1419	-	-	-	-	-[3]
SS-1-D-2	86	0.1419	-	-	-	-	-[3]
SS-1-D-3	86	0.1419	N/A	10030	10030	70682	0.822
SS-1-D-4	86	0.1419	N/A	13458	13458	94839	1.103
SS-1-D-5	86	0.1419	N/A	13966	13966	98422	1.144
NS-1-D-1	86	0.1419	-	-	-	-	-[3]
NS-1-D-2	86	0.1419	N/A	12522	12522	88246	1.026
NS-1-D-3	86	0.1419	-	-	-	-	-[3]
NS-1-D-4	86	0.1419	-	-	-	-	-[3]
NS-1-D-5	86	0.1419	N/A	14466	14466	101947	1.185
NS-1-D-6	86	0.1419	N/A	12815	12815	90309	1.050
NS-1-D-7	86	0.1419	N/A	7052	7052	49697	0.578
SS-1-S-1	86	0.1419	8104	N/A	8104	57109	0.664
SS-1-S-2	86	0.1419	7595	N/A	7595	53526	0.622
SS-1-S-3	86	0.1419	7427	N/A	7427	52339	0.609
NS-1-S-1	86	0.1419	6720	N/A	6720	47357	0.551
NS-1-S-2	86	0.1419	6520	N/A	6520	45948	0.534
NS-1-S-3	86	0.1419	6758	N/A	6758	47625	0.554

[1] Sweep length of Synergy was not long enough.
[2] No accelerometer data
[3] Unusable data due to considerable amount of AC on top load cell data record

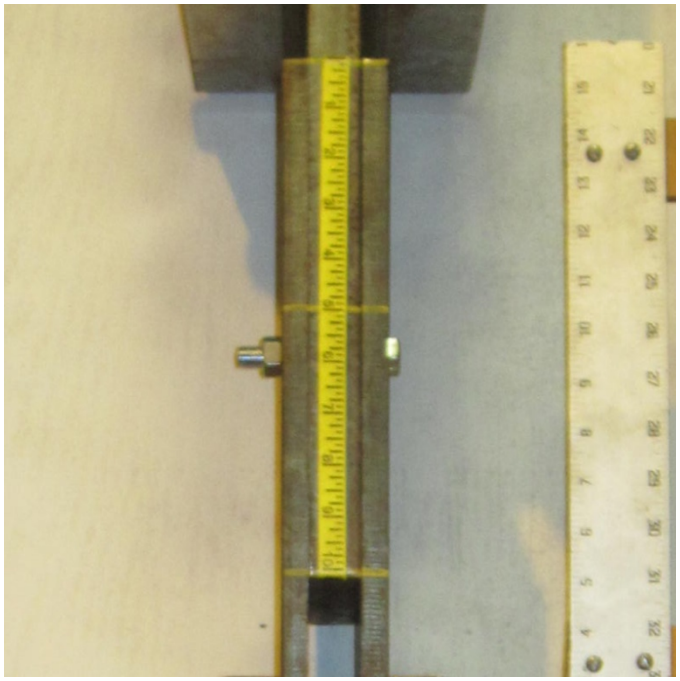

Figure 18: Typical Joint Configuration 1, Bolted, Double Shear Specimen.

Figure 19: Typical Joint Configuration 1, Bolted, Single Shear Specimen.

Table 5: Test Results of Joint Configuration 1, Riveted Specimens.

Test Name	Ultimate Tensile Strength, ksi	Stress Area, $in.^2$	Quasi-Static Load, lbf	Dynamic Load, lbf	Shear Load Per Plane, lbs	Shear Stress per plane, psi	Ratio of Ult. Shear Stress to U.T.S., ksi/ksi
RD-1-D-1	92	0.2333	N/A	30997	15498	66436	0.722
RD-1-D-2	92	0.2333	N/A	44711	22356	95830	1.042[4]
RD-1-D-3	92	0.2333	N/A	35320	17660	75702	0.823
RD-1-D-4	92	0.2333	N/A	33290	16645	71352	0.776
RD-1-S-1	92	0.2333	23973	N/A	11987	51382	0.559
RD-1-S-2	92	0.2333	20460	N/A	10230	43852	0.477
RD-1-S-3	92	0.2333	23868	N/A	11934	51156	0.556
RD-1-S-4	92	0.2333	21347	N/A	10674	45754	0.497
RS-1-D-1	92	0.2463	N/A	16149	16149	69224	0.713
RS-1-D-2	92	0.2463	N/A	15577	15577	66771	0.687
RS-1-D-3	92	0.2463	N/A	13717	13717	58799	0.605
RS-1-D-4	92	0.2463	N/A	16120	16120	69100	0.711
RS-1-S-1	92	0.2463	16745	N/A	16745	71778	0.739
RS-1-S-2	92	0.2463	15885	N/A	15885	68094	0.701
RS-1-S-3	92	0.2463	15774	N/A	15774	67618	0.696
RS-1-S-4	92	0.2463	12597	N/A	12597	53998	0.556

Figure 20: Typical Joint Configuration 1, Riveted, Double Shear Specimen.

[4] Malfunction of top accelerometer and maximum load value is omitted from analysis.

Figure 21: Typical Joint Configuration 1, Riveted, Single Shear Specimen.

5.2 Joint Configuration 2 Results

Results from fasteners tested in Joint Configuration 2 are presented in this subsection. The results from bolted specimens are presented in Table 6, and results from riveted specimens are presented in Table 7. Figure 22 and Figure 23 show a typical bolted test specimen in place for testing in double and single shear, respectively. Figure 24 and Figure 25 show a typical riveted test specimen in place for testing in double and single shear, respectively.

Table 6: Test Results of Joint Configuration 2, Bolted Specimens.

Test Name	Ultimate Tensile Strength, ksi	Stress Area, $in.^2$	Quasi-Static Load, lbf	Dynamic Load, lbf	Shear Load Per Plane, lbs	Shear Stress per plane, psi	Ratio of Ult. Shear Stress to U.T.S., ksi/ksi
SD-2-D-1	72	0.1419	N/A	42474	10619	74832	1.039
SD-2-D-2	72	0.1419	N/A	40341	10085	71074	0.987
SD-2-D-3	72	0.1419	N/A	54791	13698	96532	1.341
SD-2-D-4	72	0.1419	N/A	55001	13750	96902	1.346
ND-2-D-1	72	0.1419	N/A	29258	7314	51547	0.716
ND-2-D-2	72	0.1419	N/A	42296	10574	74518	1.035
ND-2-D-3	72	0.1419	N/A	44924	11231	79147	1.099
SD-2-S-1	72	0.1419	23941	N/A	5985	42180	0.586
SD-2-S-2	72	0.1419	24060	N/A	6015	42390	0.589
SD-2-S-3	72	0.1419	24479	N/A	6120	43127	0.599
ND-2-S-1	72	0.1419	23210	N/A	5802	40891	0.568
ND-2-S-2	72	0.1419	23542	N/A	5886	41477	0.576
ND-2-S-3	72	0.1419	23610	N/A	5903	41597	0.578
SS-2-D-1	86	0.1419	N/A	16727	8364	58940	0.685
SS-2-D-2	86	0.1419	N/A	26845	13423	94593	1.100
SS-2-D-3	86	0.1419	N/A	27975	13988	98574	1.146
NS-2-D-1	86	0.1419	N/A	24632	12316	86795	1.009
NS-2-D-2	86	0.1419	N/A	25228	12614	88893	1.034
NS-2-D-3	86	0.1419	N/A	18745	9373	66051	0.768
SS-2-S-1	86	0.1419	15239	N/A	7619	53696	0.624
SS-2-S-2	86	0.1419	15447	N/A	7724	54431	0.633
SS-2-S-3	86	0.1419	15718	N/A	7859	55385	0.644
NS-2-S-1	86	0.1419	14761	N/A	7381	52014	0.605
NS-2-S-2	86	0.1419	14273	N/A	7136	50292	0.585
NS-2-S-3	86	0.1419	14500	N/A	7250	51094	0.594

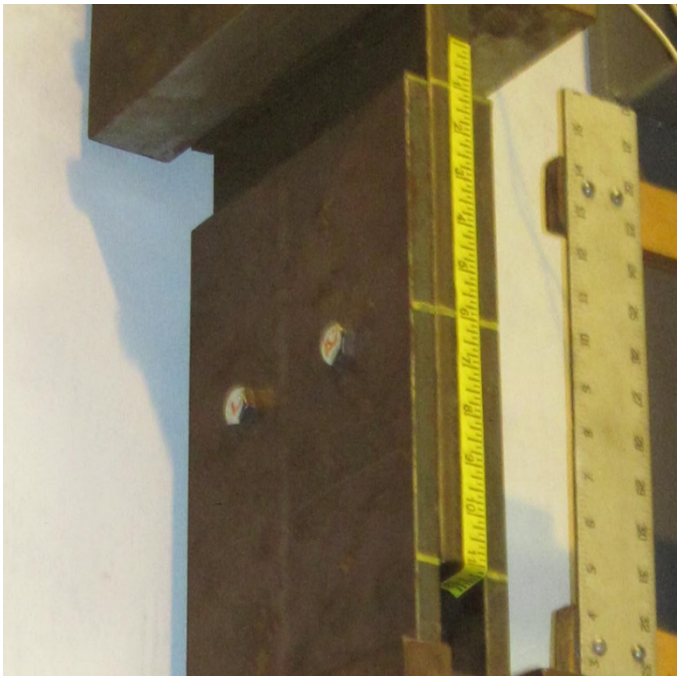

Figure 22: Typical Joint Configuration 2, Bolted, Double Shear Specimen.

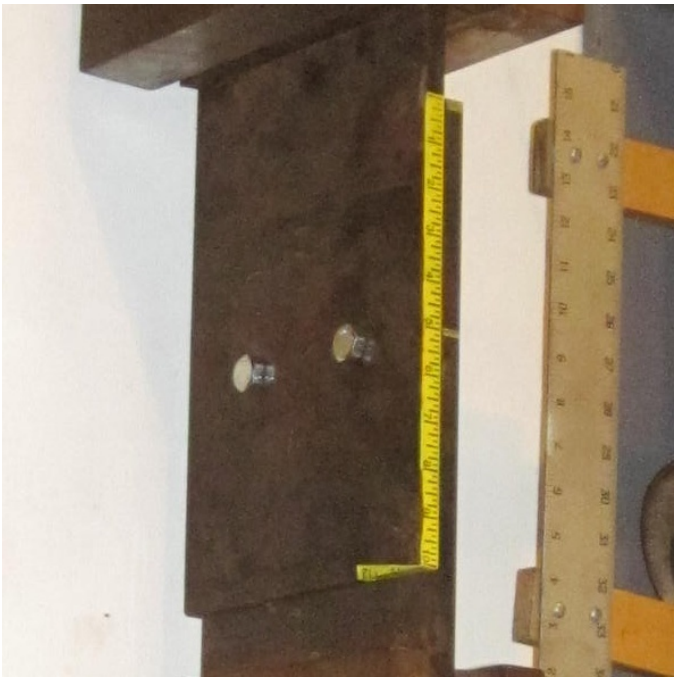

Figure 23: Typical Joint Configuration 2, Bolted, Single Shear Specimen.

Table 7: Test Results of Joint Configuration 2, Riveted Specimens.

Test Name	Ultimate Tensile Strength, ksi	Stress Area, $in.^2$	Quasi-Static Load, lbf	Dynamic Load, lbf	Shear Load Per Plane, lbs	Shear Stress per plane, psi	Ratio of Ult. Shear Stress to U.T.S., ksi/ksi
RD-2-D-1	92	0.2333	N/A	85304	21326	91417	0.994
RD-2-D-2	92	0.2333	N/A	72277	18069	77457	0.842
RD-2-D-3	92	0.2333	N/A	85538	21385	91668	0.996
RD-2-D-4	92	0.2333	N/A	55856	13964	59859	0.651
RD-2-S-1	92	0.2333	45063	N/A	11266	48292	0.525
RD-2-S-2	92	0.2333	47787	N/A	11947	51212	0.557
RD-2-S-3	92	0.2333	-	-	-	-	-[5]
RD-2-S-4	92	0.2333	41680	N/A	10420	44667	0.486
RS-2-D-1	92	0.2463	N/A	39446	19723	84546	0.870
RS-2-D-2	92	0.2463	N/A	47960	23980	102793	1.056
RS-2-D-3	92	0.2463	N/A	42505	21253	91103	0.938
RS-2-D-4	92	0.2463	N/A	79577	39789	170559	1.756
RS-2-D-5	92	0.2463	N/A	77341	38671	165767	1.707
RS-2-D-6	92	0.2463	-	-	-	-	-[6]
RS-2-S-1	92	0.2463	34049	N/A	17024	72977	0.751
RS-2-S-2	92	0.2463	29164	N/A	14582	62509	0.644
RS-2-S-3	92	0.2463	31753	N/A	15876	68056	0.701
RS-2-S-4	92	0.2463	-	-	-	-	-[5]

[5] No data were recorded.
[6] No usable data were collected.

Figure 24: Typical Joint Configuration 2, Riveted, Double Shear Specimen.

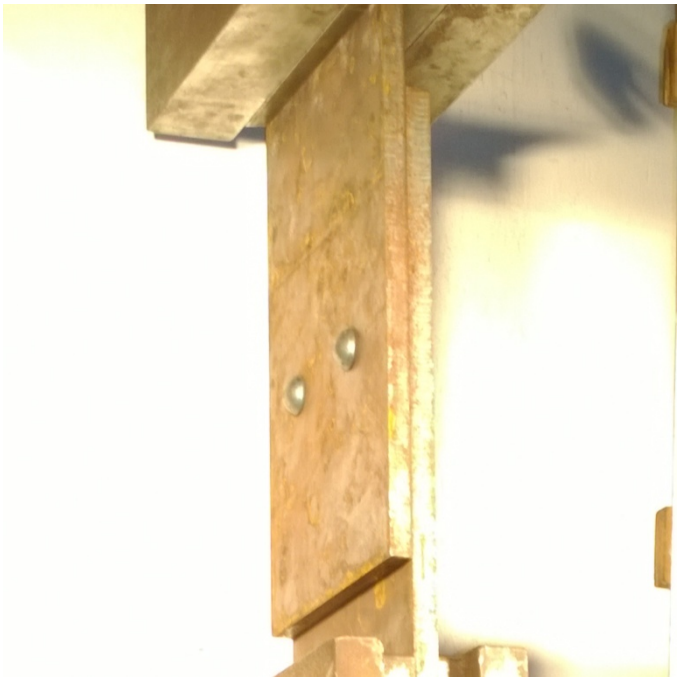

Figure 25: Typical Joint Configuration 2, Riveted, Single Shear Specimen.

5.3 Joint Configuration 3 Results

Results from fasteners in Joint Configuration 3 are presented in the tables below. The results from bolted specimens are presented in Table 8, and results from riveted specimens are presented in Table 9. Figure 26 and Figure 27 show a typical bolted test specimen in place for testing in double and single shear, respectively. Figure 28 shows a typical riveted test specimen in place for testing of single shear.

Table 8: Test Results of Joint Configuration 3, Bolted Specimens.

Test Name	Ultimate Tensile Strength, ksi	Stress Area, in^2	Quasi-Static Load, lbf	Dynamic Load, lbf	Shear Load Per Plane, lbs	Shear Stress per plane, psi	Ratio of Ult. Shear Stress to U.T.S., ksi/ksi
SD-3-D-1	72	0.1419	N/A	22513	5628	39663	0.551
SD-3-D-2	72	0.1419	N/A	30898	7725	54437	0.756
SD-3-D-3	72	0.1419	N/A	50766	12692	89441	1.242
ND-3-D-1	72	0.1419	N/A	39389	9847	69396	0.964
ND-3-D-2	72	0.1419	N/A	49142	12285	86579	1.202
ND-3-D-3	72	0.1419	N/A	39979	9995	70436	0.978
SD-3-S-1	72	0.1419	24959	N/A	6240	43973	0.611
SD-3-S-2	72	0.1419	24026	N/A	6007	42329	0.588
SD-3-S-3	72	0.1419	24702	N/A	6176	43521	0.604
ND-3-S-1	72	0.1419	24352	N/A	6088	42904	0.596
ND-3-S-2	72	0.1419	23842	N/A	5961	42005	0.583
ND-3-S-3	72	0.1419	23816	N/A	5954	41960	0.583
SS-3-D-1	86	0.1419	N/A	21268	10634	74940	0.871
SS-3-D-2	86	0.1419	-	-	-	-	-[7]
SS-3-D-3	86	0.1419	-	-	-	-	-[8]
NS-3-D-1	86	0.1419	-	-	-	-	-[9]
NS-3-D-2	86	0.1419	N/A	21537	10769	75889	0.882
NS-3-D-3	86	0.1419	N/A	19619	9809	69129	0.804
SS-3-S-1	86	0.1419	14981	N/A	7490	52786	0.614
SS-3-S-2	86	0.1419	15220	N/A	7610	53630	0.624
SS-3-S-3	86	0.1419	15103	N/A	7552	53217	0.619
NS-3-S-1	86	0.1419	14568	N/A	7284	51332	0.597
NS-3-S-2	86	0.1419	14476	N/A	7238	51008	0.593
NS-3-S-3	86	0.1419	13942	N/A	6971	49127	0.571

[7] No Accelerometer Data
[8] Unusable data due to considerable amount of AC on top load cell data record
[9] No usable data were recorded

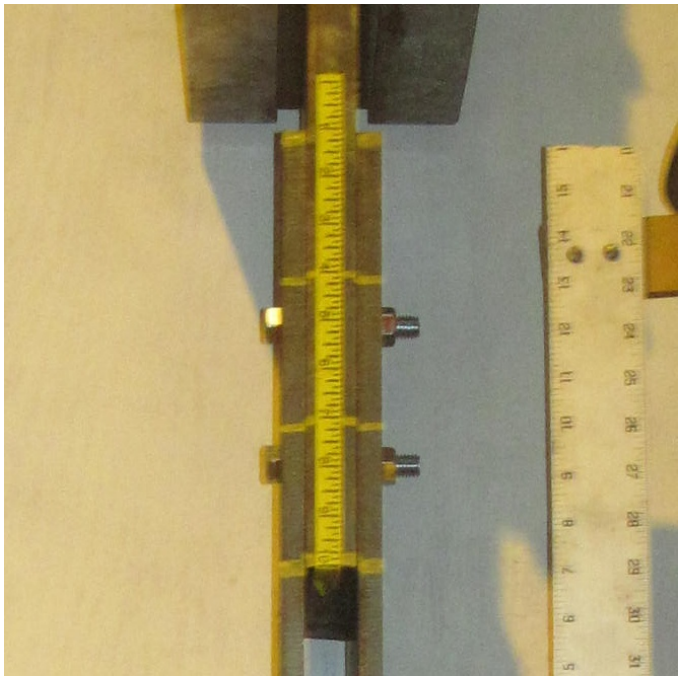

Figure 26: Typical Joint Configuration 3, Bolted, Double Shear Specimen.

Figure 27: Typical Joint Configuration 3, Bolted, Single Shear Specimen.

Table 9: Test Results of Joint Configuration 3, Riveted Specimens.

Test Name	Ultimate Tensile Strength, ksi	Stress Area, in^2	Quasi-Static Load, lbf	Dynamic Load, lbf	Shear Load Per Plane, lbs	Shear Stress per plane, psi	Ratio of Ult. Shear Stress to U.T.S., ksi/ksi
RD-3-D-1	92	0.2333	N/A	79761	19940	85476	0.929
RD-3-D-2	92	0.2333	N/A	132608	33152	142111	1.545
RD-3-D-3	92	0.2333	-	-	-	-	-[10]
RD-3-D-4	92	0.2333	N/A	106104	26526	113708	1.236
RD-3-S-1	92	0.2333	42087	N/A	10522	45103	0.490
RD-3-S-2	92	0.2333	56375	N/A	14094	60415	0.657
RD-3-S-3	92	0.2333	50915	N/A	12729	54563	0.593
RD-3-S-4	92	0.2333	42020	N/A	10505	45031	0.489
RS-3-D-1	92	0.2463	N/A	55509	27754	118973	1.225
RS-3-D-2	92	0.2463	N/A	60093	30047	128799	1.326
RS-3-D-3	92	0.2463	N/A	60332	30166	129311	1.331
RS-3-D-4	92	0.2463	N/A	54216	27108	116203	1.196
RS-3-S-1	92	0.2463	33036	N/A	16518	70806	0.729
RS-3-S-2	92	0.2463	23757	N/A	11878	50918	0.524
RS-3-S-3	92	0.2463	25103	N/A	12552	53805	0.554
RS-3-S-4	92	0.2463	29604	N/A	14802	63451	0.653

Figure 28: Typical Joint Configuration 3, Riveted, Single Shear Specimen.

[10] No data were recorded

5.4 Joint Configuration 4 Results

Results from fasteners in Joint Configuration 4 are presented in the tables below. The results from bolted specimens are presented in Table 10, and results from riveted specimens are presented in Table 11. Figure 29 and Figure 30 show a typical bolted test specimen in place for testing in double and single shear, respectively. Figure 32 and Figure 31 show a typical riveted test specimen in place for testing in double and single shear, respectively.

Table 10: Test Results of Joint Configuration 4, Bolted Specimens.

Test Name	Ultimate Tensile Strength, ksi	Stress Area, in^2	Quasi-Static Load, lbf	Dynamic Load, lbf	Shear Load Per Plane, lbs	Shear Stress per plane, psi	Ratio of Ult. Shear Stress to U.T.S., ksi/ksi
SD-4-D-1	72	0.1419	N/A	93005	11626	81929	1.138
SD-4-D-2	72	0.1419	N/A	156262	19533	137652	1.912
SD-4-D-3	72	0.1419	-	-	-	-	-[11]
SD-4-D-4	72	0.1419	N/A	103167	12896	90881	1.262
ND-4-D-1	72	0.1419	N/A	116488	14561	102616	1.425
ND-4-D-2	72	0.1419	N/A	112405	14051	99018	1.375
ND-4-D-3	72	0.1419	N/A	87507	10938	77086	1.071
SD-4-S-1	72	0.1419	47934	N/A	5992	42226	0.586
SD-4-S-2	72	0.1419	47954	N/A	5994	42243	0.587
SD-4-S-3	72	0.1419	47776	N/A	5972	42086	0.585
ND-4-S-1	72	0.1419	46720	N/A	5840	41156	0.572
ND-4-S-2	72	0.1419	47914	N/A	5989	42208	0.586
ND-4-S-3	72	0.1419	47154	N/A	5894	41538	0.577
SS-4-D-1	86	0.1419	N/A	37486	9371	66043	0.768
SS-4-D-2	86	0.1419	N/A	49237	12309	86747	1.009
SS-4-D-3	86	0.1419	N/A	34700	8675	61136	0.711
NS-4-D-1	86	0.1419	N/A	55804	13951	98317	1.148
NS-4-D-2	86	0.1419	N/A	58533	14633	103125	1.199
NS-4-D-3	86	0.1419	N/A	46405	11601	81757	0.951
SS-4-S-1	86	0.1419	28963	N/A	7241	51027	0.593
SS-4-S-2	86	0.1419	28638	N/A	7159	50454	0.587
SS-4-S-3	86	0.1419	30190	N/A	7548	53189	0.618
NS-4-S-1	86	0.1419	30040	N/A	7510	52925	0.615
NS-4-S-2	86	0.1419	28302	N/A	7076	49864	0.580
NS-4-S-3	86	0.1419	29455	N/A	7364	51894	0.603

[11] Unusable data due to considerable amount of AC on top load cell data record

Figure 29: Typical Joint Configuration 4, Bolted, Double Shear Specimen.

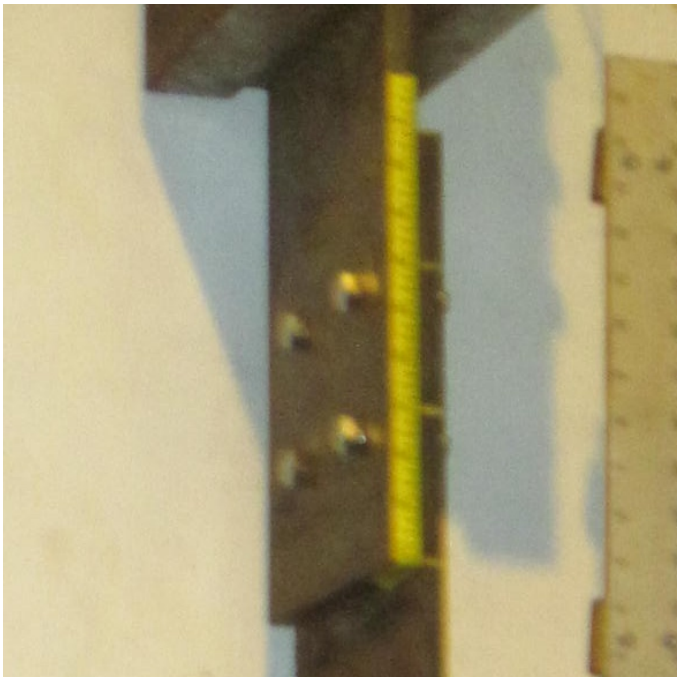

Figure 30: Typical Joint Configuration 4, Bolted, Single Shear Specimen.

Table 11: Test Results of Joint Configuration 4, Riveted Specimens.

Test Name	Ultimate Tensile Strength, ksi	Stress Area, in^2	Quasi-Static Load, lbf	Dynamic Load, lbf	Shear Load Per Plane, lbs	Shear Stress per plane, psi	Ratio of Ult. Shear Stress to U.T.S., ksi/ksi
RD-4-D-1	92	0.2333	N/A	209128	26141	112057	1.218
RD-4-D-2	92	0.2333	N/A	157324	19665	84299	0.916
RD-4-D-3	92	0.2333	N/A	113424	14178	60776	0.661
RD-4-D-4	92	0.2333	N/A	246880	30860	132286	1.438
RD-4-D-5	92	0.2333	N/A	79875	9984	42800	0.465
RD-4-D-6	92	0.2333	-	-	-	-	-[12]
RD-4-S-1	92	0.2333	85417	N/A	10677	45769	0.497
RD-4-S-2	92	0.2333	87479	N/A	10935	46874	0.509
RD-4-S-3	92	0.2333	98195	N/A	12274	52616	0.572
RD-4-S-4	92	0.2333	-	-	-	-	-[13]
RS-4-D-1	92	0.2463	N/A	66323	16581	71076	0.732
RS-4-D-2	92	0.2463	N/A	54412	13603	58311	0.600
RS-4-D-3	92	0.2463	N/A	117432	29358	125847	1.296
RS-4-D-4	92	0.2463	N/A	101994	25498	109303	1.125
RS-4-D-5	92	0.2463	N/A	85437	21359	91559	0.943
RS-4-D-6	92	0.2463	N/A	79230	19808	84908	0.874
RS-4-S-1	92	0.2463	51894	N/A	12974	55613	0.573
RS-4-S-2	92	0.2463	44832	N/A	11208	48045	0.495
RS-4-S-3	92	0.2463	51454	N/A	12864	55141	0.568
RS-4-S-4	92	0.2463	54607	N/A	13652	58520	0.602

[12] Malfunction of top accelerometer and maximum load value is omitted from analysis
[13] No data were recorded

Figure 31: Typical Joint Configuration 4, Riveted, Double Shear Specimen.

Figure 32: Typical Joint Configuration 4, Riveted, Single Shear Specimen.

5.5 Joint Configuration 5 Results

Results from fasteners in Joint Configuration 5 are presented in the tables below. The results from bolted specimens are presented in Table 12, and results from riveted specimens are presented in Table 13. Figure 33 and Figure 34 show a typical bolted test specimen in place for testing for double and single shear tests, respectively. Figure 35 and Figure 36 show a typical riveted test specimen in place for testing in double and single shear, respectively.

Table 12: Test Results of Joint Configuration 5, Bolted Specimens.

Test Name	Ultimate Tensile Strength, ksi	Stress Area, in^2	Quasi-Static Load, lbf	Dynamic Load, lbf	Shear Load Per Plane, lbs	Shear Stress per plane, psi	Ratio of Ult. Shear Stress to U.T.S., ksi/ksi
SD-5-D-1T	72	0.1419	N/A	68498	8562	60341	0.839[14]
SD-5-D-2T	72	0.1419	N/A	61838	7730	54474	0.757[14]
SD-5-D-1	72	0.1419	N/A	36835	4604	32448	0.451[14]
SD-5-D-2	72	0.1419	N/A	84346	10543	74301	1.033[14]
SD-5-D-3	72	0.1419	N/A	49161	6145	43307	0.602[14]
ND-5-D-1	72	0.1419	N/A	64407	8051	56737	0.788[14]
ND-5-D-2	72	0.1419	N/A	65598	8200	57786	0.803[14]
ND-5-D-3	72	0.1419	N/A	65891	8236	58044	0.807[14]
SD-5-S-1T	72	0.1419	-	-	-	-	[15]
SD-5-S-2T	72	0.1419	52935	N/A	6617	46631	0.648
SD-5-S-1	72	0.1419	49513	N/A	6189	43617	0.606
SD-5-S-2	72	0.1419	51127	N/A	6391	45038	0.626
SD-5-S-3	72	0.1419	51631	N/A	6454	45483	0.632
ND-5-S-1	72	0.1419	48993	N/A	6124	43159	0.600
ND-5-S-2	72	0.1419	48505	N/A	6063	42728	0.594
ND-5-S-3	72	0.1419	46673	N/A	5834	41115	0.571
SS-5-D-1	86	0.1419	N/A	53046	13262	93458	1.087
SS-5-D-2	86	0.1419	N/A	38110	9527	67143	0.781
SS-5-D-3	86	0.1419	N/A	51525	12881	90777	1.056
NS-5-D-1	86	0.1419	N/A	25648	6412	45188	0.525
NS-5-D-2	86	0.1419	N/A	28526	7132	50258	0.584
NS-5-D-3	86	0.1419	N/A	24624	6156	43383	0.504
SS-5-S-1	86	0.1419	26418	N/A	6605	46544	0.541
SS-5-S-2	86	0.1419	27477	N/A	6869	48410	0.563
SS-5-S-3	86	0.1419	31973	N/A	7993	56330	0.655
NS-5-S-1	86	0.1419	28810	N/A	7203	50759	0.590
NS-5-S-2	86	0.1419	27260	N/A	6815	48027	0.558
NS-5-S-3	86	0.1419	25549	N/A	6387	45013	0.523

[14] Malfunction of top accelerometer and maximum load value is omitted from analysis
[15] No data were recorded

Figure 33: Typical Joint Configuration 5, Bolted, Double Shear Specimen.

Figure 34: Typical Joint Configuration 5, Bolted, Single Shear Specimen.

Table 13: Test Results of Joint Configuration 5, Riveted Specimens.

Test Name	Ultimate Tensile Strength, ksi	Stress Area, in^2	Quasi-Static Load, lbf	Dynamic Load, lbf	Shear Load Per Plane, lbs	Shear Stress per plane, psi	Ratio of Ult. Shear Stress to U.T.S., ksi/ksi
RD-5-D-1	92	0.2333	N/A	147573	18447	79074	0.860
RD-5-D-2	92	0.2333	N/A	160638	20080	86075	0.936
RD-5-D-3	92	0.2333	N/A	213216	26652	114247	1.242
RD-5-D-4	92	0.2333	N/A	167113	20889	89544	0.973
RD-5-S-1	92	0.2333	86537	N/A	10817	46369	0.504
RD-5-S-2	92	0.2333	88741	N/A	11093	47550	0.517
RD-5-S-3	92	0.2333	96454	N/A	12057	51683	0.562
RD-5-S-4	92	0.2333	-	-	-	-	-[16]
RS-5-D-1	92	0.2463	-	-	-	-	-[16]
RS-5-D-2	92	0.2463	N/A	66400	16600	71159	0.733
RS-5-D-3	92	0.2463	N/A	94465	23616	101234	1.042
RS-5-D-4	92	0.2463	N/A	83951	20988	89967	0.926
RS-5-S-1	92	0.2463	-	-	-	-	-[16]
RS-5-S-2	92	0.2463	52404	N/A	13101	56160	0.578
RS-5-S-3	92	0.2463	45432	N/A	11358	48688	0.501
RS-5-S-4	92	0.2463	53620	N/A	13405	57463	0.592

[16] No data were recorded

Figure 35: Typical Joint Configuration 5, Riveted, Double Shear Specimen.

Figure 36: Typical Joint Configuration 5, Riveted, Single Shear Specimen.

6. STATISTICAL ANALYSIS

Section 6 discusses the statistical analysis conducted on the data presented in Section 5. A four-main factor experimental design was conducted using traditional analysis of variance calculations (ANOVA) on the data presented in Section 5. The four factors considered were fastener type (non pretensioned bolts, pretensioned bolts, and rivets), joint configuration (Joint Configurations 1 through 5), shear type (double and single shear), and loading type (quasi-static and dynamic). Individual comparisons of means were conducted based on the results of this ANOVA using the t-test statistic so that the full significance of the results can be better understood. All statistical calculations were computed using Microsoft EXCEL tables.

The “Ratio of Shear Strength to Ultimate Tensile Strength” value was selected as the response variable for the statistical analysis. This value provided for comparisons of the effects of the variables against one another. The “Ratio…” value is called the “specimen response” for the remainder of this section. This value was chosen because it was the maximum applied load normalized to the ultimate static tensile strength of the fastener, the number of fasteners, the surface area available for shear, and number of shear planes. This ratio of shear strength to ultimate static tensile strength was historically and is currently used in steel design and provides a good basis for the comparison of the results associated with the different specimens.

Microsoft EXCEL was used to compute the statistical analysis on all the data in this thesis. Two specific analysis techniques were used: a multivariate ANOVA and a t-

test. The typical multifactor ANOVA includes the interactions of the factors in the analysis. The effects of the factor interactions were initially computed. However, no useful information was gleaned from these results. The ANOVA's were then computed again without factor interactions, which allowed for a focused analysis of the main factors. These results were used for the statistical analysis presented in this section. The following paragraphs explain the calculations performed in the Microsoft EXCEL spreadsheets.

Traditional ANOVA relationships were used to compute the multivariate ANOVA to determine which factor had a significant effect on the response. The F-distribution was used for all the ANOVA tests completed for the statistical analysis of the research results to determine if a factor has a significant effect on the specimen response. The F-Ratio value was calculated by first determining the sum of squares of each factor, which is sum of all the squared distances between individual sample means and the overall sample mean. The mean square value of each factor was then calculated by dividing the sum of squares by the degrees of freedom within each sample. Each mean square value was divided by the mean square of the error, or the sum of squared distances between the sample average values and actual values divided by the number of error degrees of freedom, to determine the F-Ratio. The F-Ratio value, along with the degrees of freedom, corresponds to a probability that the null hypothesis is true, or that the factor does not affect the specimen's response. Any probability of the F-Ratio less than the alpha value of 0.05, the typical value for statistical analysis techniques and indicates a 95% confidence of the null hypothesis (compared samples are not statistically

different from each other) being true, indicated that a factor has a statistically significant effect on the specimen response. Probabilities less than the alpha value were denoted by bolded and underlined probability values in the ANOVA tables.

A t-test was completed on the samples from factors that were indicated by the ANOVA as having a significant effect on the specimen response. The individual t-tests were conducted between a set of samples from a single factor, i.e., comparing dynamic to quasi-static loading type, or riveted samples only comparing double shear to single shear. The t-test statistics were based on the differences between the means and standard deviations of the samples since the analysis focused on determining whether samples were statistically different from each other. The t-test statistic, degrees of freedom, and the probability using a t-distribution were determined using the method and equations for comparing independent samples assuming the compared samples had unequal variances and unequal sample sizes from Hayter (2002). This was the correct assumption for the samples tested in this thesis' analysis. The t-test statistic to determine statistical differences between two samples was computed by dividing the difference of the sample means by the standard error of the difference between the means. Hayter (2002) uses Satterthwaite's Formula, shown in Equation (5), to calculate the effective degrees of freedom for compared samples with unequal variances (s_1^2 and s_2^2) and unequal sample sizes (n_1 and n_2). Equation (5) results were rounded down to the nearest integer to use in determining the probability of the null hypothesis. The probability of the sample comparison satisfying the null hypothesis (the sample means are not different) was two-sided and calculated using the t-distribution.

$$Eff.Deg.of\ Freedom = \frac{\left(\frac{s_1^2}{n_1} + \frac{s_2^2}{n_2}\right)^2}{\frac{\left(\frac{s_1^2}{n_1}\right)^2}{n_1 - 1} + \frac{\left(\frac{s_2^2}{n_2}\right)^2}{n_2 - 1}} \quad \textbf{(5)}$$

All types of a significant factor were compared to one another using the t-test in order to make all possible comparisons between samples. For example, the factor of joint configuration will have 10 different t-tests completed for the 5 separate joint configurations: Joint Configuration 1 was compared with Joint Configurations 2, 3, 4, and 5, individually; Joint Configuration 2 compared with Joint Configurations 3, 4, and 5; Joint Configuration 3 compared with Joint Configurations 4 and 5; Joint Configuration 4 compared with Joint Configuration 5. The results of the t-test allowed the samples to be grouped based on statistical differences. Samples that are grouped together are not statistically different from each other, whereas samples from separate groups are statistically significantly different from each other. For example, the t-tests on the joint configuration factor might indicate two different groups: Joint Configurations 2, 3, and 4 and Joint Configurations 1 and 5.

Plots of the sample data points and statistical means, standard errors, and standard deviations of the samples were produced using JMP10 statistical analysis software. These plots allowed for a visual representation of the data and differences of the means. The following sentences explain the important portions of the plots. The individual dots were the measured data points, and the solid line across the entire plot

indicated the mean of all the data points analyzed for all figures from the statistical analysis in this section. Along the y-axis was the value of the specimen's response, or the ratio of shear stress to ultimate static tensile strength. The x-axis was the specific samples within the factor that were being compared to one another. The medium length line near the middle of the sample distribution was the sample mean. The first short line on either side of the mean line indicated the error bars of the mean; ± 1.96 standard errors on each side of the sample mean is the range where any new sample mean will fall with 95% confidence. The outer-most short lines from the mean line indicate one standard deviation from the sample mean. Plots in the following subsections are only shown for comparisons between samples with only one of the four main factors affecting the response.

A table of values from the t-test for certain individual t-tests is also presented in the analysis. The values presented for each set of compared samples were the absolute difference in means, the standard error of the difference, the t-test statistic, and the probability of the null hypothesis being true for the respective t-test statistic. The alpha value, or threshold, for statistical significance was 0.05. A shaded t-test probability value indicated the probability that the samples were similar fell below the alpha value of 0.05.

6.1 Initial Analysis on All Specimen Responses

The data were initially analyzed by comparing the specimens' responses using an ANOVA on all four factors of interest. The results of the first ANOVA test are shown in Table 14. All Joint Configuration 5 specimens had to be excluded because results of all

bolted, double shear, dynamic tests were invalidated by a faulty accelerometer reading. The table indicated that loading type had the most significant effect on the specimen response. Whether a specimen was subjected to a quasi-static or dynamic loading type was expected to have the most significant effect on the response due to the suspected specimen strength increase, with respect to the fastener's ultimate static tensile strengths, caused by dynamic loadings on the specimen.

Table 14: Results of ANOVA on All Specimens.

Effect Source	Degrees of Freedom	Sum of Squares	Mean Sum of Squares	F-Ratio	Probability of F-Ratio
Loading Type	1	7.716	7.716	182.281	<0.0001
Fastener Type	2	0.039	0.020	0.466	0.628
Shear Type	1	0.001	0.001	0.017	0.898
Joint Configuration	3	0.240	0.080	1.890	0.134
Error	152	6.434	0.042		
Total	159	14.430			

A t-test comparing the two loading types was conducted using all specimens' data prior to performing any further statistical analysis. This test compared the shear stress response based on the loading type, since the loading type was indicated as the most significant factor for the specimen response. This analysis technique was used to quantify an overall increase in ultimate shear strength with respect to the fastener's ultimate static tensile strength due to dynamic loads, if applicable. All fastener types were lumped together into a single data set as the initial ANOVA (Table 14) indicated

that fasteners, when comparing ultimate shear strengths with respect to its respective ultimate static tensile strength, should have similar responses. Figure 37 shows the sample data comparing the specimen responses for each loading type. The mean of the dynamic loading type specimen response was 1.024 (Standard Deviation, (SD) of 0.280, Coefficient of Variation (CV) of 28%), and the mean of the quasi-static loading type specimen response was 0.584 (SD of 0.059, CV of 10%). The mean difference was 0.439 and the standard error of the difference was 0.032. These values resulted in a t-statistic of 13.874 and corresponding probability of loading type not having an effect on the specimen response of less than 0.0001. This result overwhelmingly indicated that loading type significantly affects the specimen response for all specimen types.

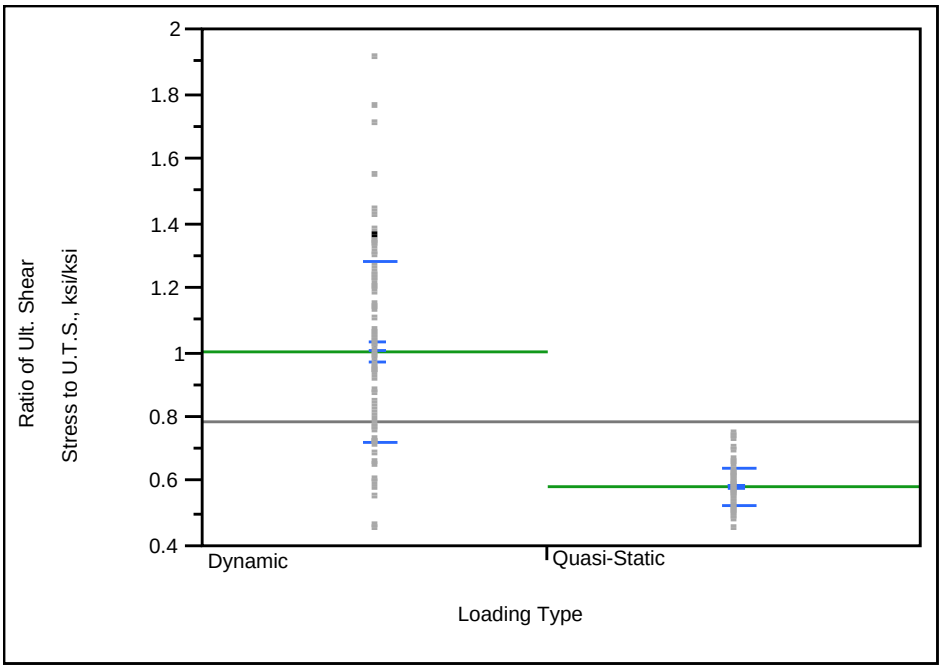

Figure 37: Comparison of All Specimens Response by Loading Type.

Since the samples were statistically significantly different, an increase in shear strength with respect to fastener ultimate static strength could be quantified, herein referred to as the “dynamic increase ratio”. Computing the dynamic increase ratio for the fastener response was done by dividing the mean of the specimens subjected to dynamic loading type by the mean of the specimens subjected to quasi-static loading type. The order is specific because the increase ratio is made with respect to the ultimate static strength of a fastener. The dynamic increase ratio for all specimens was 1.72.

Since the t-test and ANOVA indicated a significant effect on specimen response due to loading type, a separate ANOVA for each loading type was conducted. This was to determine if the factors had an effect on the dynamic specimen response and to verify that the factors did not have an effect on the quasi-static specimen response.

6.2 Analysis of Significant Factors on Dynamic Loading Type Specimen Response

A three-factor ANOVA was completed on the dynamic loading type specimen data for the remaining three factors, fastener type, shear type, and joint configuration to determine whether any of these factors have a significant effect on the dynamic response of the specimens. The results of this ANOVA are presented in Table 15.

Table 15: Results of ANOVA on All Specimens Subjected to Dynamic Loading Type.

Effect Source	Degrees of Freedom	Sum of Squares	Mean Sum of Squares	F-Ratio	Probability of F-Ratio
Fastener Type	2	0.067	0.033	0.414	0.662
Shear Type	1	0.081	0.081	1.009	0.318
Joint Configuration	3	0.242	0.081	1.000	0.397
Error	75	6.053	0.081		
Total	81	6.444			

Table 15 indicated that there were no statistically significant effects on specimen response by fastener type, shear type, or joint configuration. Therefore it can be said that, in general, the three factors, fastener type, shear type, and joint configuration, do not cause a statistically significant difference in the specimen responses. This was more than likely due to the large variations in the samples as the majority of the variation was included in the error sum of squares. Therefore, it was shown that dynamic loading type caused a wide variation of specimen response regardless of the specimen type. It is possible that a larger sample size could provide a different result, but for the specimens tested in this thesis, a conclusion that the three main factors do not affect specimen response must be drawn.

6.3 Analysis of Significant Factors on Quasi-Static Loading Type Specimen Response

Quasi-static loading type specimen data were given a three-factor ANOVA in the same manner as the dynamic specimens to verify that the three factors do not

significantly affect the shear response of fasteners. The results of the quasi-static specimen ANOVA are shown in Table 16.

Table 16: Results of ANOVA on All Specimens Subjected to Quasi-Static Loading Type.

Effect Source	Degrees of Freedom	Sum of Squares	Mean Sum of Squares	F-Ratio	Probability of F-Ratio
Fastener Type	2	0.013	0.007	2.487	0.089
Shear Type	1	0.028	0.028	10.498	**0.002**
Joint Configuration	4	0.023	0.006	2.157	0.080
Error	90	0.244	0.003		
Total	97	0.309			

Table 16 indicated that shear type has the most statistically significant effect on the response of quasi-static loading type specimens. Further analysis using the t-test statistic was completed to determine whether the difference in quasi-static specimen response due to shear type was statistically significant.

A t-test was performed to compare the responses based on the shear type. The plot of the sample data is shown in Figure 38. The t-test indicated a significant statistical difference between double and single shear samples subjected to quasi-static loadings. The means were 0.562 and 0.605 for double and single shear, respectively. The mean difference of 0.043 resulted in a ratio of mean difference (RMD) of 7%. The standard error of the difference was 0.011. The corresponding t-statistic and probability of the samples not being affected by shear type was 4.029 and 0.0001, respectively (degrees of

freedom was 90). However, the mean difference equated to an approximate 3 ksi (400 lbf) difference in the mean ultimate shear strength. This mean difference was small enough to be caused by variability in the actual strength of the specimens (Table 1 showed that the ultimate static tensile strength of bolts varied by approximately 400 lbf), or by a possible substantial difference in ultimate shear strength due to shear type caused by the riveted specimens. Previous research indicated that the grip length of a rivet (distance between rivet heads) caused a difference in ultimate shear strength. This possibility is explored in Section 6.4. It was also possible that the very small variation of specimen response, shown by the very small error mean sum of squares value in Table 16, increased the sensitivity of the statistical tests. Therefore, the difference was not large enough to be considered a practical difference from an engineering standpoint.

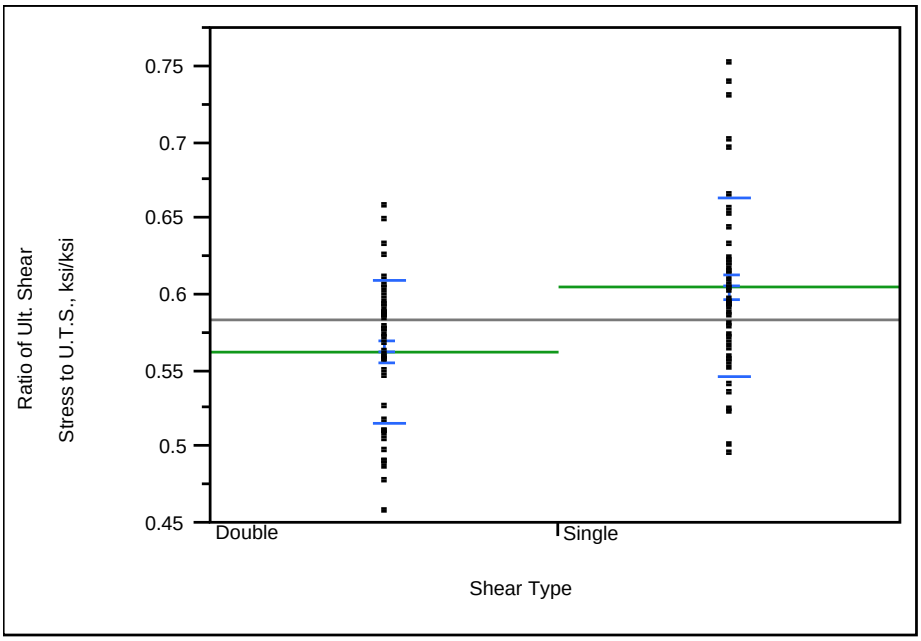

Figure 38: Comparison by Shear Type for All Quasi-Static Loading Type Specimens.

The quasi-static loading type specimen response is statistically significantly affected by shear type. These differences were possibly caused by the riveted specimen responses to shear type. This was further analyzed in the Section 6.4. Although the differences between other samples were considered to be statistically significant, the actual differences between them were small enough to be considered practically insignificant from an engineering standpoint. Therefore, the testing in this thesis verified that the shear type, joint configuration, and fastener type did not have a significant practical effect on the specimen response.

6.4 Analysis of Riveted Specimen Response

The data from the rivet specimens was analyzed separately because of two things. First, the normalization of the rivet data was based on an estimated ultimate driven static tensile strength that was calculated from the average ultimate undriven static tensile strength from ASTM E8 specimens (ASTM 2013), rather than actual testing to determine the ultimate driven static tensile strength. Second, the rivets possibly caused statistically significant differences in the quasi-static specimen analysis. The rivet specimen data were analyzed using the multifactor ANOVA, similar those used in the previous analyses. The remaining three factors, loading type, joint configuration, and shear type, were inserted into a three factor ANOVA on the riveted specimen data. The results of the rivet specimen data ANOVA is shown in Table 17. The table indicated the most significant factor affecting the specimen response is loading type, as expected due

to the results of the overall ANOVA. Joint configuration also caused a statistically significantly different specimen response.

Table 17: Results of ANOVA on All Riveted Specimens.

Effect Source	Degrees of Freedom	Sum of Squares	Mean Sum of Squares	F-Ratio	Probability of F-Ratio
Loading Type	1	3.227	3.227	71.566	**<0.0001**
Shear Type	1	0.125	0.125	2.780	0.100
Joint Configuration	4	0.628	0.157	3.482	**0.012**
Error	69	3.111	0.045		
Total	75	7.092			

A t-test was completed on the riveted specimen data for the loading type since the ANOVA indicated it to be the most significant factor on specimen response. Figure 39 is the plot of the sample data. The t-test indicated that, for riveted specimens, the two loading types caused statistically significantly differences in the specimen response. The sample means were 0.992 (CV of 30%) and 0.577 (CV of 14%) for dynamic and quasi-static loading types, respectively. The mean difference was 0.413 and standard error of the difference was 0.048, resulting in a t-statistic of 8.531 and probability of the samples not being affected by loading type of less than 0.0001 (degrees of freedom were 47). The mean difference between the samples equated to a DIF of 1.72. This difference was as expected since the DIF for all specimens was 1.72.

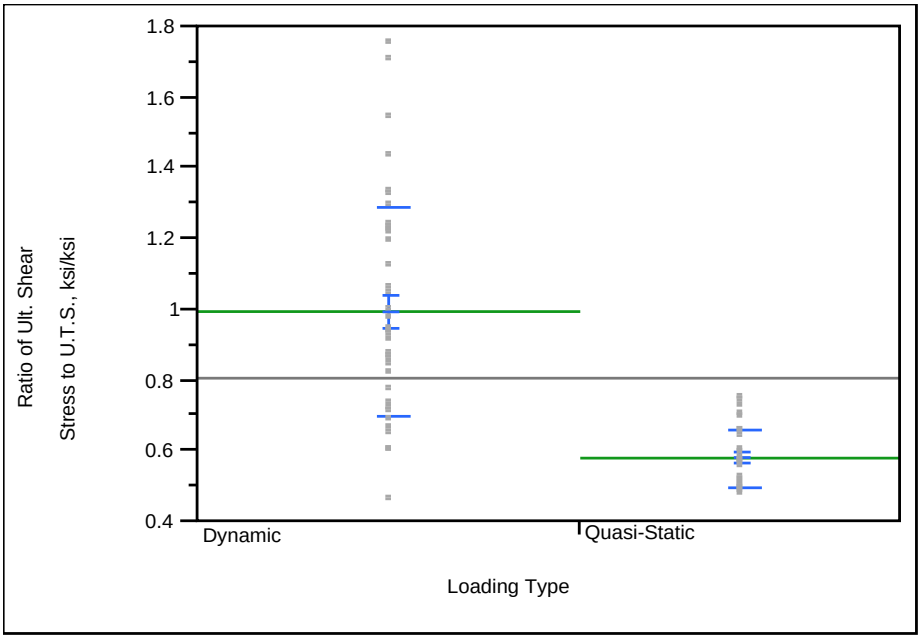

Figure 39: Comparison by Loading Type for Riveted Specimens.

Although the joint configuration factor was indicated as causing a statistical difference, the next analysis performed was a separate ANOVA for riveted specimens subjected to dynamic loading type and quasi-static loading type since it had been shown that loading type did cause an extreme significant difference in the specimen response. This was to make sure that the statistical significance was not caused by the extreme difference caused loading type and to clearly see if shear type had an effect on specimen response as shown in previous research. The ANOVA results from the riveted specimens subjected to dynamic loading type and riveted specimens subjected to quasi-static loading type are shown in Table 18 and Table 19, respectively. Table 18 indicated a statistically significant difference in the specimen response due to the joint

configuration. Table 19 indicated a statistically significant difference in specimen response due to shear type.

Table 18: Results of ANOVA on All Riveted Specimens Subjected to Dynamic Loading Type.

Effect Source	Degrees of Freedom	Sum of Squares	Mean Sum of Squares	F-Ratio	Probability of F-Ratio
Shear Type	1	0.030	0.030	0.431	0.516
Joint Configuration	4	1.137	0.284	4.022	**0.009**
Error	35	2.474	0.071		
Total	40	3.642			

Table 19: Results of ANOVA on All Riveted Specimens Subjected to Quasi-Static Loading Type.

Effect Source	Degrees of Freedom	Sum of Squares	Mean Sum of Squares	F-Ratio	Probability of F-Ratio
Shear Type	1	0.067	0.067	14.932	**0.001**
Joint Configuration	4	0.025	0.006	1.395	0.260
Error	29	0.130	0.004		
Total	34	0.223			

The first factor analyzed using the t-test was the joint configuration for riveted specimens subjected to dynamic loading type. The plot of the sample data of the riveted, dynamic loading type specimens for each joint configuration is shown in Figure 40.

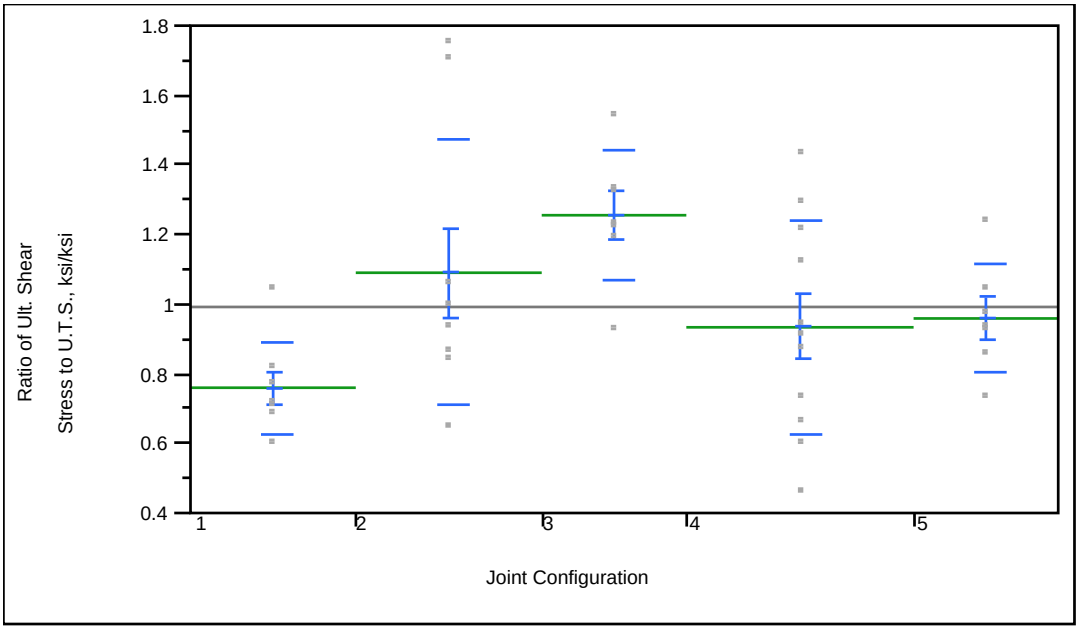

Figure 40: Comparison by Joint Configuration for Riveted, Dynamic Loading Type Specimen Response.

The comparisons of each configuration indicated that there were statistically significant differences in riveted specimen responses due to joint configurations. The t-test comparison values for each configuration comparison are shown in Table 20. There was a significant statistical and practical difference between some configuration means. However, the variation of the data was high (numerous outliers in Joint Configuration 2 and 3), and the sample size was small (each joint configuration has at most 12 data points). Therefore, it was difficult to determine the cause of the difference. More tests are needed to get a better sample distribution. Some of the difference, however, may have been due to the acceleration/inertial force data or individual sample strengths.

Table 20: t-test Values Comparing Joint Configurations for Riveted, Dynamic Loading Type Specimens.

Sample A	Sample B	Absolute Value of Mean Difference	SD of Difference	Deg. of Fr.	t-test Statistic	Probability of t-test
Configuration 1	Configuration 2	0.3419	0.1330	10	2.5701	0.0279
Configuration 1	Configuration 3	0.5268	0.1414	10	3.7269	0.0039
Configuration 1	Configuration 4	0.2076	0.1276	14	1.6276	0.1259
Configuration 1	Configuration 5	0.2252	0.1414	11	1.5932	0.1394
Configuration 2	Configuration 3	0.1848	0.1330	12	1.3892	0.1900
Configuration 2	Configuration 4	0.1343	0.1183	15	1.1357	0.2739
Configuration 2	Configuration 5	0.1167	0.1330	11	0.8775	0.3990
Configuration 3	Configuration 4	0.3191	0.1276	15	2.5019	0.0244
Configuration 3	Configuration 5	0.3051	0.1414	11	2.1333	0.0563
Configuration 4	Configuration 5	0.0176	0.1276	15	0.1380	0.8921

The next t-test was completed on the effects of shear type on the riveted specimens subjected to quasi-static loadings. Previous research referenced in this thesis's literature review had concluded that there was a difference in the response of the specimen when the grip length of compared rivets was different. The grip lengths for the rivets tested for this thesis were 1 inch and 2 inches for single and double shear, respectively.

The results for riveted, quasi-static specimens indicated a statistically significant difference in the specimen response due to shear type. The sample means are 0.620 (CV of 13%) and 0.532 (CV of 9%) for single and double shear, respectively. The mean difference was 0.088, and the standard error of the difference was 0.022. These values resulted in a t-statistic of 3.945 and probability that the specimen were not affected by shear type of 0.001 (degrees of freedom were 27). This was a significant difference and

was practically different as well. The difference can be easily seen in the plot of the sample data shown in Figure 41. This comparison also shows that riveted specimen response contributed significantly to the statistically significant difference due to shear type in the overall quasi-static loading type specimens comparison.

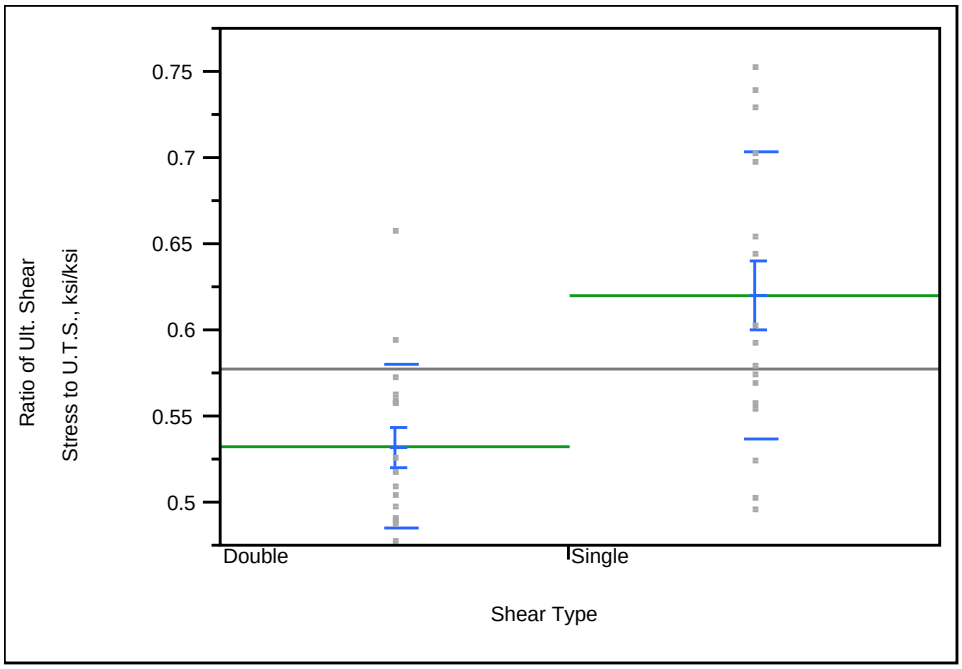

Figure 41: Comparison by Shear Type of Riveted, Quasi-Static Loading Type Specimen Response.

The difference in double and single shear specimens was likely due to the longer grip length with double shear rivets having more initial tension. Wilson and Oliver (1930) observed this effect in their testing of many rivets with multiple gauge lengths. They stated that the initial stress is higher in longer grip rivets and that rivets with a "2 inch grip had a slightly greater tension if driven with a press riveter…" (Wilson and

Oliver 1930). If the double shear rivets have a greater initial stress (which is closer to the yield limit than single shear rivets), they would not have the same amount of available strength in shear, using Mohr's circle or the interaction curve shown in Figure 2. This would be confirmed by testing and comparing the tensile strength of the rivets with the same grip length as the double and single shear specimens. However, this type of testing could not be conducted for the rivets tested in this thesis. It is important to note that this effect was not necessarily caused by the fact the rivet is in double or single shear, but instead by the length of the rivet, i.e., a single shear rivet with a grip length the same size as a double shear should have similar responses.

The riveted specimens subjected to dynamic loading type were also given a t-test comparing the response due to shear type. The results indicated no statistically significant difference, although the single shear specimens did have a greater mean than the double shear specimens. However, the CV of the samples was 32% and 28% for single and double shear, respectively. This large amount of variation in these samples may have masked any statistical differences in the riveted, dynamic specimen responses that were seen in the riveted, quasi-static specimens.

Design guides have adjusted the design shear strength to a factor of the undriven rivet ultimate tensile strength. The value for the ratio of shear strength to undriven rivet ultimate tensile strength used for design purposes was 0.75. A separate analysis was completed on the normalized measured shear strength to the ultimate undriven rivet tensile strength to compare the results to the design value of 0.75 since testing was completed to determine the undriven rivet ultimate tensile strength. The quasi-static

specimen mean normalized to the undriven ultimate tensile strength was 0.690. It is less than 0.75, but the mean of single and double shear, quasi-static specimens was 0.741 and 0.636, respectively. This falls in line with the range of values given in Kulak et al. (1987), Wilson and Oliver (1930), and Schenker (1954).

To summarize the analysis of riveted specimens, the loading type has the most significant effect on specimen response as a rivet under dynamic loading has a 72% (SD of 8.7%) increase in ultimate shear capacity when compared to a similar rivet subjected to quasi-static loading. The configuration of the joint under dynamic loading has some statistically significant effect on the specimen response. The shear type of the specimen under quasi-static loading has a statistically significant effect on the specimen response due to the grip length increasing the initial stress (decreasing available shear strength). However, the dynamic specimens show a similar result due to shear type but there was no statistically different response, more than likely due to variation of the results.

6.5 Analysis of Bolt Pretension Effects and All Bolted Specimens.

The non-pretensioned and pretensioned bolted specimens were directly compared to each other to determine if there were any statistical differences in the specimen response due to initial tension in the bolt for dynamic loading type and to verify that there were no differences when a quasi-static loading type was applied. Also analyzed was the response of all bolted specimens combined versus the four factors of interest. This can be done since bolts from the same lot were used for each bolted fastener type,

and the different size bolts have been normalized to an average measured ultimate tensile strength capacity for each size of bolt used.

A t-test of all bolted samples comparing response to loading type was completed since this variable was shown to have the most statistically significant effect on the specimen response. The sample means were 0.5862 (CV of 6%) and 1.043 (CV of 25%) for quasi-static and dynamic loading types, respectively. The mean difference was 0.456, and the standard error of the difference was 0.0363. These values resulted in a t-statistic of 12.580 and a probability that the specimen response was not affected by the loading type of less than 0.0001 (degrees of freedom were 108). Therefore, the specimen response was statistically significantly affected by the loading type. The dynamic increase ratio for all bolted specimens was 1.78 (SD of 0.062). Therefore the next analysis completed was an ANOVA for the remaining three factors for each loading type, and results are shown in Table 21 and Table 22 for bolted specimens subjected to dynamic and quasi-static loading types, respectively. Joint Configuration 5 results have been omitted from the bolted, dynamic loading type analyses due to instrumentation malfunctions on all bolted, dynamic loading type, double shear specimens.

Table 21: Results of ANOVA on All Bolted Specimens Subjected to Dynamic Loading Type.

Effect Source	Degrees of Freedom	Sum of Squares	Mean Sum of Squares	F-Ratio	Probability of F-Ratio
Fastener Type	1	0.026	0.026	0.484	0.491
Shear Type	1	0.312	0.312	5.839	**0.020**
Joint Configuration	3	0.341	0.114	2.129	0.111
Error	42	2.241	0.053		
Total	47	2.919			

Table 22: Results of ANOVA on All Bolted Specimens Subjected to Quasi-Static Loading Type.

Effect Source	Degrees of Freedom	Sum of Squares	Mean Sum of Squares	F-Ratio	Probability of F-Ratio
Fastener Type	1	0.012	0.012	12.618	**0.001**
Shear Type	1	0.005	0.005	5.421	**0.024**
Joint Configuration	4	0.017	0.004	4.640	**0.003**
Error	55	0.051	0.001		
Total	61	0.085			

The dynamic loading type ANOVA indicated that bolt fastener type does not affect the response of the fastener. Therefore, analysis of the other factors for bolted specimens subjected to the dynamic loading type was performed. Table 21 indicates that only shear type may have a statistically significant effect on the bolted specimen response when subjected to a dynamic loading type. Table 22 indicated that all factors may have a significant effect on the bolted specimen response when subjected to a quasi-static loading type. The effect of fastener type, which checks the effect of bolt pretension

on specimen response, was checked first using the t-test. If this analysis showed no difference in specimen response based upon bolt pretension, a series of t-test analyses would be conducted to determine the effects of the remaining factors on specimen response.

The first t-test analysis for dynamic loading type specimens was conducted on both bolted fastener types combined and compared the specimen response by double and single shear. A plot of the sample data is shown in Figure 42. The samples had means of 1.114 (CV of 25%) and 0.953 (CV of 19%) for double and single shear samples, respectively. The mean difference was 0.162 (RMD of 16%), and standard error of the difference was 0.065. These difference values result in a t-statistic of 2.502 and probability that the specimen response is affected by shear type of 0.016 (degrees of freedom were 44). This result indicated shear type caused a statistically significant effect on the specimen response. A possible cause for the difference in response due to shear type may be the presence of bending (tensile/compression forces) in the bolt. The longer bolt length for double shear specimens may have had axial forces applied causing an incremental increase in strength. This theory can be proven by examining the failure surfaces of the bolt. However, the tested bolt failure surfaces were damaged during testing as the surface slid along and banged against the specimen plates, and conclusive determination could not be made.

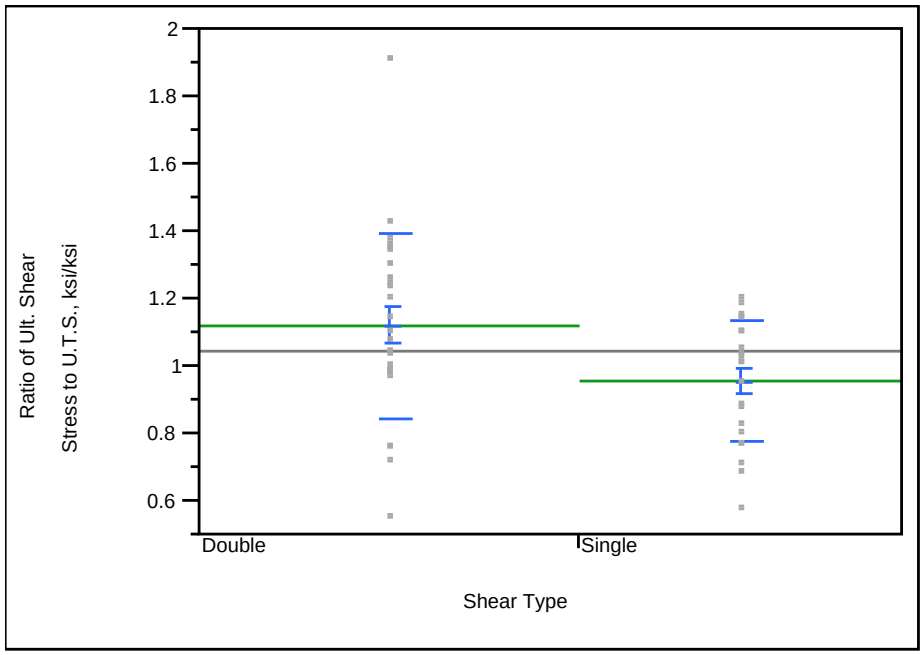

Figure 42: Comparison by Shear Type of Bolted, Dynamic Loading Type Specimens.

A separate analysis was performed to compare non-pretensioned bolted specimens and pretensioned bolted specimens, individually, by shear type. These individual comparisons of bolted fastener types indicated that there was no statistically significant difference in dynamic specimen response for either fastener type. It was interesting, however, that a statistically significant difference appeared when all bolted fastener type, dynamic loading type specimen data were combined and compared by the shear type. This indication of statistical significance, or lack thereof, may have been due to the relative sizes of the samples. The all bolted specimens data set has a larger sample size (48 data points) while the individual fastener type sample size is much smaller (24 for each bolted fastener type). The sample variation may have forced any differences between the samples to be deemed insignificant because of the relatively small sample

size. The sample variation may have been reduced enough to allow the difference to become significant if the sample size was sufficiently large enough. This may have been the case for the individual bolted samples. Generally, the double shear specimens' response means for the individual data sets was larger than those subjected to single shear. The sample variation may have caused any difference to be deemed statistically insignificant.

The first t-test analysis on bolted specimens subjected to quasi-static loading type compared all bolted specimens by their fastener type to determine if bolt pretension significantly affected the specimen response. The plot of the sample data is shown in Figure 43. The means were 0.572 (CV of 5%) and 0.600 (SD of 6.5%) for non-pretensioned and pretensioned specimens, respectively. The mean difference was 0.027 (RMD of 4.8%), and the standard error of the difference was 0.009. These values resulted in a t-statistic of 3.099 and probability that the specimens were not affected by bolt pretension of 0.003 (degrees of freedom were 52). These results indicate the specimen response was statistically significantly affected by bolt pretension. However, the mean difference correlated to approximately 300 lbf (2 ksi). This difference could be attributed to variability in the individual specimen strengths, very low response variations, or instrumentation, as stated for the overall quasi-static specimen comparisons in Section 6.3. Therefore, this difference was not significant from a practical engineering standpoint. Since there was no practical difference in response caused by bolt pretension, other factors affecting the responses from all bolted specimens combined were analyzed.

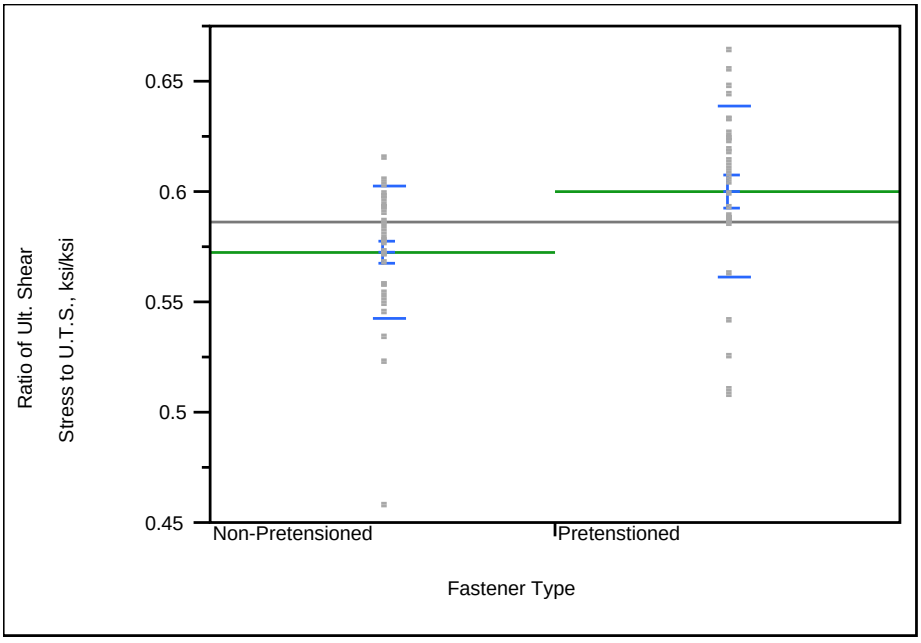

Figure 43: Comparison by Fastener Type for All Bolted, Quasi-Static Loading Type Specimens.

The second t-test analysis compared all bolted, quasi-static specimens by the shear type. A plot of the sample data is shown in Figure 44. The samples have means of 0.577 (CV of 6.5%) and 0.595 (CV of 6%) for double and single shear specimens, respectively, and the mean difference was 0.018 (RMD of 3.1%). The standard error of the difference was 0.009. The difference values result in a t-statistic of 1.980 and probability that the samples were not affected by shear type of 0.052 (degrees of freedom were 60). This indicated a nearly statistically significant difference in the sample means. The mean difference correlated to approximately 200 lbf (1.5 ksi) and can be attributed to the variability in the individual specimen strengths, very low response variations, or instrumentation. Therefore, this difference was not significant from a practical engineering standpoint. The non-pretensioned and pretensioned bolts

were compared to each other for single and double shear response individually. This analysis concluded that there was no statistical difference for double shear and statistically significant difference for single shear.

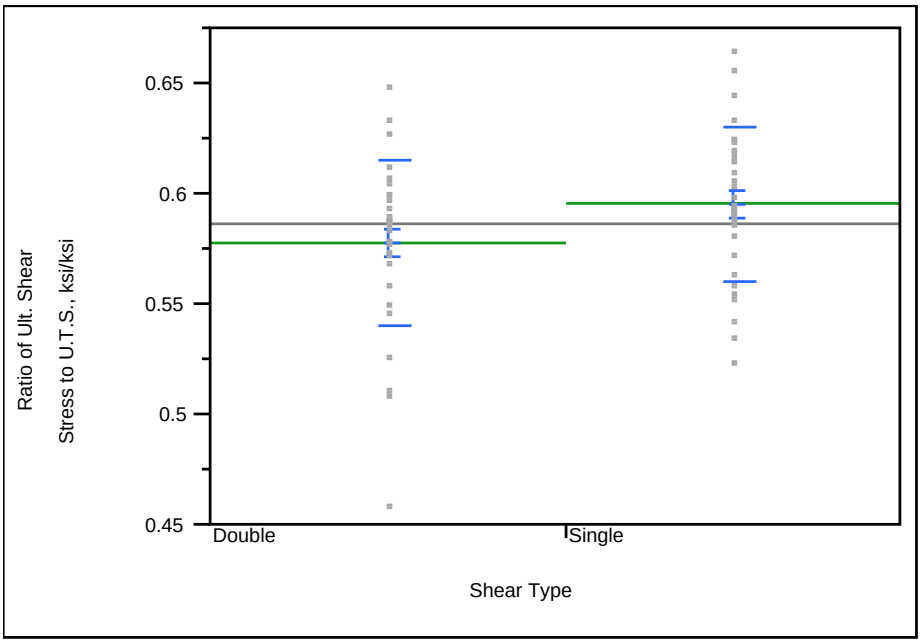

Figure 44: Comparison by Shear Type for All Bolted, Quasi-Static Loading Type Specimens.

The final t-test analysis on bolted specimens subjected to quasi-static loading type compared the response across all the configuration types. The values for the set of t-tests are shown in Table 23. The table indicated that all the joint configurations were not statistically different from each other except for Joint Configuration 1. The plot of the sample data is shown in Figure 45. The means of Joint Configuration 2 through 5 were at most different by 0.010 (or roughly 100 lbf, or 0.8 ksi) from one another. The mean of Joint Configuration 1 was 0.553 (CV of 10%) and had an average mean

difference of 0.042 (RMD of 6.9%) to the other configurations. This difference correlated to approximately 450 lbf (3 ksi). This difference was not practically significantly different from an engineering standpoint due to the variability of individual specimen strength, very low response variation, and instrumentation. Non-pretensioned and pretensioned specimens subjected to quasi-static loading type were compared to each other for each individual joint configuration. This analysis indicated that the means of the fastener types were different by a similar amount as in the overall comparison. Therefore, bolt pretension did not affect the shear response of a fastener placed in multiple joint configurations.

Table 23: t-test Values Comparing Joint Configuration for All Bolted, Quasi-Static Loading Type Specimens.

Sample A	Sample B	Absolute Value of Mean Difference	SD of Difference	Deg. of Fr.	t-test Statistic	Probability of t-test
Configuration 1	Configuration 2	0.0457	0.0136	7	3.3653	0.0120
Configuration 1	Configuration 3	0.0459	0.0136	7	3.3775	0.0118
Configuration 1	Configuration 4	0.0425	0.0133	7	3.1898	0.0153
Configuration 1	Configuration 5	0.0354	0.0136	7	2.6048	0.0352
Configuration 2	Configuration 3	0.0002	0.0139	8	0.0123	0.9905
Configuration 2	Configuration 4	0.0033	0.0136	8	0.2404	0.8161
Configuration 2	Configuration 5	0.0103	0.0139	8	0.7453	0.4774
Configuration 3	Configuration 4	0.0034	0.0136	6	0.2524	0.8092
Configuration 3	Configuration 5	0.0105	0.0139	6	0.7576	0.4774
Configuration 4	Configuration 5	0.0071	0.0136	10	0.5202	0.6142

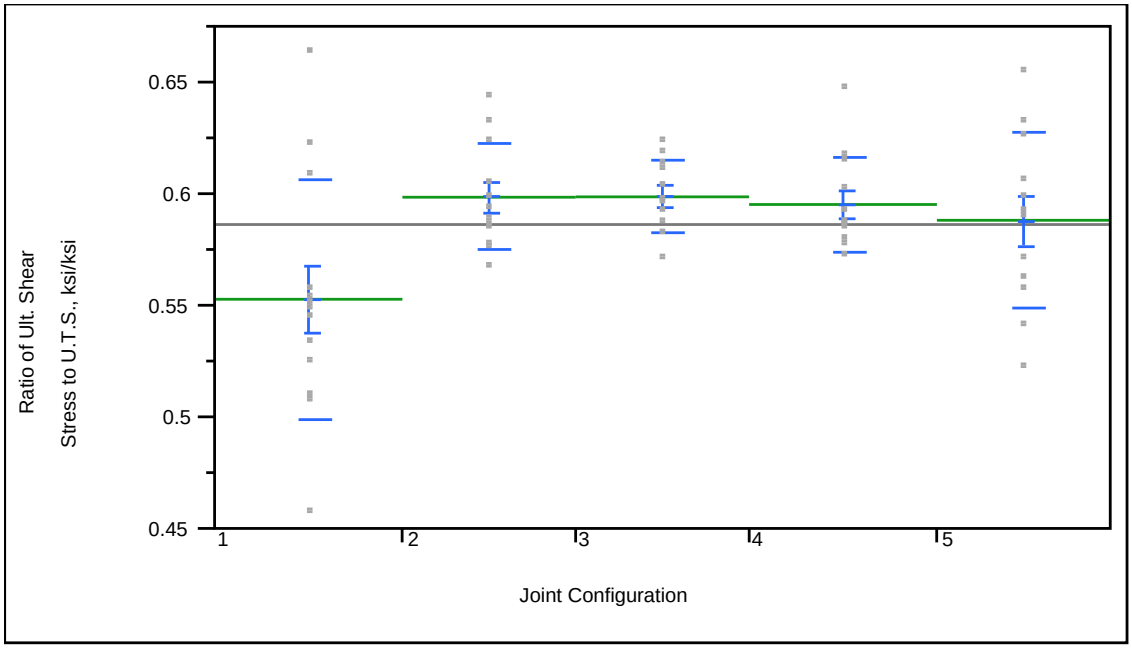

Figure 45: Comparison by Joint Configuration for All Bolted, Quasi-Static Loading Type Specimens.

In summary, the analysis of bolted specimens tested in this thesis indicated that all bolted fasteners subjected to dynamic loading type have 78% more ultimate shear strength than specimens subjected to quasi-static loadings, with respect to the fastener's ultimate static tensile strength. It also indicated that bolt pretension does not affect the ultimate shear capacity of a bolt fastener for either loading type. This verified previous research that had concluded bolt pretension did not affect the fastener shear strength when subjected to quasi-static loadings. Analysis of the research gathered for this thesis indicated this conclusion holds true for bolts subjected to monotonic dynamic loadings. However, the larger variations seen in the dynamic loading type specimen data may have masked any effects on the shear response.

Further analysis of the data showed that bolt pretension did not affect the response of the fastener when observing the effects of other factors, such as shear type or joint configuration, for either loading type. Additionally when analyzing all bolted specimens data, the analysis of specimens subjected to the dynamic loading type indicated that double shear specimens have a statistically significant greater response than single shear specimens, although analysis of each bolted fastener type individually did not indicate such, more than likely due to a smaller sample size and similar response variation masking any differences. The increase in strength for bolts in double shear could be attributed to the presence of a bending (tensile or compressive) force or failure in the longer bolt, but it cannot be proven due to damage of the bolt failure surfaces.. All bolted specimens under quasi-static loadings showed a statistically significant difference in the response based on all the factors, but the sample differences were small enough to be considered not practically different from an engineering standpoint.

7. CONCLUSIONS

The analysis of results of the tests performed in this thesis justified the following conclusions about the shear strength of various structural fasteners under multiple loadings, shear types, and joint configurations.

1. Loading type (dynamic or quasi-static) had the most significant effect on the shear strength of a fastener, regardless of the type of fastener, configuration, or shear type. The dynamic increase ratio, which compares ultimate dynamic shear strength to ultimate quasi-static shear strength (each normalized to the fastener's ultimate static tensile strength), was 1.75 for all fasteners combined and was 1.78, 1.78, and 1.72 for non-pretensioned bolts, pretensioned bolts, and rivets, respectively.

2. Overall, specimens subjected to the quasi-static loading type were not practically affected by shear type, joint configuration, and fastener type.

3. Overall, specimens subjected to the dynamic loading type were not affected by shear type, joint configuration, and fastener type. Note that all Joint Configuration 5 specimens subjected to the dynamic loading type were excluded from analysis; therefore, the relationship of this configuration to others was not established.

4. Riveted specimens subjected to the quasi-static loading type were statistically significantly affected by the shear type. The riveted, double shear specimen response was statistically significantly less than the riveted, single shear specimen response and may be caused by an increase in initial tension (causing less available shear strength) in

longer grip lengths (single shear rivets were half the length of double shear rivets, 1 inch to 2 inches).

5. All bolted specimens combined subjected to the dynamic loading type were statistically significantly affected by shear type. The bolted specimens showed a difference (double shear specimens were stronger than single shear specimens) when both types were combined, even though individually no difference was indicated.

6. Riveted specimens subjected to the dynamic loading type were statistically significantly affected by joint configuration. The sample means, however, had very high sample variations (almost ±40% of the sample mean), and the sample sizes were small. Therefore, it is difficult to determine the cause of this effect.

7. Bolt initial tension did not affect the specimen ultimate shear strength regardless of loading type, shear type, or joint configuration.

8. The quasi-static shear strength of bolts (average ratio of 0.587 for ultimate shear stress to ultimate tensile strength) was similar to the design strength in AISC Steel Design Manual (0.563 for bolts using the bolt's actual cross-sectional area), to the strength found in the "Guide to Design Criteria…" (0.620), and to available shear strength according to von Mises failure criterion (0.577).

9. The quasi-static shear strength of rivets, normalized to the undriven rivet ultimate tensile strength (0.690 overall, 0.741 for single shear, 0.638 for double shear), was within the range of values for the ratio of shear stress to tensile strength determined by Kulak et al. (1987) and Schenker (1954).

10. The increase factor of 1.2 was a good estimate for undriven rivet ultimate tensile strength to driven rivet ultimate tensile strength. The mean ratio of rivet, quasi-static specimen shear strength to the estimated ultimate driven rivet tensile strength was 0.577, which is similar to the bolt design shear strengths and von Mises failure criterion for ductile material shear strength.

11. The dynamic loading type induced a higher variability in the data than the quasi-static loading type (coefficient of variation of 26% and 6% for dynamic and quasi-static, respectively), possibly masking any significant differences in the data.

12. Riveted specimens had more variation than the bolted specimens (30% to 25% and 14% to 6% for dynamic and quasi-static loading types, respectively).

The conclusions stated above are based solely on the data gathered during testing of the 224 specimens. Their individual responses may or may not be indicative of the global responses of the specimen types.

8. RECOMMENDATIONS FOR FUTURE TESTING

The following recommendations for future testing have been established following the analysis of the test data.

1. Retest the bolted, Configuration 5 specimens, since the data were excluded because of instrumentation malfunctions,
2. Add a mechanical damper to the accelerometers to eliminate possible noise/ringing from being recorded,
3. Perform several more tests on all bolted sample types to reduce the variation and determine whether some of the effects seen in the combined bolted sample analysis are true for individual bolt types.

REFERENCES

ASTM (2003). "Standard Specification for Rivets, Steel, Structural." Standard A502-03, ASTM International, West Conshohoken, PA.

ASTM (2010). "Standard Specification for Carbon Steel Bolts and Studs, 60,000 PSI Tensile Strength." Standard A307-10, ASTM International, West Conshohoken, PA.

ASTM (2011). "Standard Test Methods for Determining the Mechanical Properties of Externally and Internally Threaded Fasteners, Washers, Direct Tension Indicators, and Rivets." Standard F606-11a, ASTM International, West Conshohoken, PA.

ASTM (2013). "Standard Test Methods for Tension Testing of Metallic Materials." Standard E8-13a, ASTM International, West Conshohoken, PA.

Baron, Frank and Larson Jr., E. W. (1955). "Comparison of Bolted and Riveted Joints." *Transactions*, Vol 120, Paper 2778. Pages 1322-1335. ASCE, VA.

Bendigo, R. A., Hanson, R. M., and Rumpf, J. L. (1963). "Long Bolted Joints." *Journal of the Structural Division*, Vol 89. No ST6, Proc. Paper 3727. Pages 187-213. ASCE, VA.

Carleton, H. D. (1970). "Digital Filters for Routine Data Reduction." *Miscellaneous Paper*, N-70-1. U.S. Army Engineer Waterways Experiment Station. Vicksburg, MS.

Carter, Jack W., Lenzen, Kenneth H., and Wyly, Lawrence T. (1955). "Fatigue in Riveted and Bolted Single-Lap Joints." *Transactions*, Vol 120. Paper 2778. Pages 1353-1380. ASCE, VA.

Clements, E. W. (1956). "Properties of Bolts Under Shock Loading." *NRL Report*, 4817. Naval Research Laboratory, Washington, D.C.

Chesson, E., Jr. (1964). "High Strength Fasteners Versus Rivets." *Building Research Institute Conference*. Washington, D.C. Found in Munse (1970).

Flathau, W. J. (1971). "Dynamic Tests of Large Reinforcing Bar Splices." *Technical Report* N-71-2. U.S. Army Engineer Waterways Experiment Station, Vicksburg, MS.

Foreman, Robert T. and Rumpf, John L. (1961). "Static Tension Tests of Compact Bolted Joints." *Transactions*, Vol 126. Paper 3125. Pages 228-254. ASCE, VA.

Hayter, Anthony J. (2002). "Comparing Two Population Means." *Probability and Statistics: For Engineers and Scientists*, 2nd Edition, Duxbury, Pacific Grove, CA. Pages 432-438.

Hechtman, R. A., Young, D. R., Chin, A. G., and Savikko, E. R. (1955). "Slip of Joints Under Static Loads." *Transactions*, Vol 120. Paper 2778. Pages 1335-1352. ASCE, VA.

Higgins, T. R. (1951). "Bolted joints found better under fatigue." *Engineering News-Record*. Vol. 147. Pages 35-36.

Higgins, T. R. and Munse, W. H. (1952). "How much combined stress can a rivet take?" *Engineering News-Record*. Vol. 149. No. 23. Pages 40-42.

Higgins, T. R. and Ruble, E. J. (1955). "Structural Uses of High-Strength Bolts." *Transactions*, Vol 120. Paper 2778. Pages 1389-1398. ASCE, VA.

Jones, Jonathon (1956). "Effect of Bearing Ratio on Static Strength of Riveted Joints." *Journal of the Structural Division*. Vol 82. No. ST6. Paper 1108. ASCE, VA.

Kaplan, S. (1959). "Double Shear Tests of High Strength Bolts." *Fritz Laboratory Reports*, Paper 271.4. Lehigh University, Bethlehem, PA.

Kulak, Geoffrey L., Fisher, John W., and Struik, John H. A. (1987). "Guide to Design Criteria for Bolted and Riveted Joints, Second Edition." *Research Council on Structural Connections*. American Institute of Steel Construction, Chicago, IL.

Maney, G. A. (1946). "Predicting Bolt Tension." *Fasteners*, Vol. 3, No. 5.

McKinnon, Dane (2007). "Tension vs. Torque Explained (sort of…)." *FAQ: Ask the Expert*. http://www.portlandbolt.com/faqs/tension-vs-torque-explained-sort-of/. (June 2013).

Munse. W. H. (1970). "Final Report on Riveted and Bolted Structural Joints, Project IHR-5." *Structural Research Series* No. 365. August. University of Illinois Engineering Experiment Station, Champaign, IL.

Munse, W. H., Wright, D. T. and Newmark N. M. (1955). "Laboratory Tests of Bolted Joints." *Transactions*, Vol 120. Paper 2778. Pages 1299-1318. ASCE, VA.

Munse, W. H. and Cox, H. L. (1956). "The Static Strength of Rivets Subjected to Combined Tension and Shear." *University of Illinois Engineering Experiment Station Bulletin*. Vol 54, No. 437. University of Illinois Engineering Experiment Station, Champaign, IL.

Rupmf, John L. (1958). "Shear Resistance of High Strength Bolts." *Fritz Laboratory Reports*, Paper 271.3. Lehigh University, Bethlehem, PA.

Schenker, Leo, Salmon, Charles G., Johnston, Bruce Gilbert (1954). "Structural Steel Connections." *Engineering Research Institute*, AFSWP Report No. 352. University of Michigan, Ann Arbor, MI.

Stewart, W.C. (1955). "History of the Use of High-Strength Bolts." *Transactions*, Vol 120. Paper 2778. Pages 1296-1298. ASCE, VA.

"Silicone Fluid Resources." (2014). *ESCO Products, Inc.* http://buysiliconefluid.com/resources.html#compressibility.

"Torque-Tension Relationship for Metric Fasteners." (2009). *Fastenal*. http://www.fastenal.com/content/feds/pdf/Torque-Tension%20Chart%20for%20Metric%20Fasteners.pdf. (June 2013).

Wallaert, James J. and Fisher, John W. (1962). "Shear Strength of High-Strength Bolts." *Fritz Laboratory Reports*. Paper 1822. Lehigh University, Bethlehem, PA. http://preserve.lehigh.edu/engr-civil-environmental-fritz-lab-reports/1822

Wilson, W. M. and Oliver, W. A. (1930). "Tension Tests of Rivets." *University of Illinois Engineering Experiment Station Bulletin*. Vol. 27, No. 43. University of Illinois Engineering Experiment Station, Champaign, IL.

Wright, D. T. and Munse, W. H. (1952). "Static Tests of Bolted and Riveted Joints." Structural Research Series No. 20. University of Illinois Engineering Experiment Station, Champaign, IL.

Additional Sources

Fisher, J. W. and Beedle, L. S. (1964). "Bibliography on Bolted and Riveted Structural Joints, ASCE Manual No. 48 (67-15)." *Fritz Laboratory Reports*, Paper 201. Lehigh University, Bethlehem, PA. http://preserve.leheigh.edu/engr-civil-environmental-fritz-lab-reports/201

Fisher, J.W., Kormanik, Robert, Allan, R. N. (1966). "Supplement to Bibliography on Bolted and Riveted Structural Joints." *Fritz Laboratory Reports*, Paper 302.2. Lehigh University, Bethlehem, PA.

APPENDIX A

SHOP DRAWINGS FOR SPECIMEN CONFIGURATIONS

This appendix contains the shop drawings for each of the five different specimen configurations.

Configuration 1

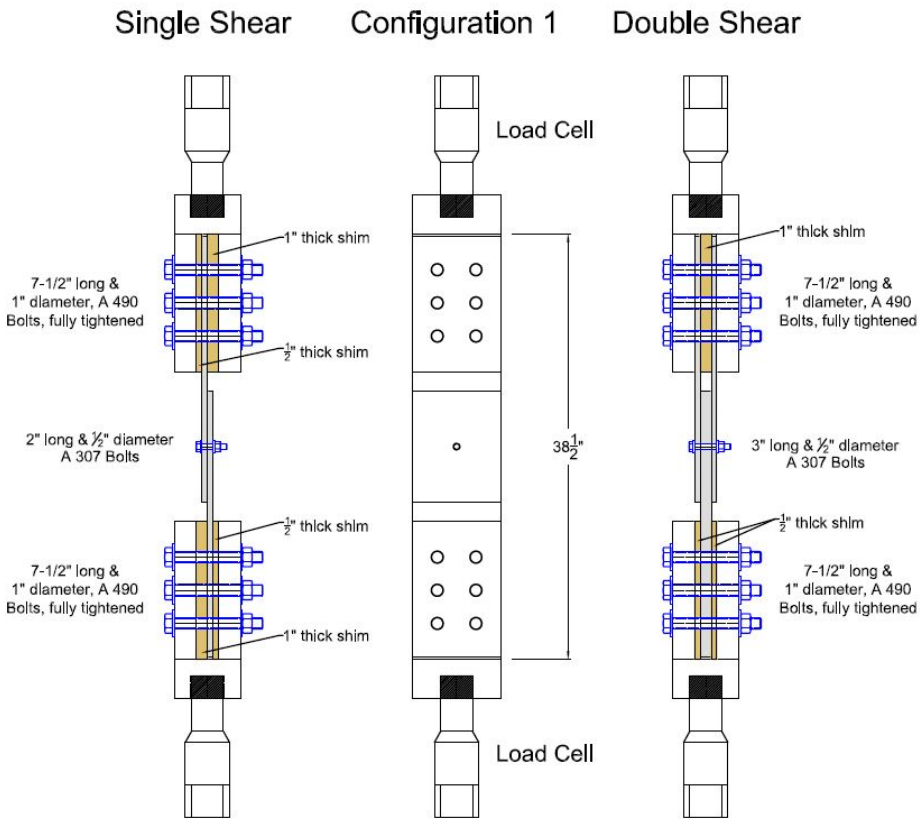

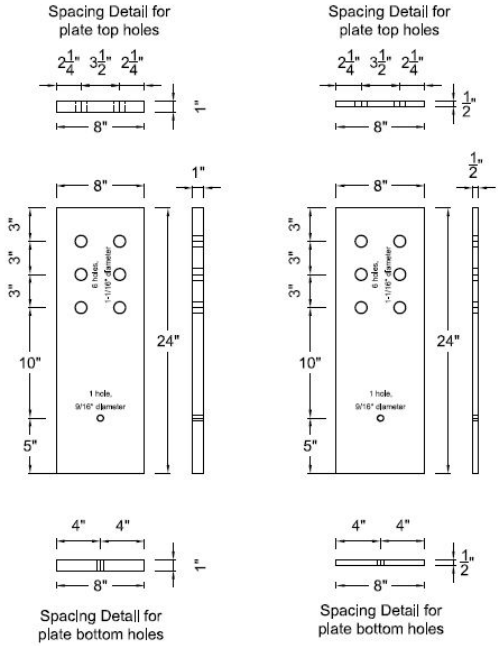

Configuration 2

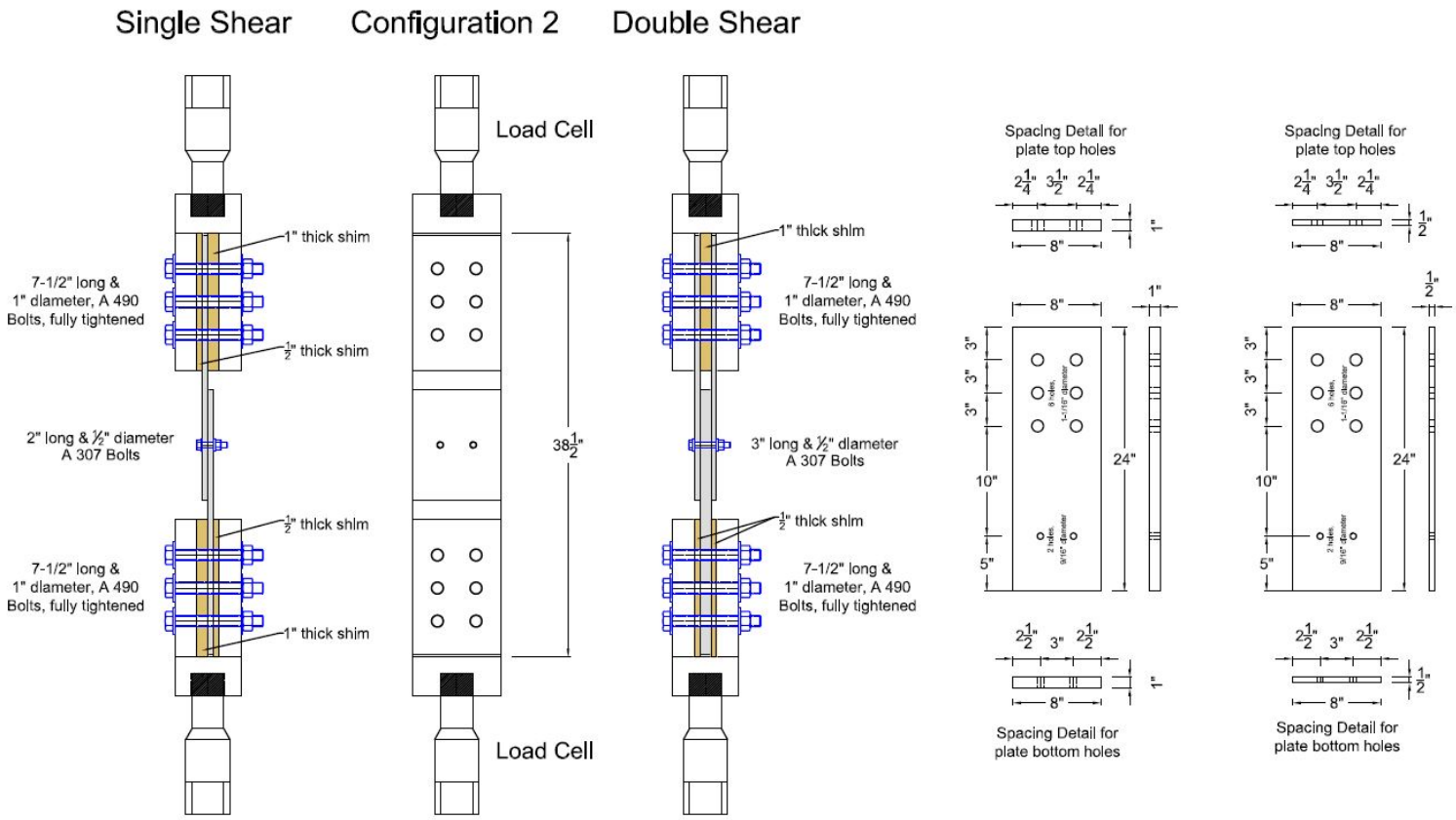

Configuration 3

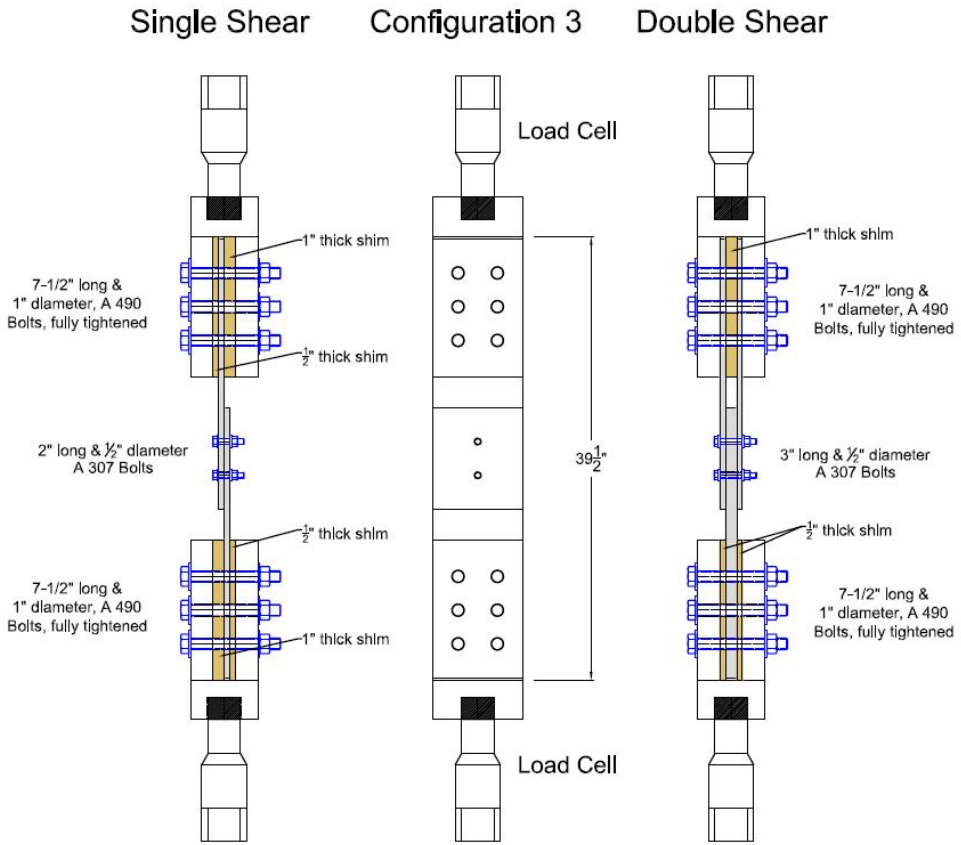

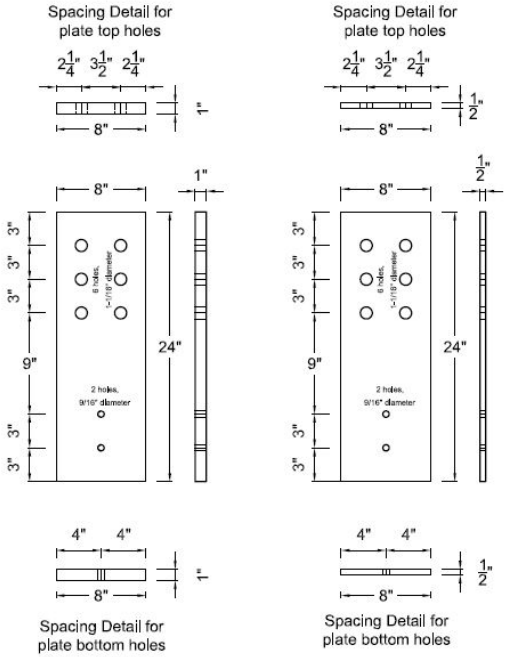

Configuration 4

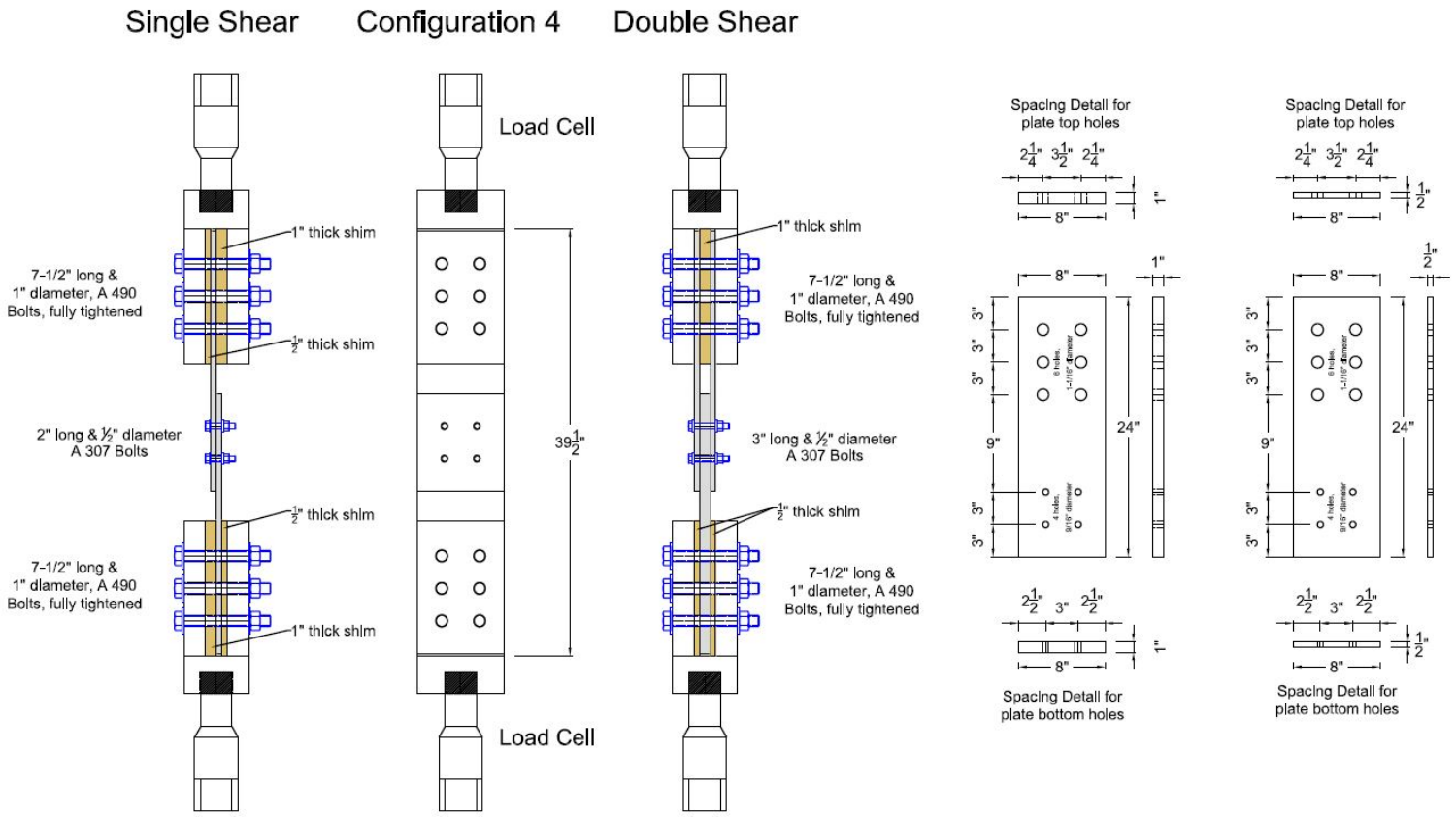

Configuration 5

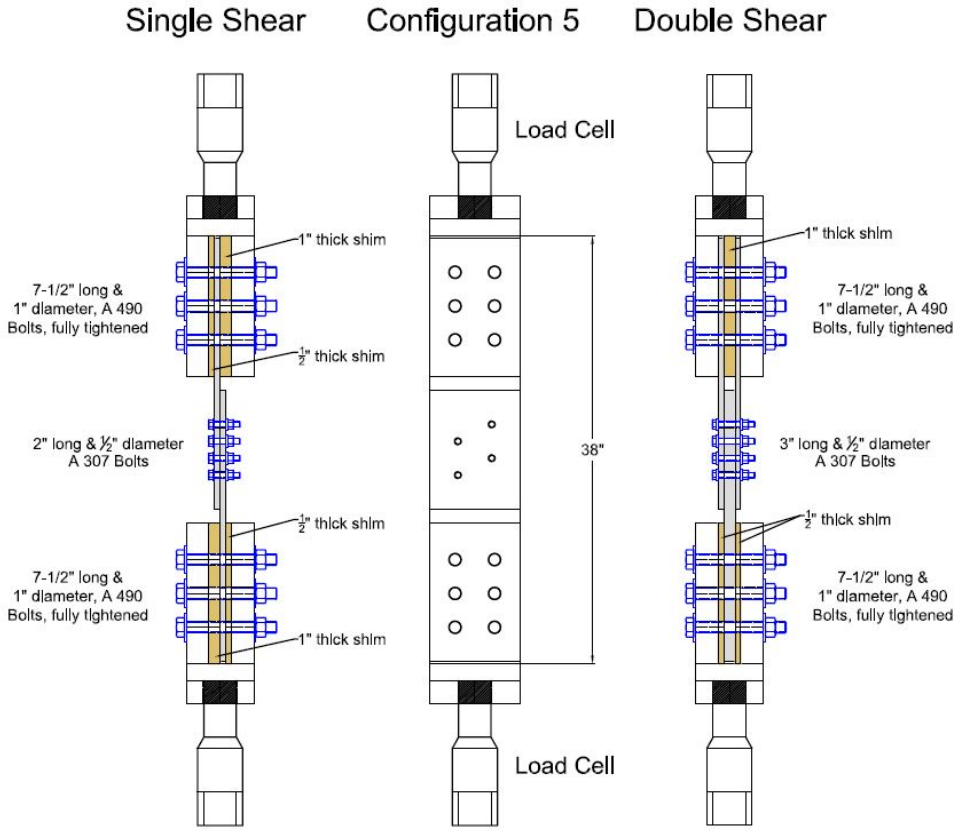

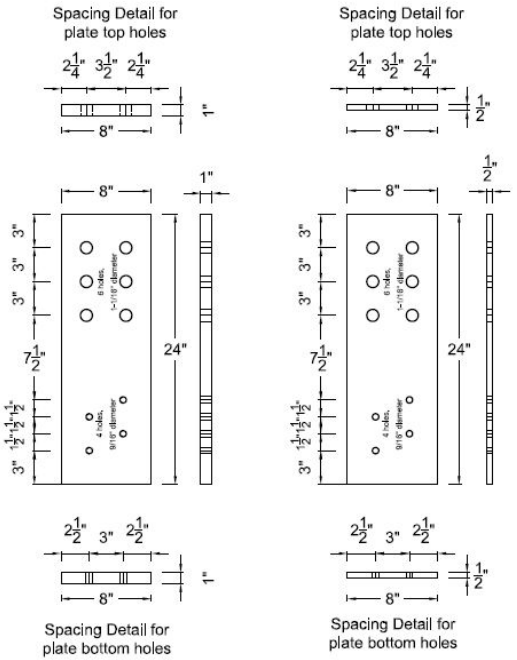

APPENDIX B

200-KIP DYNAMIC LOADER TECHNICAL DETAILS

This appendix details the testing machine used for loading the bolted and riveted specimens. Included is a description of the area where testing was conducted, information and schematics about the dynamic loader and its operation, as well as the specific components that allow the machine to adjust amount and rate of force applied. Also included are details of the specific instrumentation used in the testing as well as the established procedure for processing the load cell and accelerometer data collected.

B.1 Site Overview

The site where the test series was conducted is located in a temperature-controlled room containing the 200-Kip Dynamic Loader at USACE-ERDC in Vicksburg, MS, shown in Figure 46. The main components of the site are labeled by letters in Figure 46. 'A' is the "command center" for the operation of the dynamic loader. This is where the data acquisition system, high-speed camera recording system, and pressurizing control system is located. 'B' is the location of the high-speed camera, when it is used. The two (2) 1000-watt lamps used to provide adequate lighting for high-speed camera footage are placed closer to the 200-kip dynamic loader, 'C'. 'C' is also the location of the test specimen which is surrounded by the reaction structure (tall, grey, steel tower and red and grey base) of the 200-kip dynamic loader, which is detailed in section B.2.1. 'D' is the location of the pressurizing system, detailed in section B.2.2. 'E'

is the location of the rapid-opening valve (not seen as it is behind the “command center”), detailed in section B.2.3.

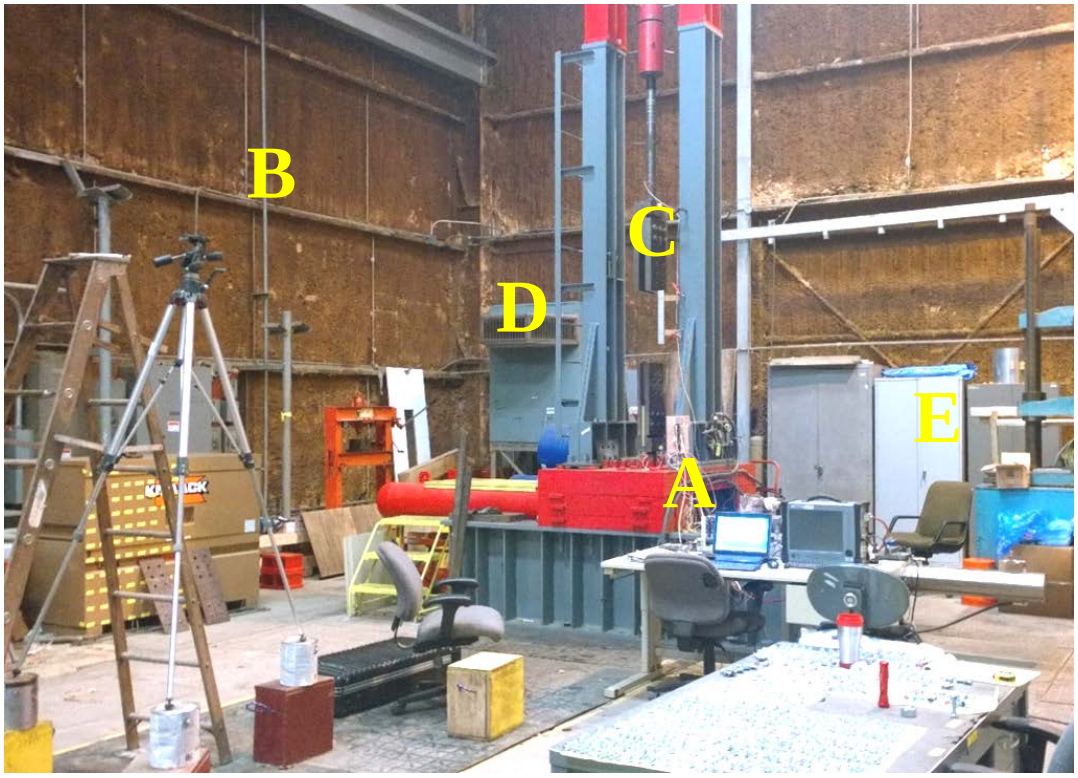

Figure 46: Overall View of Experimental Site.

B.2 200-Kip Dynamic Loader Information

All the tests for this thesis were conducted using the 200-Kip Dynamic Loader shown in Figure 46, which is hydraulically actuated with a rigid support system (reaction structure) and is capable of applying up to a 200-kip load in 1.5 milliseconds by rapidly releasing the pressure of a compressed fluid (Flathau 1971). The maximum stroke of the loader is 4 inches. The 200-kip loader has three main components, detailed in the

subsections below, the ram operation and reaction structure, pressurization system, and the rapid-opening valve.

B.2.1 Ram Operation and Reaction Structure

Three (3) components (indicated by some of the letters in Figure 47) make up the inner workings of the 200 kip loader. The first component, the ram (A) and piston (D) assembly, is the only component of the 200-Kip Dynamic Loader that moves. The ram attaches to the bottom of the test specimen through the bottom load cell and bottom grip. The piston provides the surface area for the pressure contained in the upper chamber (B) and the lower chamber (C) to act on to keep the test specimen in place during test preparations or to apply the breaking force once the loader is fired. Pressure tanks (F) are attached to the upper chamber. 'E' (as shown) is the expansion tube that is used post-firing. The expansion tube shown in Figure 47 was moved when the rapid-opening valve was added to the loader in 2011, which now occupies the area denoted by 'E'.

Prior to firing the ram, a preload of 1000-2000 lbf is placed on the test specimen, in order to allow the loader to fire correctly. Then, up to 6000 psi of pressure is slowly placed into the upper and lower chambers. The preload and unequal surface areas on the top and bottom of the piston cause a slight difference in the pressures between the chambers. When pressurized to the desired level, the loader is fired. Upon firing, the rapid-opening valve releases the pressure in the lower chamber. Due to a pressure differential between the two chambers, the pressure above the piston forces the ram to

move downward, as indicated by the red arrow in Figure 47. The setup of the pressure release valve allows the piston/ram to only move in the downward direction.

The top of the test specimen is attached to the reaction structure, the majority of which is located above the pressure chambers. The reaction structure has a few components that were designed so that when correcting load applications, it can be said the reaction structure is completely rigid. These components are shown in Figure 48. ‘A’ is the solid rod that connects the top of the test specimen to the cross-beam, ‘B’. It also has the top load cell integrated into it as shown in section B.3.1. The cross-beam, ‘B’, is mounted on the tower legs, ‘C’, which dissipate the remaining force to the strong floor through the bottom reaction structure, ‘D’ and ‘E’. The bottom reaction structure contains the ram and pressure chambers.

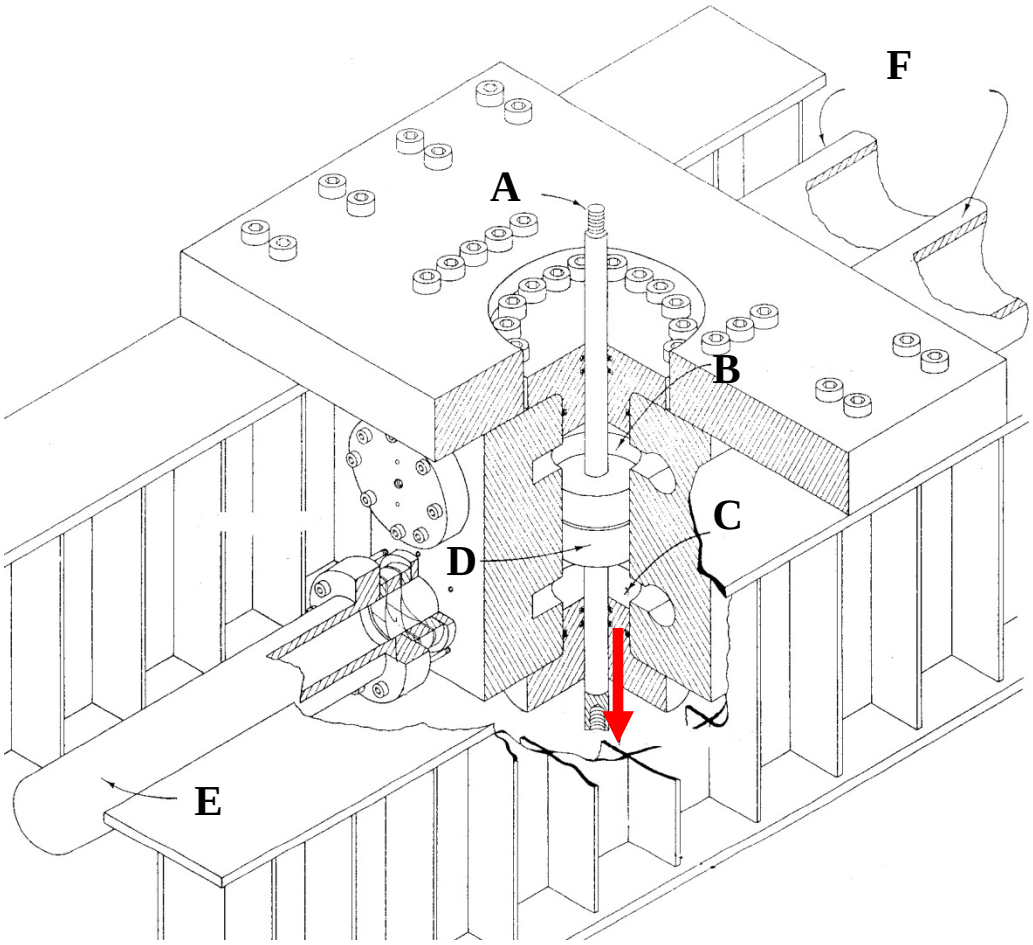

Figure 47: Sectioned View of Internal Components of Rapid Loading Machine (Flathau 1971).

Figure 48: Reaction Structure of 200 kip Dynamic Loader.

B.2.2 Pressurization System

Since the loader operates based on the principle of pressure differentials, the pressurization system is critical in correctly testing a test specimen. The chambers described in the previous section are filled with compressible fluid called Xiameter (formerly Dow Corning) PMX-200 Silicon Fluid 100cst (see Figure 49 for the fluid

compressibility chart), which is stored in drums ‘B’ and ‘C’ in Figure 50. This allows for the use of a constant volume (CV) pump, ‘D’ in Figure 50, to pressurize the two chambers. Pressure in the chambers is slowly built up to the desired level by strokes of the pump, powered by a pneumatic airline pressurized to about 110 psi, which injects a small amount of the fluid at a time into the chambers. Approximately one pint of fluid will be pumped into the chambers. The flow of the fluid is directed into one or both of the chambers by the use of solenoid valves. The solenoid valves and CV pump are controlled by software specifically developed for this loader, which operates on a laptop in the “command center”. The software also allows for monitoring of quasi-static pressure changes inside the upper and lower chambers.

Prior to pressurizing the chambers, a constant flow course adjustment pump, ‘A’ in Figure 50, is used to completely fill the chambers with fluid (air enters the lower chamber post-firing and must be bled out) and to move the piston into the correct firing position. The course pump forces the fluid into the chambers through two gate valves (note: this is a completely separate system from the CV pump). A manual lever controls which chamber has fluid added to it and the direction the ram moves; moving the lever up will fill the lower chamber forcing the ram up, and moving the lever down will fill the upper chamber forcing the ram down. The course adjustment pump will also place the preload on the specimen by adding fluid to the upper chamber. The course adjustment pump fluid lines are closed off prior to the operation of the CV pump and pressurization of the chambers.

During the pressurization of the chambers, the pressurization system needs to be constantly monitored using the loader software and by watching a readout of the force seen by one of the load cells, due to the upper and lower chambers pressurizing at different rates because of the uneven surface area above and below the piston and maintaining the preload on the sample. Monitoring the chamber pressure is accomplished using the same loader software that operates the CV pump and solenoid valves. Monitoring of the preload is accomplished using the instruments shown in Figure 51. From left to right in Figure 51, a Fluke 45 Dual Display Multimeter is used to read the load cell output, and a PR-300 Compound Regulated Power Supply is used to supply a very clean electrical signal to the bridge (object on top of the multimeter), which connects the load cell to the multimeter. The bridge is calibrated in such a way that a value of 0.1 mV on the multimeter display equals approximately 100 lbf applied to the load cell and specimen. The preload during pressurization is kept at ± 500 lbf from the initial preload.

For the test series in this thesis, the operating pressures ranged from 2000 psi to 3000 psi.

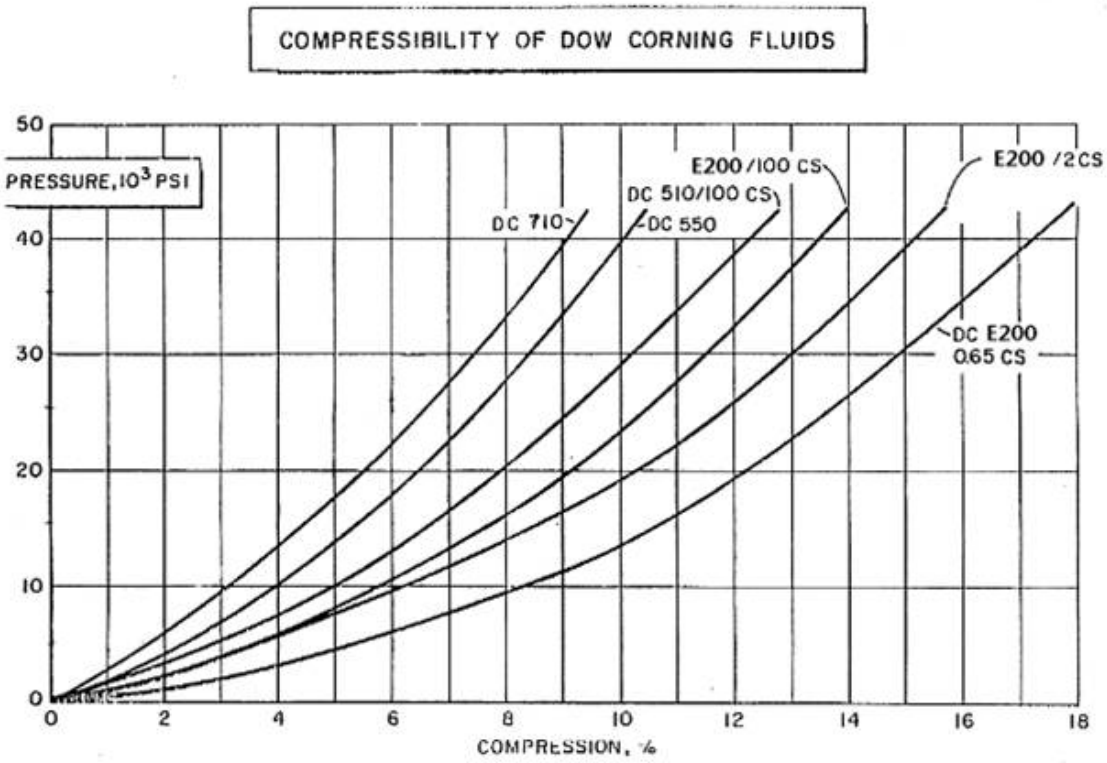

Figure 49: Typical Compressibility of Xiameter/Dow Corning Silicone Fluids (Silicone 2014).

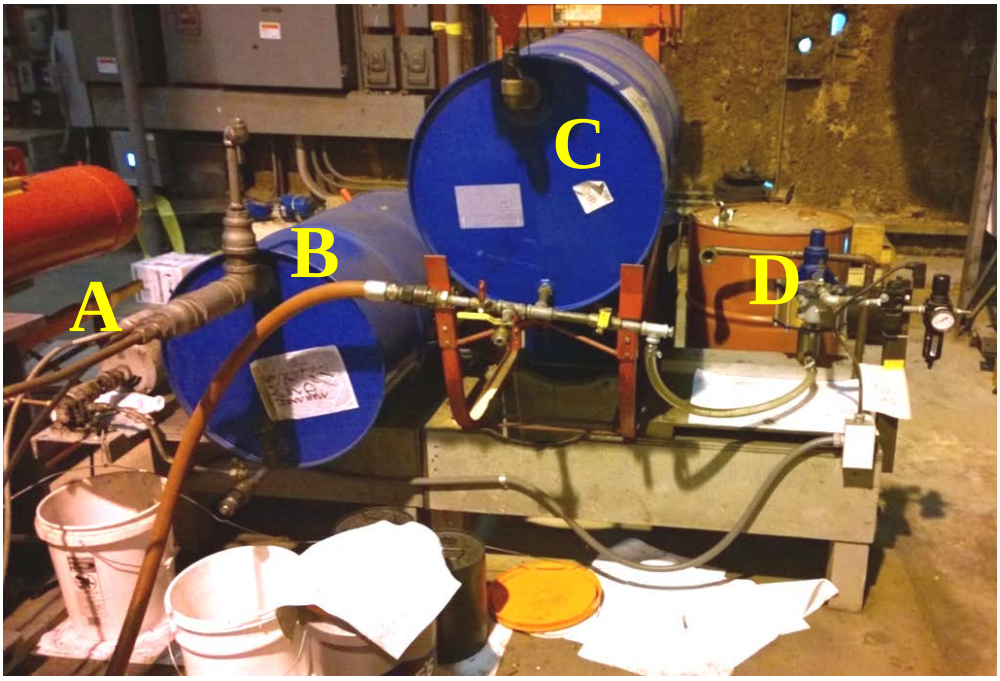

Figure 50: Components of Loader Pressurization System.

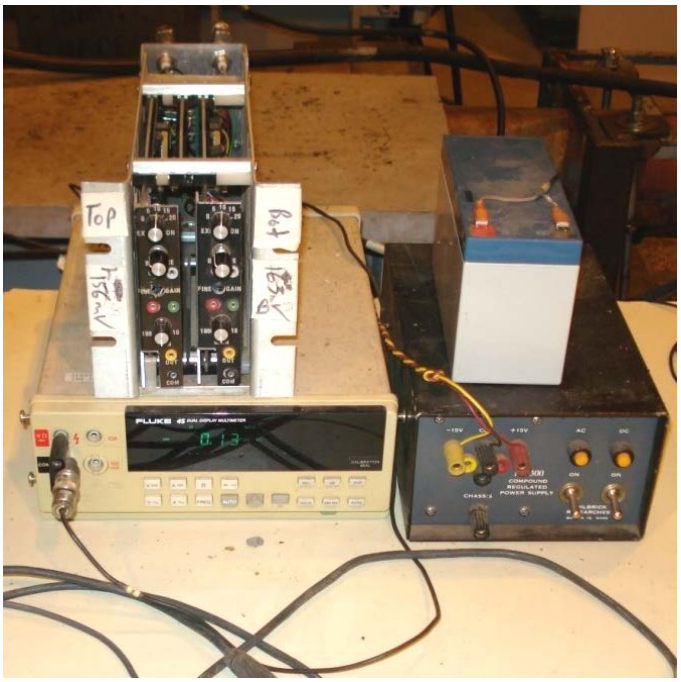

Figure 51: Components for Monitoring Pressurization Process.

B.2.3 Rapid Opening Valve

The 200-kip dynamic loader is able to apply large dynamic loads because of the rapid-opening valve shown in Figure 52. This valve, model #225-4.5-6000, was designed by Dynamic Systems and Research in Albuquerque, NM. Installed in 2011, the valve is capable of handling up to 6000 psi of a fluid flowing through a 4.5-inch-diameter orifice and allows for drastically reduced time between tests when compared to previous firing mechanisms installed on the 200-kip dynamic loader. The typical time between tests for this test series was at most 45 minutes compared to at least 1-2 hours using the previous firing mechanisms, a rupture disk firing system or a now-retired rapid opening valve, which had a capacity of 3000 psi.

The orifice is adjustable to almost any diameter between 4.5 inches (100% open) to 0 inches (fully closed). By controlling the diameter of the orifice, the flow rate of the fluid exiting the lower chamber is able to be controlled, therefore controlling the loading rate applied to the test specimen. For tests where a very slow load rate is required, the orifice is fully closed, and a very small bypass orifice (typically 1/16 inch to ¼ inch in diameter) is installed on the tube between the loader and the valve.

The major components of the valve are denoted by the letters A through F in Figure 52. ‘A’ is the housing of the rapid opening solenoid valve. ‘B’ is the adjustable orifice. ‘C’ is the bypass orifice. ‘D’ is the expansion tube, where the fluid exiting the lower chamber enters the valve. ‘E’ is where a supply of pure nitrogen is attached. Nitrogen at 225 psi is needed to ‘arm’ or ‘prime’ the valve for firing. This pressure physically moves the solenoid gate inside the valve. Nitrogen is used to eliminate

possible corrosion inside the valve. ‘F’ is the two co-axial cable inputs (‘ARM’ and ‘FIRE’) for remote control of the valve and a co-axial output for a trigger (sent to data acquisition system and high-speed camera).

The valve is fired correctly by first arming the valve by pressurizing the valve with nitrogen. There is not an exact time allotment for arming. When the “ARM” button is pressed and held, the operator listens until the sound of hissing (from nitrogen entering the valve) subsides. Second, while still holding the “ARM” button (otherwise the valve will de-pressurize), the “FIRE” button is pressed and held until the test is completed (specimen breaking). Finally, the “FIRE” button is released followed by the “ARM” button. The two buttons remain pressed during the test to ensure the solenoid valve remains open for the duration of the test because once the electrical signal sent to the valve is stopped, the solenoid valve will return to the closed position.

For the test series in this thesis, two orifice sizes were used: 4.5-inch diameter (100% open) for the dynamic tests and 1/16 bypass orifice (main orifice is fully closed) for the quasi-static tests.

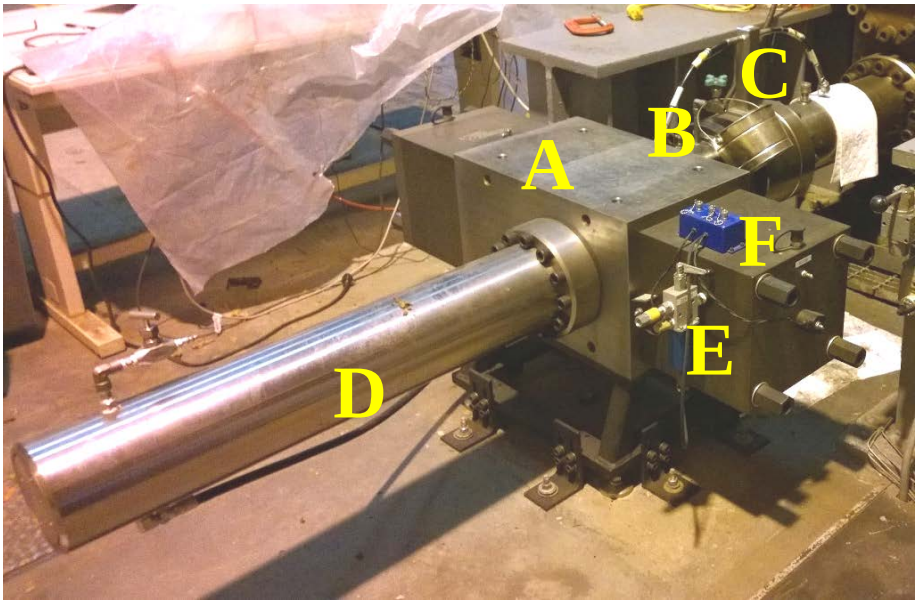

Figure 52: Rapid-Opening Valve.

B.3 Instrumentation

The following subsections detail the instrumentation used for the testing. Included are the primary instrumentation that was used to measure the data of interest, a data acquisition system, and a high-speed camera to capture the test on video.

B.3.1 Primary Instrumentation

Two load cells and two accelerometers are used to collect the primary data during testing. Figure 53 shows the location of these instruments on the testing apparatus and test specimen. A load cell is placed in tandem with an accelerometer above and below the test specimen. The location of the load cells and accelerometers is limited by the setup of the gripping mechanism and testing apparatus. The load cell below the specimen (bottom load cell) is shown in Figure 54. The load cell above the test specimen

(top load cell), shown in Figure 55, is integrated into the upper reaction structure and cannot be removed from the testing apparatus. In Figure 53, the letter A corresponds to the location of the top load cell, and the letter B corresponds to the location of the bottom load cell. The accelerometers can be moved easily and placed in the best possible location. They are mounted on the gripping mechanism, like the bottom accelerometer shown in Figure 56, as close as possible to one of the load cells in order to measure the acceleration at that load cell, which is critical for determining the influence of inertial effects, as detailed in Section B.4. In Figure 53, the letter C corresponds to the location of the top accelerometer, and the letter D corresponds to the location of the bottom accelerometer. Due to the nature of shear stress planes and testing mechanism, it was not feasible to add any other primary instruments, such as strain gauges or displacement measuring devices.

The top and bottom load cells are custom made strain gauged load cells for the testing apparatus with a maximum working capacity of 200 kips. The load cells were designed and constructed by the Sensors, Measurement, and Instrumentation Branch at ERDC. They are calibrated in such a way that a positive reading corresponds to tension and negative reading corresponds to compression in the load cell. After nearly half of the tests listed in the test matrix were completed, the top load cell permanently malfunctioned due to a gauge becoming un-mounted. The gauges were replaced, and the load cell was re-calibrated.

The accelerometers above and below the test specimen (denoted as top accelerometer and bottom accelerometer, respectively) were designed, manufactured,

and calibrated by two electronics companies. In total, four (4) different accelerometers, each with a peak sensitivity of 20,000 g's, were used in the test series. All four gauges measure acceleration along the axis it is oriented. For this thesis, the accelerometers were mounted to the specimen in a vertical orientation as to measure the acceleration of the specimen in the direction of loading. The accelerometers are calibrated in the data acquisition system in such a way that a positive acceleration corresponds to the specimen accelerating up and a negative acceleration corresponds to the specimen accelerating down. During the test series, if the lead wires from the gauge were damaged or cut, the accelerometer was replaced. The initial accelerometers used were Sigma 7270A 20K piezoresistive accelerometers, but they were damaged during testing. Two (2) PCB Electronics Model 3991A1120KG piezoresistive accelerometers were used for the remainder of the tests.

Figure 53: Overall View of Gauge Locations.

Figure 54: Bottom Load Cell.

Figure 55: Top Load Cell.

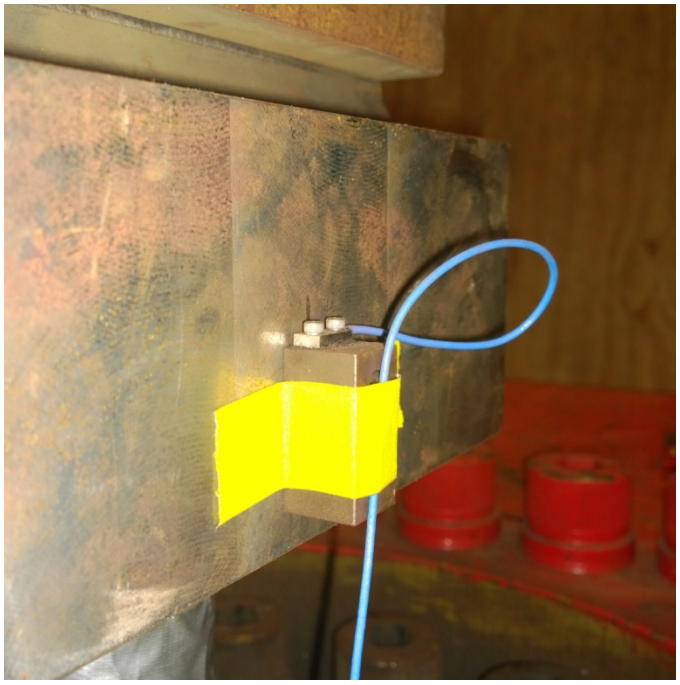

Figure 56: Typical Mounting of an Accelerometer to Specimen Grip.

B.3.2 Data Acquisition

The data from the primary instruments was collected using a Hi-Techniques Synergy P data acquisition system, shown in Figure 57. This system requires no other peripherals to record the data. The system contains its own operating system (Windows XP or 7), data input hardware, and data collection software. The Synergy is capable of collecting up to 16 channels (or gauges) of data at a 2-MHz sampling rate. The gauge outputs are correctly calibrated, and data are recorded using the Hi-Techniques Synergy software. The data from four (4) channels used for this test series are collected at a 100-kHz to 1000-kHz sampling rate for the dynamic tests and at a 10-kHz sampling rate for quasi-static tests. Acquisition of the data is triggered remotely when the rapid-opening valve discussed in Section B.2.3 is opened.

Figure 57: Hi-Techniques Synergy Data Acquisition System.

B.3.3 High-Speed Camera

A high-speed camera was used to record video footage of the tests, which helps to corroborate data collected on the Synergy. A Phantom v4.3 high-speed camera, shown in Figure 58, is used to record footage at 8113 fps for dynamic tests and 1000 fps for quasi-static tests. The resolution of the footage is limited to 256 pixels by 256 pixels because of the frame rate needed to accurately capture footage for dynamic tests. Later tests used a Phantom v5.1, which operated at same resolution but was able to use a higher frame rate. The camera is triggered using the same trigger as the data acquisition system. Two (2) 1000-watt lamps are used to provide adequate lighting on the specimens during recording of the testing. Camera footage is recorded and stored on a computer

connected to the camera using Phantom v675.2 software. The high-speed camera footage was used to aid in determining the time of maximum load and failure in the specimen.

Figure 58: Phantom High-Speed Camera.

B.4 Processing Load Cell and Accelerometer Data

When dealing with dynamic forces and moving masses, it is critical to account for the forces due to inertia, or moving mass, as it will have an effect on the measurements recorded by both the top and bottom load cells. That is why it is critical that accelerometers were used in this test series as the acceleration of the mass of the grips and ram needs to be considered to determine the true load applied to the test

specimen. The formula for calculating the force due to inertia of a mass is known as Newton's Second Law of Motion.

To simplify the processing of results of the test series, the mass and displacement of the grips, ram, and specimen are lumped together as shown in Figure 59. M_1 and x_1 are the mass and displacement of the upper grip assembly and half of the test specimen (approximately 425 lbf). M_2 and x_2 are the mass and displacement of the lower grip assembly and the other half of the test specimen (approximately 305 lbf). M_3 and x_1 are the mass and displacement of the ram and piston assembly. $\ddot{x}_1$ and $\ddot{x}_2$ are accelerations measured by the accelerometers.

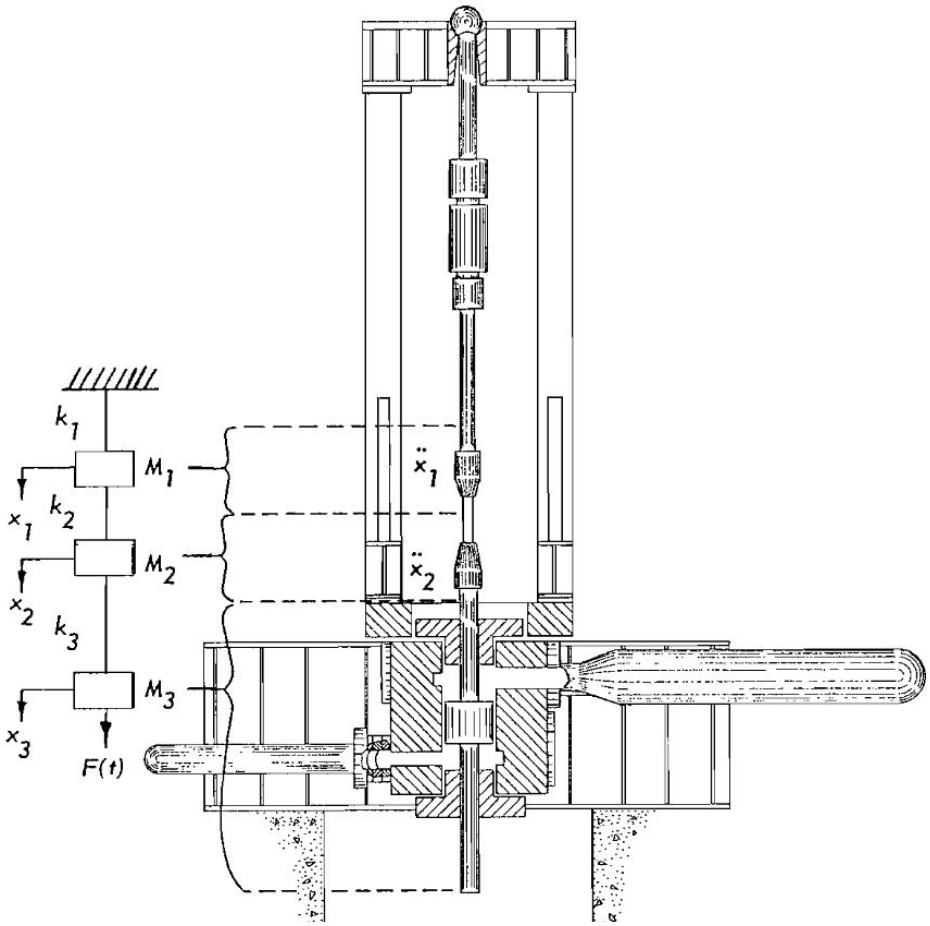

Figure 59: Spring-Mass Model of Test Configuration (Flathau 1971).

The uncoupled mass models with accompanying free-body diagrams and equilibrium equations are shown in Figure 60. The expressions k_1x_1 and $k_3(x_3 - x_2)$ in Figure 60 represent the load recorded by the upper and lower load cells, respectively. The expressions $M_1\ddot{x_1}$ and $M_2\ddot{x_2}$ represent the inertial force due to acceleration of the upper and lower grip assembly and test specimen, respectively. The expression $k_2(x_2 - x_1)$ represents the load applied to the test specimen. By performing equation substitution, equation (5) is the equilibrium of the actual forces in the top and bottom load cells.

$$k_3(x_3 - x_2) - M_2\ddot{x}_2 = k_1x_1 + M_1\ddot{x}_1 \quad (6)$$

This equation indicates that the inertial term for the top assembly is additive and for the bottom assembly is subtractive, assuming a positive acceleration is the downward direction. The orientation and calibration of the accelerometers assume a positive acceleration is in the upward direction; therefore equation (5) is changed to equation (6).

$$k_3(x_3 - x_2) + M_2\ddot{x}_2 = k_1x_1 - M_1\ddot{x}_1 \quad (7)$$

For tests where the acceleration on top and bottom is almost zero (like in the quasi-static set of tests), equation (6) is simplified to equation (7).

$$k_3(x_3 - x_2) = k_1x_1 \quad (8)$$

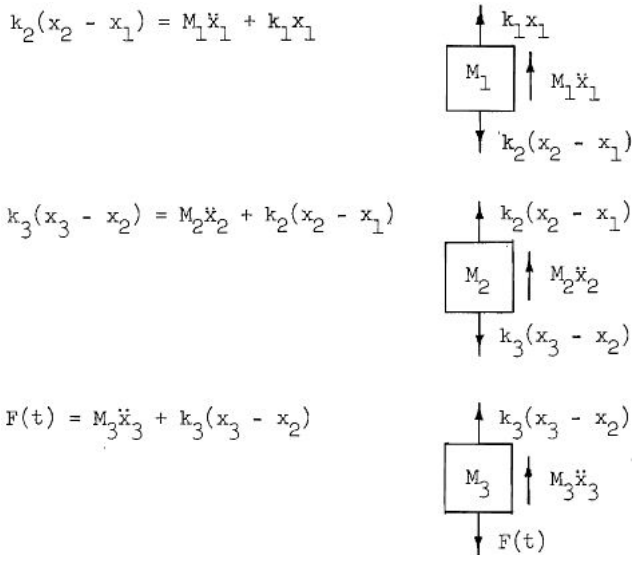

Figure 60: Uncoupled Mass Model and Free-Body Diagram with Equations of Motion and Equilibrium (Flathau 1971).

Analysis of the bottom load cell and accelerometers for inertial effects proved to be difficult due to the extremely complex nature of the accelerometer data compared to the load cell. The energy in the accelerometer data (a Fast-Fourier Transform of the data is squared and then integrated) is dominated by high-frequencies, those over 5000 Hz, whereas almost all of the energy in the load cell data is below 1000 Hz. The data results can be quickly dominated by inertial effects, even when the accelerometer data are filtered since the calculated amount of inertial force can be become large compared to original test data due to the large mass of the grips. Further analysis of the bottom load cell and accelerometer data should be completed in order to compare with the results of the top load cell and accelerometer.

Only data from the top load cell and accelerometer are used to determine the maximum applied force on the test specimen for the results presented in the following subsections. Therefore equation (8) is used to determine the applied force on the specimen.

$$\boldsymbol{k_2(x_2 - x_1) = k_1 x_1 - M_1 \ddot{x}_1} \qquad \textbf{(9)}$$

Dynamic tests have measured accelerations (even though the amount is small, the inertial effect must be accounted for due to the large amount of mass moving), therefore the equation to determine the applied force on the test specimen is used as is. However, quasi-static tests have accelerations of essentially zero; therefore equation (8) is simplified to equation (9) to determine the applied force on the specimen.

$$k_2(x_2 - x_1) = k_1 x_1 \qquad (10)$$

The graphing and data processing software DPlot was used to determine the correct maximum applied load on the test specimen. To correctly account for the inertial forces present in the dynamic loading tests, the load cell and accelerometer data had to be processed in a specific manner. The load cell and accelerometer data were placed on the same graph and shifted to where the constant values prior to the arrival of the load were essentially zero. The curves were then filtered using a robust built-in low pass filter, Option 4-Low Pass. This filter has a cut-off frequency of about 3-4% of the sampling frequency (Carleton 1970); the cut-off value for the filter is based on where the amplitude response is reduced by 3 dB. For the data collected in this research, this equates to a cutoff frequency of 3 kHz (dynamic) and 300 Hz (quasi-static). A velocity time history was calculated by integrating the acceleration time history. The acceleration time history is then multiplied by the mass of the top grip and test specimen to become the inertial force time history. This time history was subtracted from the original load cell time history, as described in equation (8). The resulting time history was the load applied to the test specimen accounting for inertial effects. The original load cell time history and applied load time history were shifted again by the value of the mean of the data after the applied load subsides and becomes a constant value again. The value of the leading mean is now the amount of preload measured on the specimen.

APPENDIX C

DATA PLOTS FOR ALL TEST SPECIMENS

This appendix contains all the data plots (Figure 61 through Figure 194) for tests conducted for this thesis. All dynamic tests are plotted individually. All quasi-static tests of the same fastener type, shear type, and joint configuration are plotted on the same graph. The plot order is pretensioned dynamic, non-pretensioned dynamic, pretensioned quasi-static, non-pretensioned quasi-static, riveted dynamic, and riveted quasi-static for each joint configuration from 1 to 5.

The labeling system for test names in the test series is in the following order: *Structural Fastener Type/Shear Type-Joint Configuration-Loading Type-Test Number.*

Test Characteristic	Label	Description
Structural Fastener Type	N	Non-Pretensioned Bolts
	R	Rivets
	S	Pretensioned Bolts
Shear Type	D	Double Shear
	S	Single Shear
Joint Configuration	1	Single Fastener
	2	Two Fasteners—Horizontal
	3	Two Fasteners—Vertical
	4	Four Fasteners—Square
	5	Four Fasteners—Staggered
Loading Type	D	Dynamic
	S	Quasi-Static

For the data plots of each dynamic test given in this appendix, a total of four curves are present: original load data, total load data, inertial force due to acceleration, and the velocity time history. The velocity time history was important in determining where to take the maximum load, as after the test specimen fails, the corrected time history can be highly dominated by inertial effects. Where the velocity time history becomes positive for the final time (again, down is negative and up is positive like the acceleration data), a maximum displacement down has occurred in the test. It was generally assumed that any data after this point occurred after the test specimen failed and was therefore invalid. In some tests, the velocity time history became positive twice. This was due to any sort of slip that can occur in the test sample causing the top grip to move upward. Therefore, the maximum applied load on the test specimen was taken prior to the velocity becoming positive for the final time. The point of failure of the specimen was corroborated by observing the significant slip of the specimen in the high-speed video footage. The time stamps on the high-speed footage and data plots are synced and allow for accurate corroboration.

The data plots shown for the quasi-static tests in this appendix have all time histories for tests of the same fastener type, joint configuration, and shear type on a single plot. Only the top load cell time history was used, since the movement seen by the top accelerometer was essentially zero for the quasi-static tests. Each load time history was still shifted and filtered in the same manner as the load time histories were for dynamic tests.

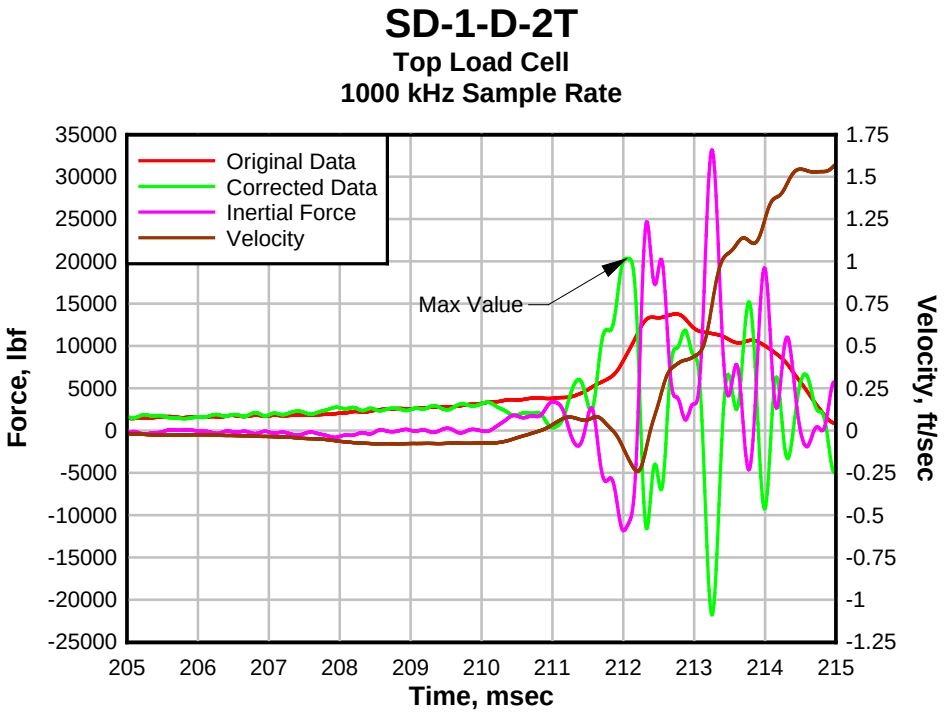

Figure 61: SD-1-D-2T Test Data.

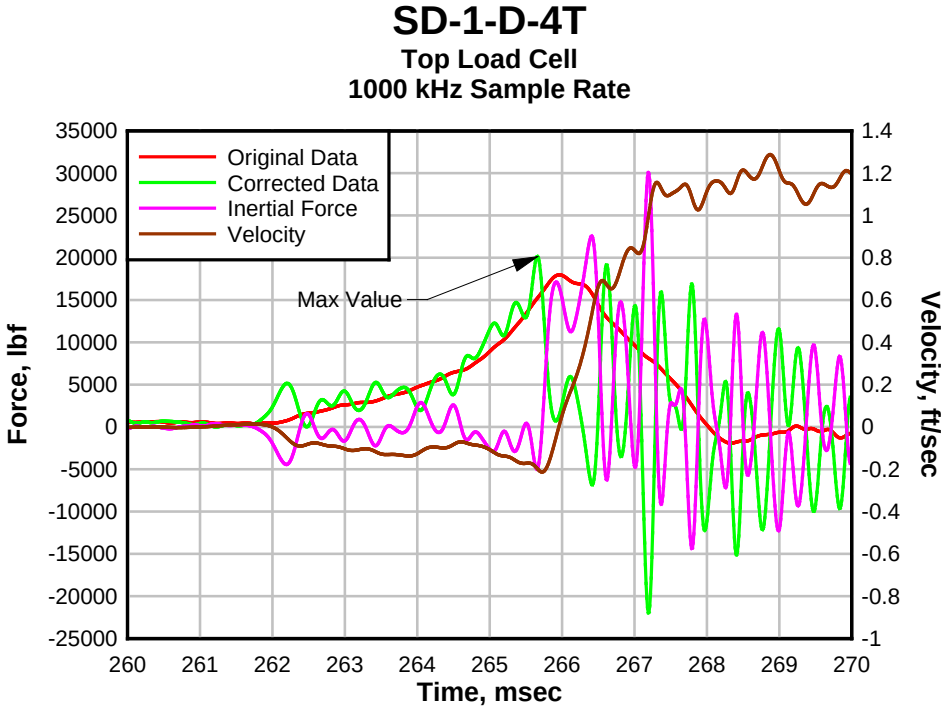

Figure 62: SD-1-D-4T Test Data.

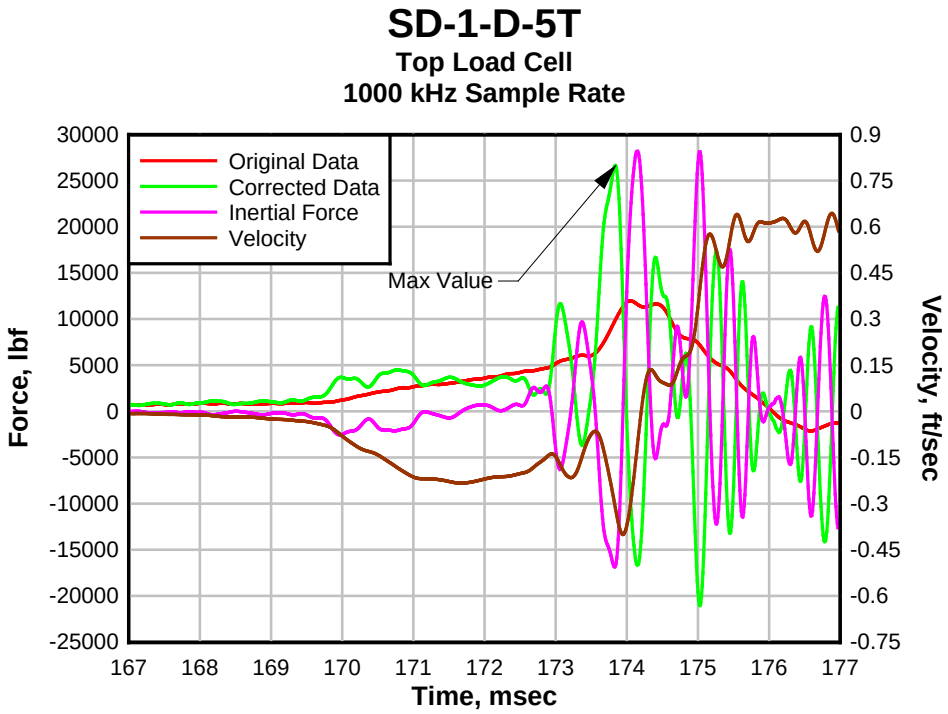

Figure 63: SD-1-D-5T Test Data.

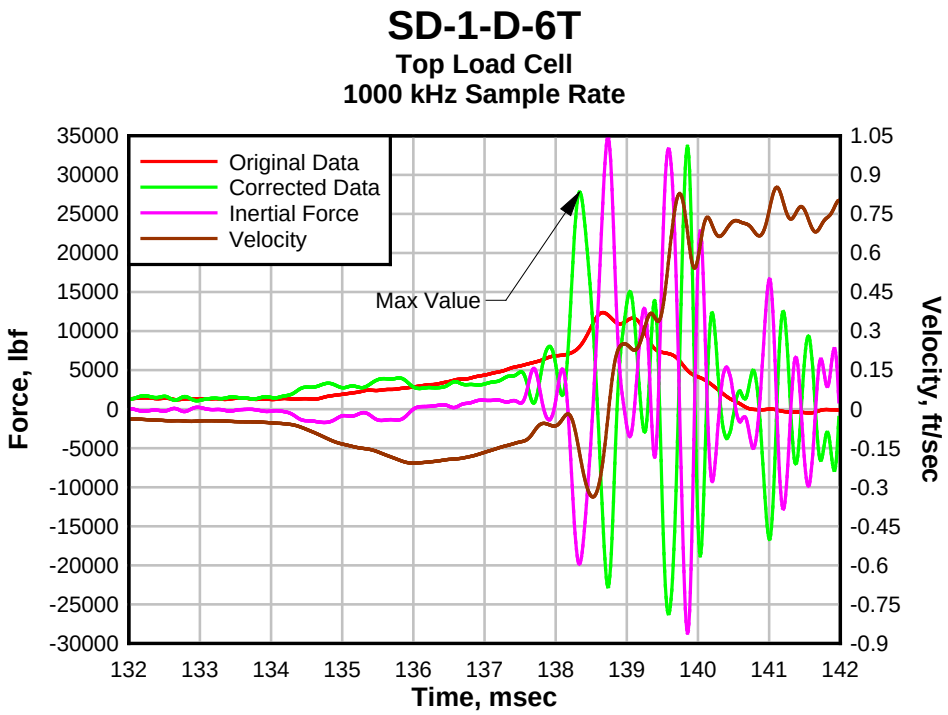

Figure 64: SD-1-D-6T Test Data.

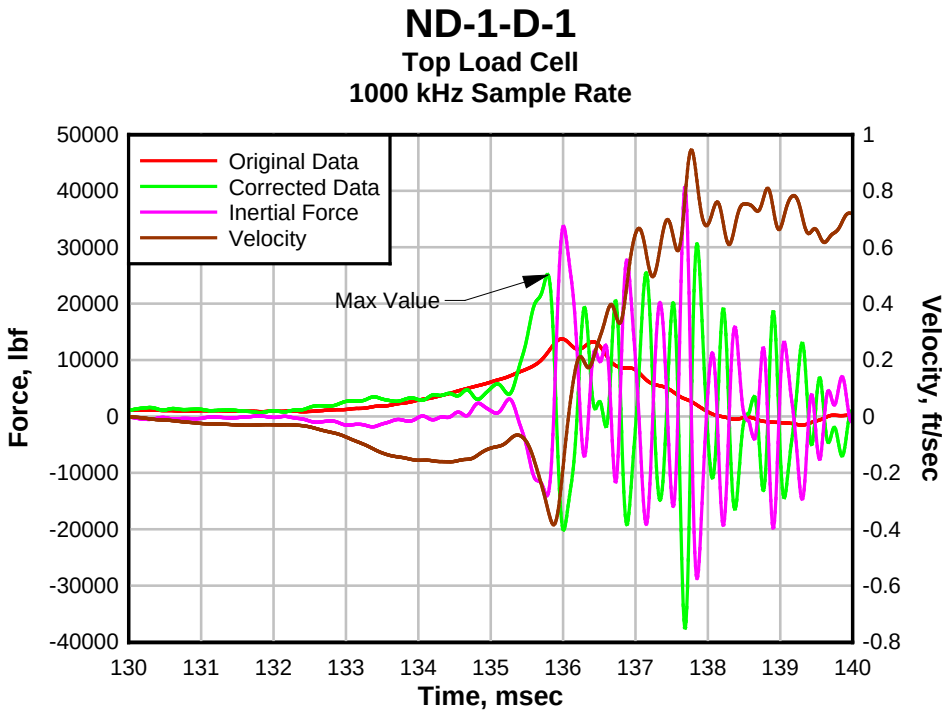

Figure 65: ND-1-D-1 Test Data.

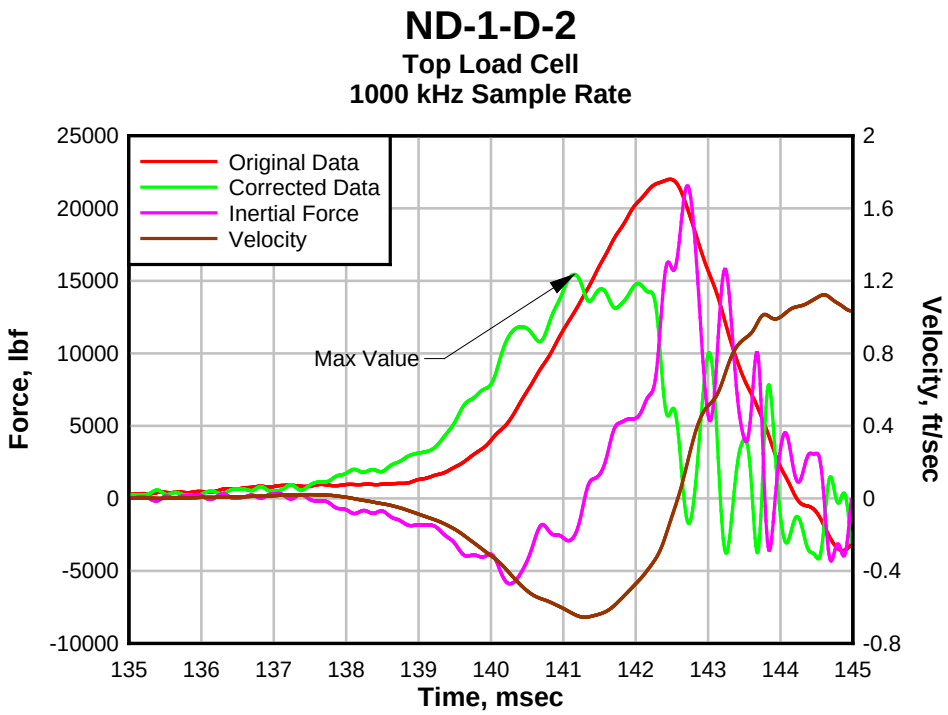

Figure 66: ND-1-D-2 Test Data.

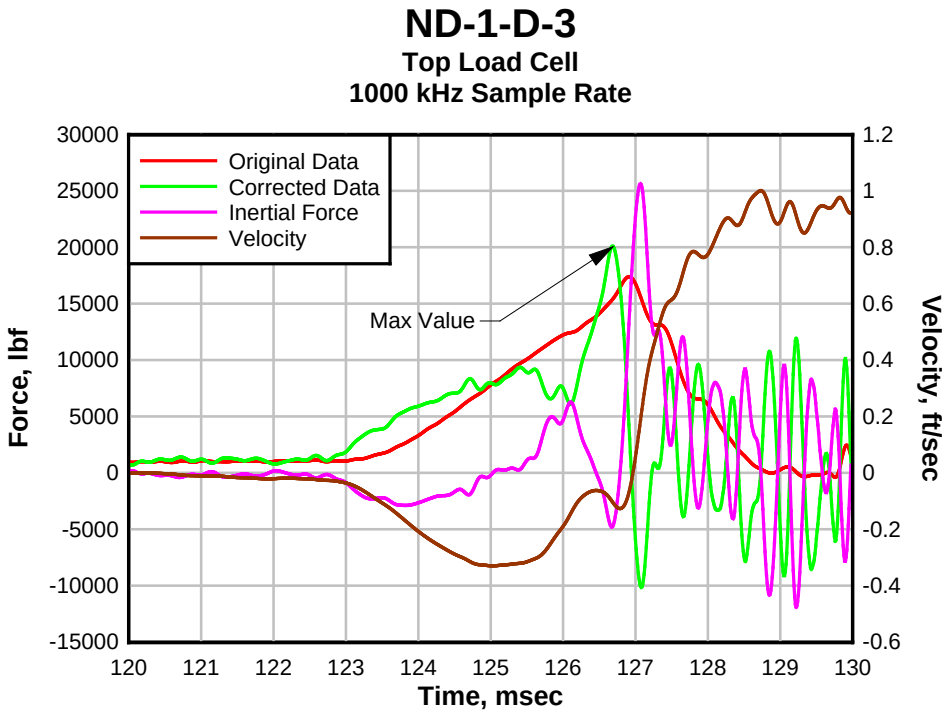

Figure 67: ND-1-D-3 Test Data.

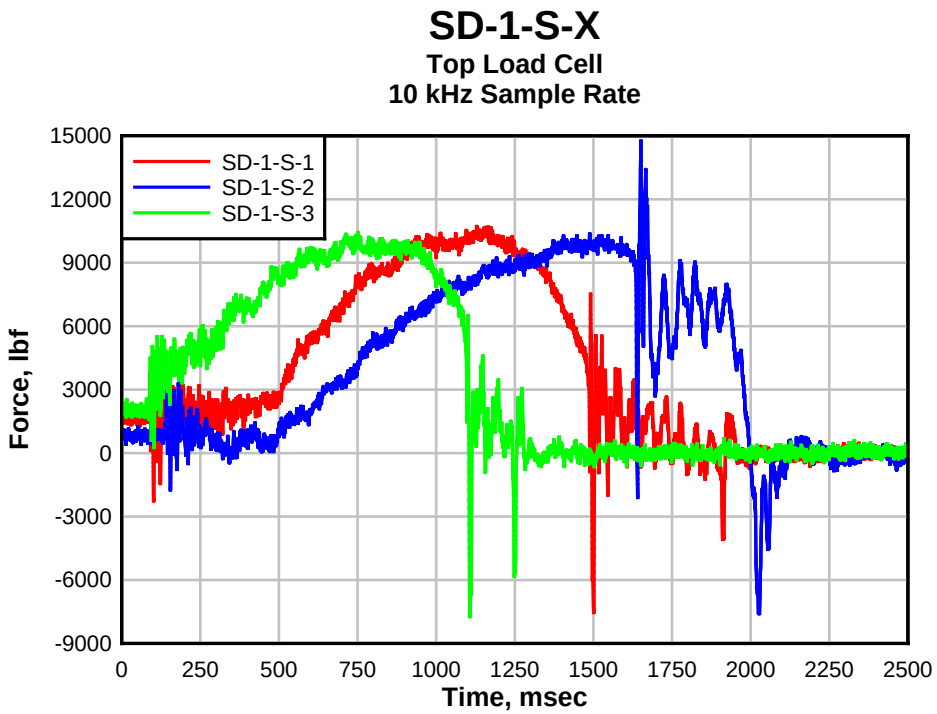

Figure 68: SD-1-S-X Tests Data.

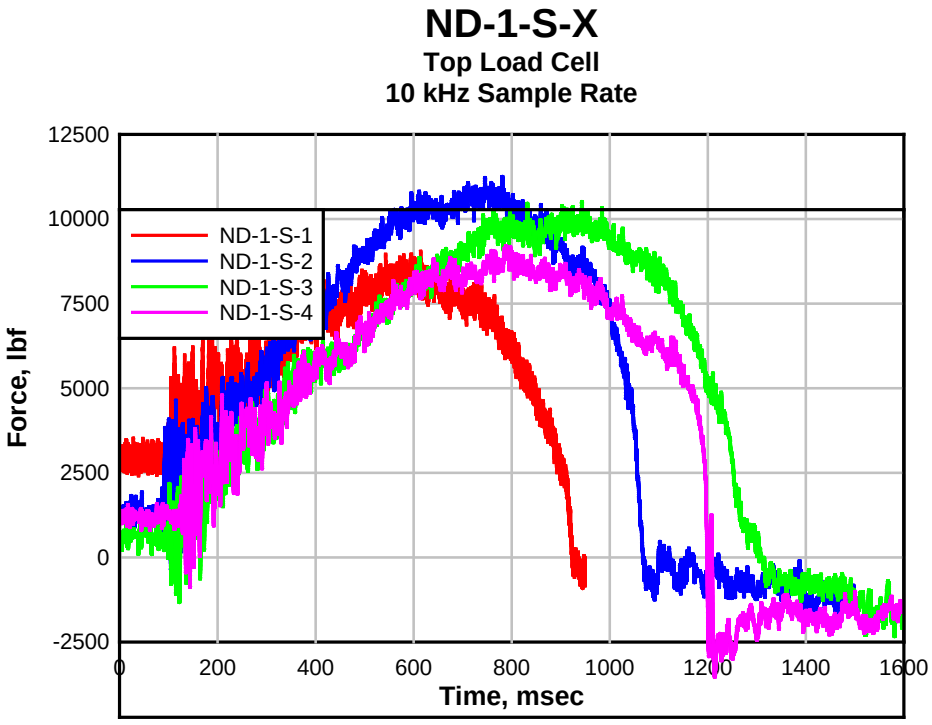

Figure 69: ND-1-S-X Tests Data.

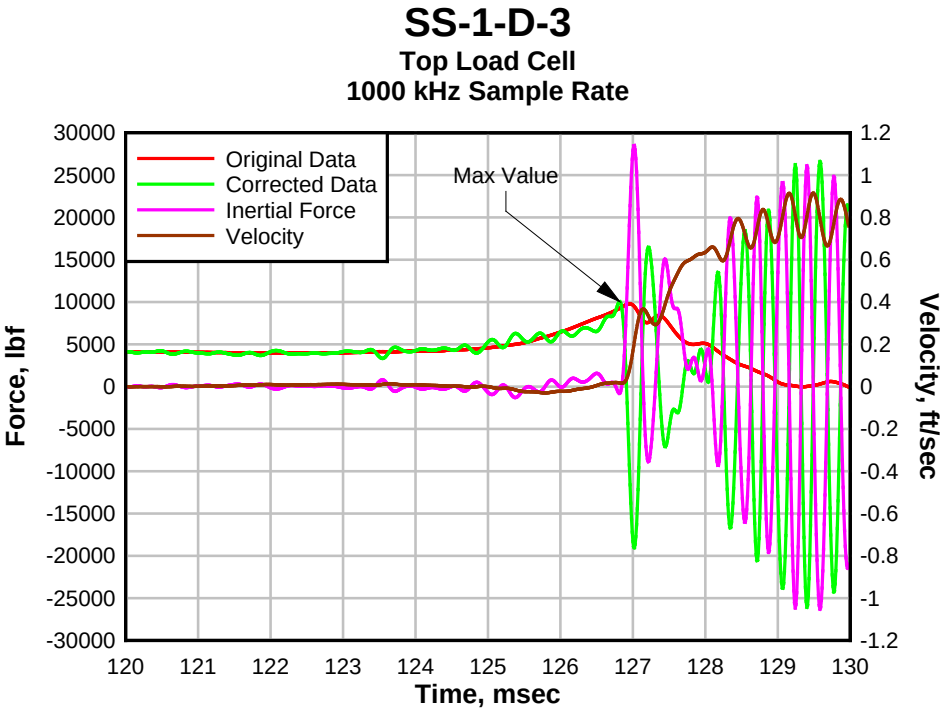

Figure 70: SS-1-D-3 Test Data.

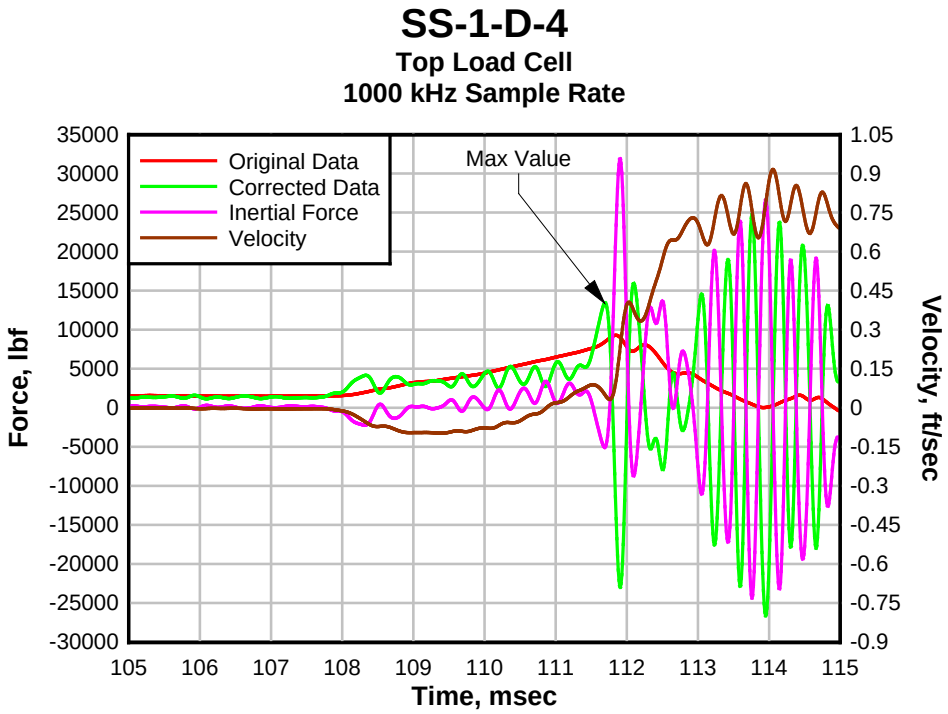

Figure 71: SS-1-D-4 Test Data.

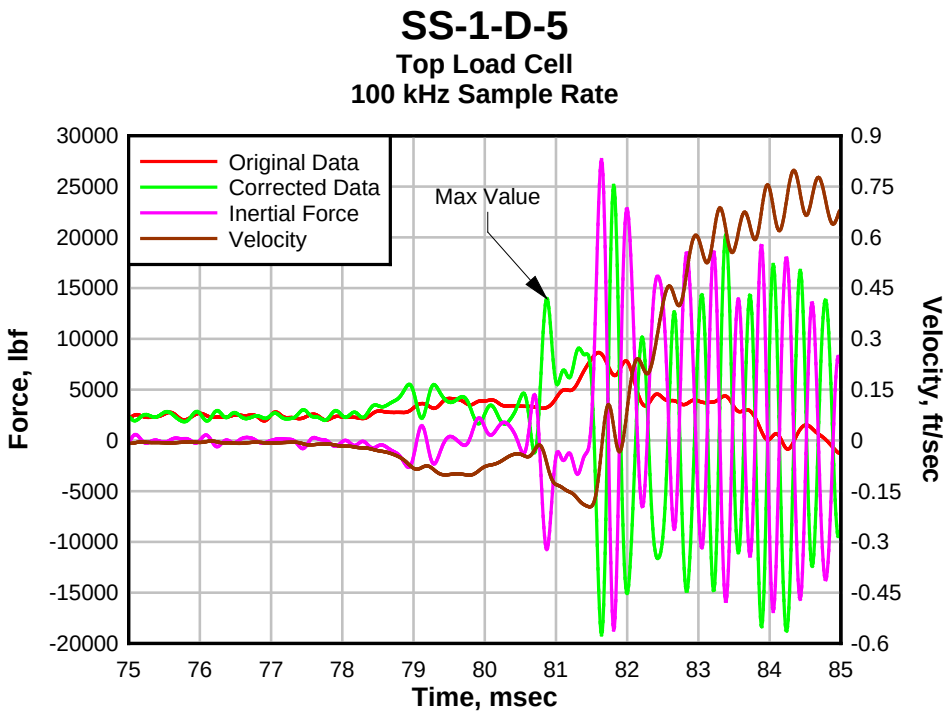

Figure 72: SS-1-D-5 Test Data.

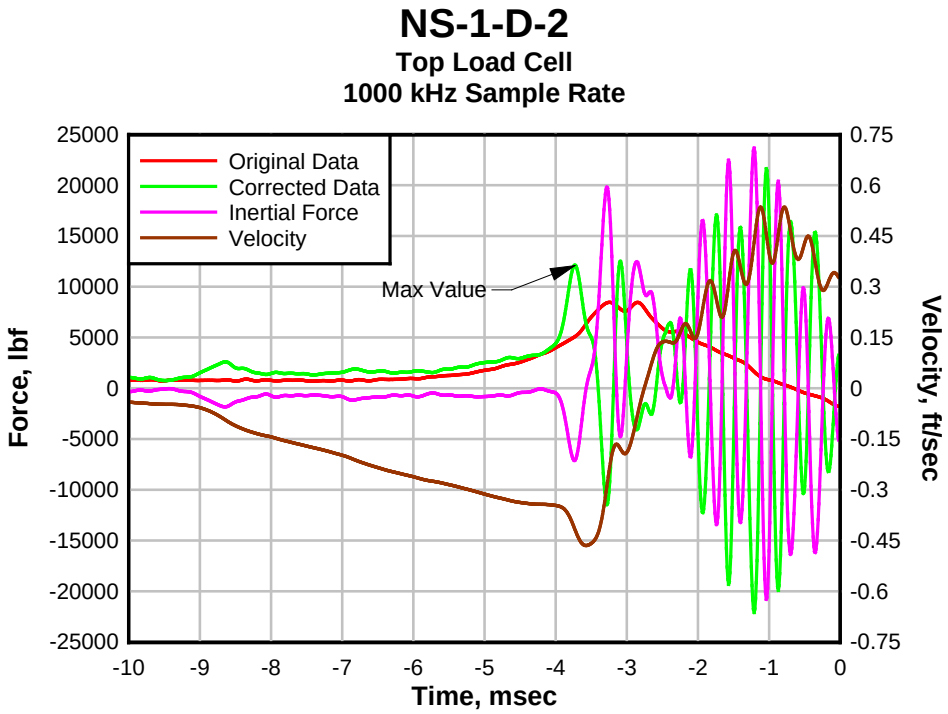

Figure 73: NS-1-D-2 Test Data.

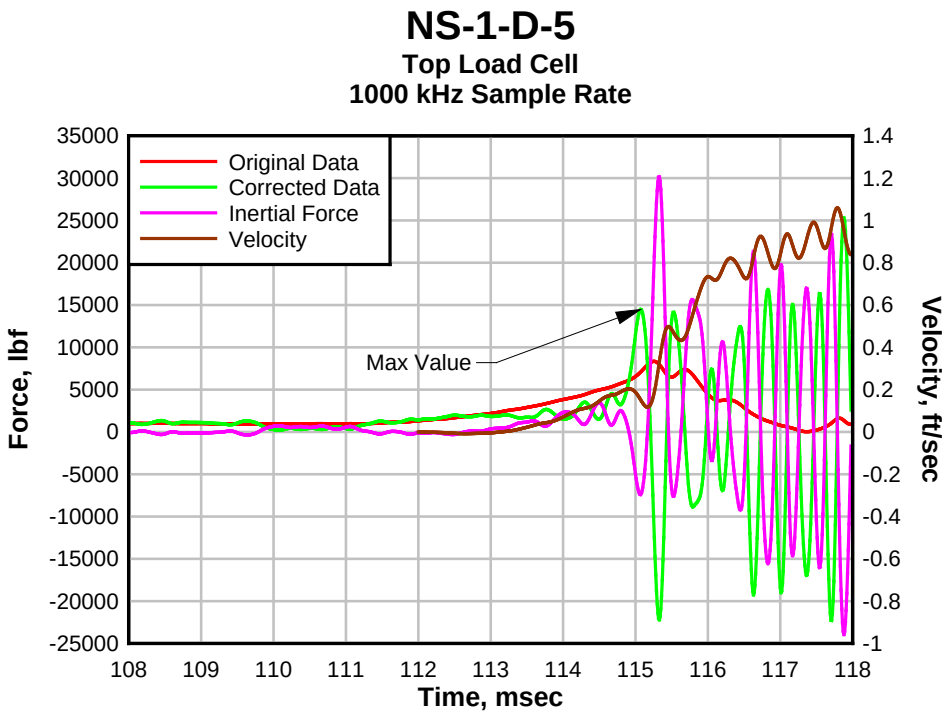

Figure 74: NS-1-D-5 Test Data.

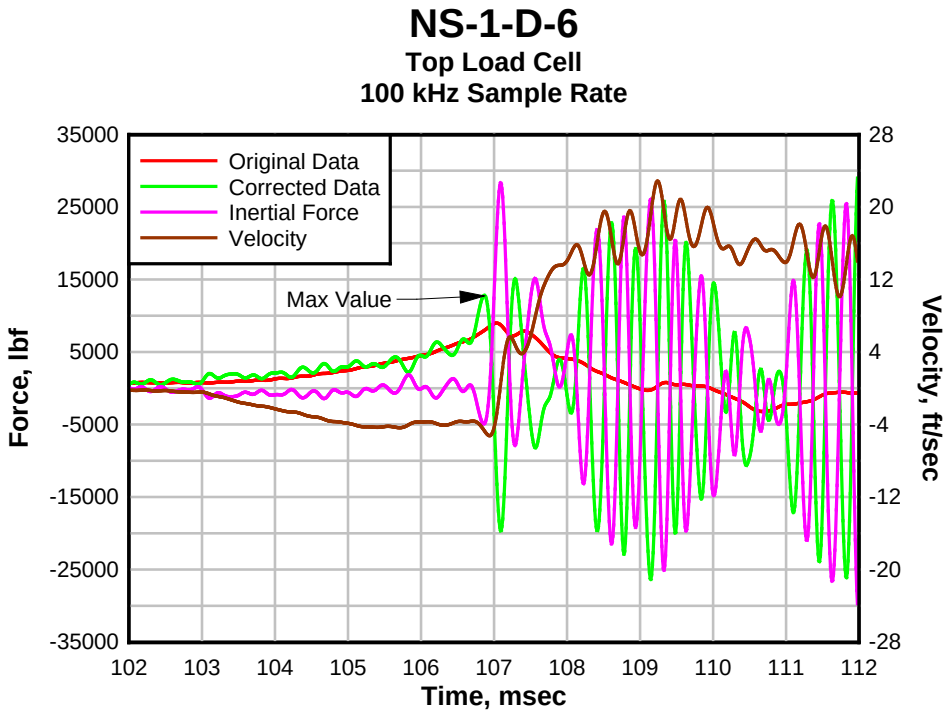

Figure 75: NS-1-D-6 Test Data.

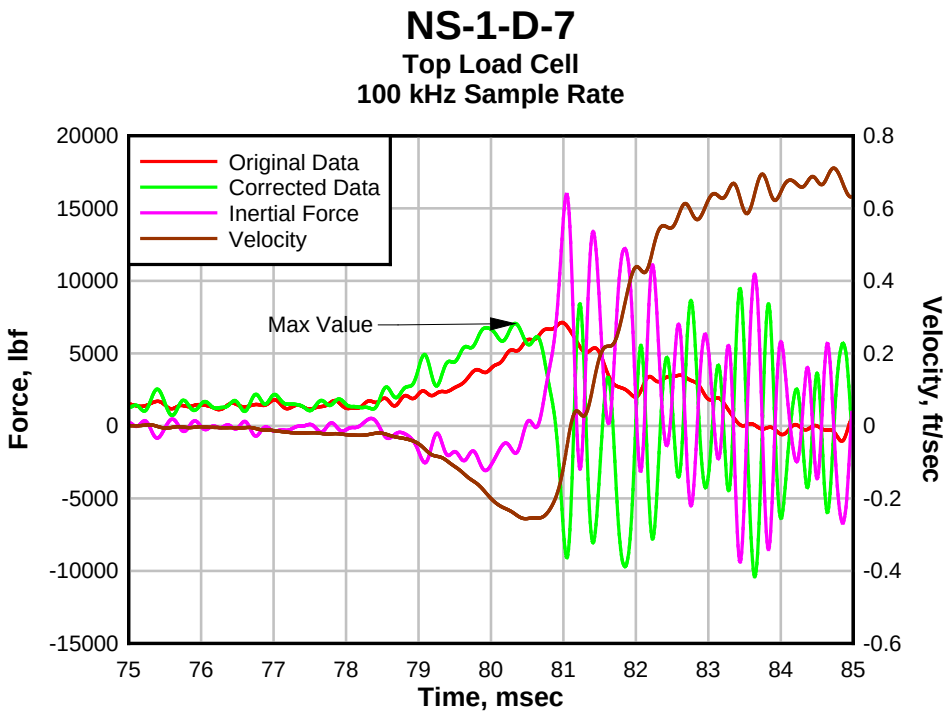

Figure 76: NS-1-D-7 Test Data.

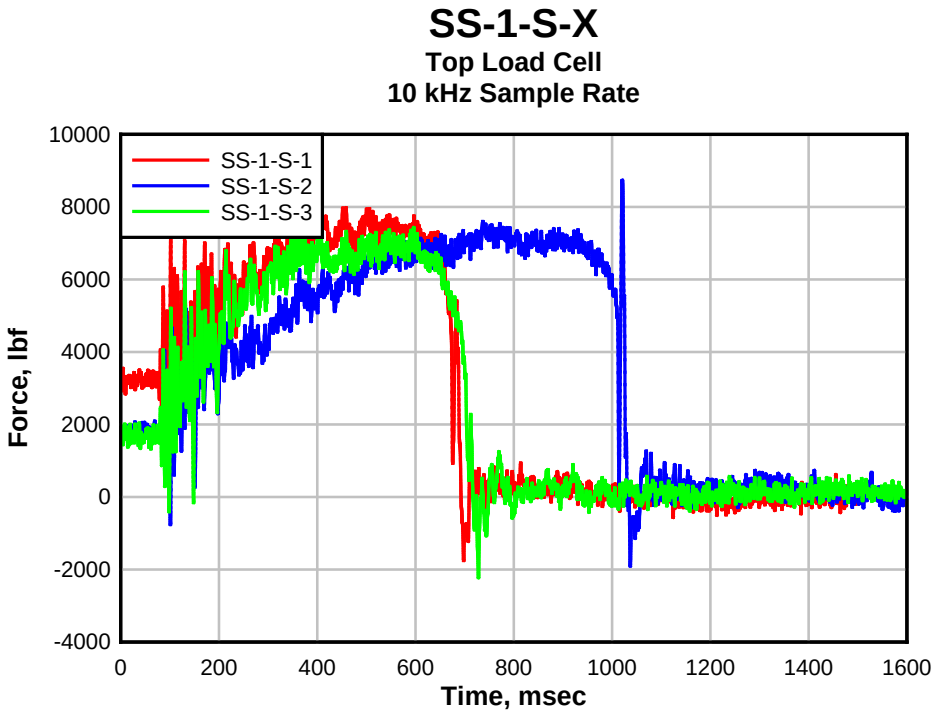

Figure 77: SS-1-S-X Tests Data.

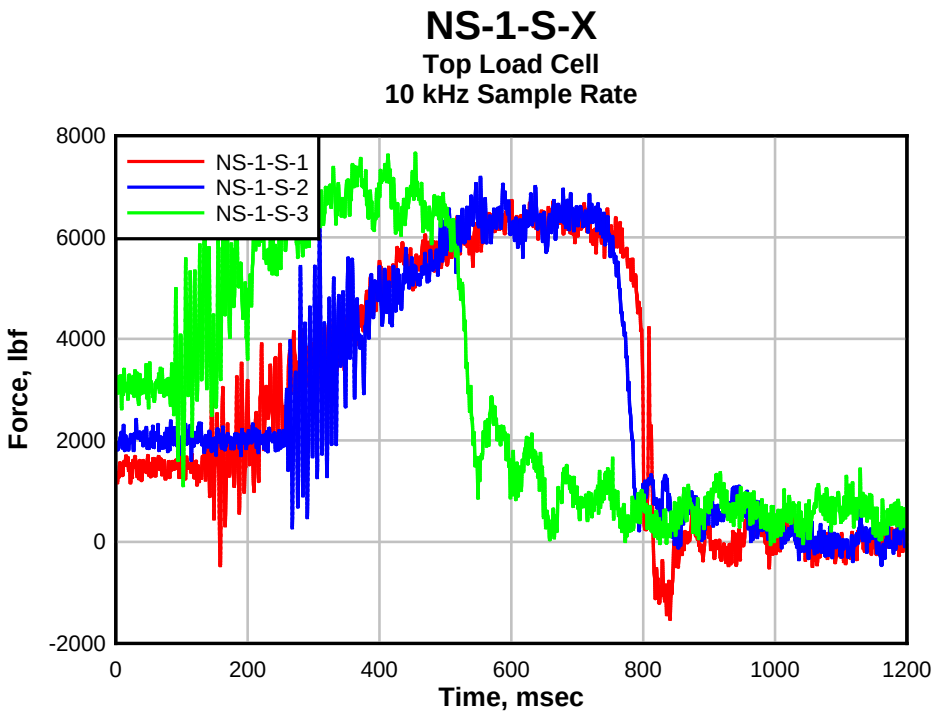

Figure 78: NS-1-S-X Tests Data.

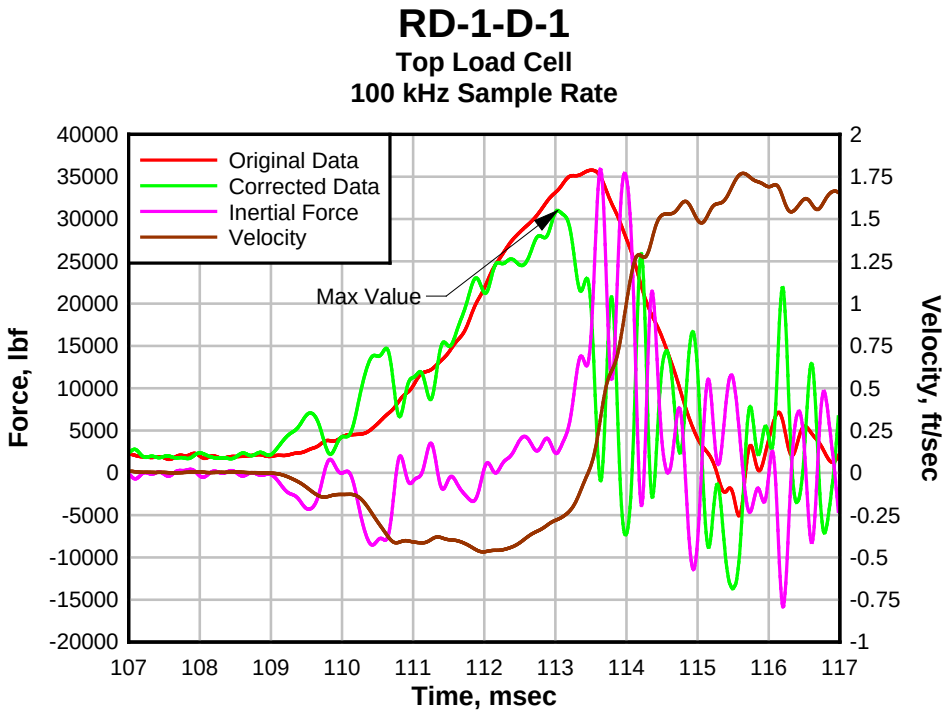

Figure 79: RD-1-D-1 Test Data.

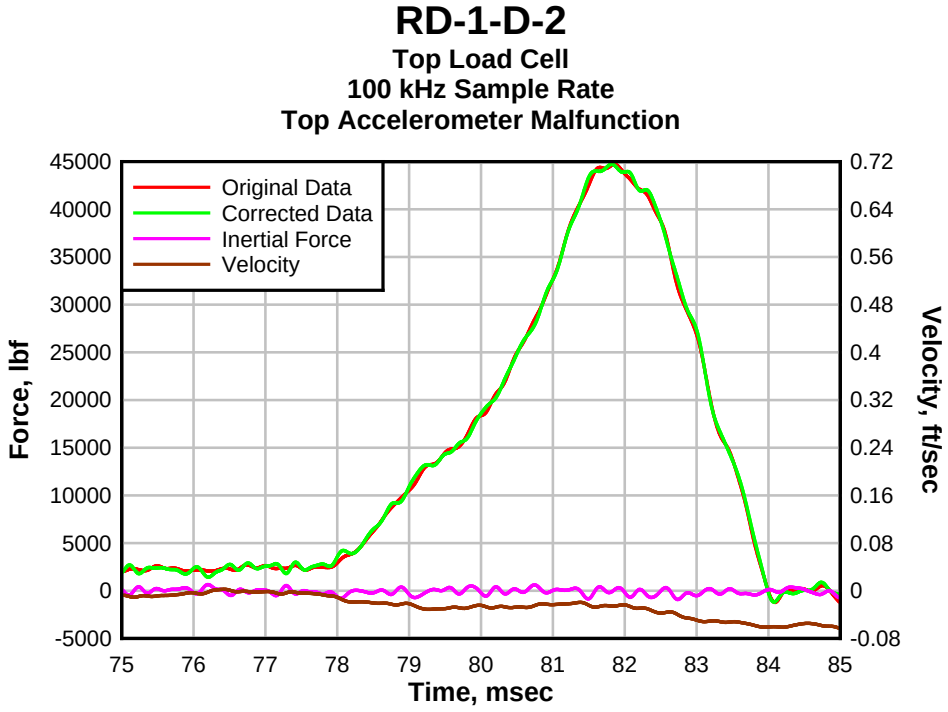

Figure 80: RD-1-D-2 Test Data.

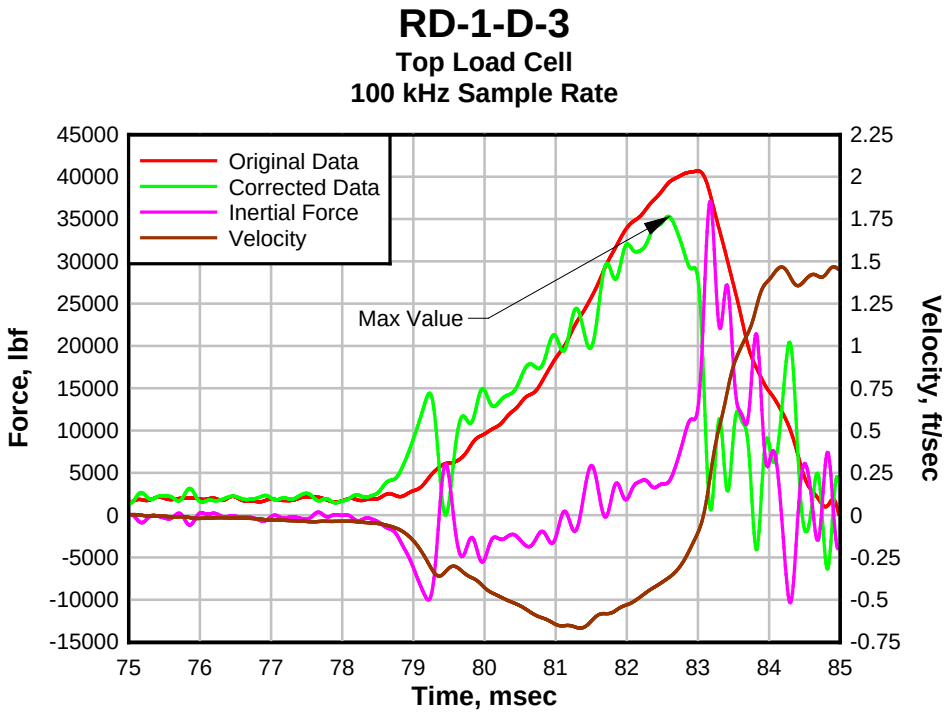

Figure 81: RD-1-D-3 Test Data.

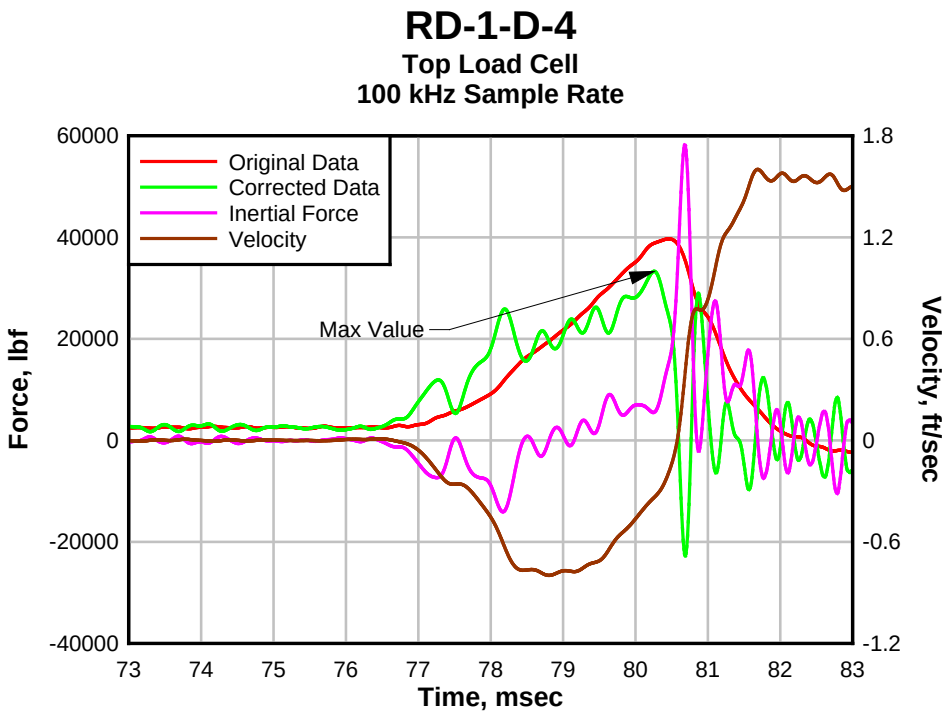

Figure 82: RD-1-D-4 Test Data.

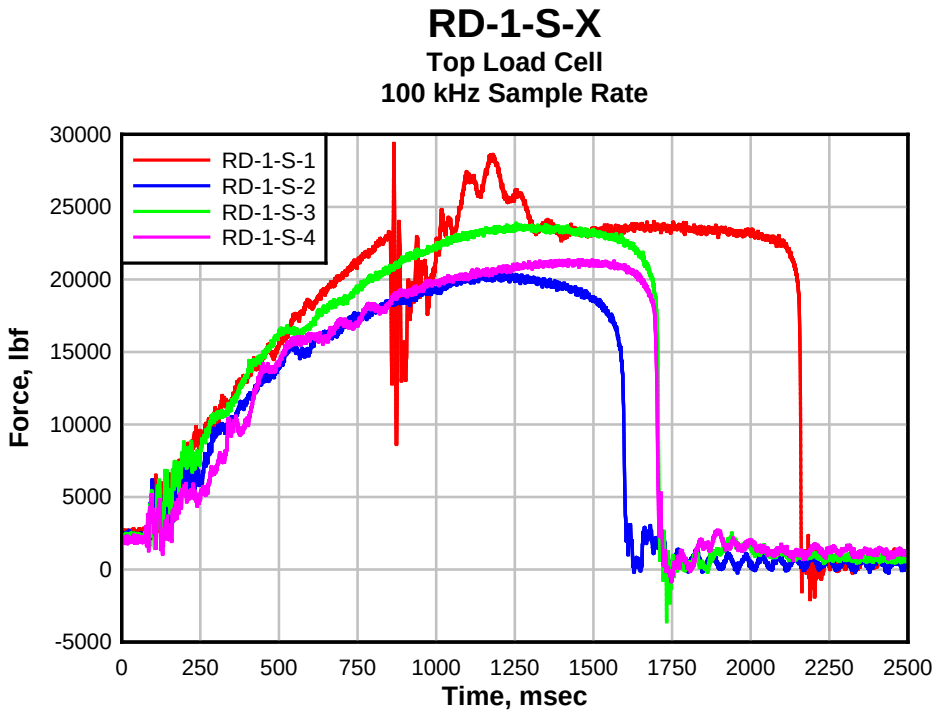

Figure 83: RD-1-S-X Tests Data.

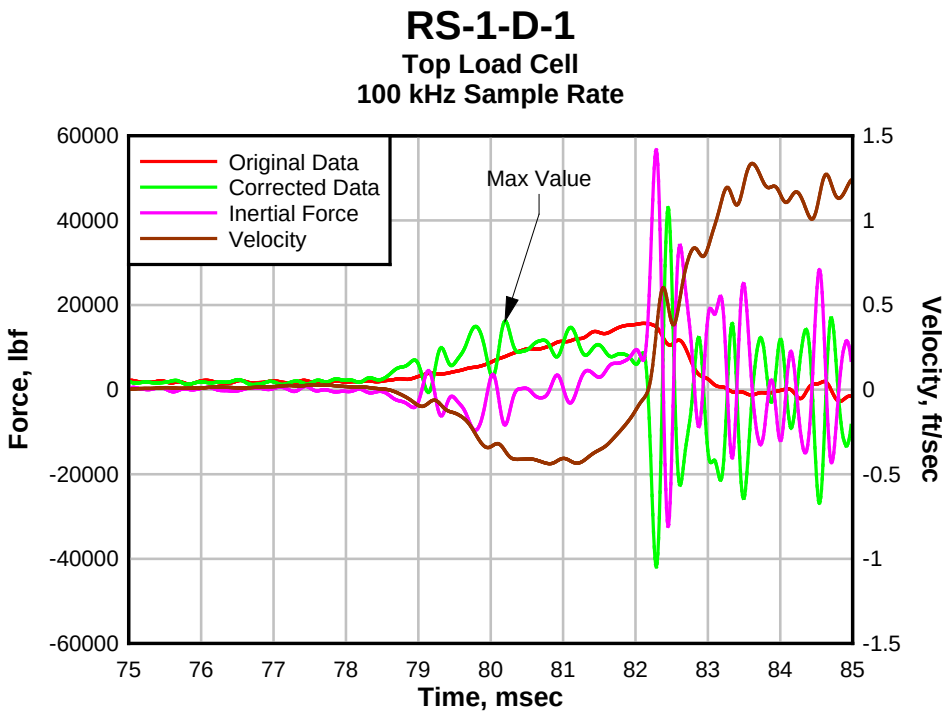

Figure 84: RS-1-D-1 Test Data.

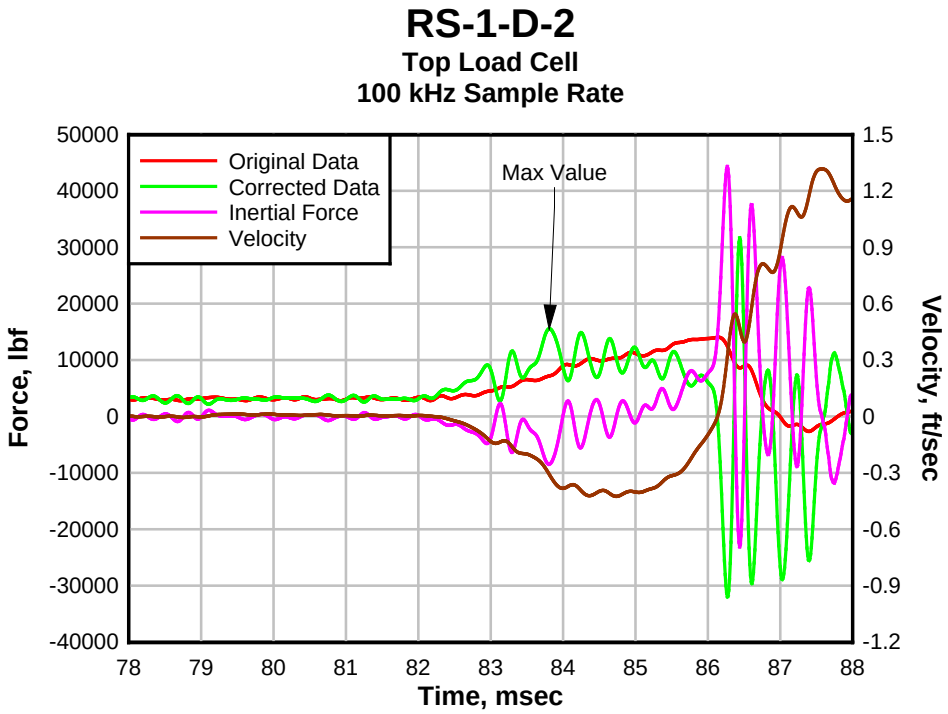

Figure 85: RS-1-D-2 Test Data.

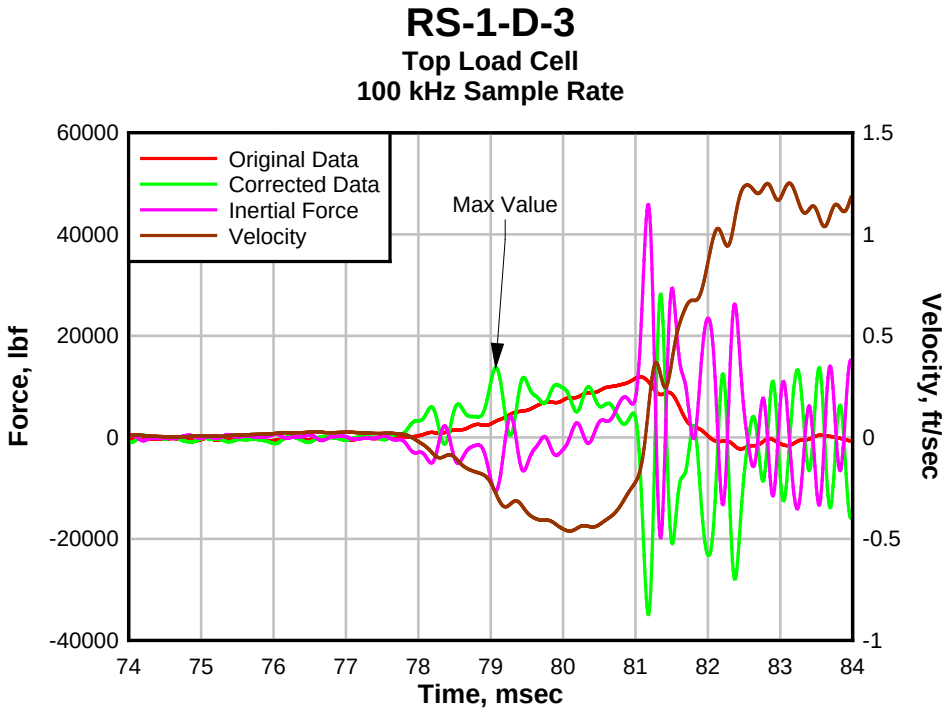

Figure 86: RS-1-D-3 Test Data.

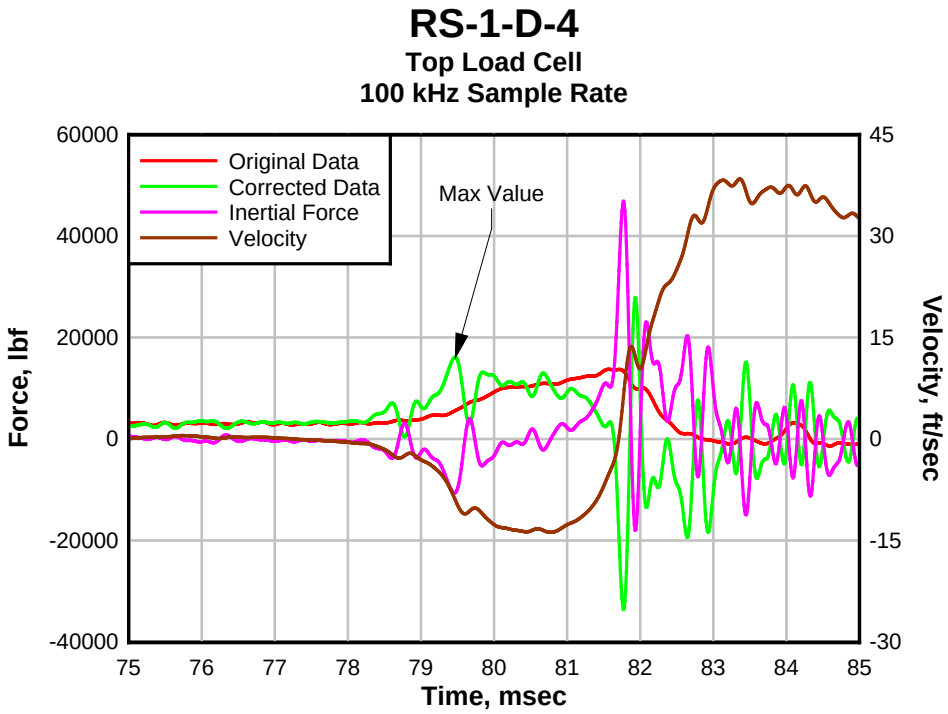

Figure 87: RS-1-D-4 Test Data.

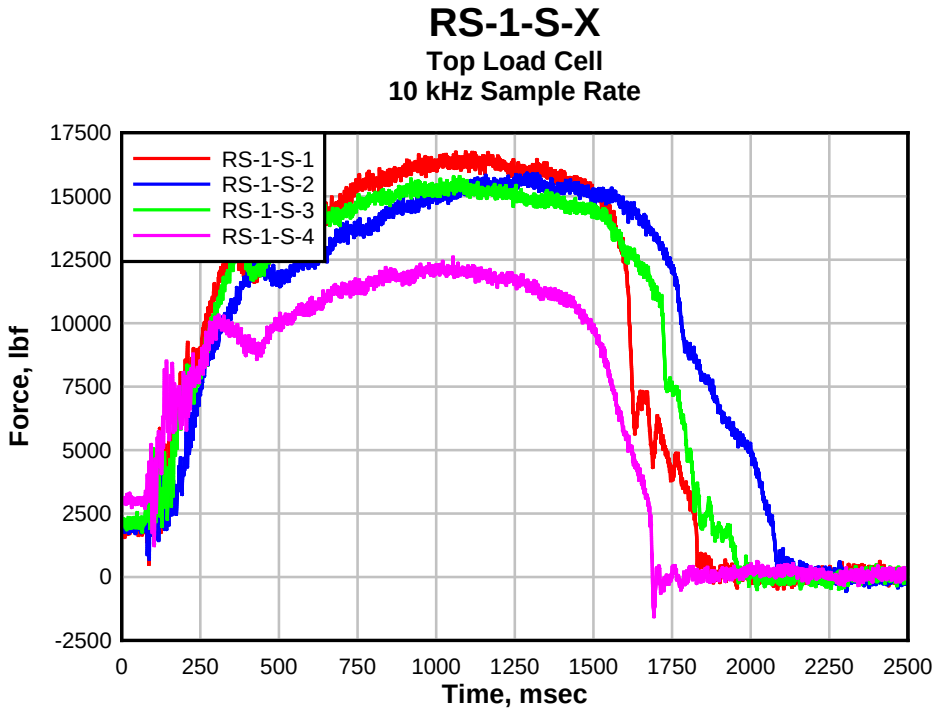

Figure 88: RS-1-S-X Tests Data.

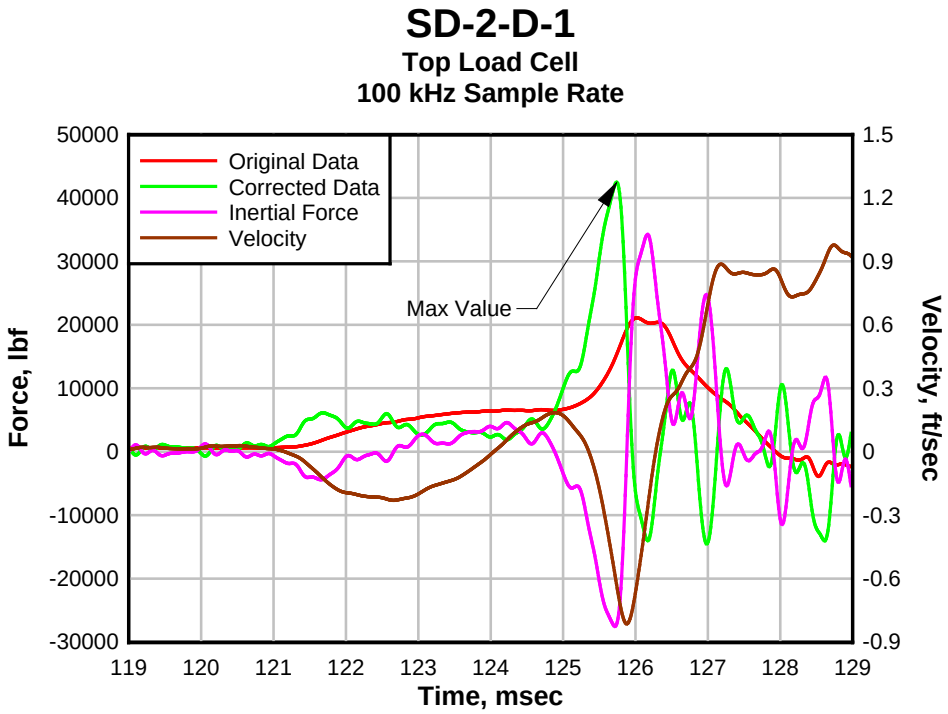

Figure 89: SD-2-D-1 Test Data.

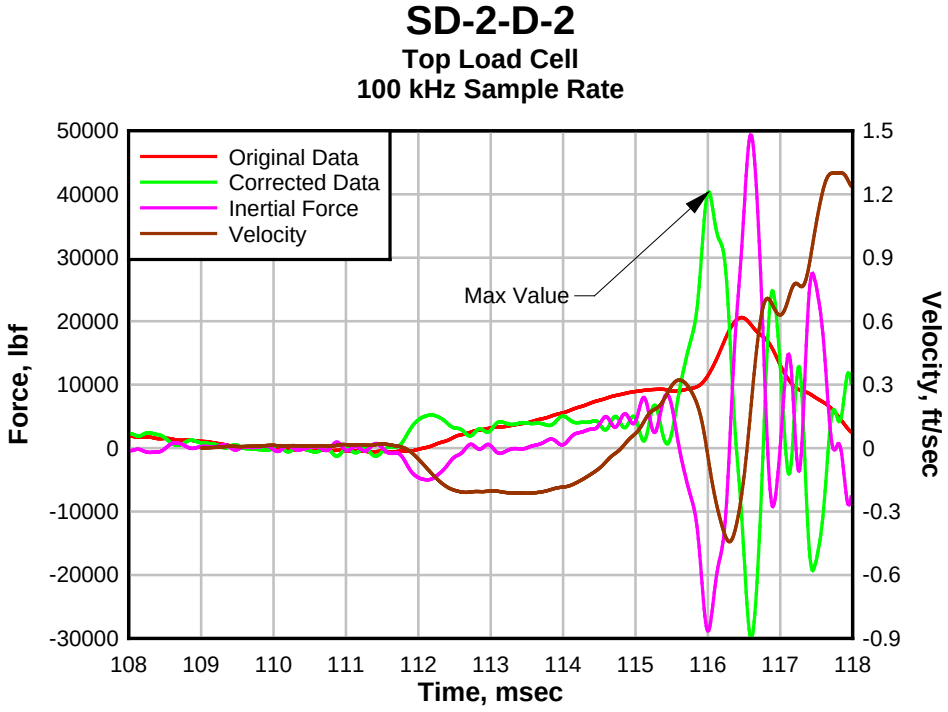

Figure 90: SD-2-D-2 Test Data.

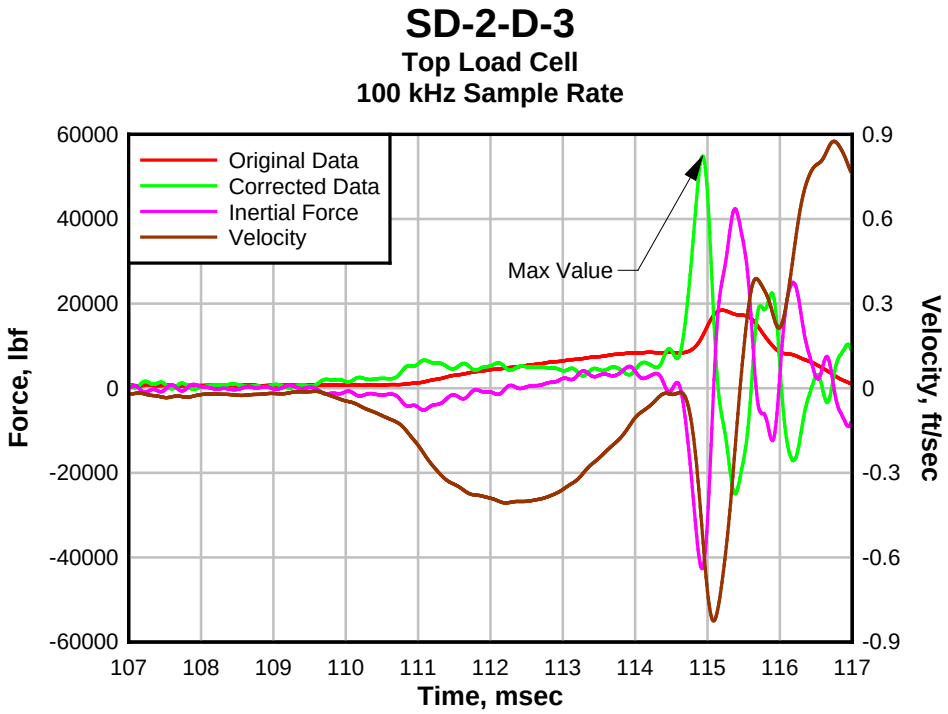

Figure 91: SD-2-D-3 Test Data.

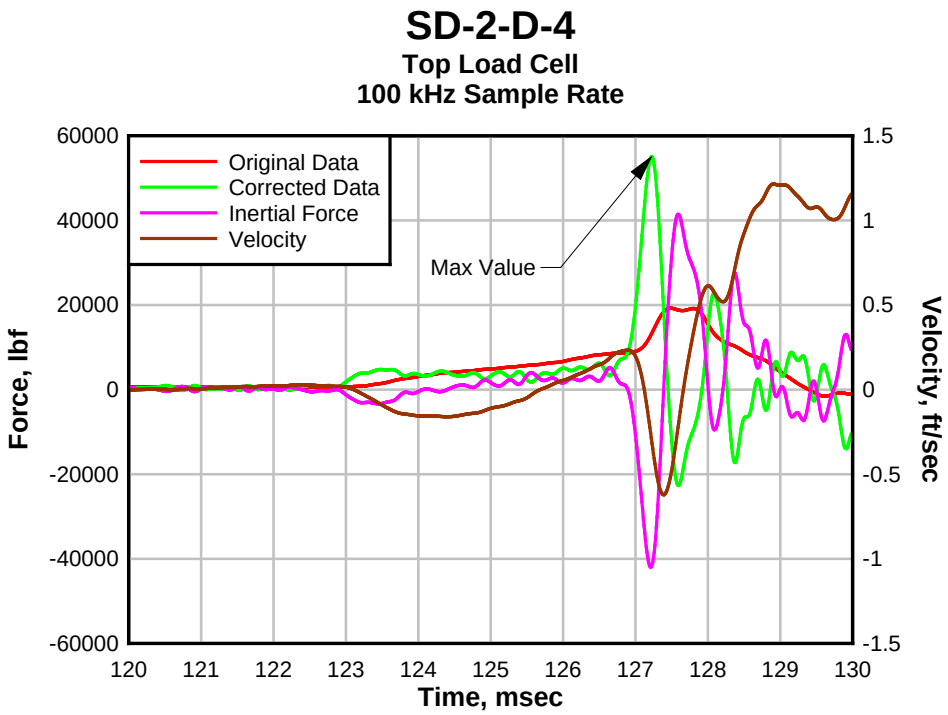

Figure 92: SD-2-D-4 Test Data.

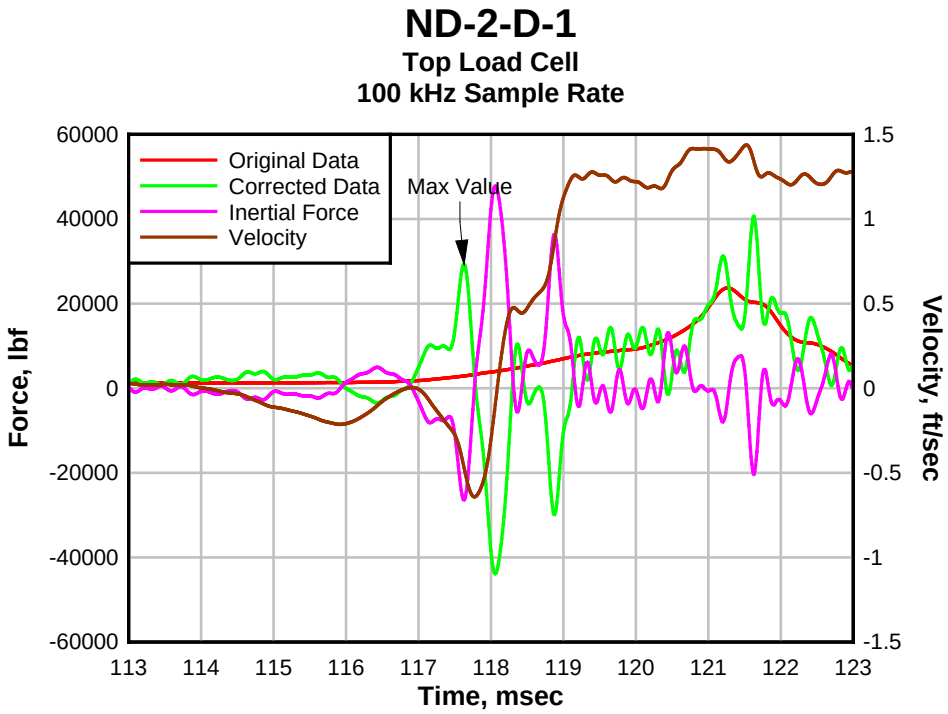

Figure 93: ND-2-D-1 Test Data.

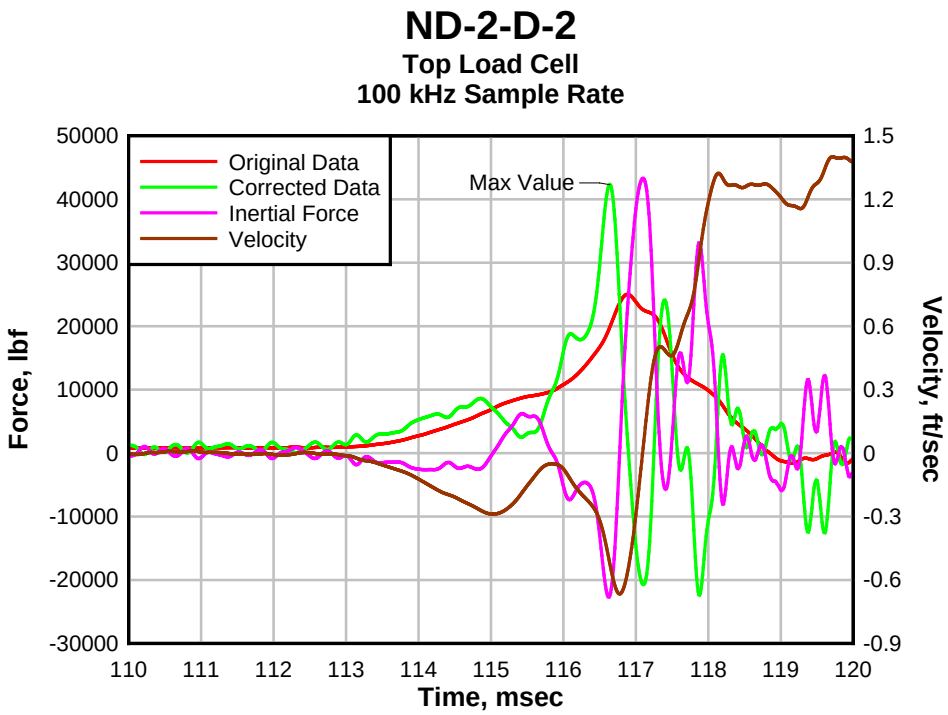

Figure 94: ND-2-D-2 Test Data.

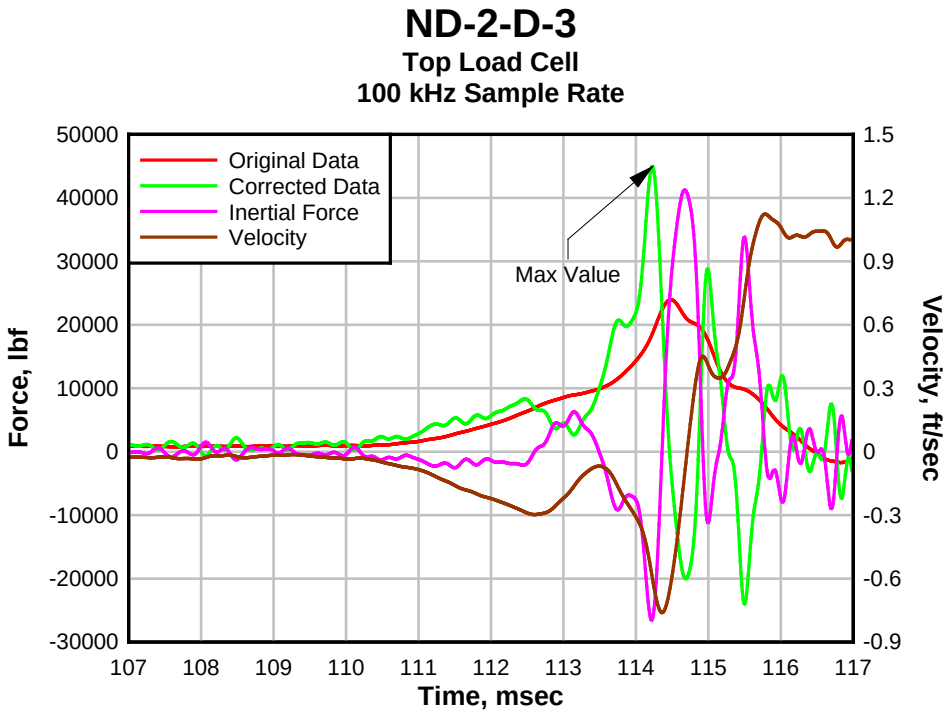

Figure 95: ND-2-D-3 Test Data.

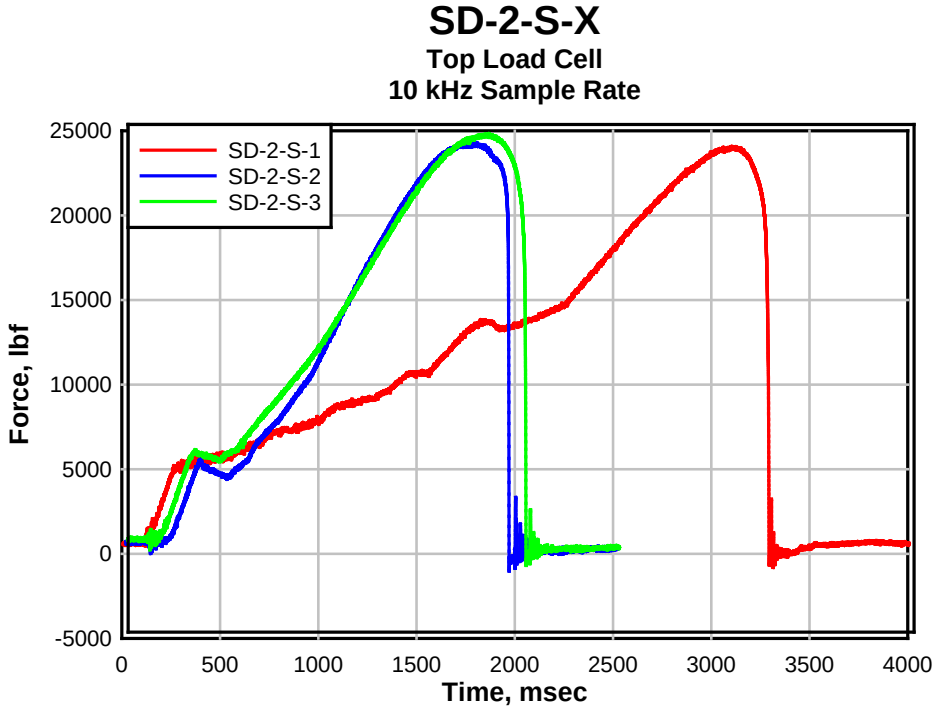

Figure 96: SD-2-S-X Tests Data.

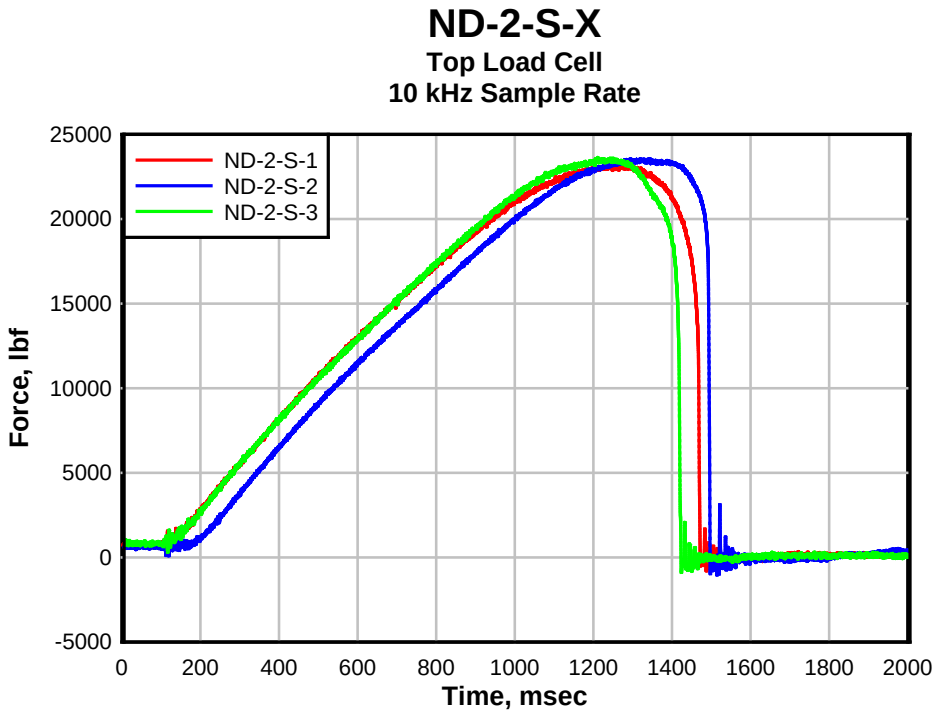

Figure 97: ND-2-S-X Tests Data.

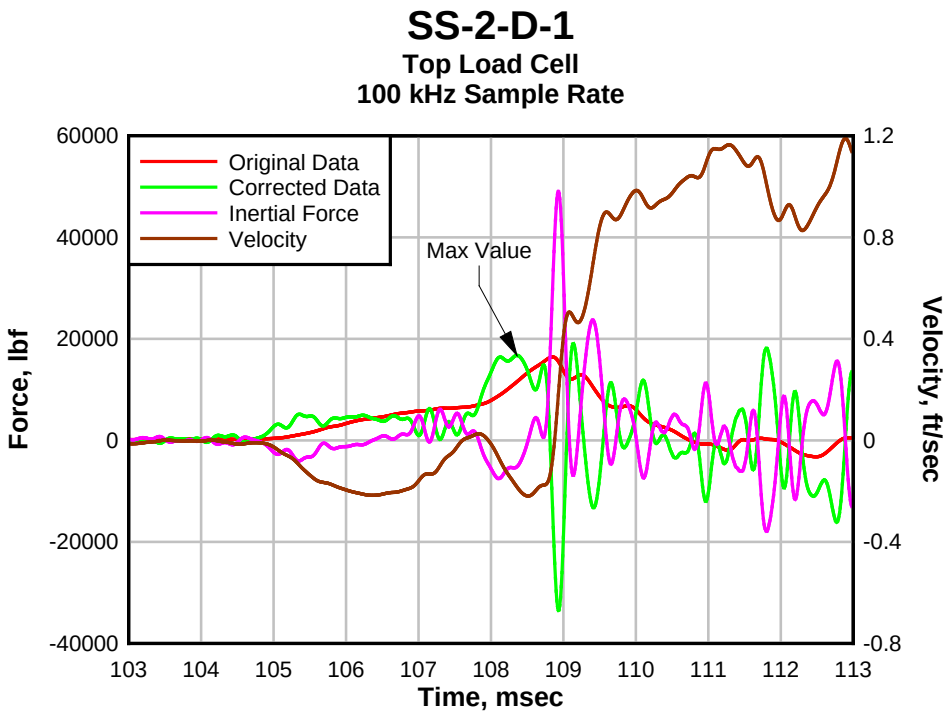

Figure 98: SS-2-D-1 Test Data.

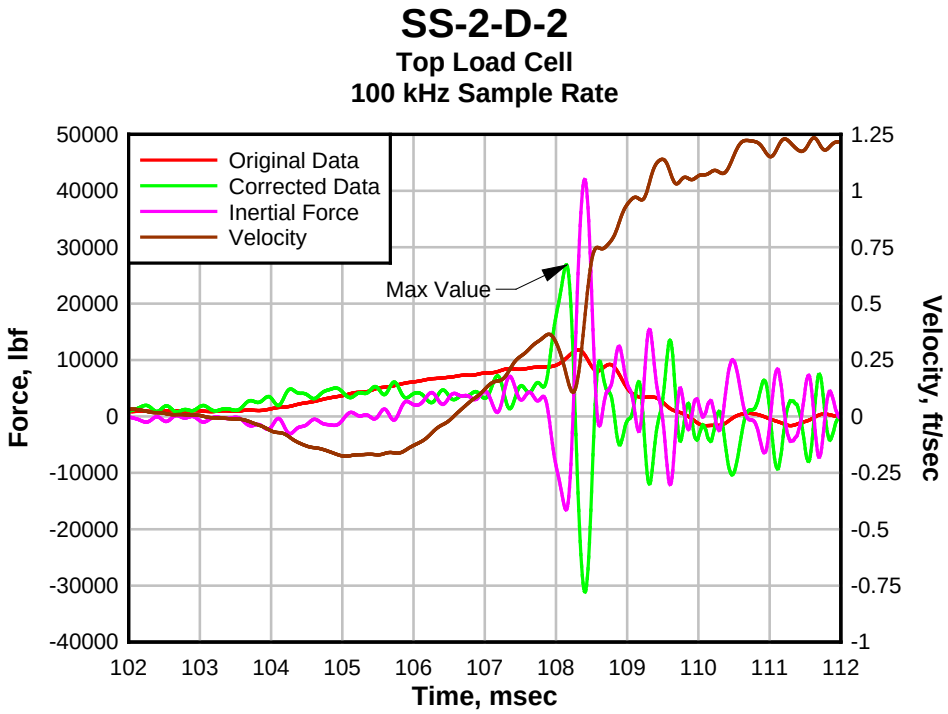

Figure 99: SS-2-D-2 Test Data.

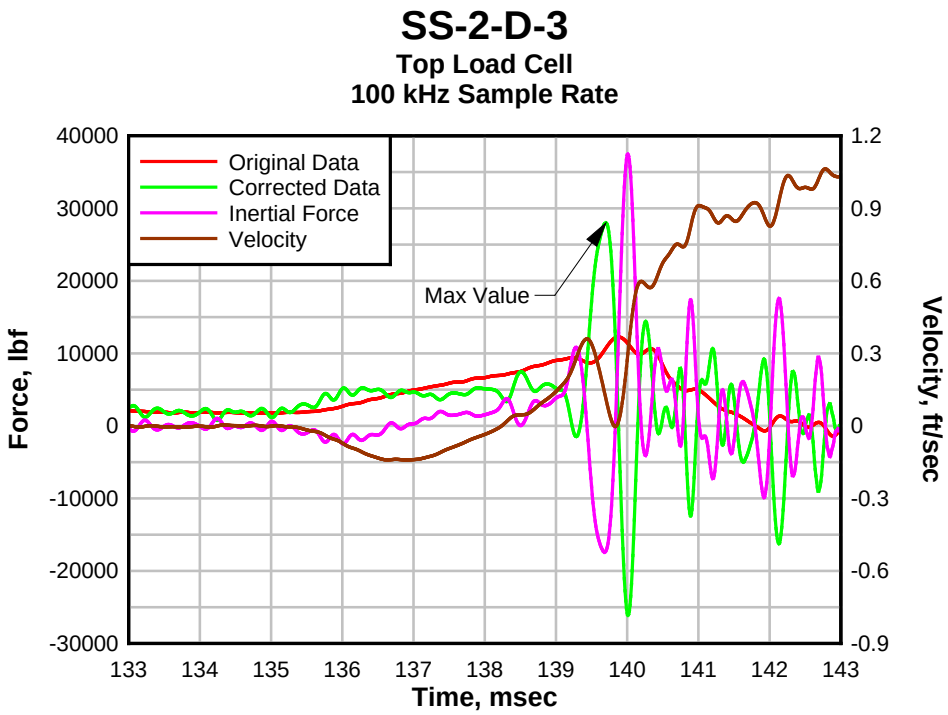

Figure 100: SS-2-D-3 Test Data.

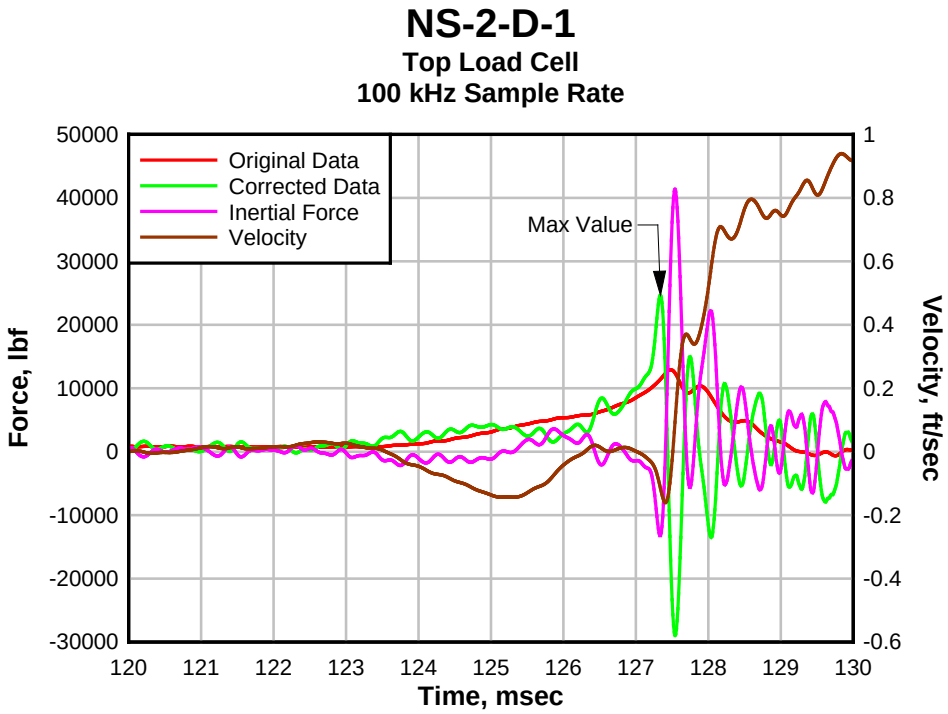

Figure 101: NS-2-D-1 Test Data.

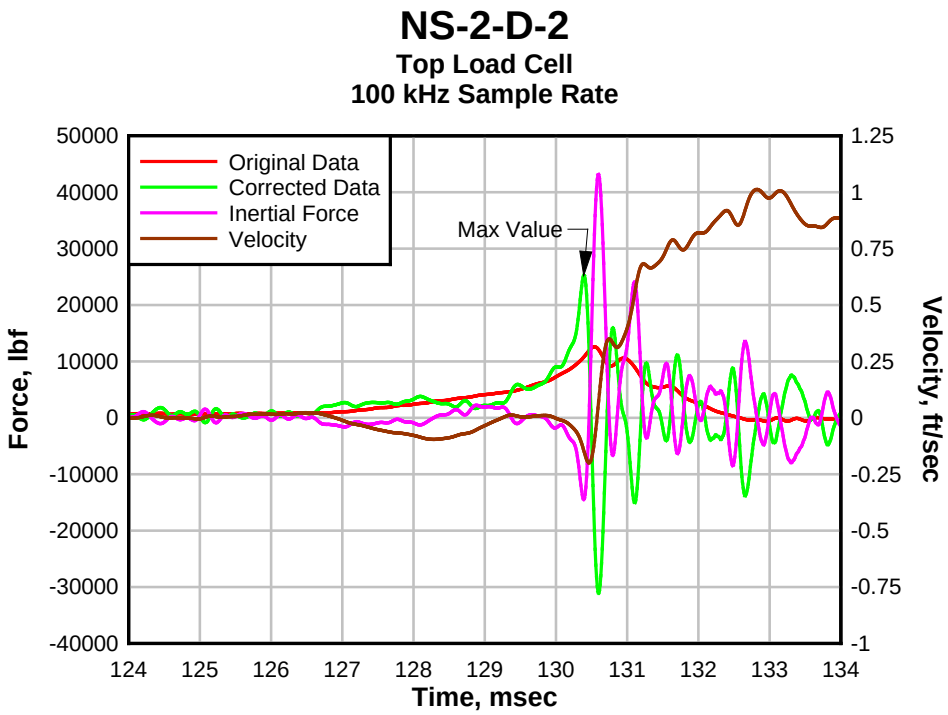

Figure 102: NS-2-D-2 Test Data.

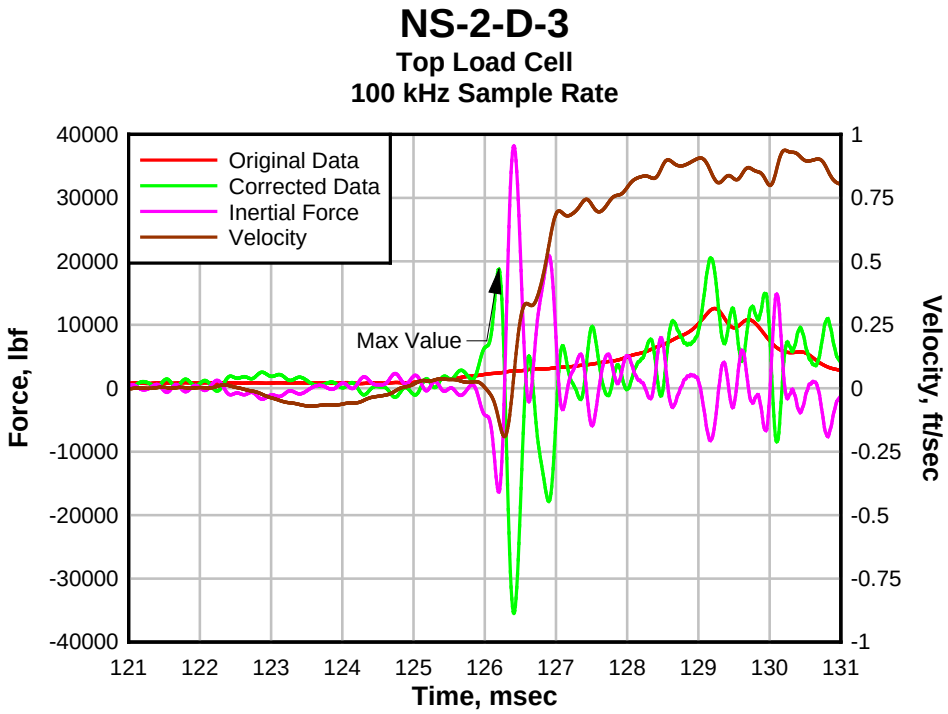

Figure 103: NS-2-D-3 Test Data.

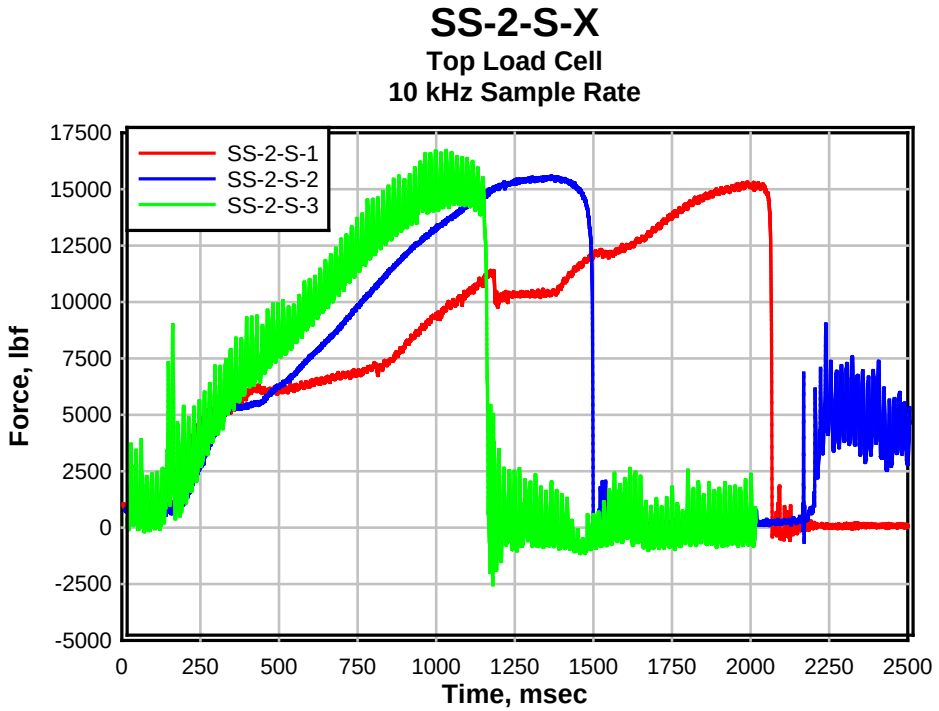

Figure 104: SS-2-S-X Tests Data.

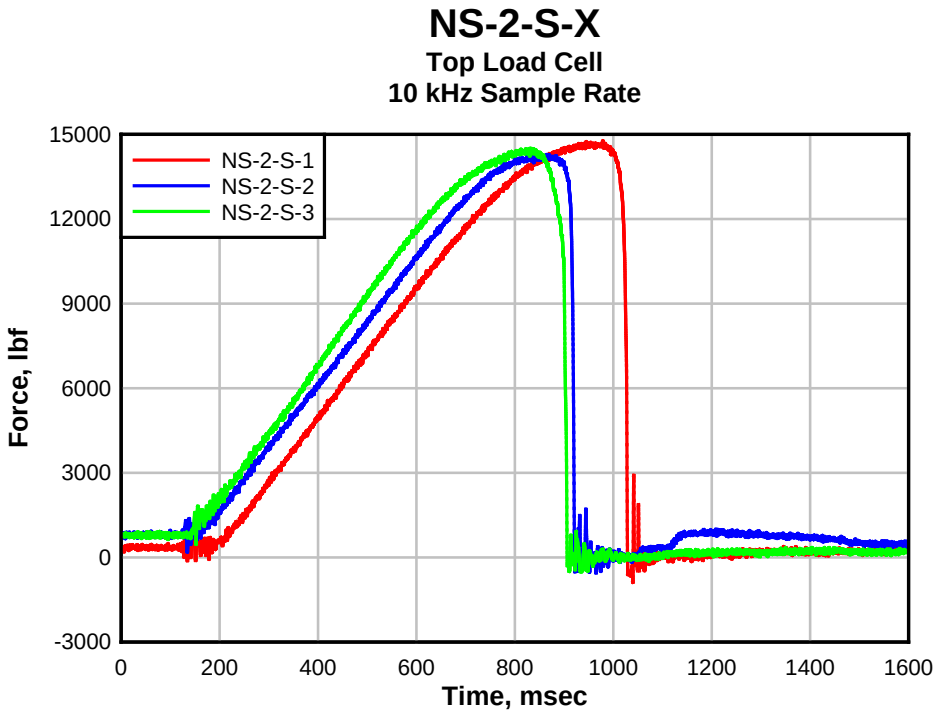

Figure 105: NS-2-S-X Tests Data.

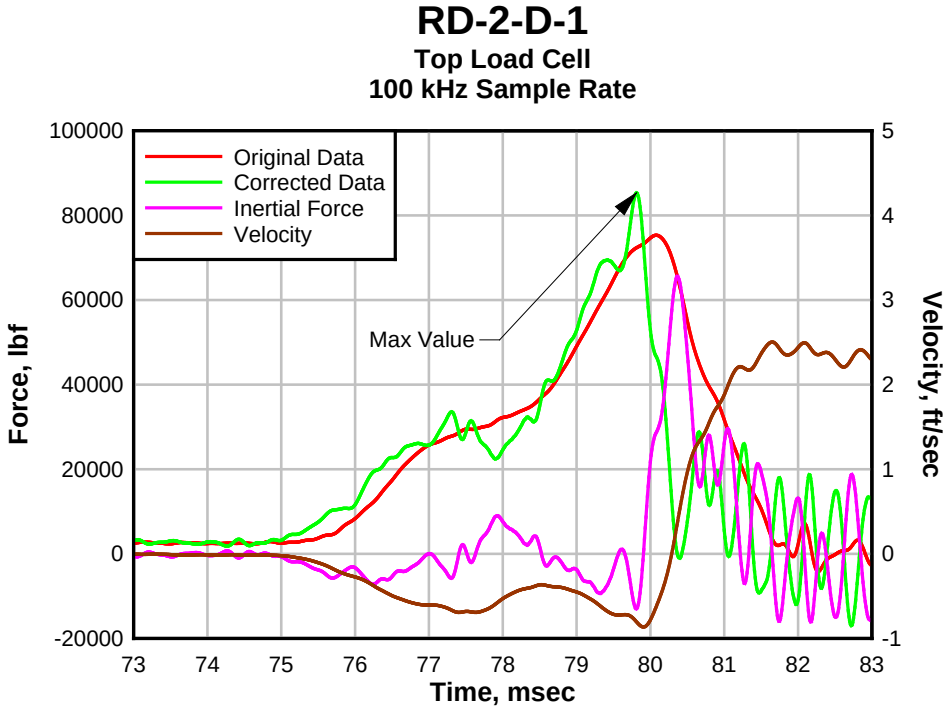

Figure 106: RD-2-D-1 Test Data.

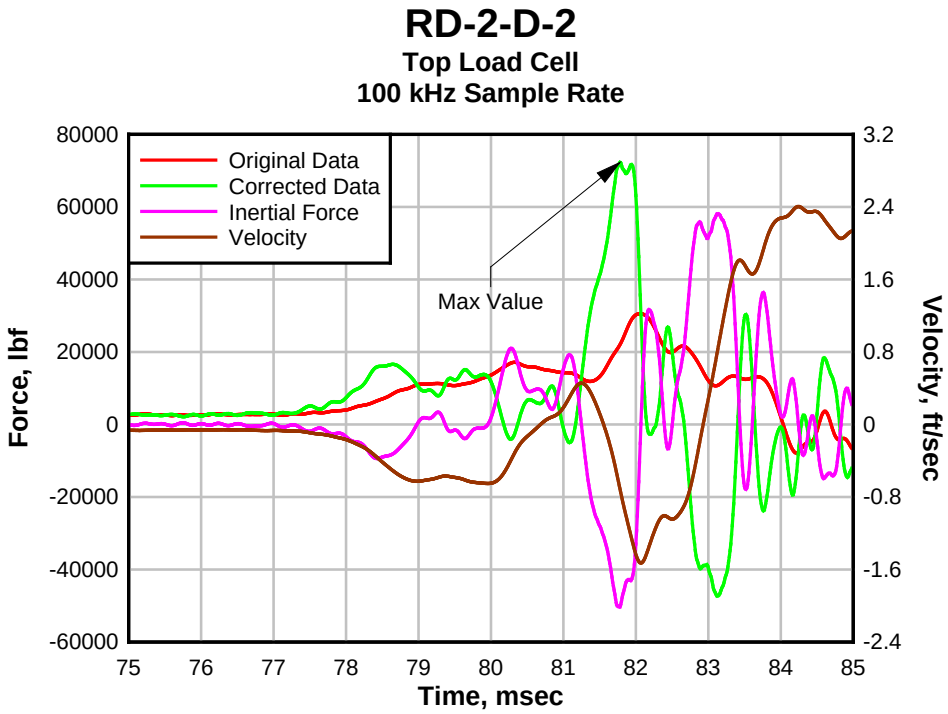

Figure 107: RD-2-D-2 Test Data.

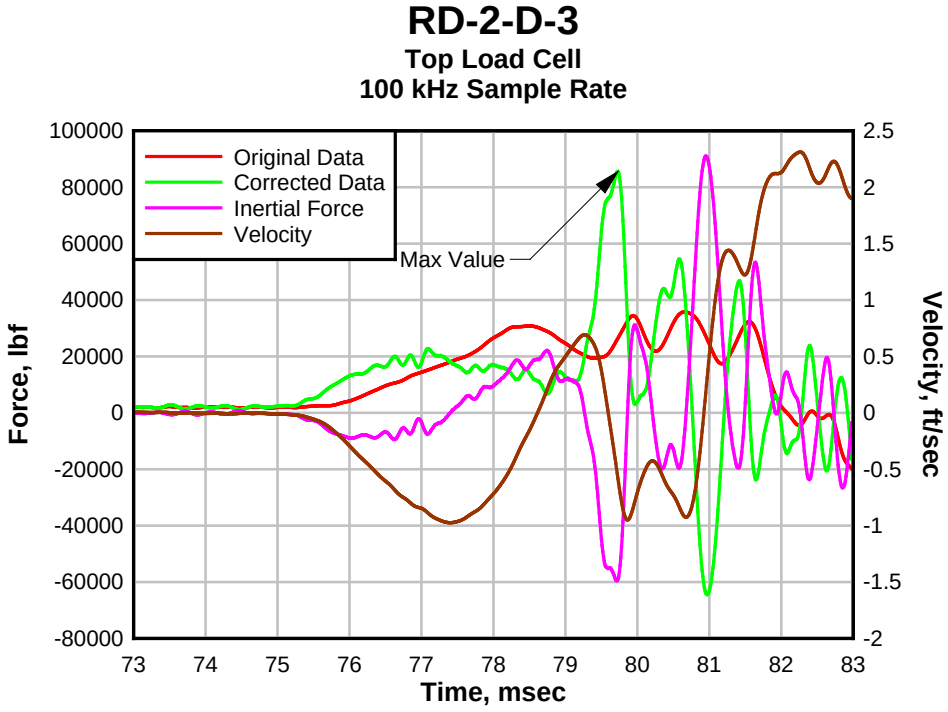

Figure 108: RD-2-D-3 Test Data.

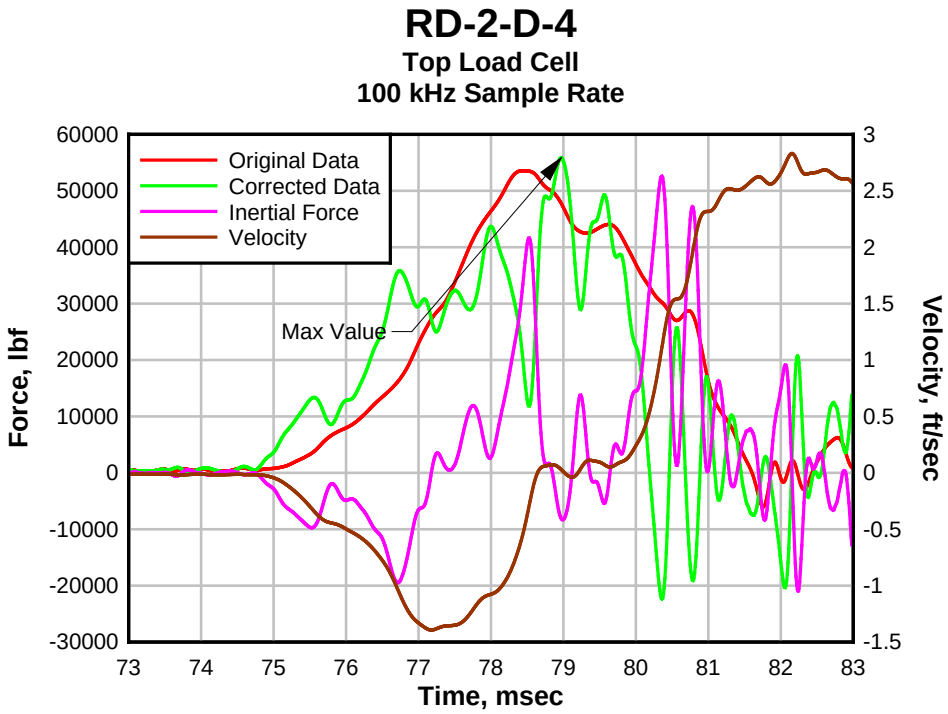

Figure 109: RD-2-D-4 Test Data.

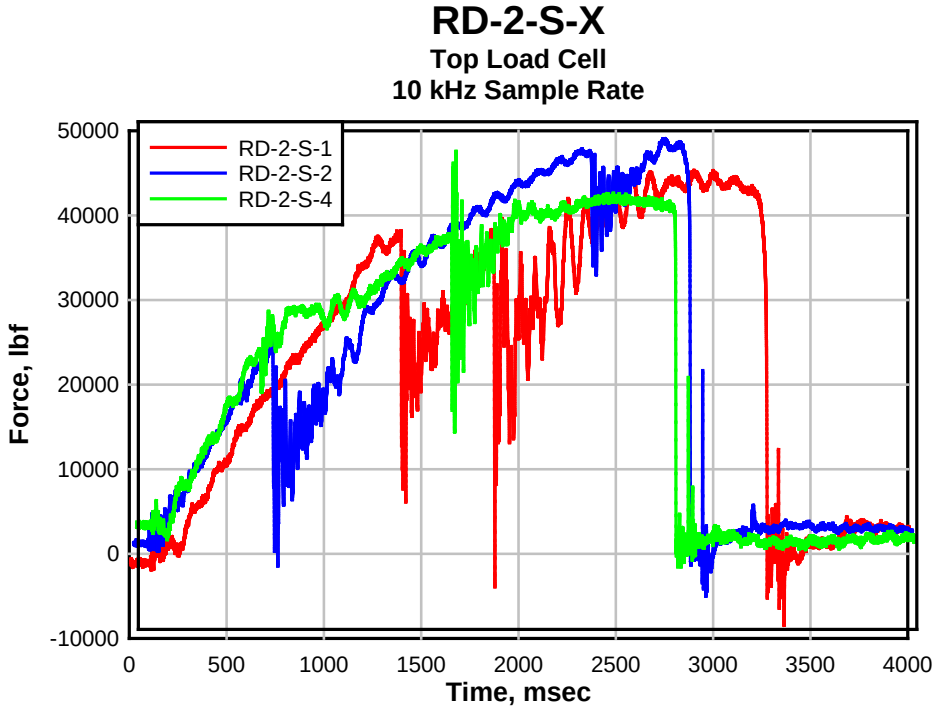

Figure 110: RD-2-S-X Tests Data.

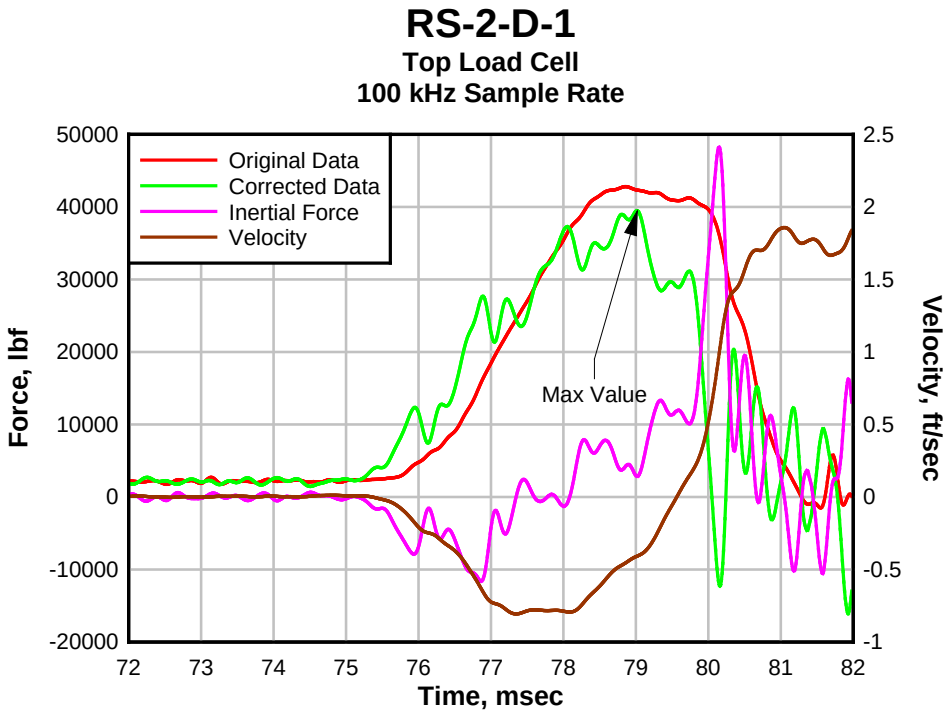

Figure 111: RS-2-D-1 Test Data.

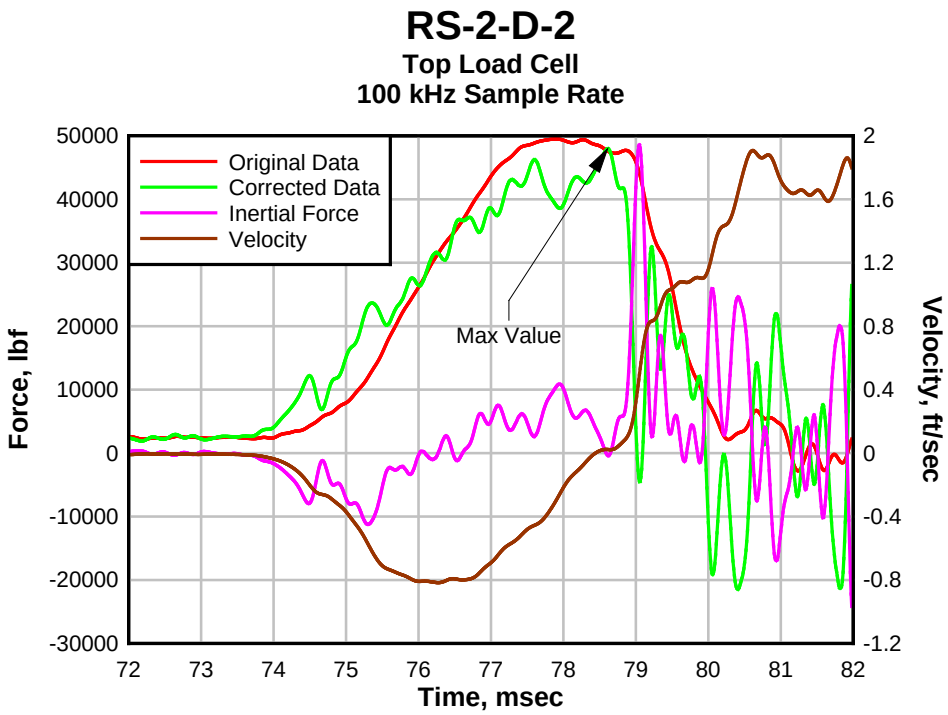

Figure 112: RS-2-D-2 Test Data.

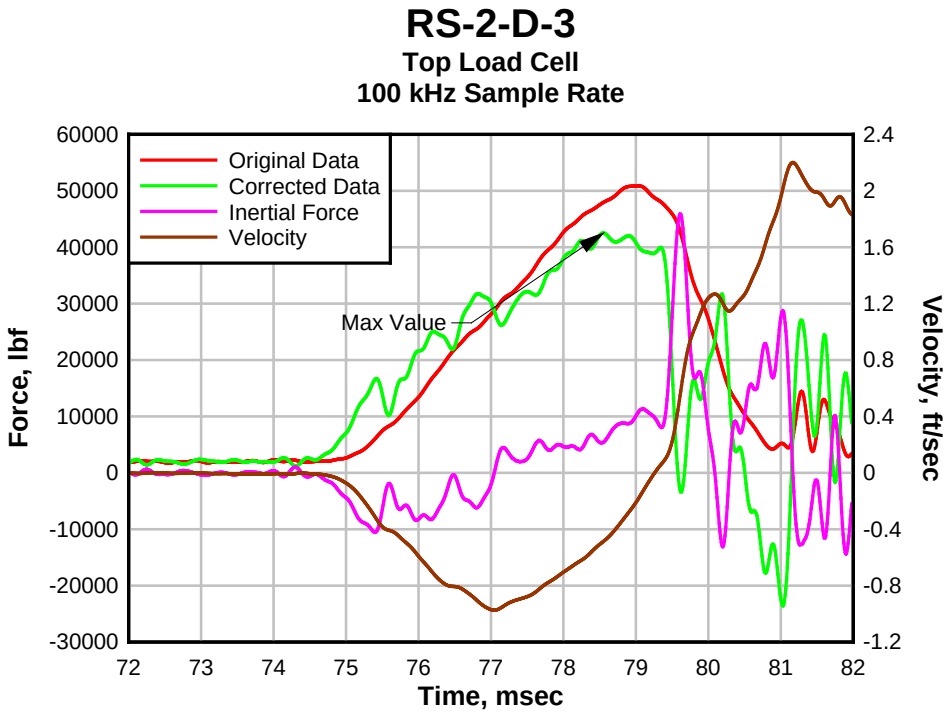

Figure 113: RS-2-D-3 Test Data.

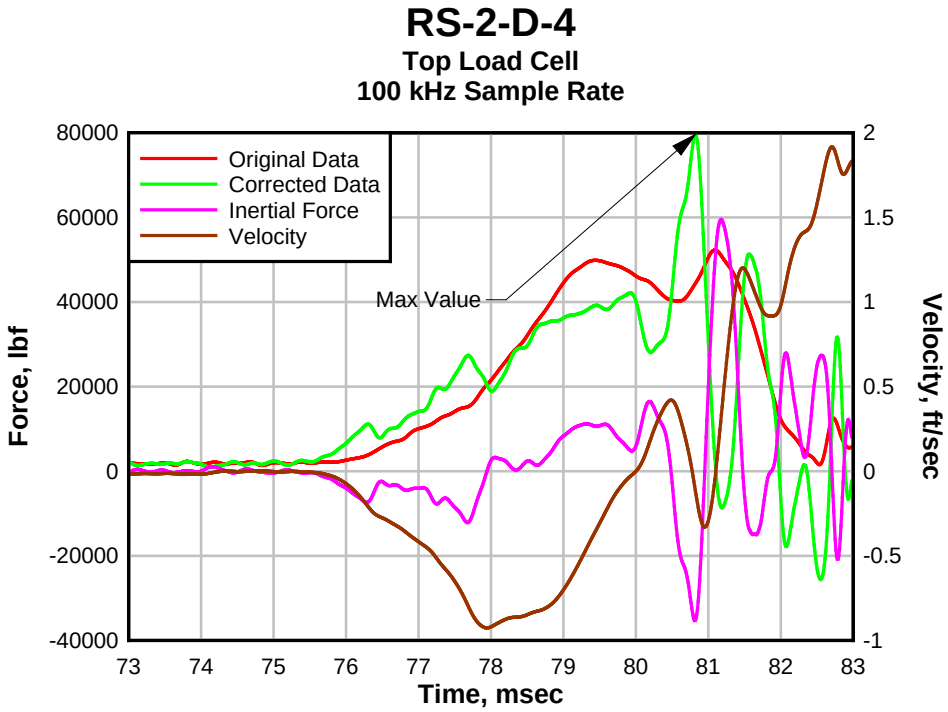

Figure 114: RS-2-D-4 Test Data.

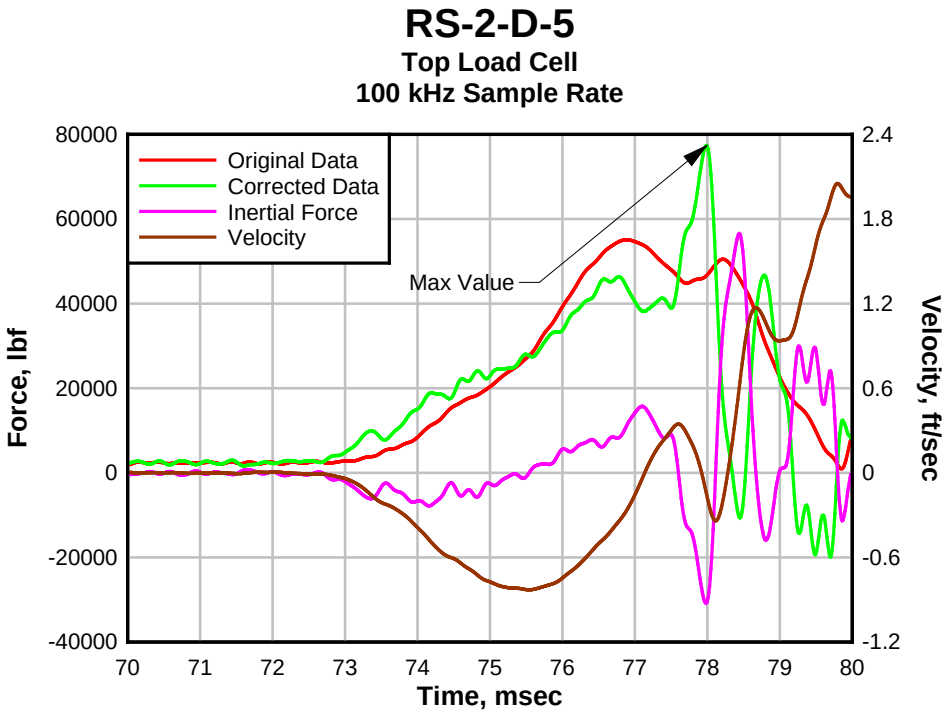

Figure 115: RS-2-D-5 Test Data.

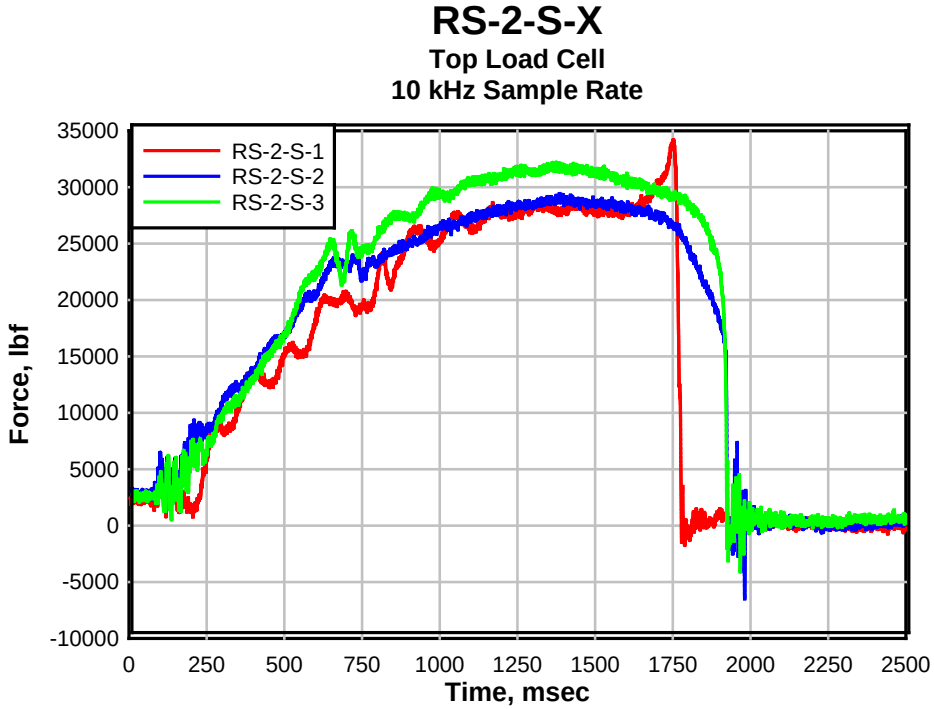

Figure 116: RS-2-S-X Tests Data.

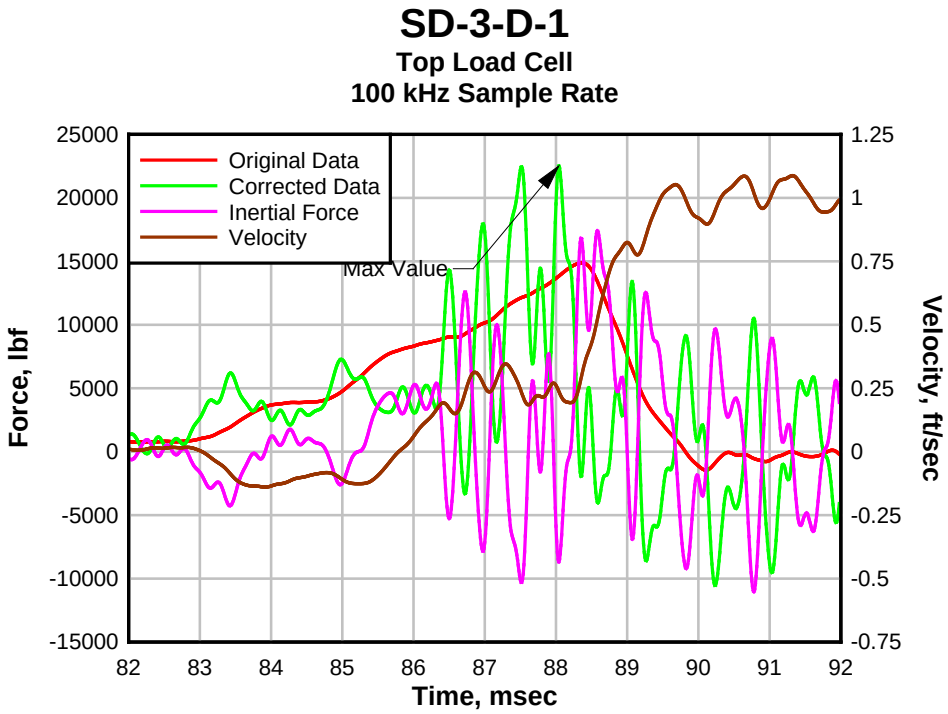

Figure 117: SD-3-D-1 Test Data.

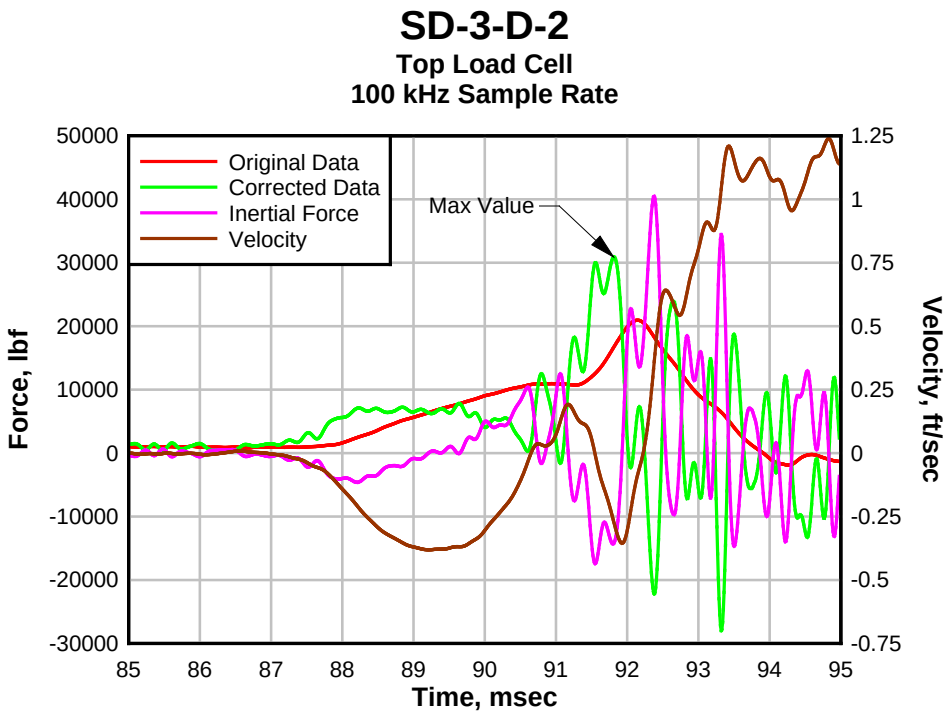

Figure 118: SD-3-D-2 Test Data.

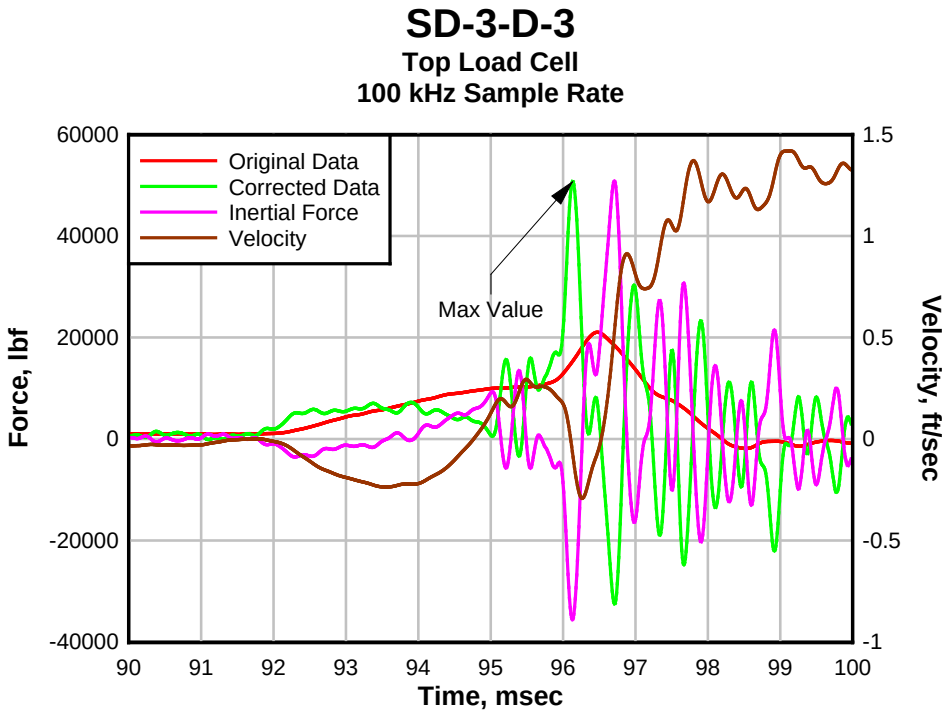

Figure 119: SD-3-D-3 Test Data.

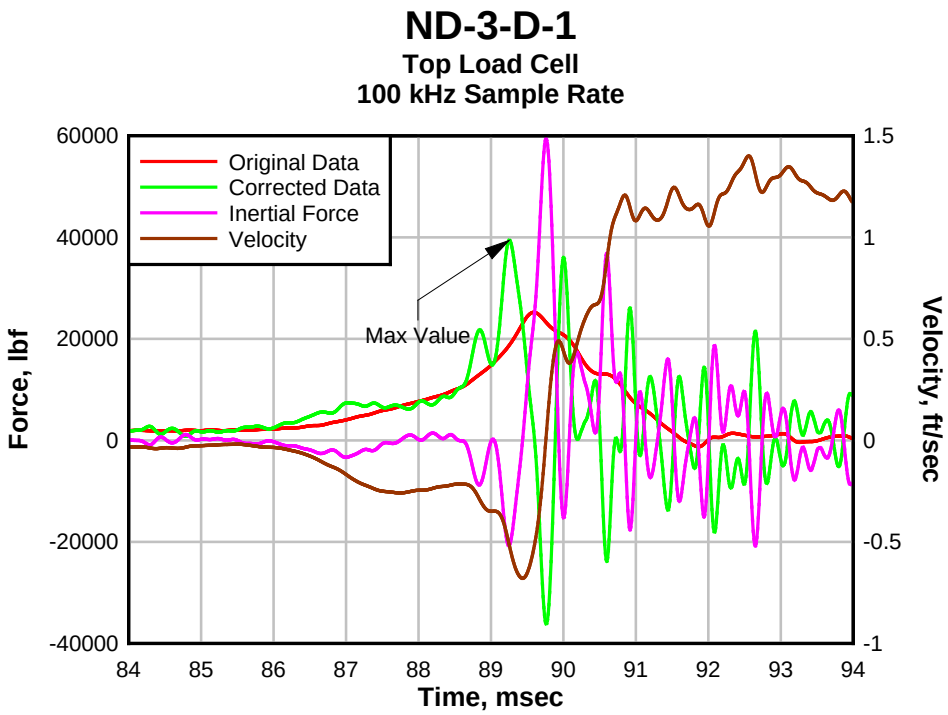

Figure 120: ND-3-D-1 Test Data.

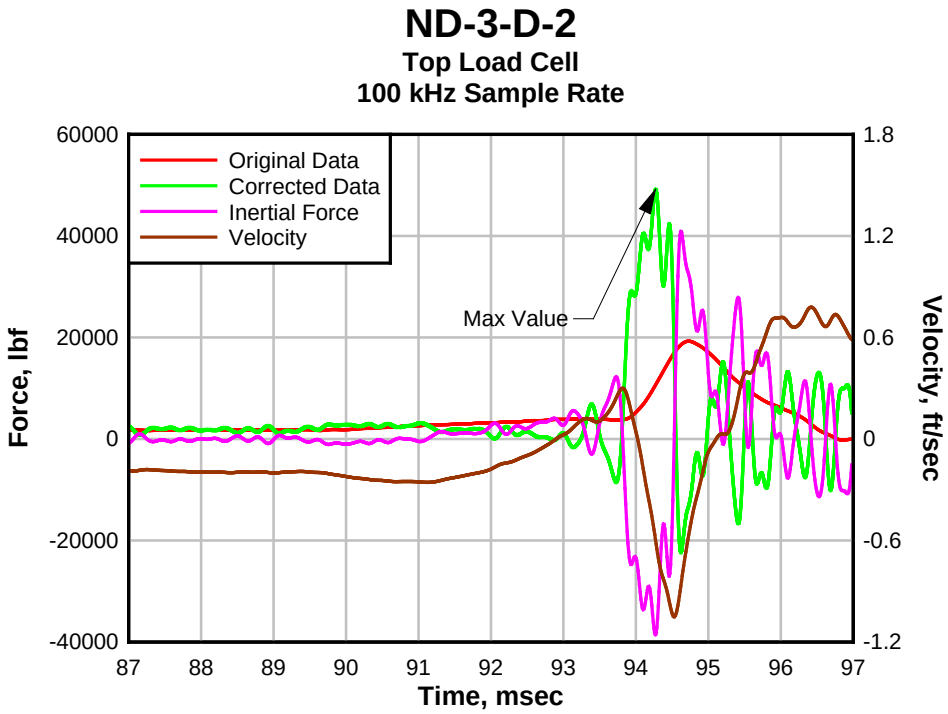

Figure 121: ND-3-D-2 Test Data.

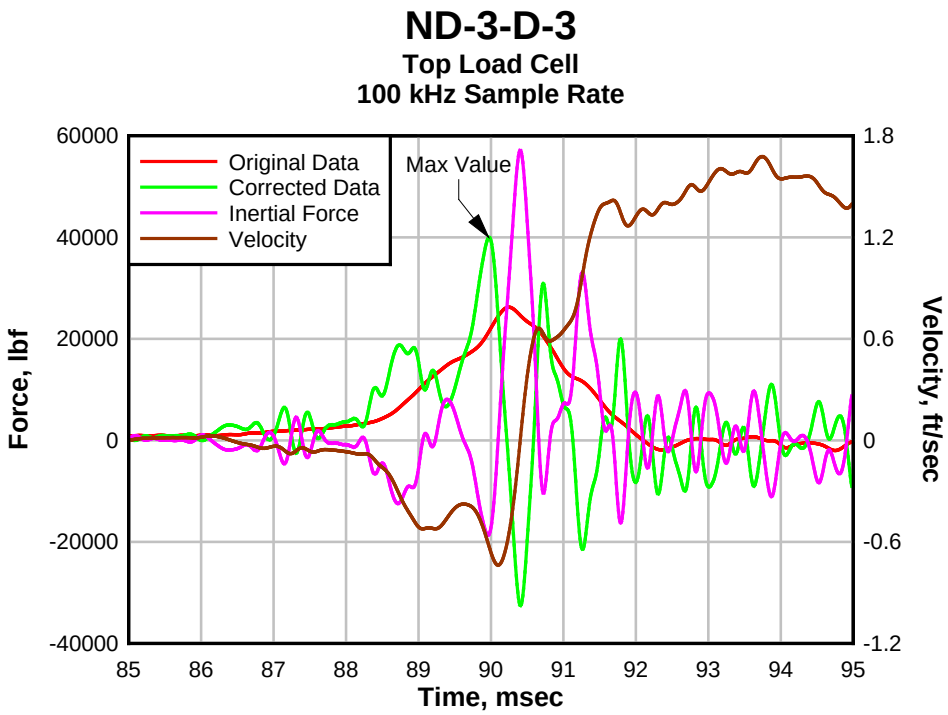

Figure 122: ND-3-D-3 Test Data.

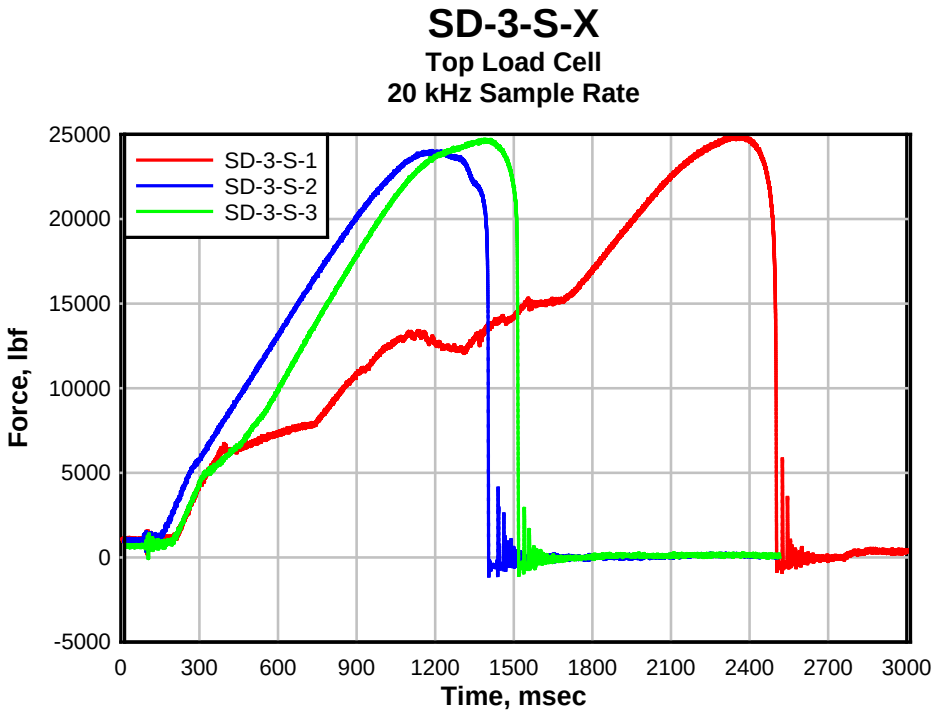

Figure 123: SD-3-S-X Tests Data.

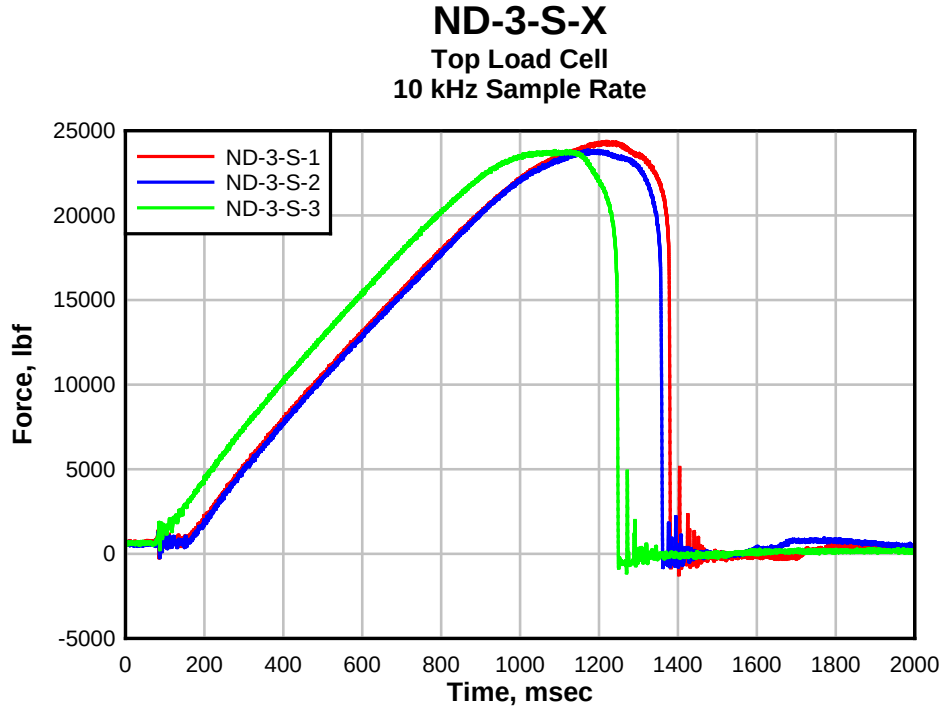

Figure 124: ND-3-S-X Tests Data.

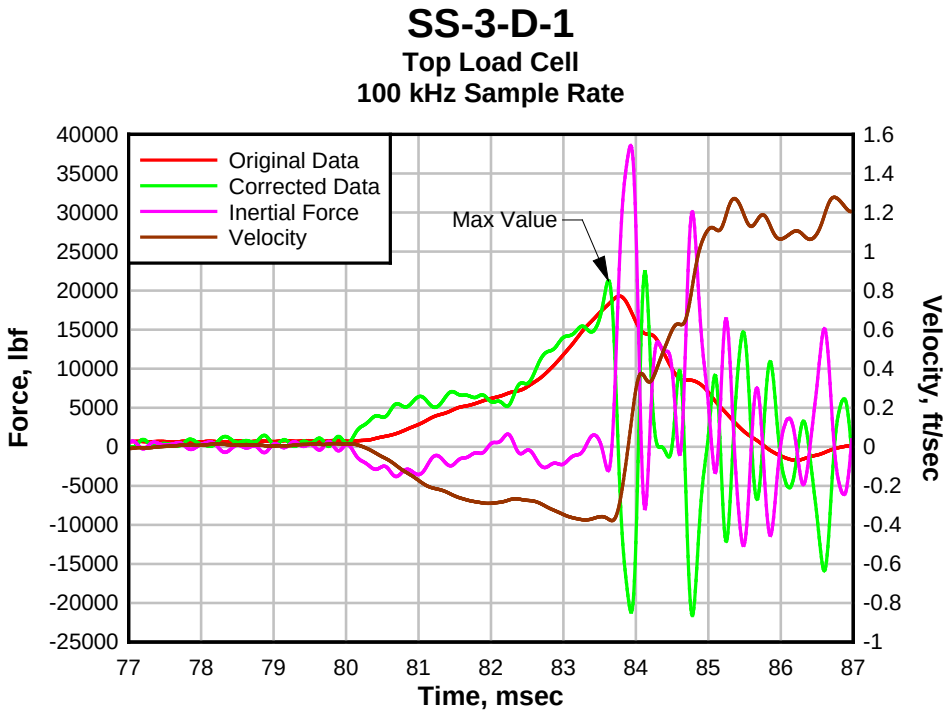

Figure 125: SS-3-D-1 Test Data.

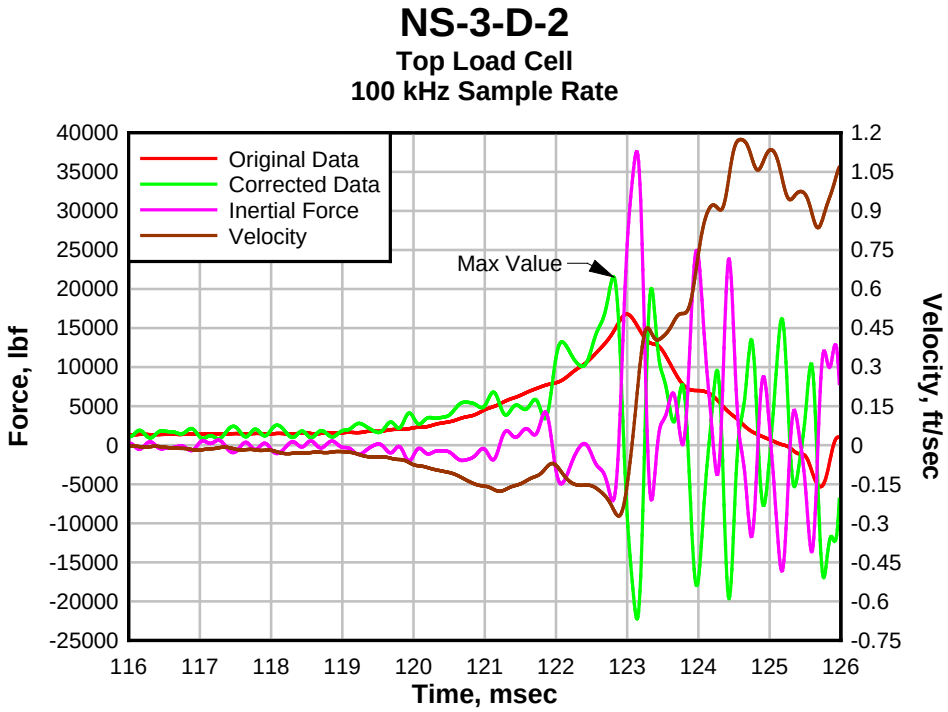

Figure 126: NS-3-D-2 Test Data.

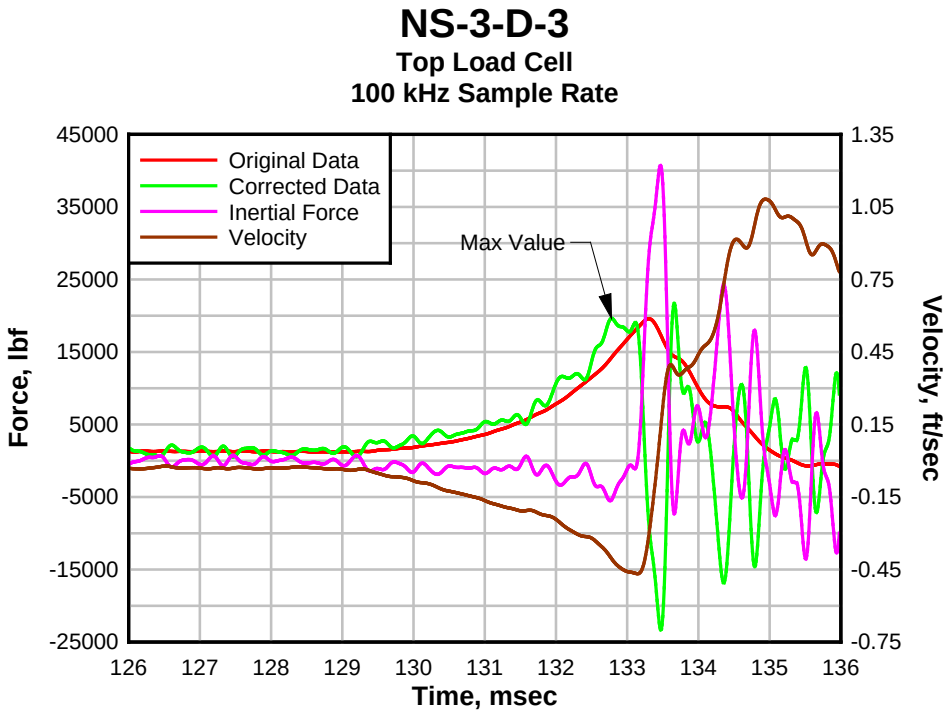

Figure 127: NS-3-D-3 Test Data.

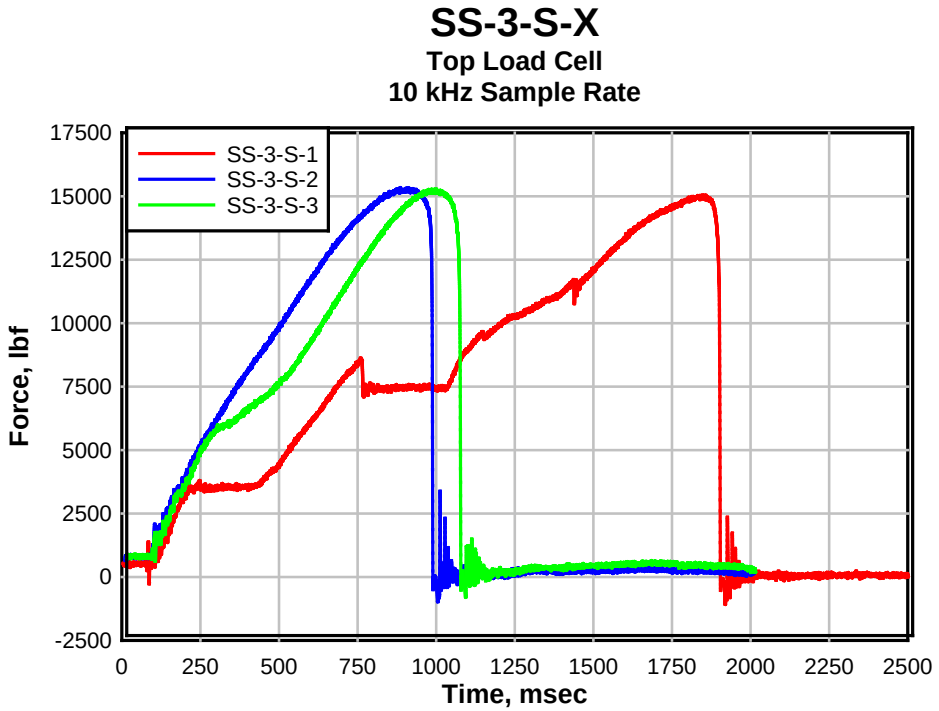

Figure 128: SS-3-S-X Tests Data.

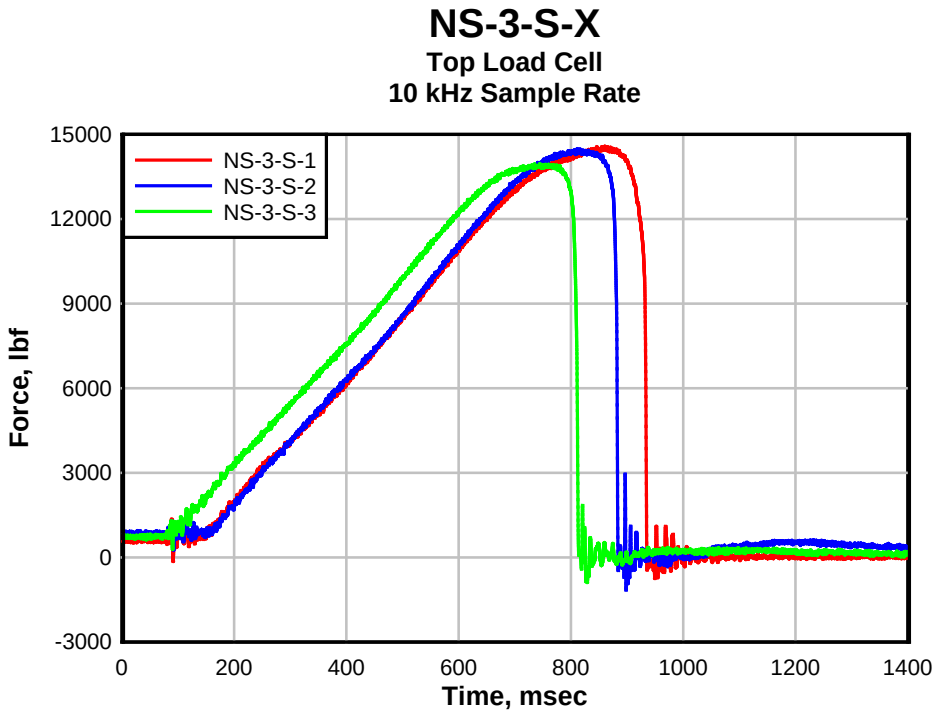

Figure 129: NS-3-S-X Tests Data.

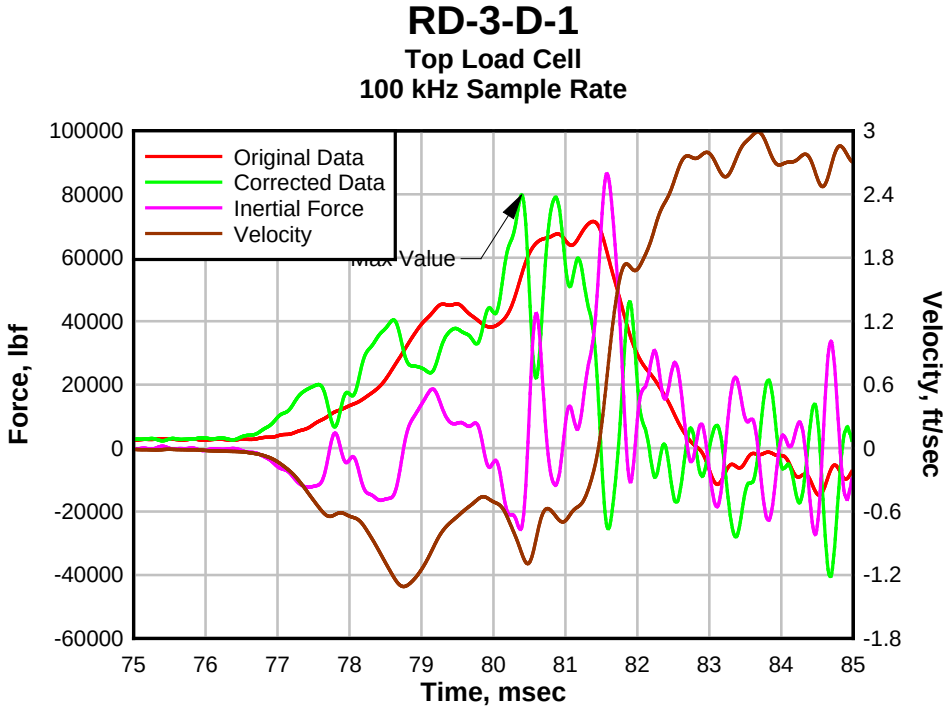

Figure 130: RD-3-D- Test Data.

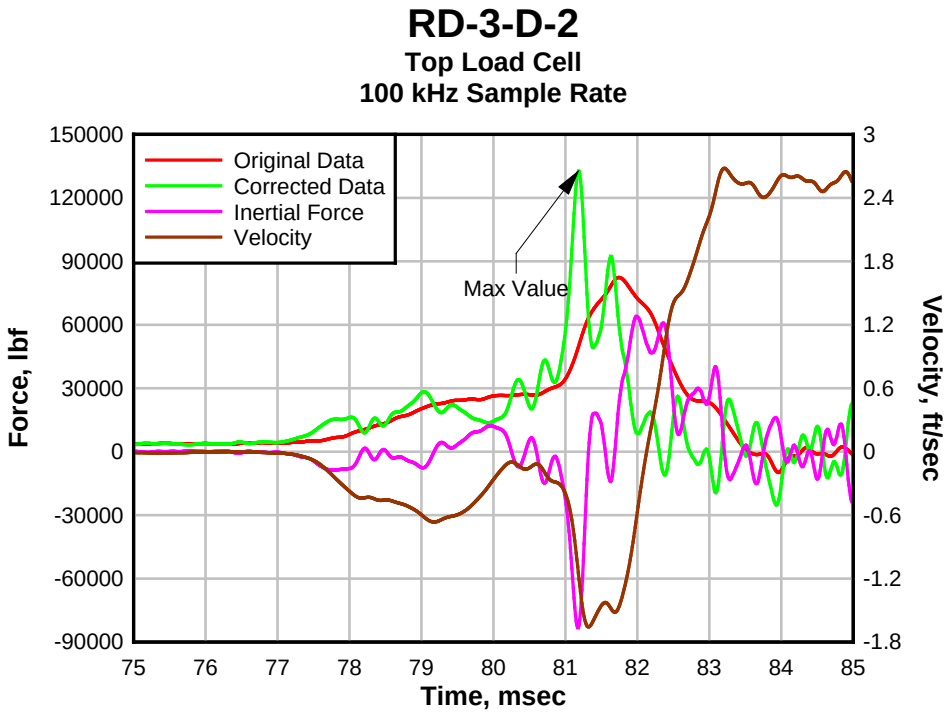

Figure 131: RD-3-D-2 Test Data.

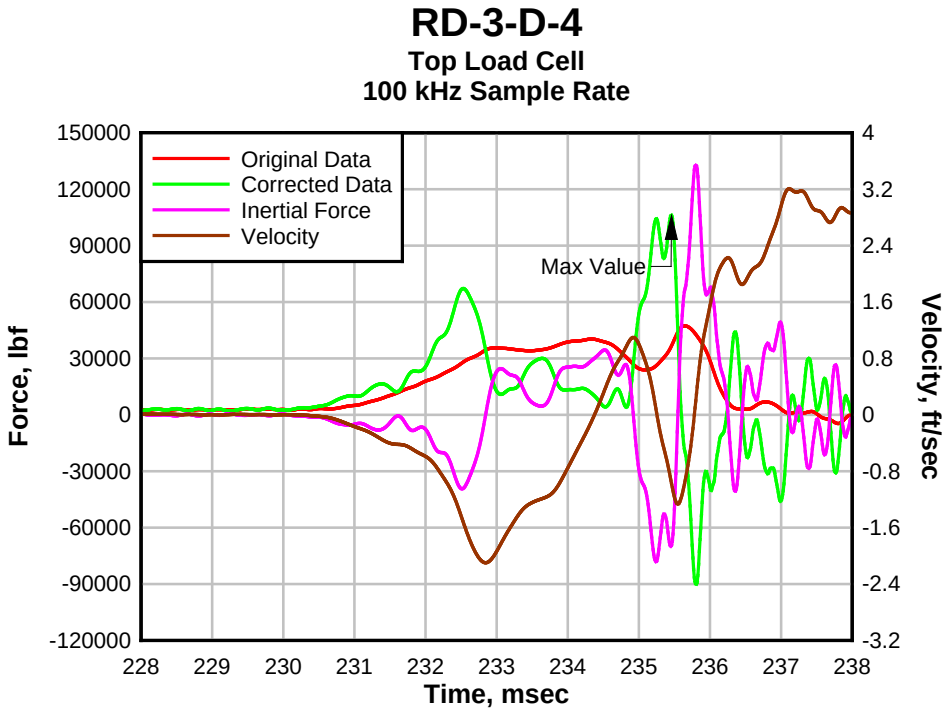

Figure 132: RD-3-D-4 Test Data.

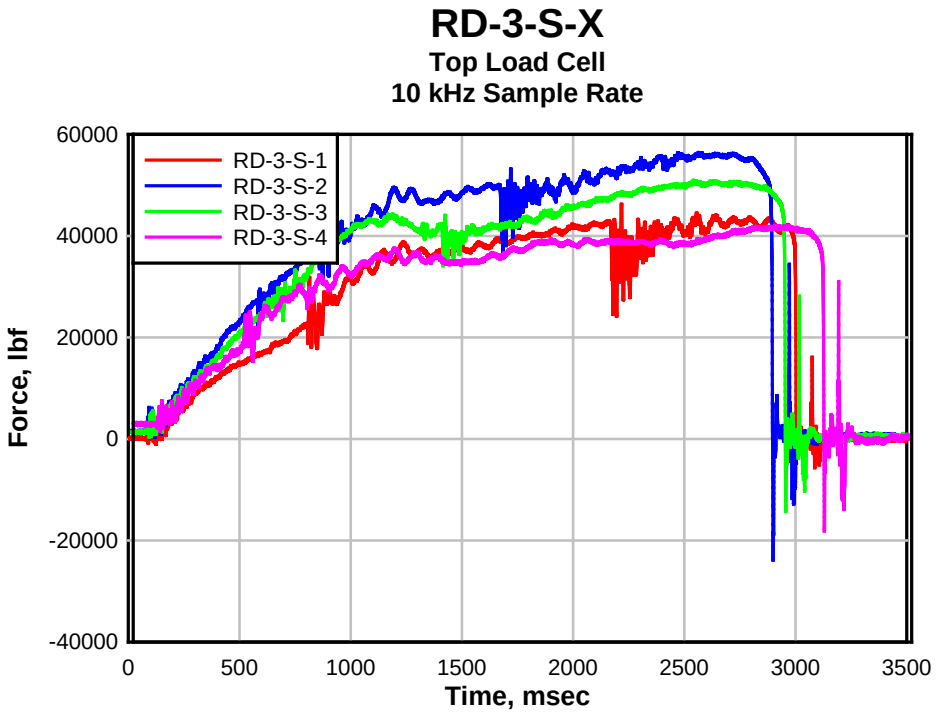

Figure 133: RD-3-S-X Tests Data.

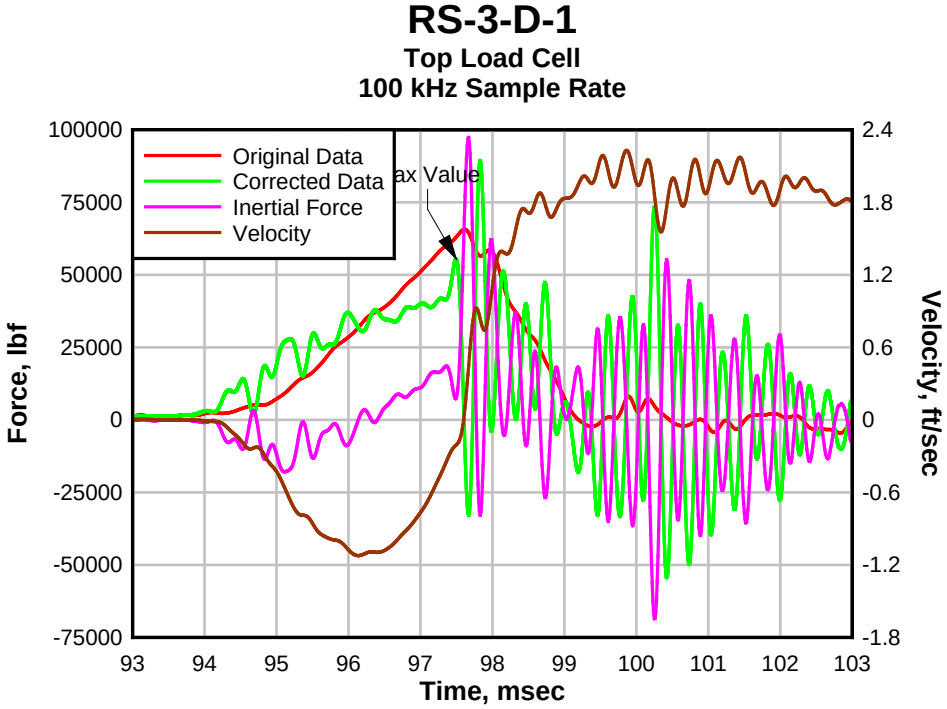

Figure 134: RS-3-D-1 Test Data.

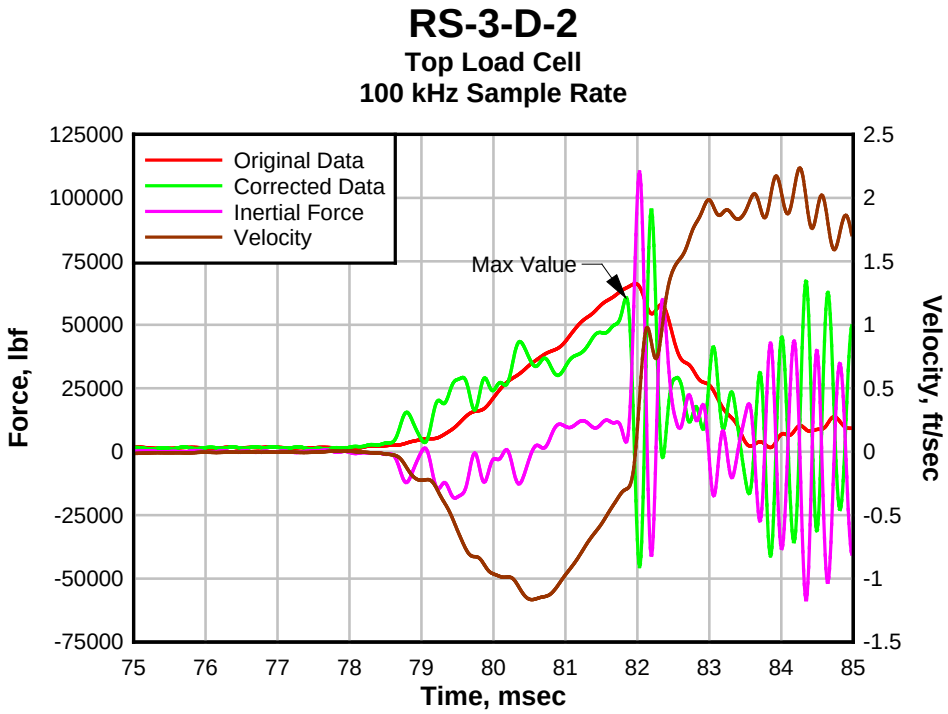

Figure 135: RS-3-D-2 Test Data.

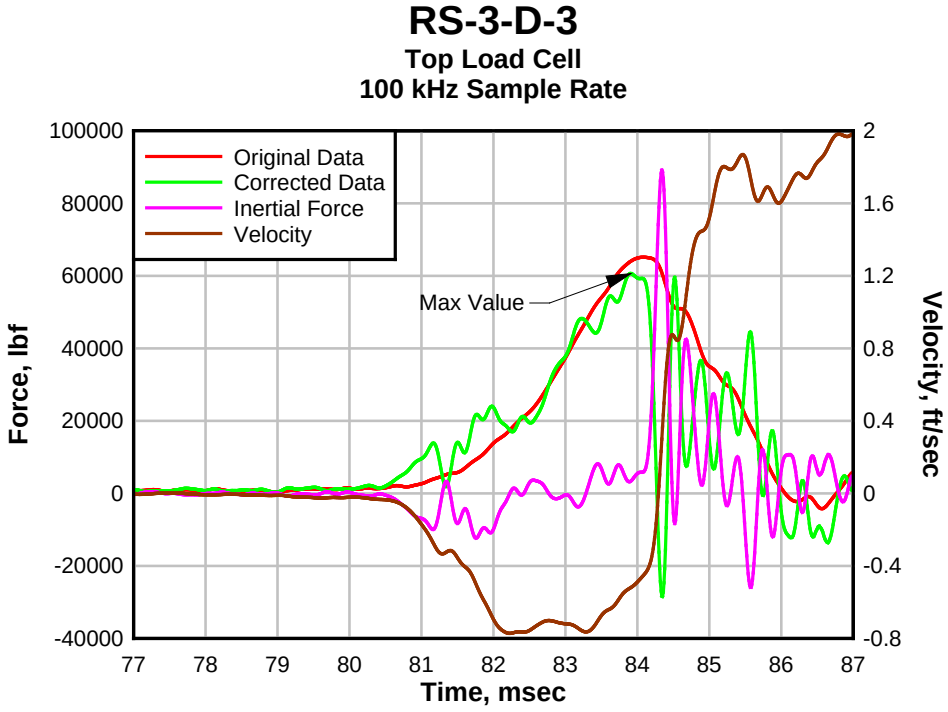

Figure 136: RS-3-D-3 Test Data.

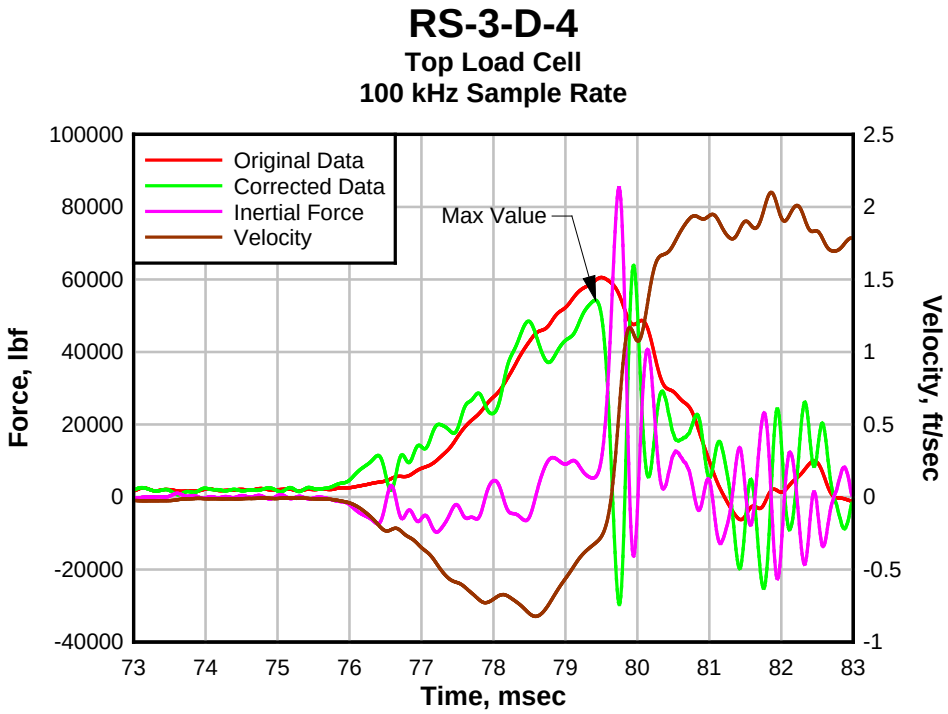

Figure 137: RS-3-D-4 Test Data.

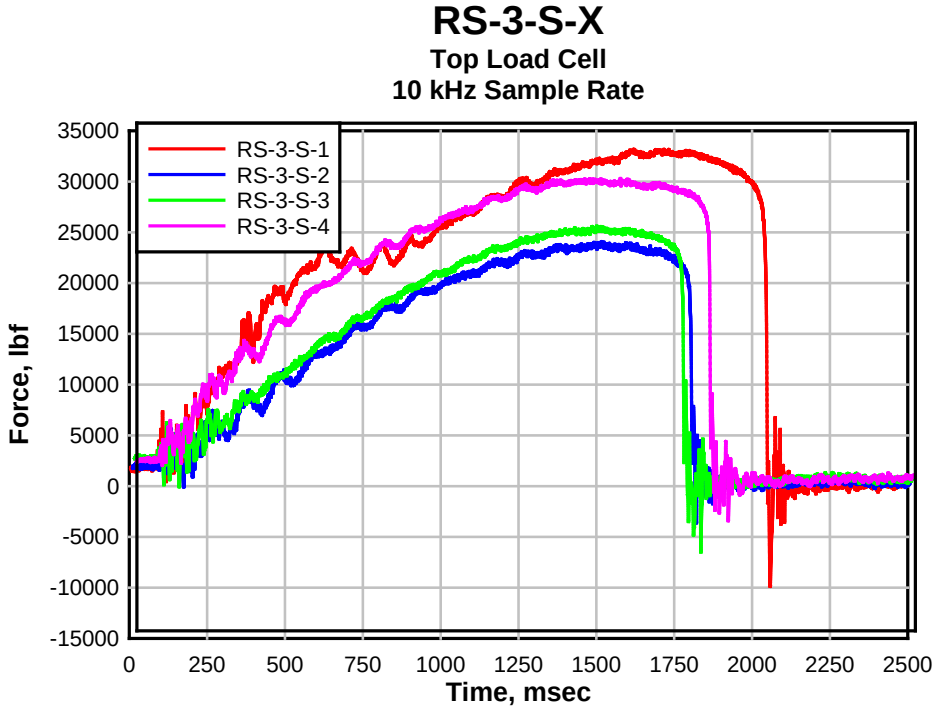

Figure 138: RS-3-S-X Tests Data.

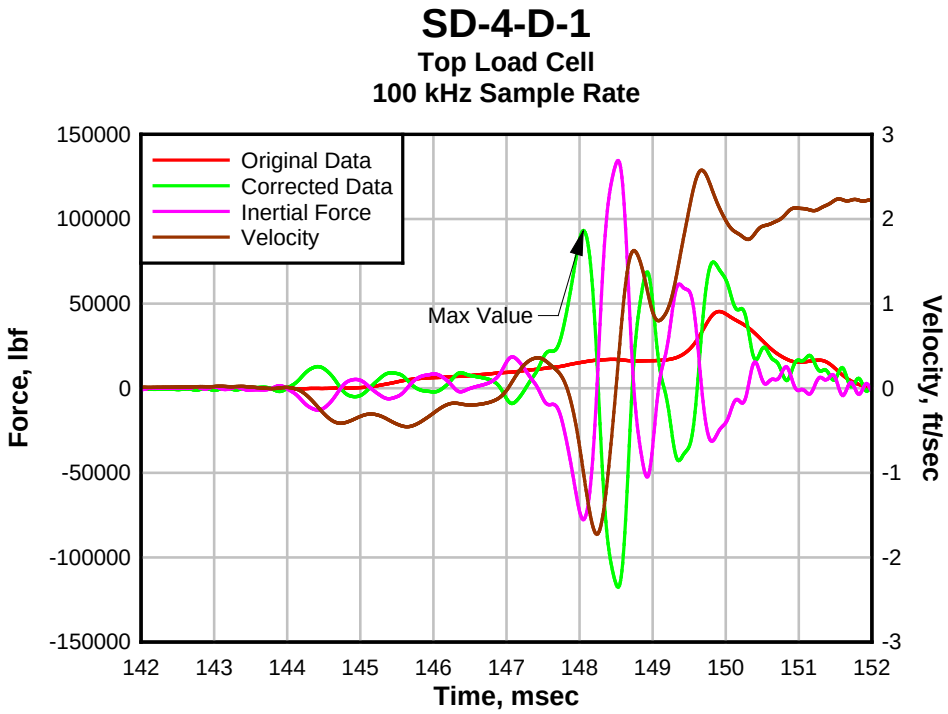

Figure 139: SD-4-D-1 Test Data.

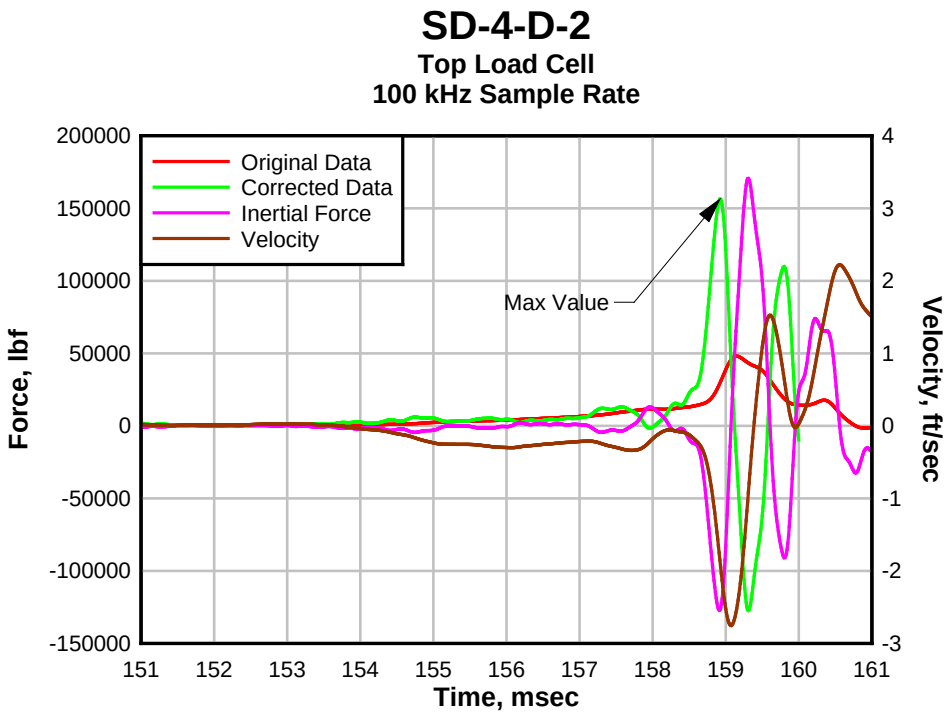

Figure 140: SD-4-D-2 Test Data.

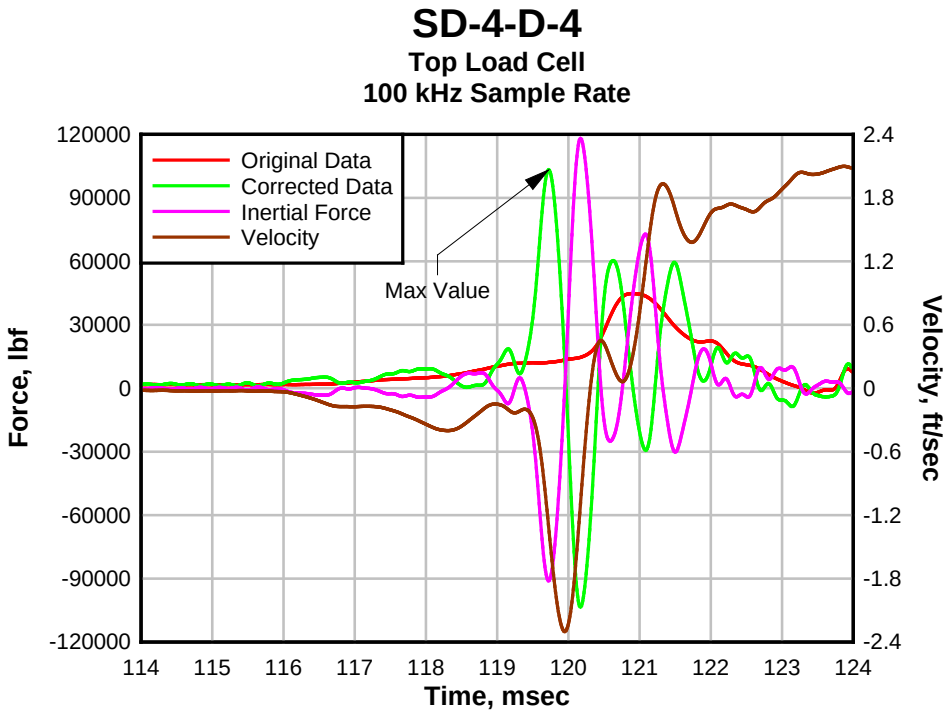

Figure 141: SD-4-D-4 Test Data.

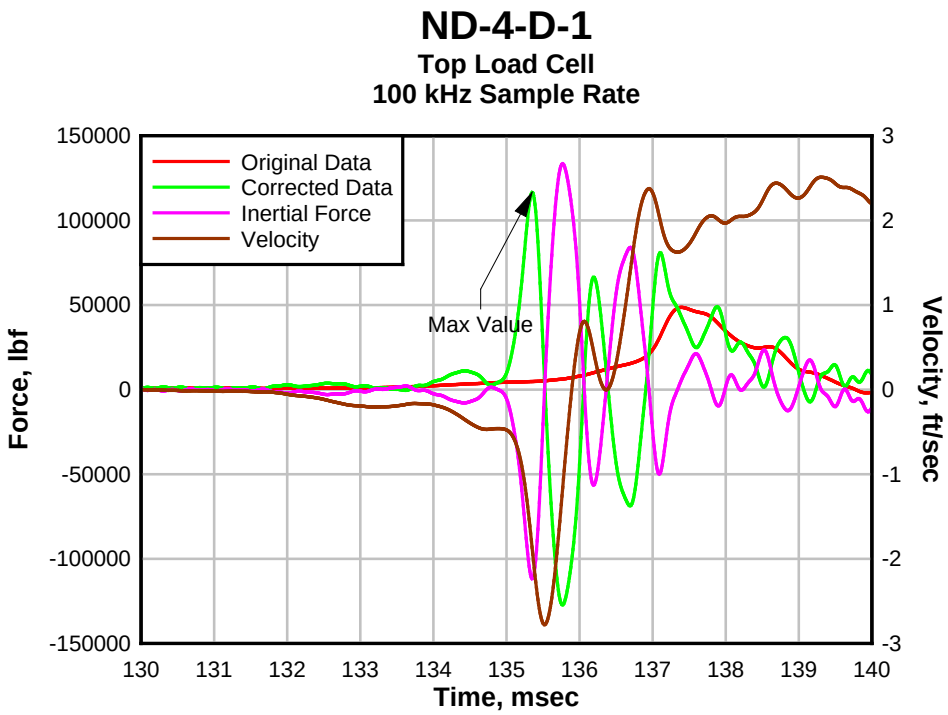

Figure 142: ND-4-D-1 Test Data.

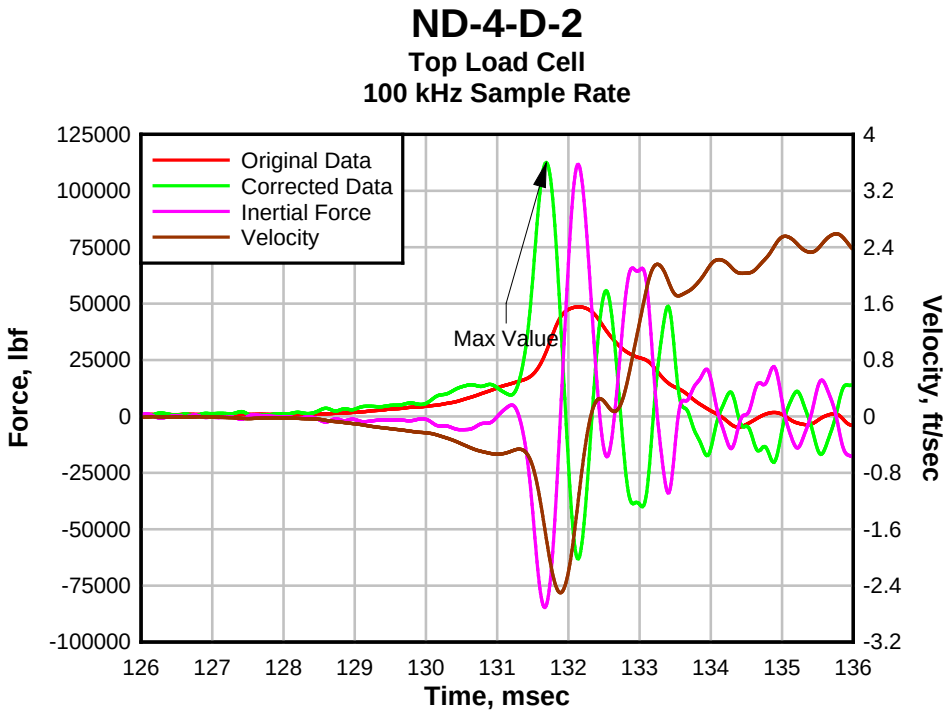

Figure 143: ND-4-D-2 Test Data.

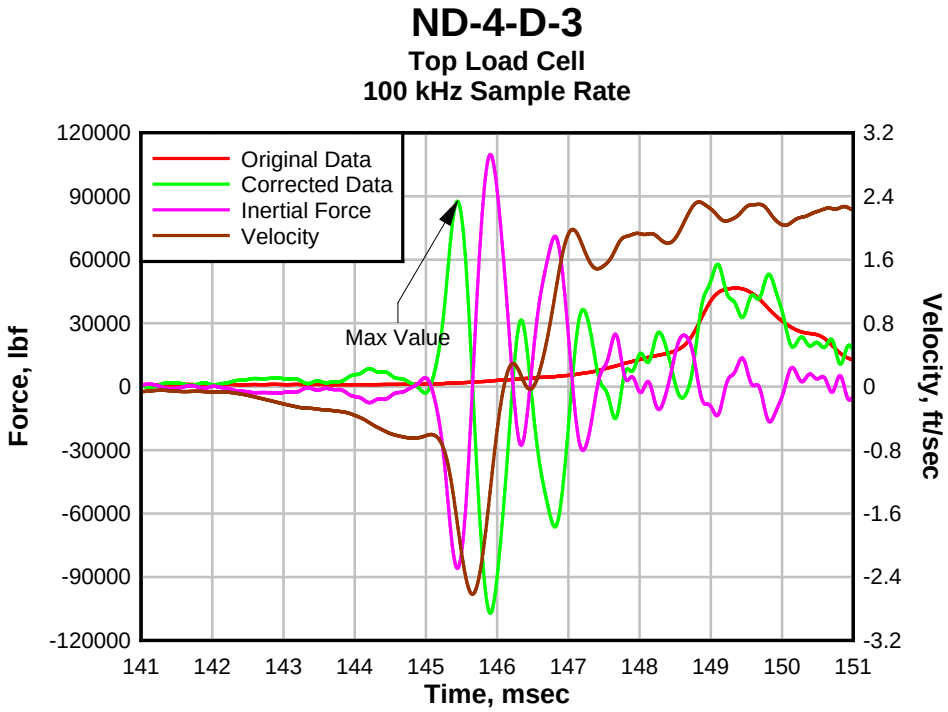

Figure 144: ND-4-D-3 Test Data.

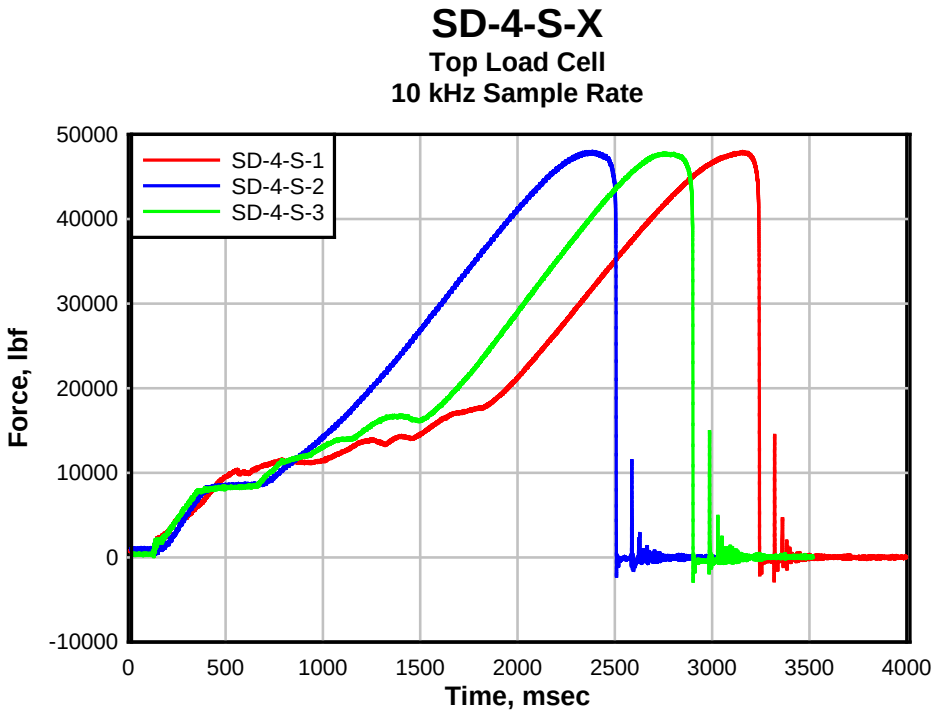

Figure 145: SD-4-S-X Tests Data.

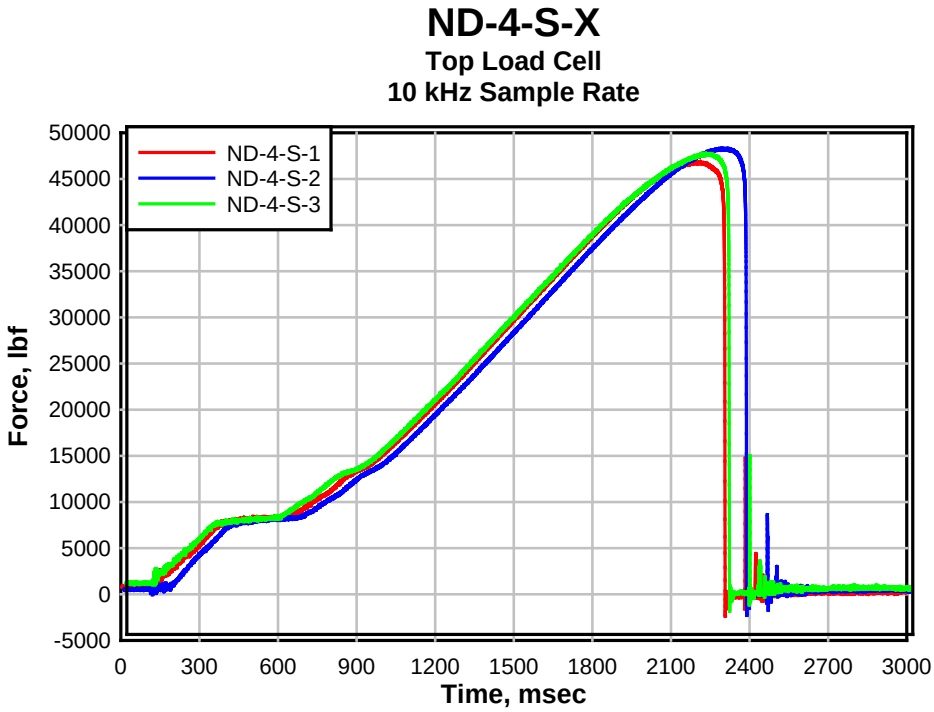

Figure 146: ND-4-S-X Tests Data.

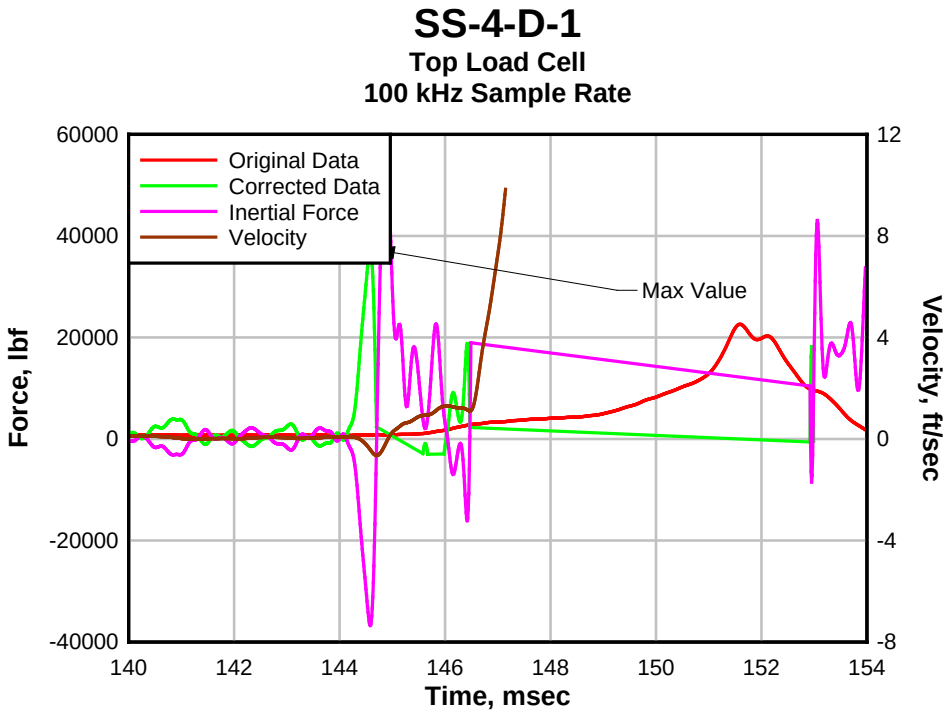

Figure 147: SS-4-D-1 Test Data.

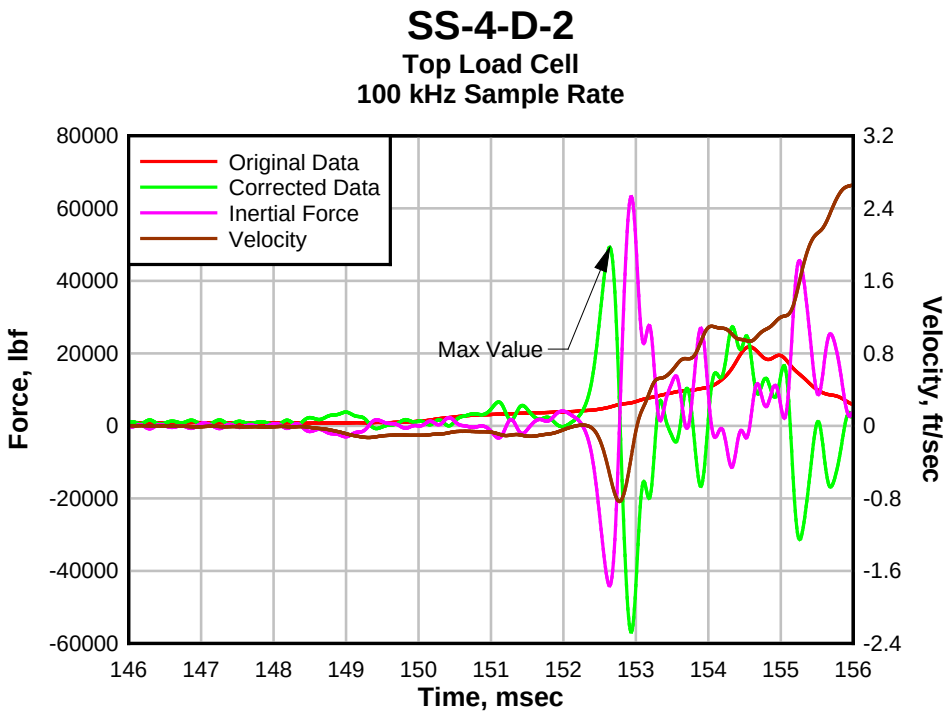

Figure 148: SS-4-D-2 Test Data.

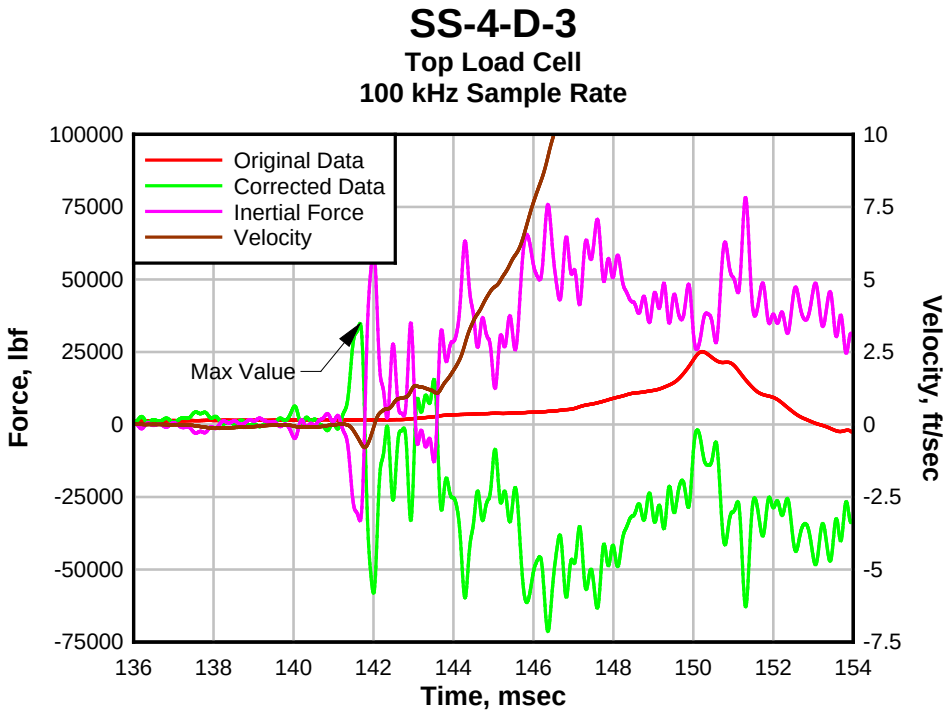

Figure 149: SS-4-D-3 Test Data.

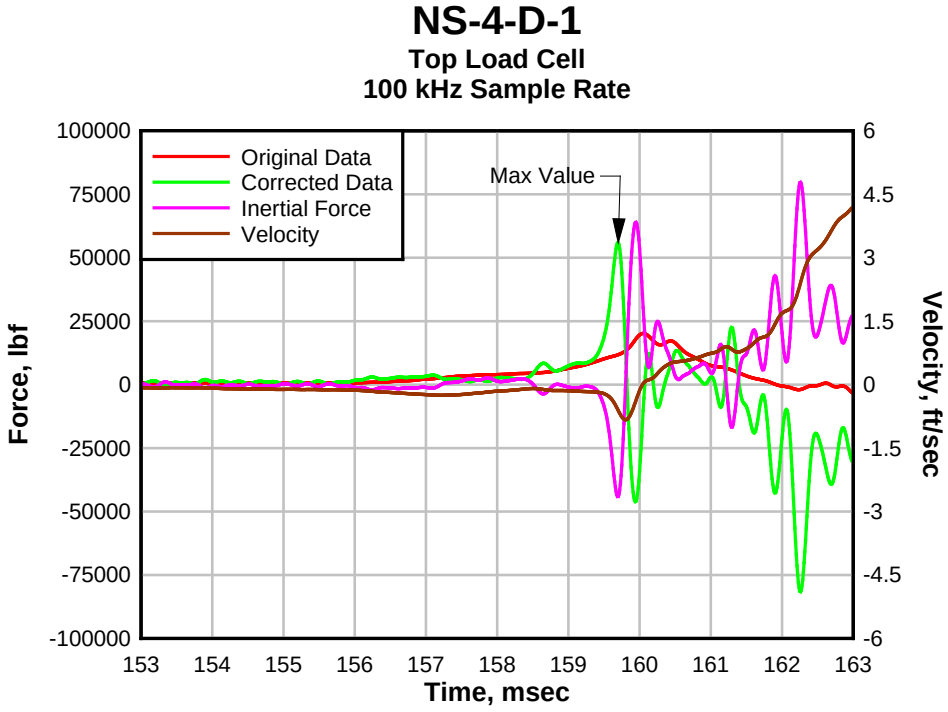

Figure 150: NS-4-D-1 Test Data.

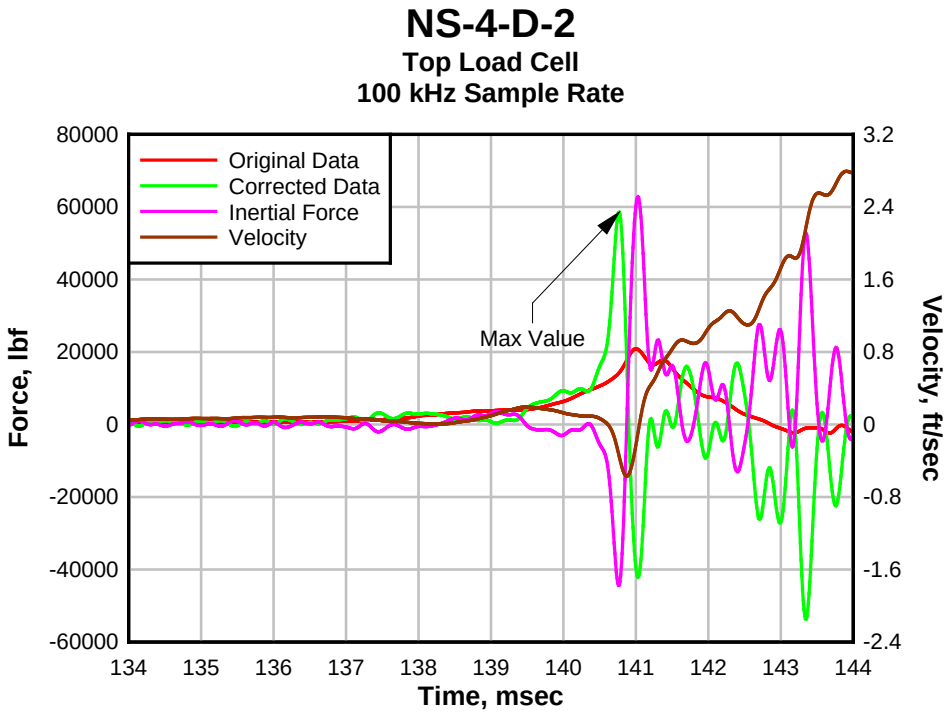

Figure 151: NS-4-D-2 Test Data.

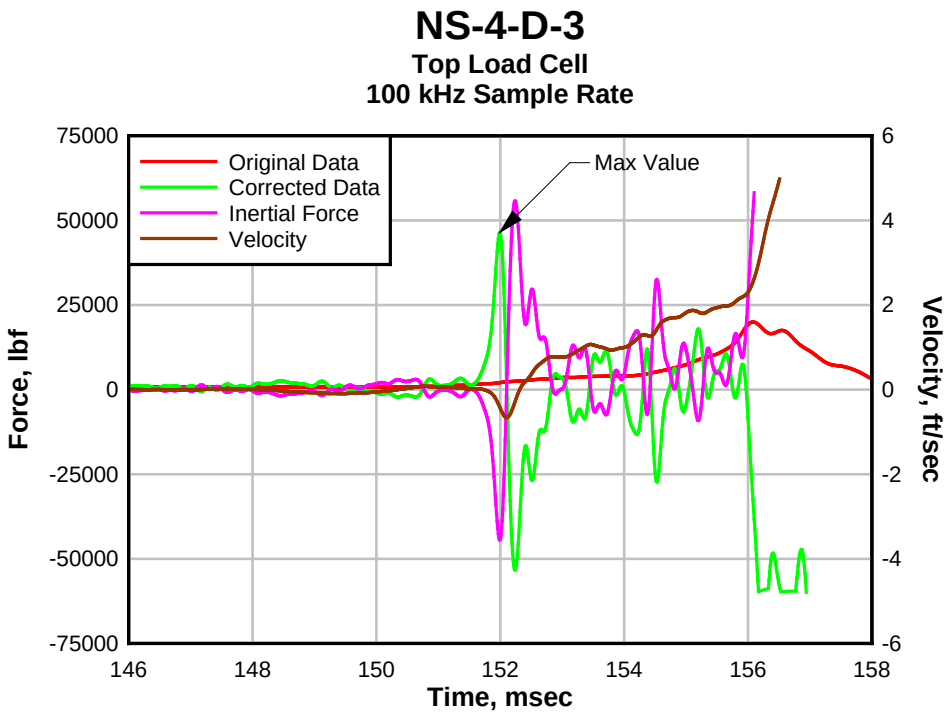

Figure 152: NS-4-D-3 Test Data.

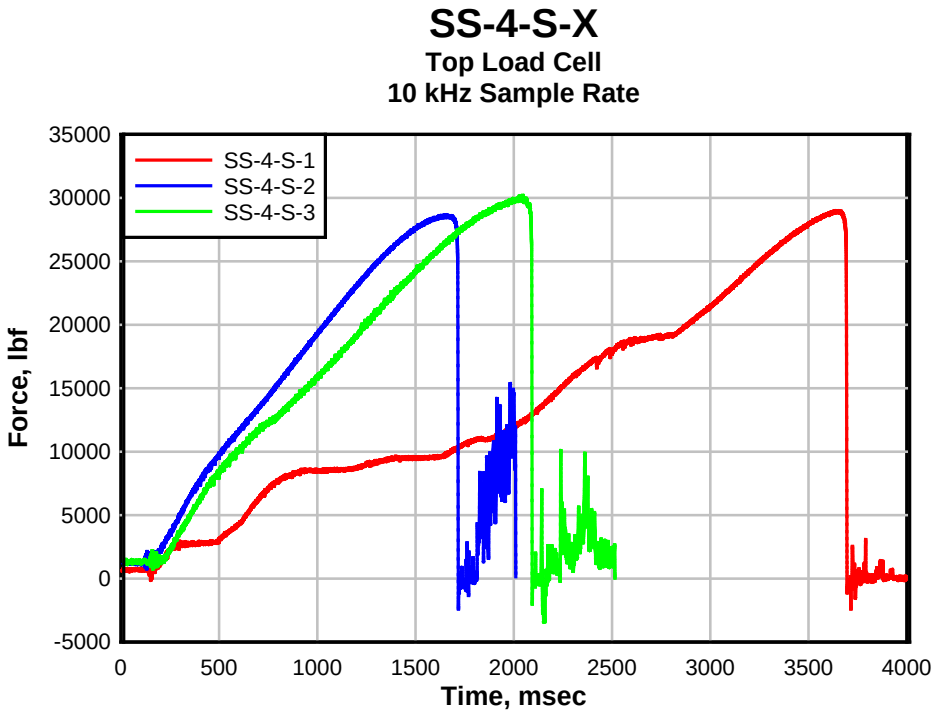

Figure 153: SS-4-S-X Tests Data.

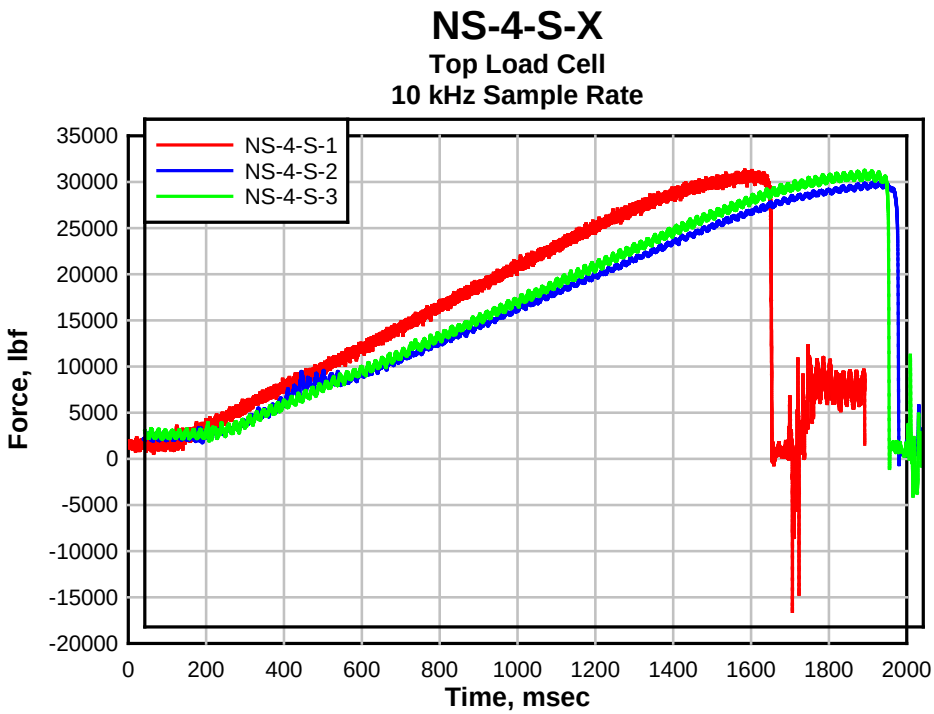

Figure 154: NS-4-S-X Tests Data.

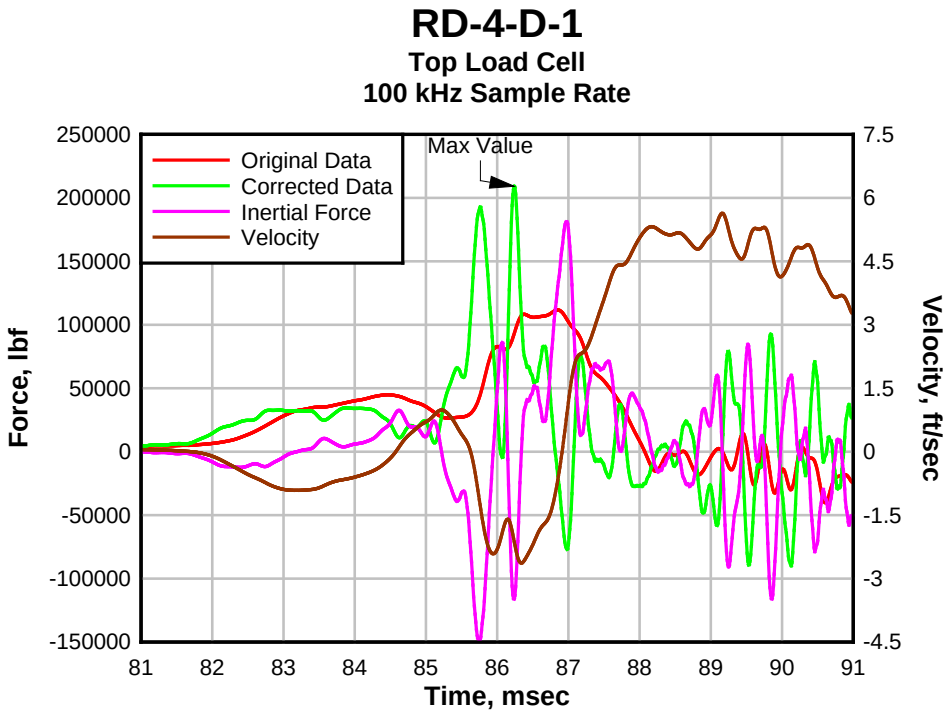

Figure 155: RD-4-D-1 Test Data.

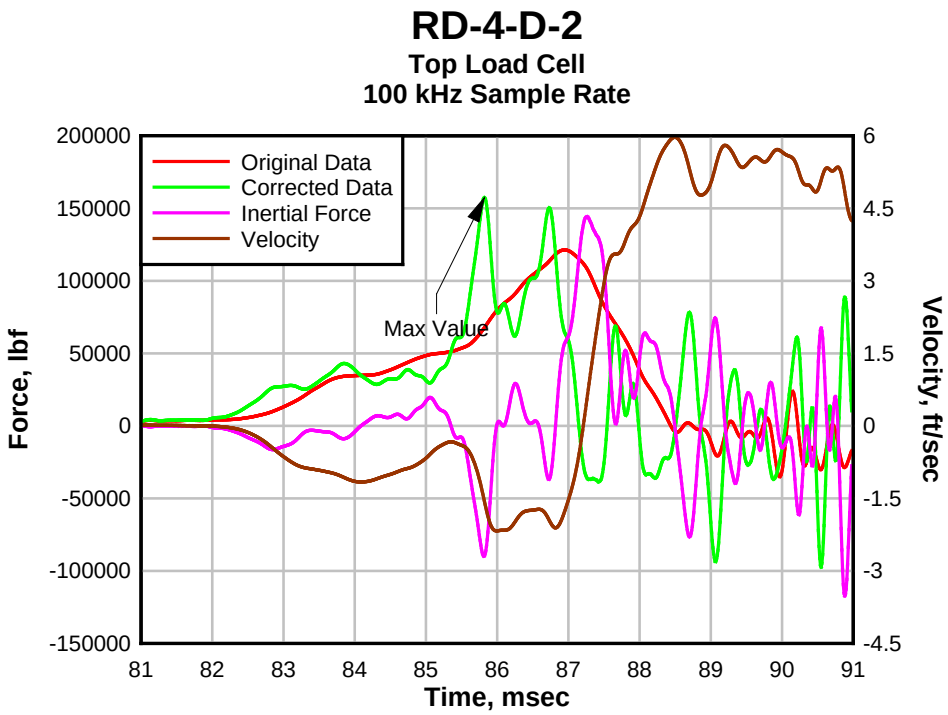

Figure 156: RD-4-D-2 Test Data.

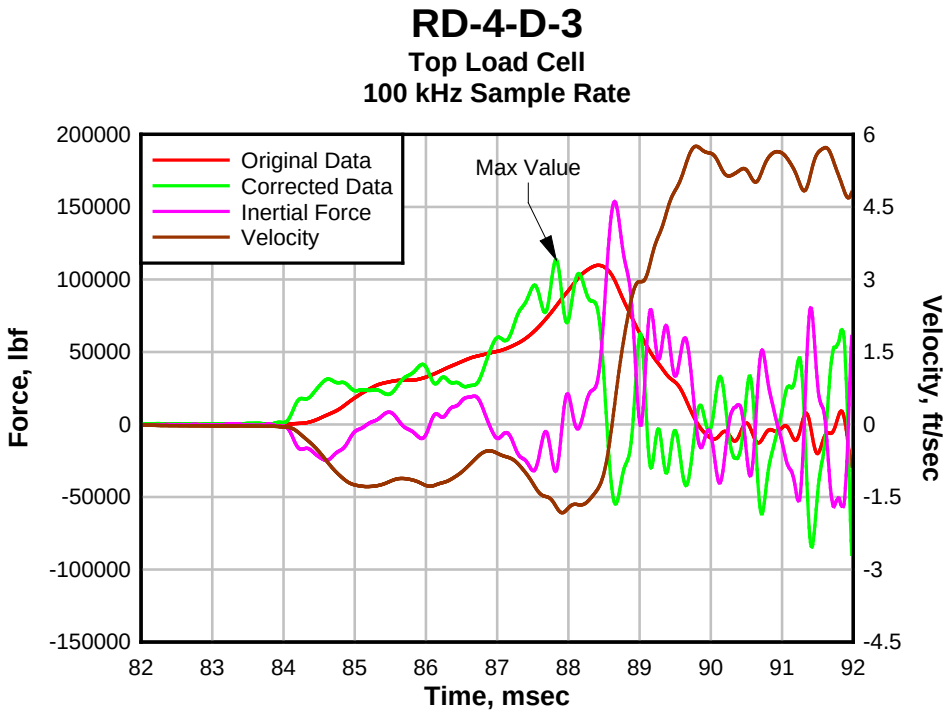

Figure 157: RD-4-D-3 Test Data.

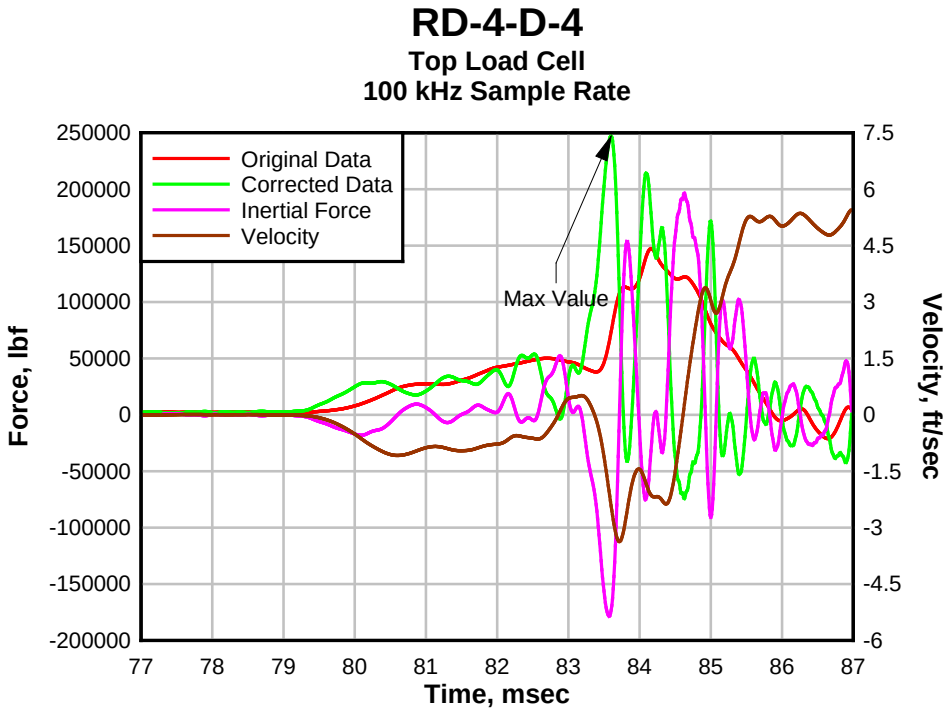

Figure 158: RD-4-D-4 Test Data.

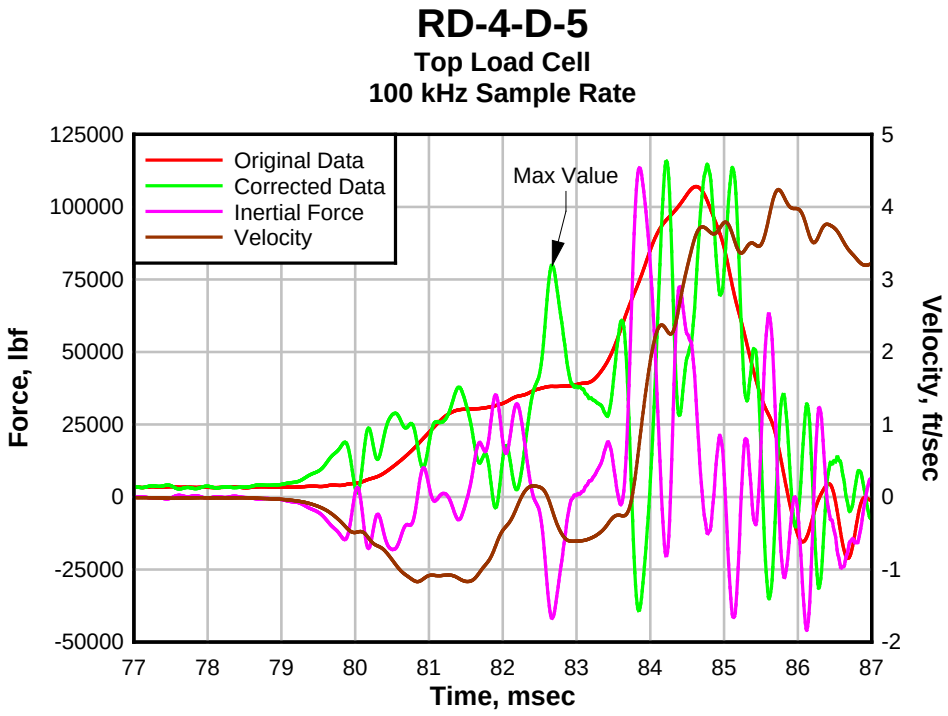

Figure 159: RD-4-D-5 Test Data.

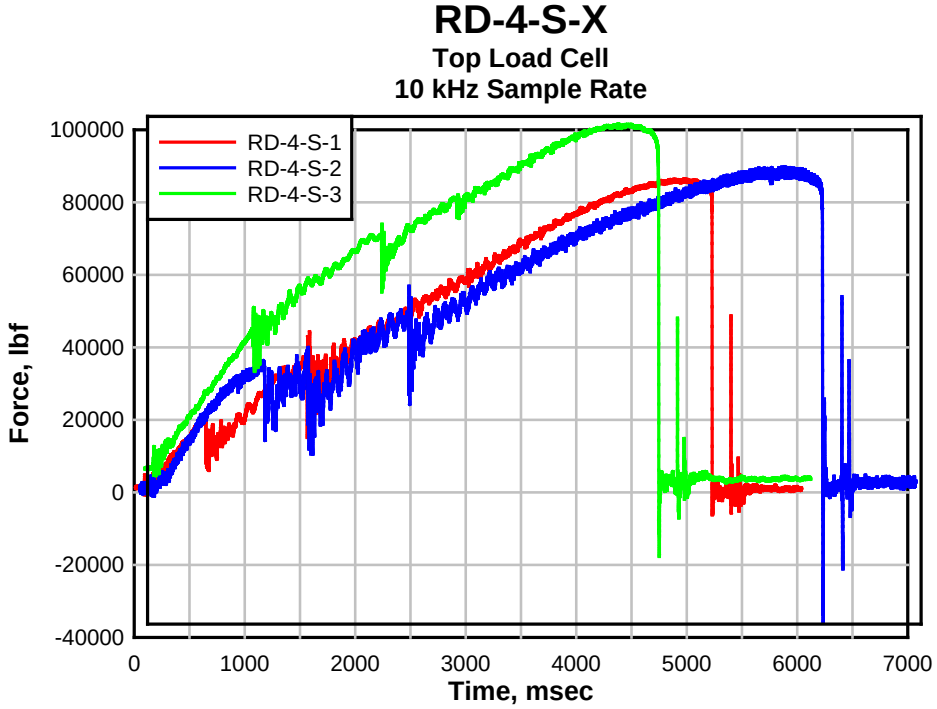

Figure 160: RD-4-S-X Tests Data.

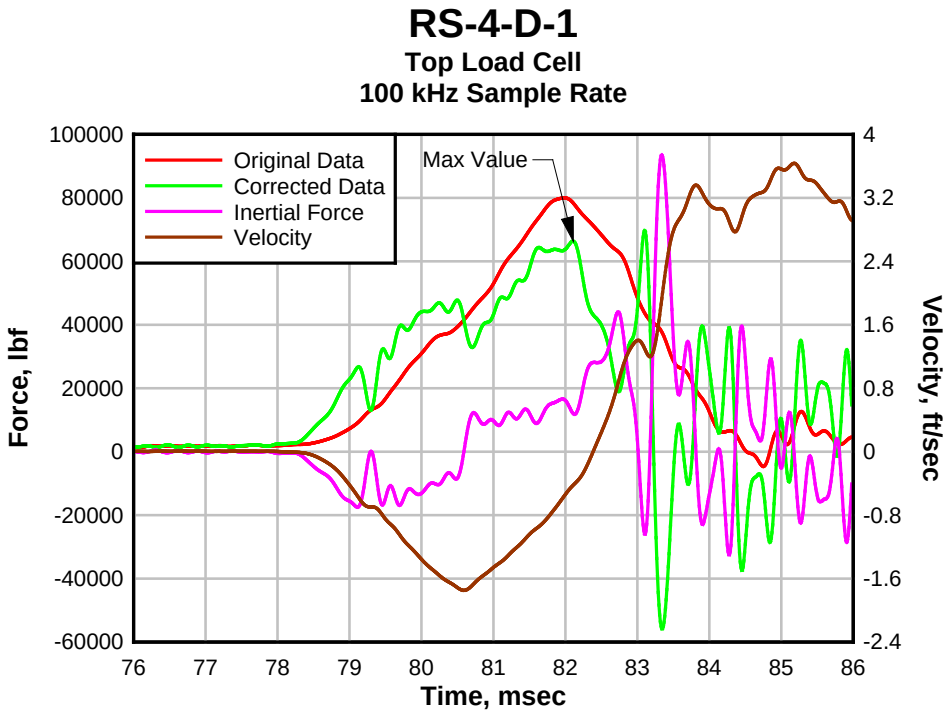

Figure 161: RS-4-D-1 Test Data.

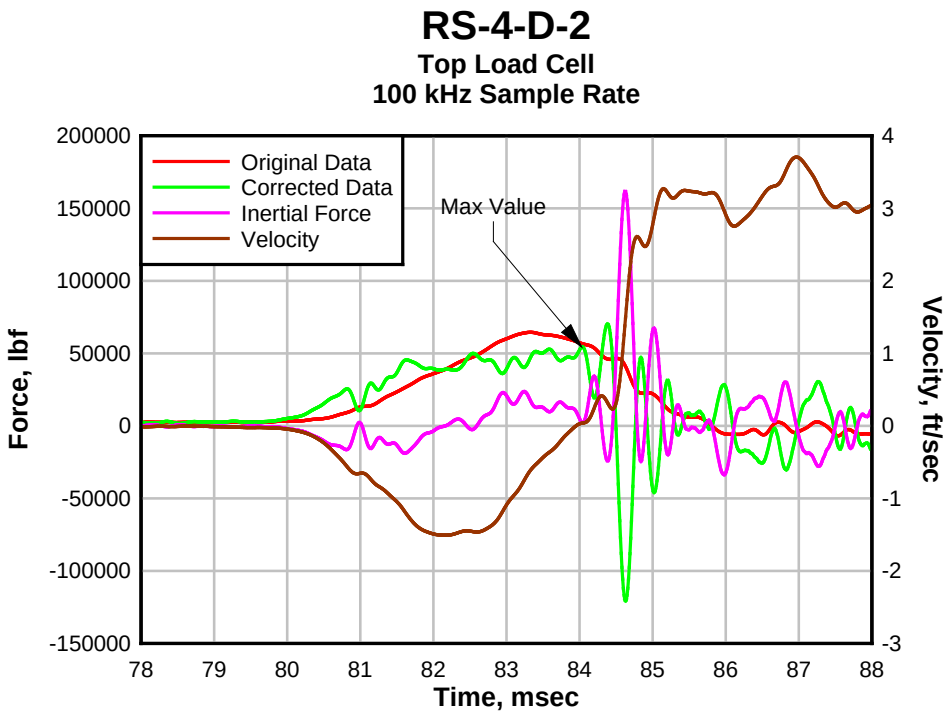

Figure 162: RS-4-D-2 Test Data.

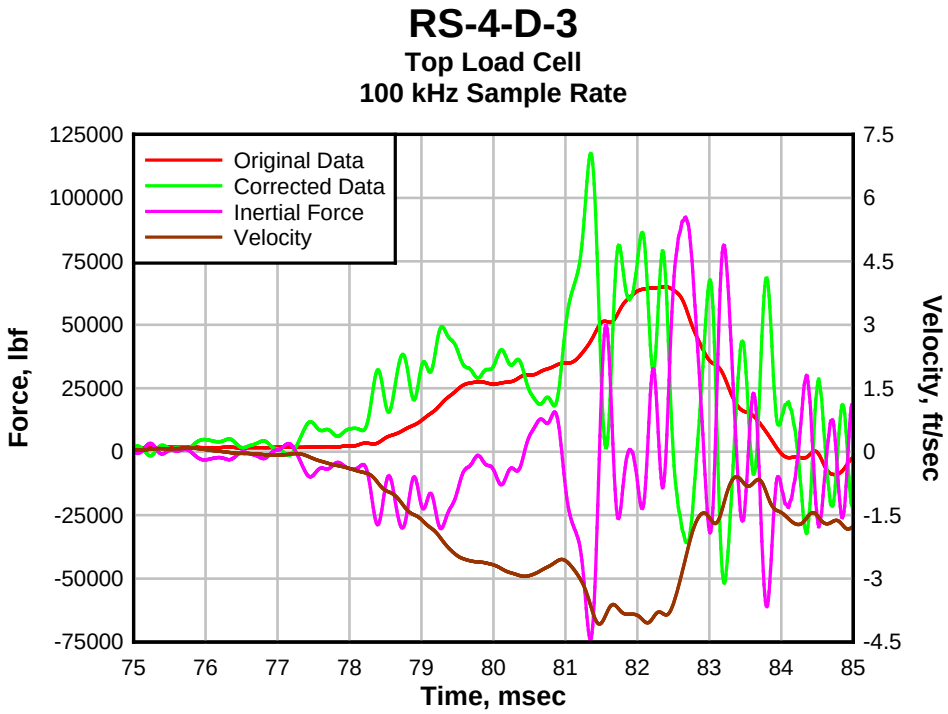

Figure 163: RS-4-D-3 Test Data.

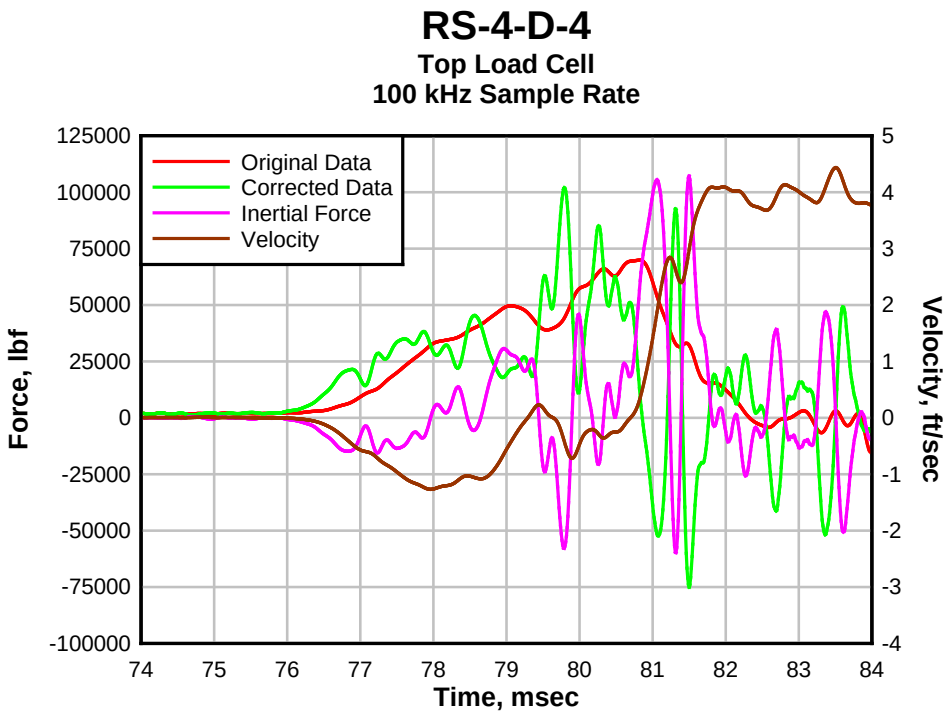

Figure 164: RS-4-D-4 Test Data.

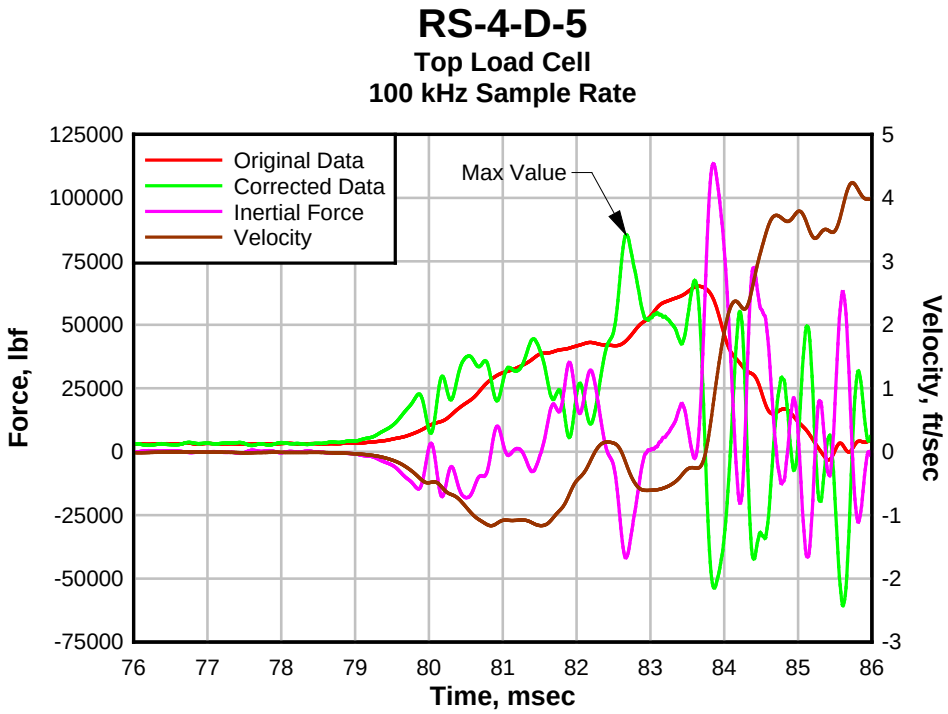

Figure 165: RS-4-D-5 Test Data.

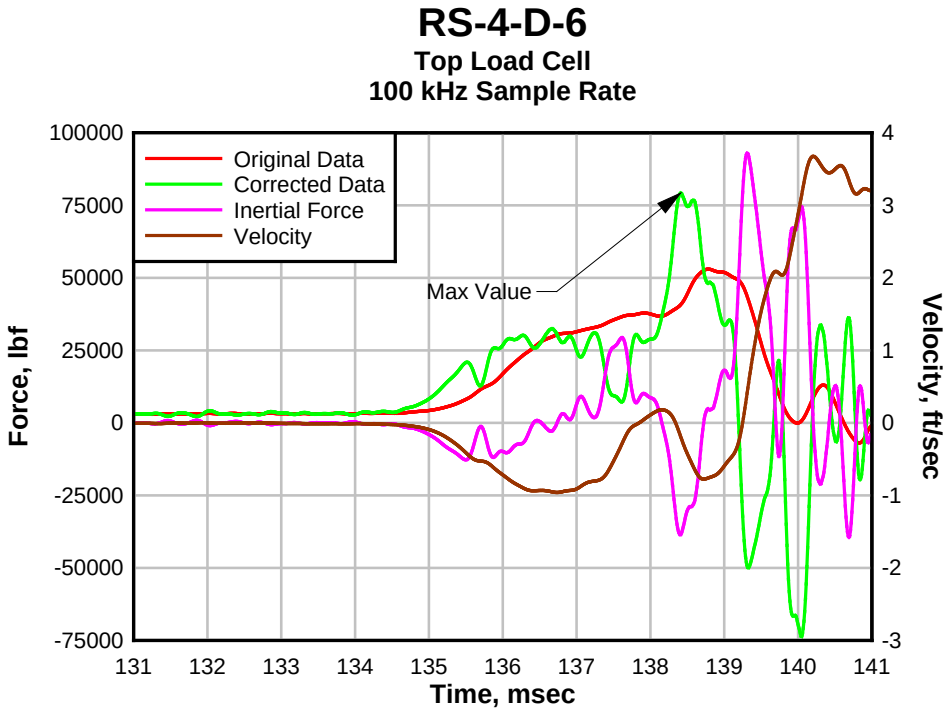

Figure 166: RS-4-D-6 Test Data.

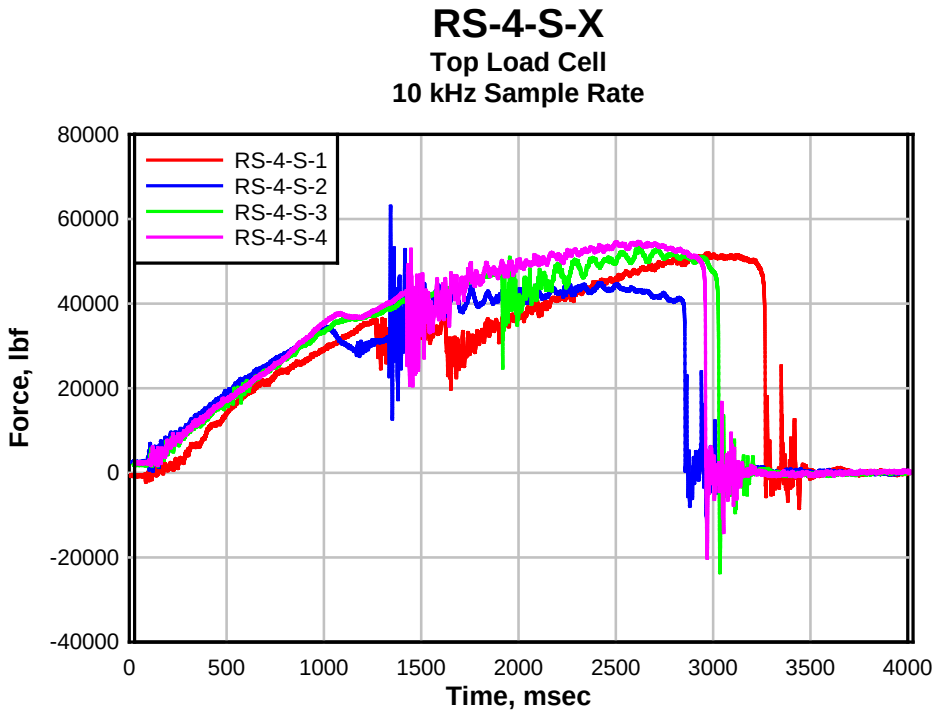

Figure 167: RS-4-S-X Tests Data.

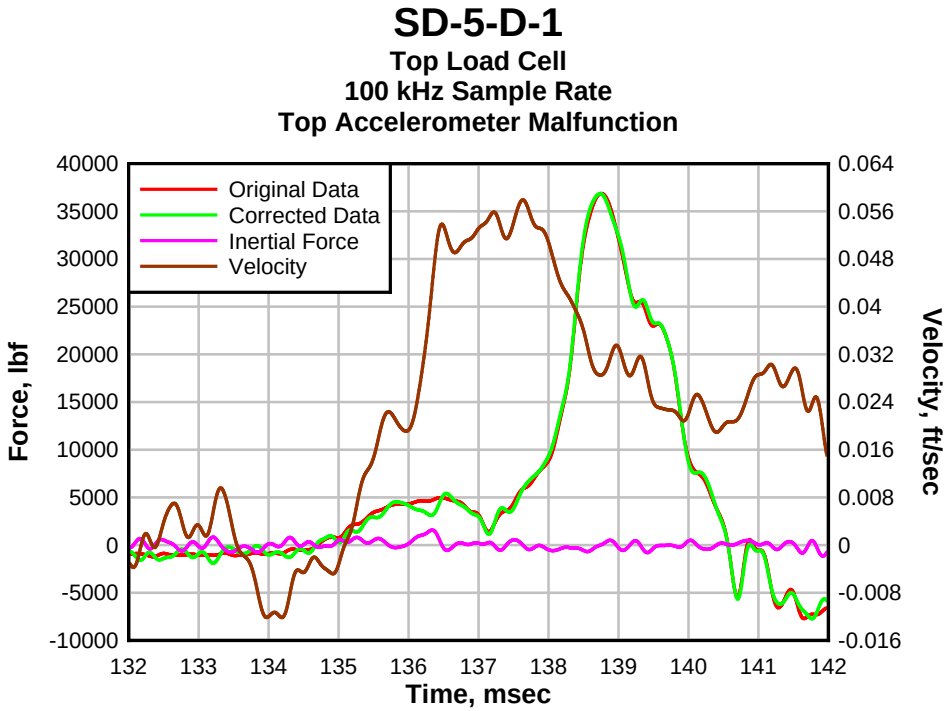

Figure 168: SD-5-D-1 Test Data.

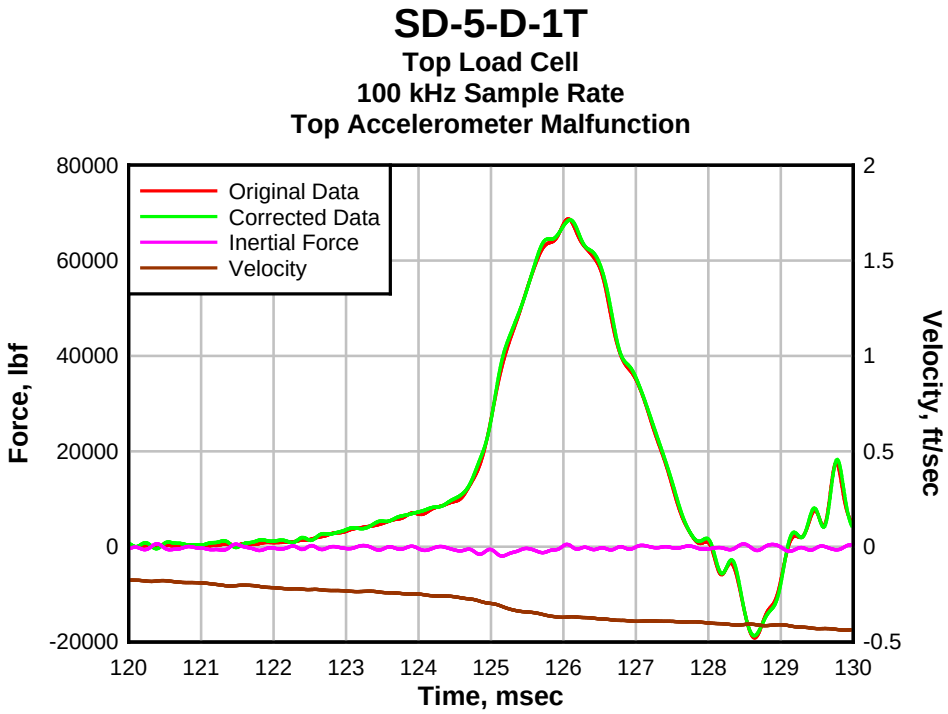

Figure 169: SD-5-D-1T Test Data.

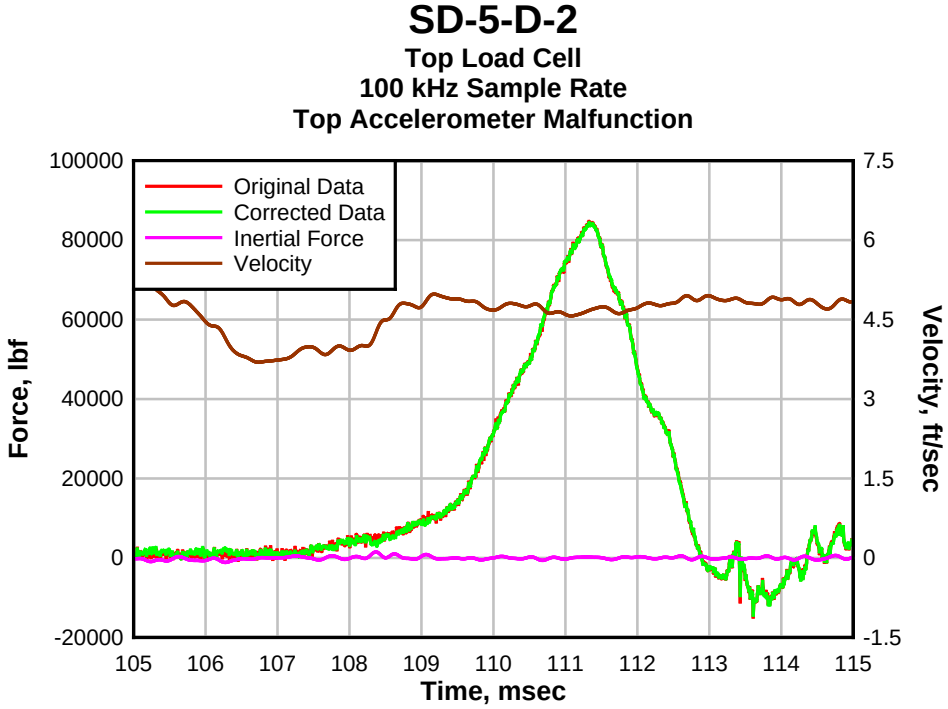

Figure 170: SD-5-D-2 Test Data.

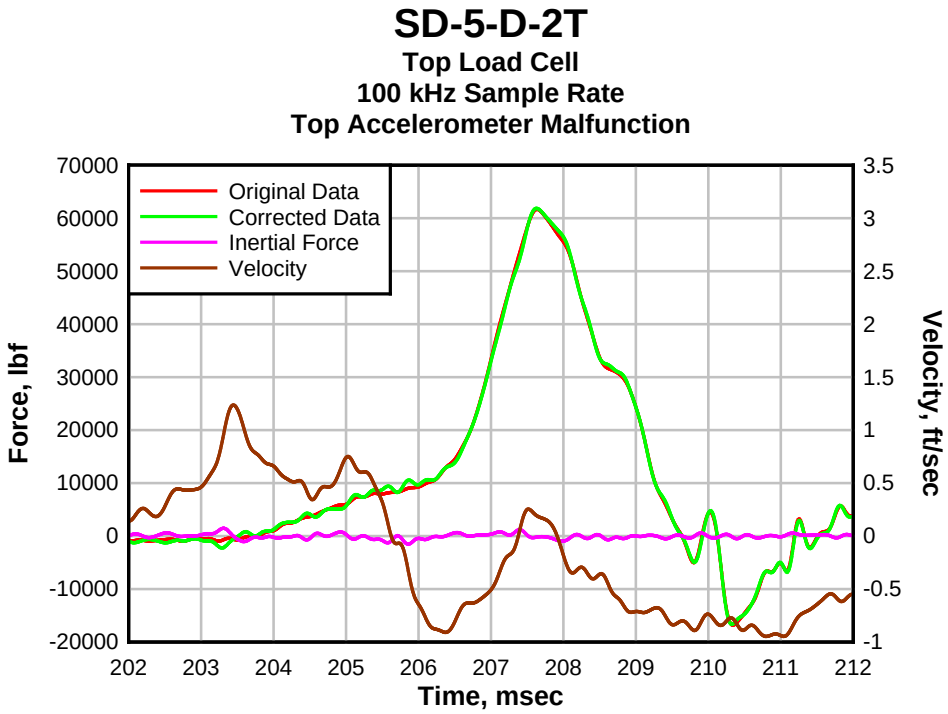

Figure 171: SD-5-D-2T Test Data.

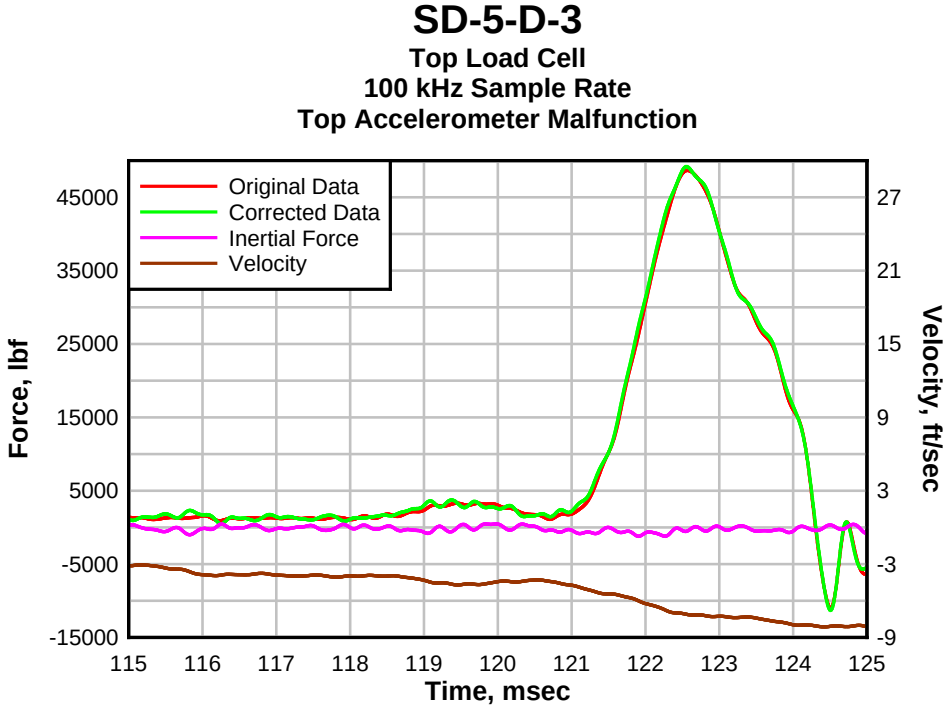

Figure 172: SD-5-D-3 Test Data.

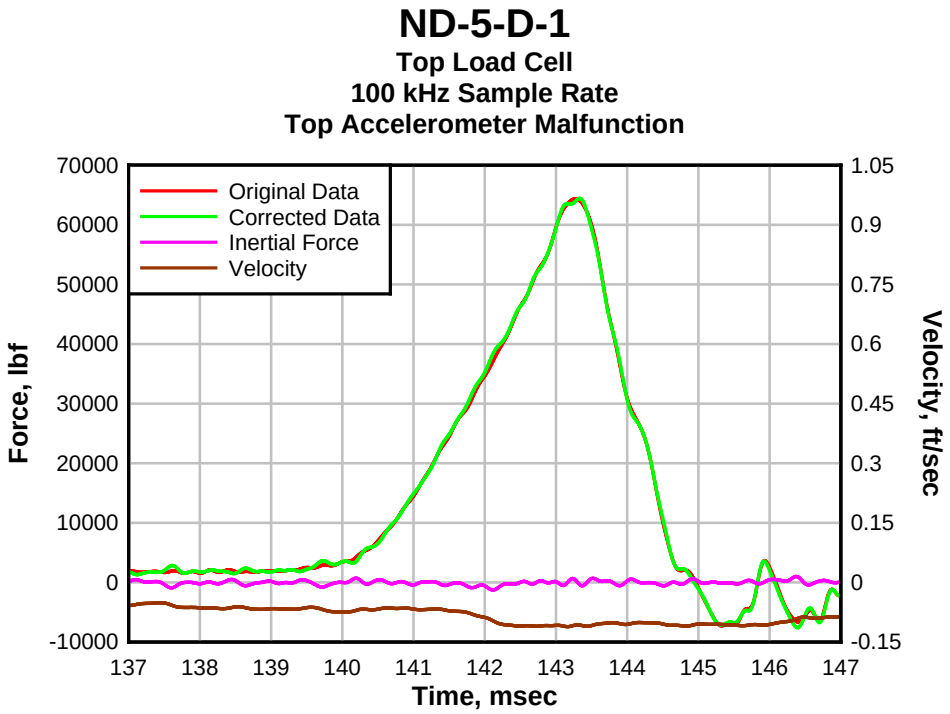

Figure 173: ND-5-D-1 Test Data.

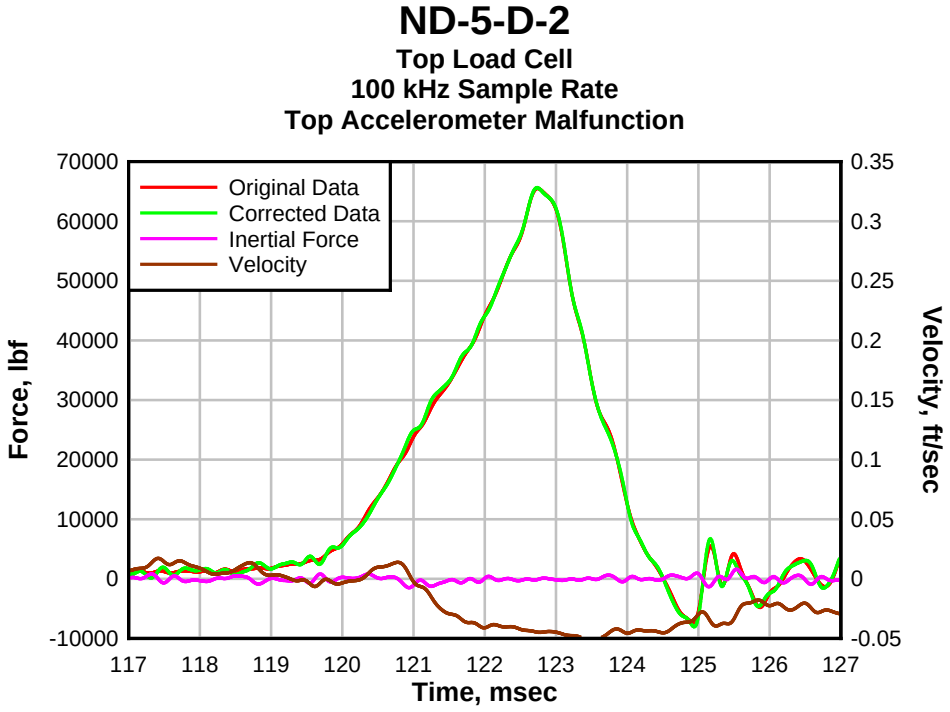

Figure 174: ND-5-D-2 Test Data.

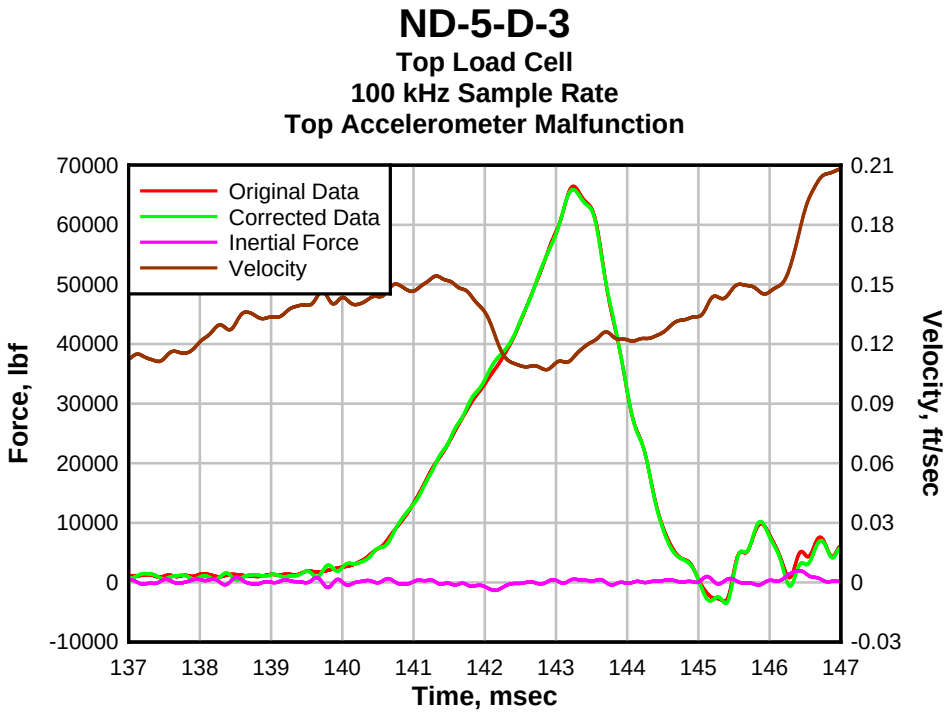

Figure 175: ND-5-D-3 Test Data.

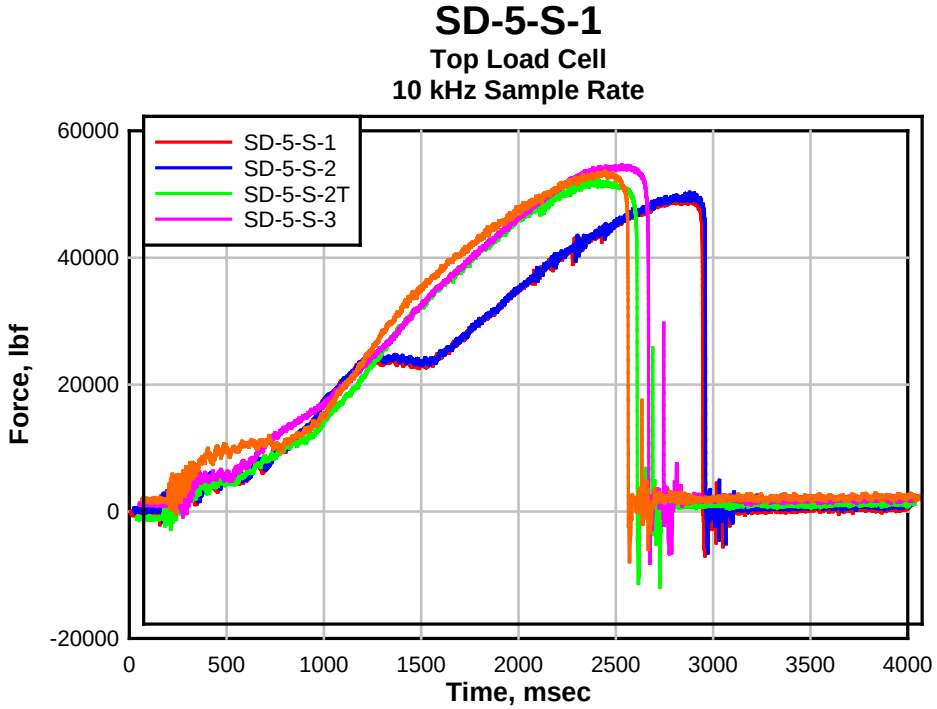

Figure 176: SD-5-S-X Tests Data.

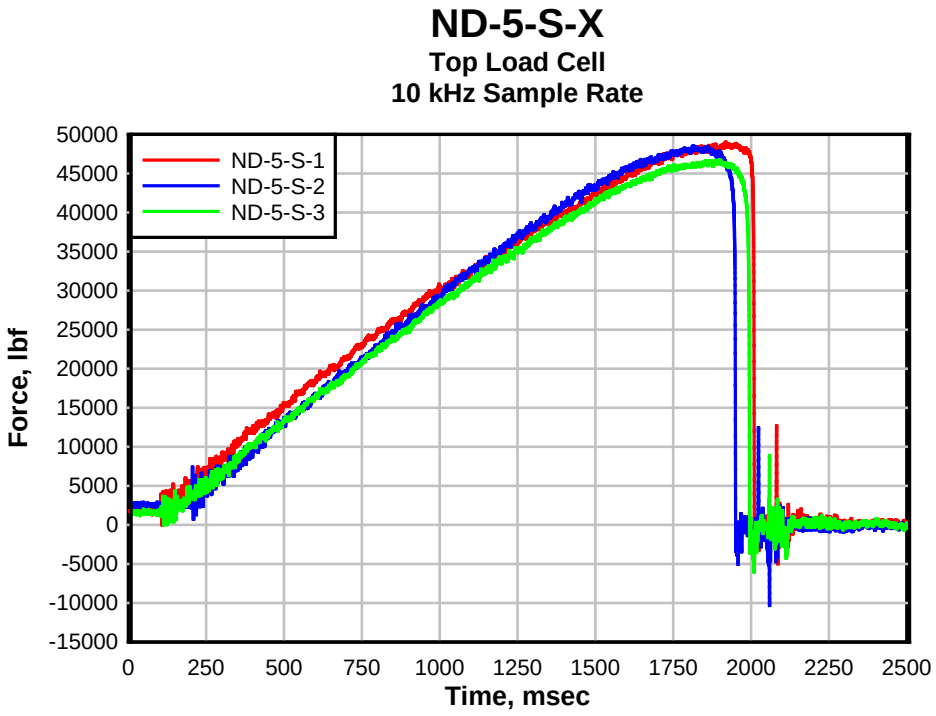

Figure 177: ND-5-S-X Tests Data.

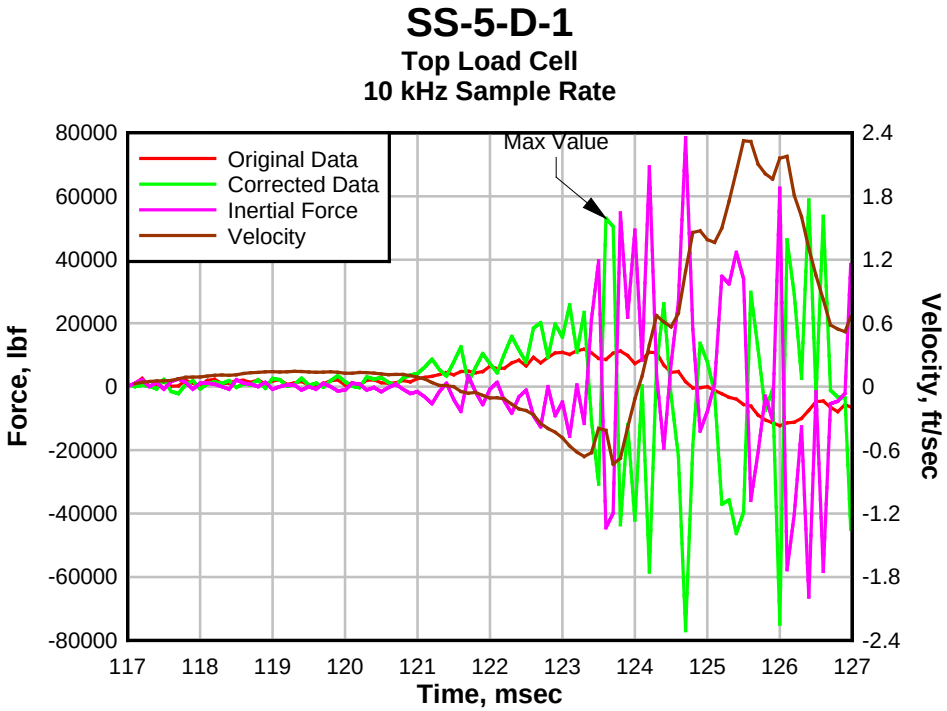

Figure 178: SS-5-D-1 Test Data.

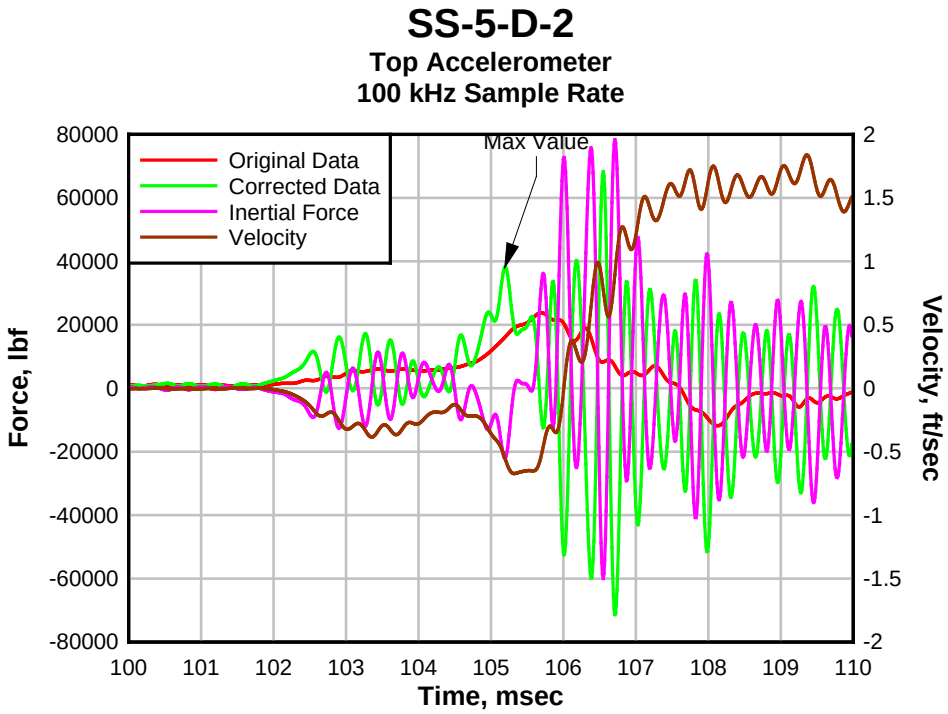

Figure 179: SS-5-D-2 Test Data.

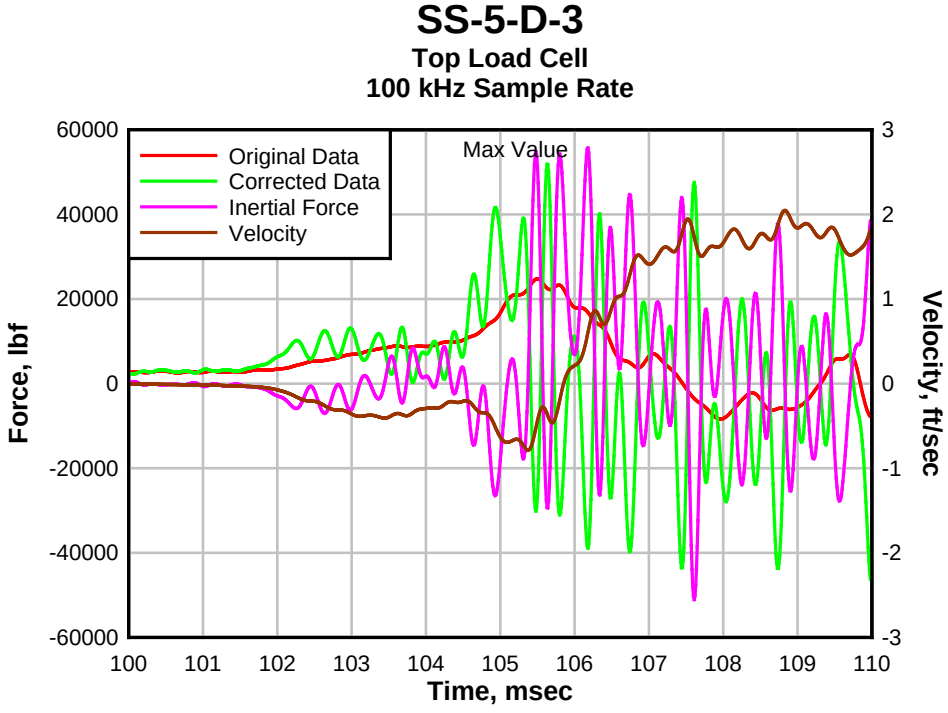

Figure 180: SS-5-D-3 Test Data.

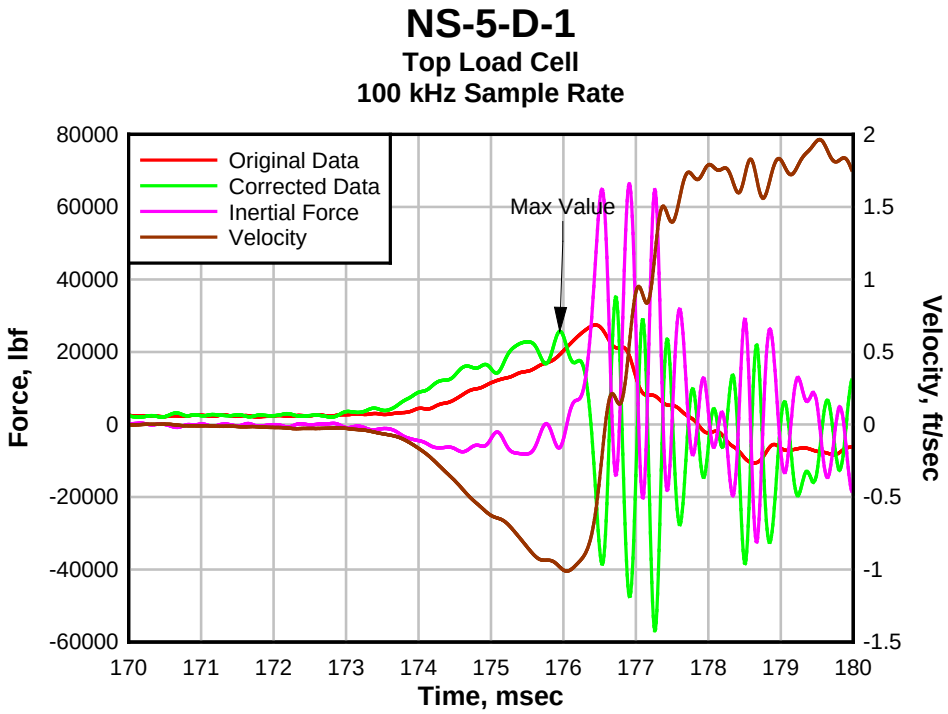

Figure 181: NS-5-D-1 Test Data.

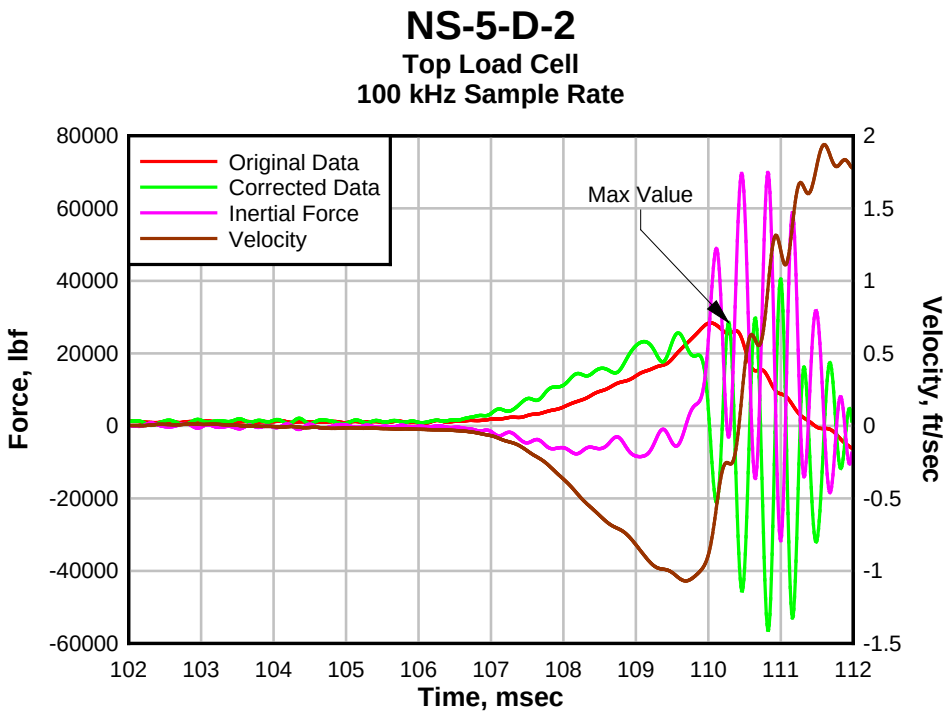

Figure 182: NS-5-D-2 Test Data.

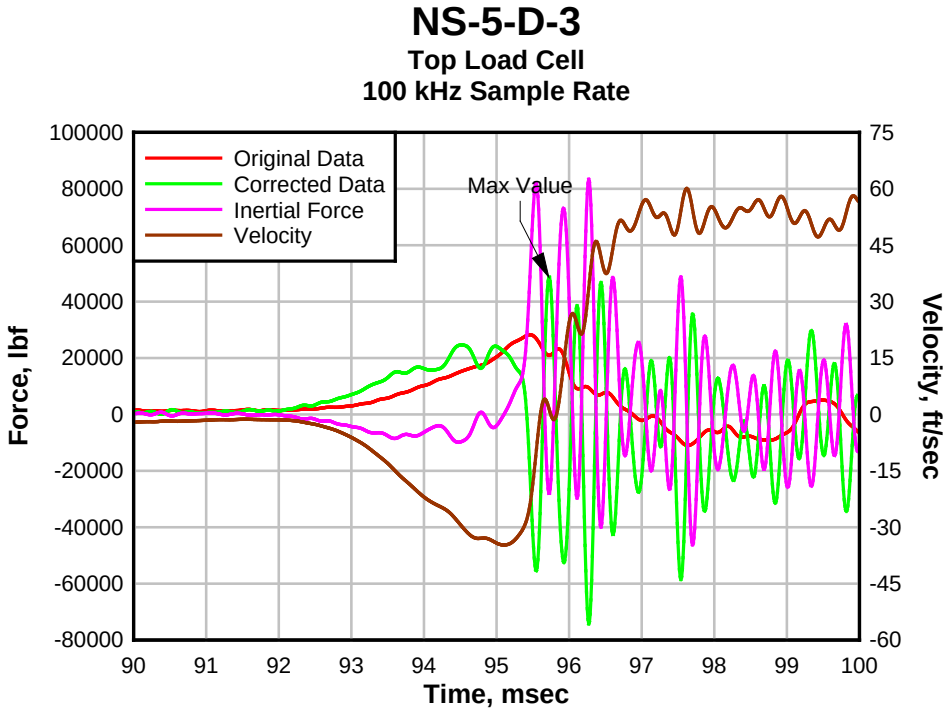

Figure 183: NS-5-D-3 Test Data.

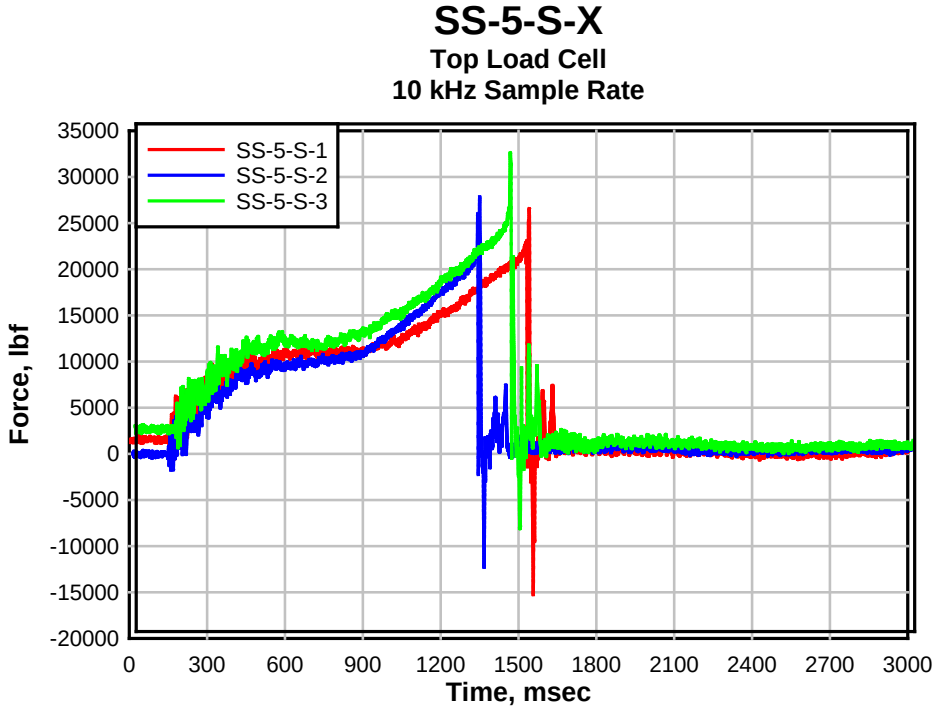

Figure 184: SS-5-S-X Tests Data.

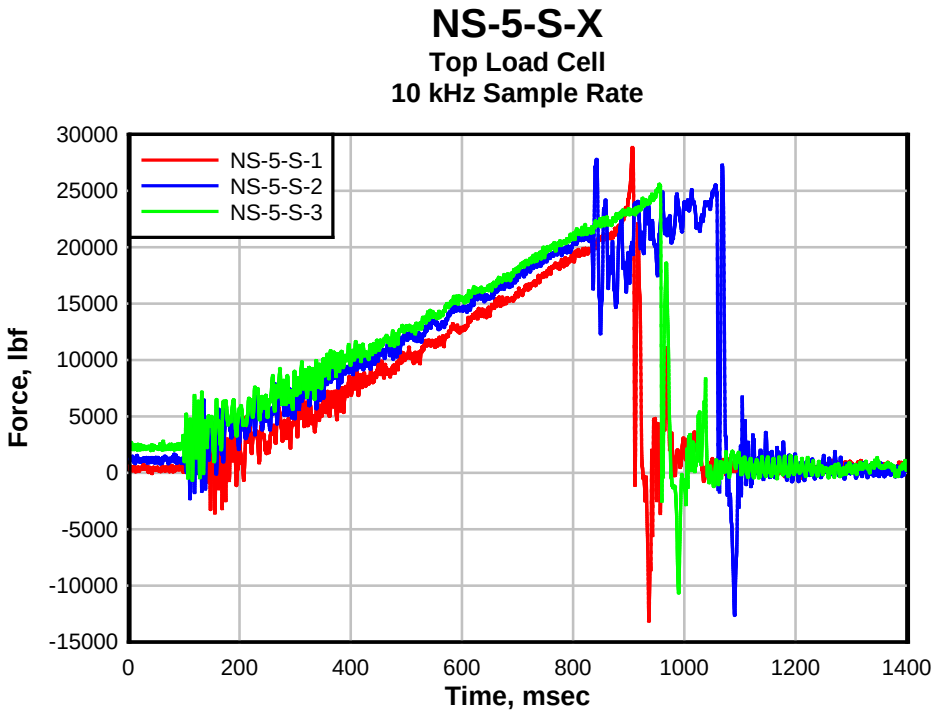

Figure 185: NS-5-S-X Tests Data.

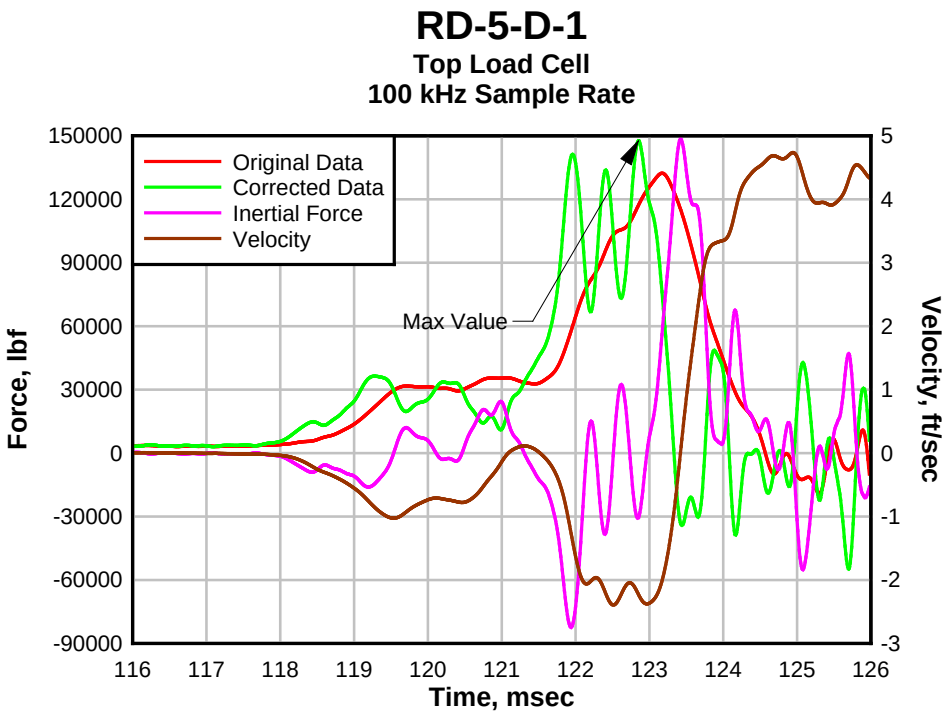

Figure 186: RD-5-D-1 Test Data.

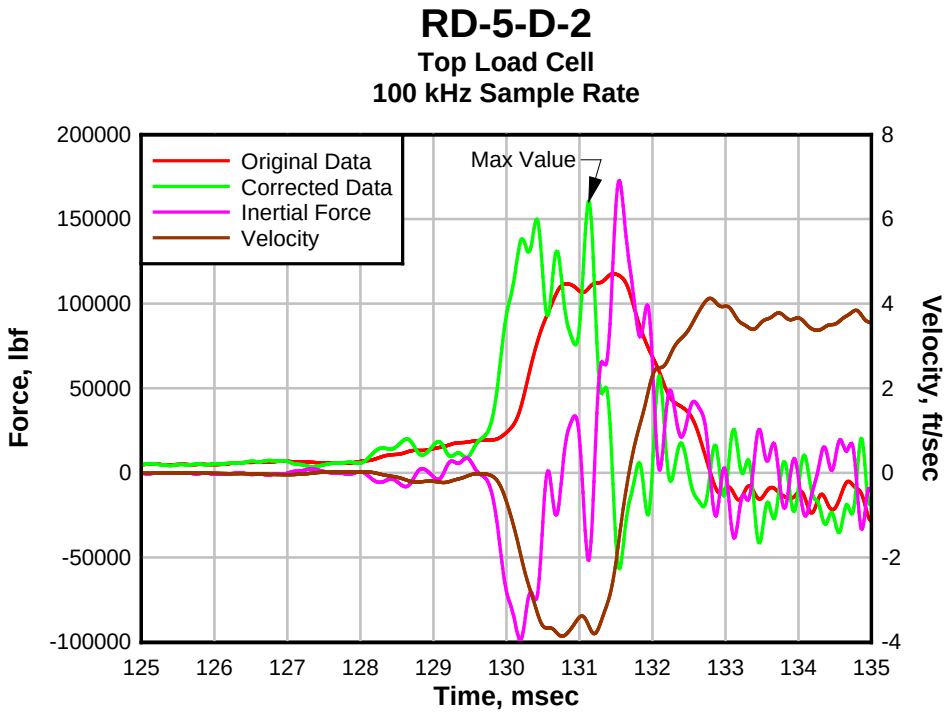

Figure 187: RD-5-D-2 Test Data.

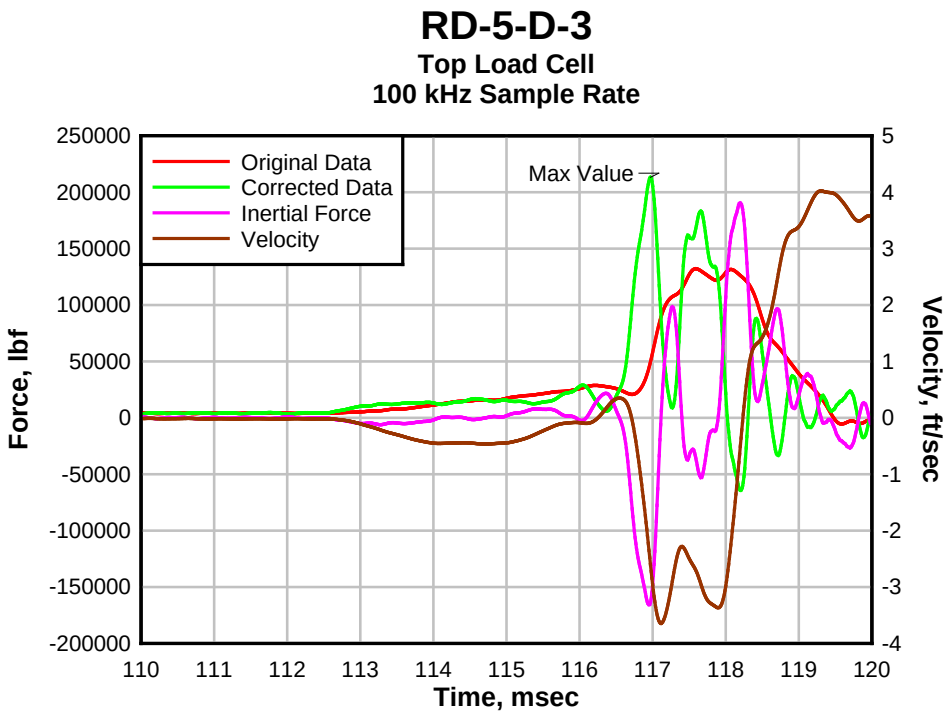

Figure 188: RD-5-D-3 Test Data.

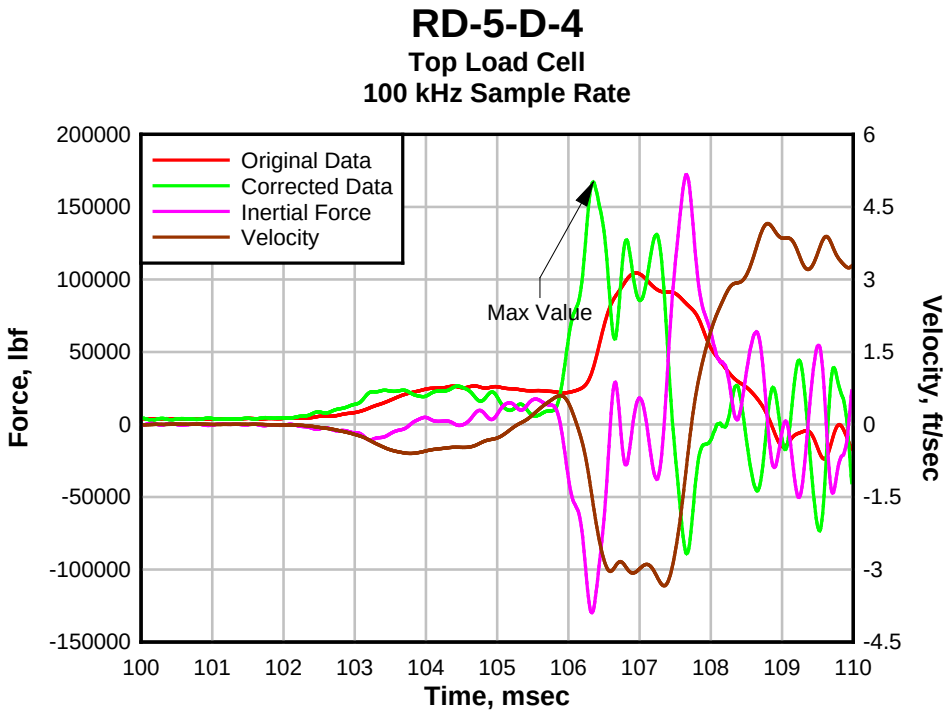

Figure 189: RD-5-D-4 Test Data.

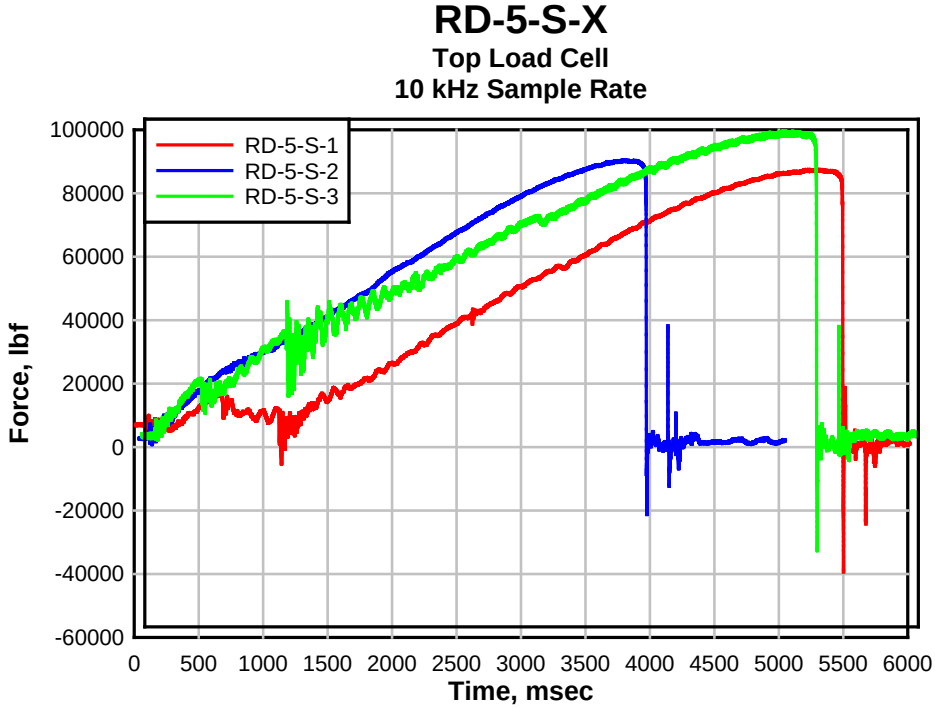

Figure 190: RD-5-S-X Tests Data.

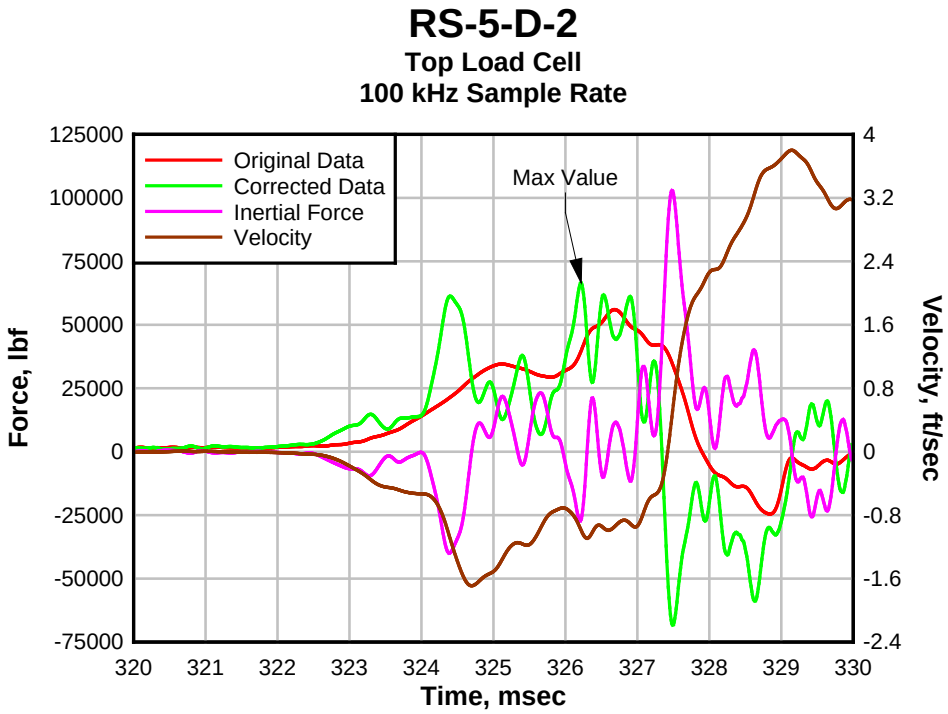

Figure 191: RS-5-D-2 Test Data.

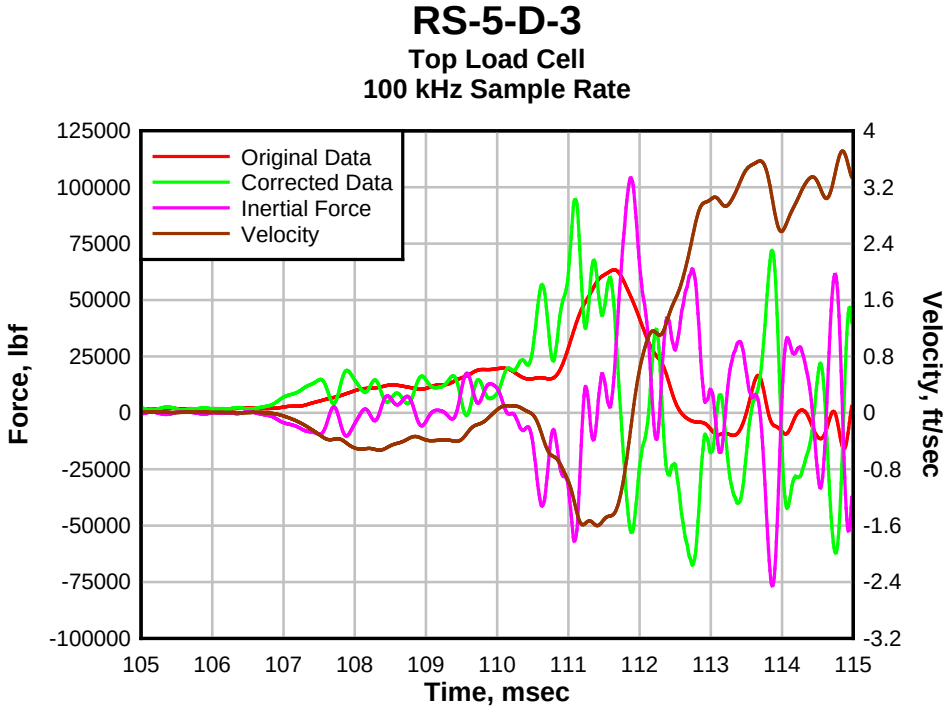

Figure 192: RS-5-D-3 Test Data.

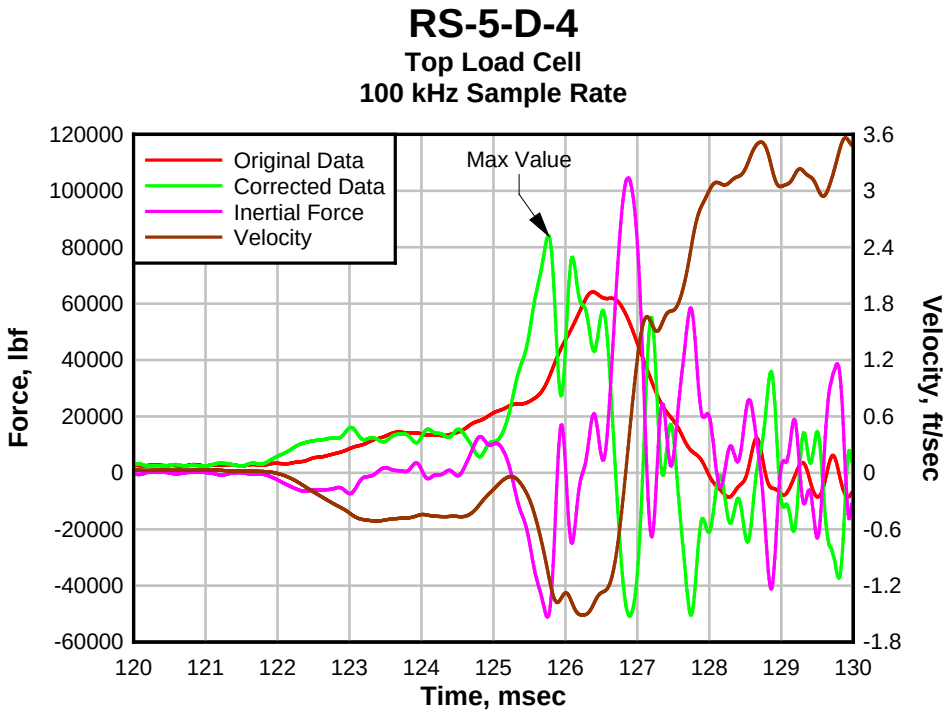

Figure 193: RS-5-D-4 Test Data.

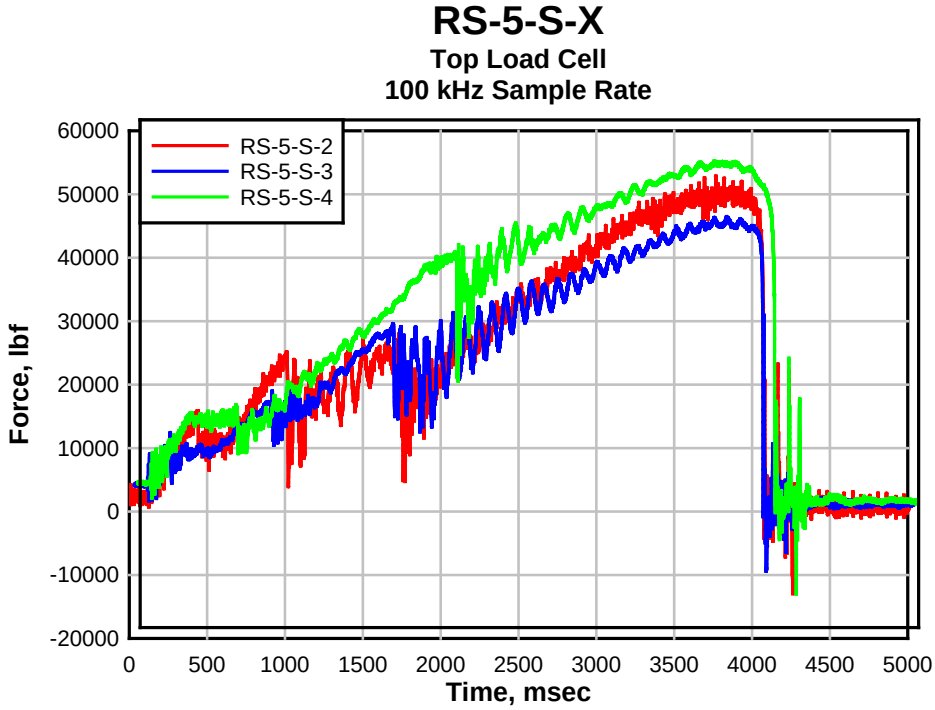

Figure 194: RS-5-S-X Tests Data.